

Electronic Thesis and Dissertation Repository

---

7-31-2019 1:30 PM

# Pregestational Diabetes Induced Congenital Heart Defects and Coronary Artery Malformations; Mechanisms and Preventative Therapies

Anish Engineer  
*The University of Western Ontario*

Supervisor  
Feng, Qingping  
*The University of Western Ontario*

Graduate Program in Physiology and Pharmacology  
A thesis submitted in partial fulfillment of the requirements for the degree in Doctor of Philosophy  
© Anish Engineer 2019

Follow this and additional works at: <https://ir.lib.uwo.ca/etd>



Part of the [Cardiovascular Diseases Commons](#), [Cellular and Molecular Physiology Commons](#), [Developmental Biology Commons](#), and the [Pharmacology Commons](#)

---

## Recommended Citation

Engineer, Anish, "Pregestational Diabetes Induced Congenital Heart Defects and Coronary Artery Malformations; Mechanisms and Preventative Therapies" (2019). *Electronic Thesis and Dissertation Repository*. 6328.  
<https://ir.lib.uwo.ca/etd/6328>

This Dissertation/Thesis is brought to you for free and open access by Scholarship@Western. It has been accepted for inclusion in Electronic Thesis and Dissertation Repository by an authorized administrator of Scholarship@Western. For more information, please contact [wlsadmin@uwo.ca](mailto:wlsadmin@uwo.ca).

## Abstract

Congenital heart defects (CHDs) arise from perturbations in complex molecular and cellular processes underlying normal embryonic heart development. CHDs are the most common congenital malformation, occurring in 1 to 5% of live births, and are the leading cause of pediatric mortality. Adverse genetic and environmental factors can impede normal cardiogenesis, and increase the likelihood of CHDs. Pregestational maternal diabetes increases the risk of CHDs in children by more than four-fold. As the prevalence of diabetes rapidly rises among women of childbearing age, there is a need to investigate the mechanisms and potential preventative strategies for these defects. The aim of this thesis was to explore the pathogenesis of pregestational diabetes-induced CHDs and coronary artery malformations (CAMs), while testing the efficacy of two clinically relevant pharmacotherapies. To this end, using a mouse model of pregestational diabetes, I examined the impact of hyperglycemia-induced elevations in oxidative stress and miR-122 on heart development, concurrently determining the preventative capabilities of sapropterin or antimiR-122 treatment. I confirmed that pregestational diabetes results in spectrum of CHDs, CAMs and cardiac function deficits, and that their incidence is significantly lowered with either sapropterin or antimiR-122. Specifically, sapropterin treatment lowered the incidence of CHDs and CAMs from 59% and 50% to 27% and 21%, respectively. Similarly, antimiR-122 therapy reduced this incidence of CHDs from 57% to 23%. These morphological malformations range in severity, and include septal and outflow defects (OFT), myocardium deficiencies, and hypoplastic coronary arteries. Lineage tracing experiments revealed a diminished commitment of second heart field progenitors to the OFT, endocardial cushions and ventricular myocardium in embryonic hearts from diabetic dams. In addition, deficits in

cardiogenic gene expression, enzyme activity, cell proliferation, and epicardial EMT, induced by pregestational diabetes, contribute to these defects, and were prevented by both treatments. Specifically, sapropterin treatment reestablished the functional eNOS dimer and restored its phosphorylation in embryonic hearts of diabetic dams, leading to normal cardiovascular development. Conversely, antimiR-122 attenuated the targeting and inhibition of key genes responsible for cardiogenesis by miR-122. These results suggest that sapropterin and antimiR-122 may have therapeutic potential in preventing CHDs in children of women with pregestational diabetes.

**Key words:**

Pregestational diabetes, congenital heart defects, embryonic heart development, sapropterin, tetrahydrobiopterin, oxidative stress, coronary artery development, miR-122, antimiR-122

## Lay Summary

The most common birth defects are congenital malformations of the heart, accounting for 1-5% of live births. Newborns with congenital heart defects have an increased risk of mortality, as proper function of the heart is compromised when specific development is not attained during gestation. Congenital heart defects can go unnoticed by doctors at birth, however, as the child matures and is involved in increasing amounts of physical activity, the congenital malformations can manifest themselves. Therefore, it is vital that research be conducted into how and why these malformations develop, and more significantly, what remedies during pregnancy can prevent their occurrence. In terms of how these defects arise, it has been previously shown that pregestational diabetes in the mother increases the risk for congenital heart defects in the child by over 50%. Studies in animal models have confirmed diabetes as a risk factor for newborns with malformed hearts. This connection is alarming as the incidence of diabetes in a younger demographic is seemingly increasing. This is also true for the female population, specifically in North America. More and more women are being diagnosed as diabetic at a younger age, and if these women have children, their offspring may have a serious, life-threatening medical condition. Therefore, it is beneficial not only to the lives of these children, but also to the health-care system to find a solution to this problem. This research will attempt to do just that, as we will investigate whether administration of sapropterin or antimicroRNA-122 will decrease the presence of heart defects in the offspring of diabetic mouse mothers.

## Co-Authorship Statement

The studies outlined in **Chapters 2-4** were performed by Anish Engineer in the laboratory of Dr. Qingping Feng, with the assistance of co-authors listed below.

Dr. Qingping Feng contributed to experimental design, data interpretation and manuscript preparation for all experiments. In addition, Dr. Sharon Lu assisted with scientific training and troubleshooting in all experiments.

**Chapter 2:** Dr. Sharon Lu assisted with intrauterine fetal echocardiography (**Figure 2.3 T-W**), sample collection, and all other technical aspects of this project. Ms. Tana Saiyin helped with tissue processing and histology. Mr. Andrew S. Kucey and Dr. Brad L. Urquhart measured biopterin levels by UPLC and mass spectrometry analysis (**Figure 2.2 E-G**). Dr. Thomas A. Drysdale and Dr. Kambiz Norozi provided valuable comments and revised this manuscript.

**Chapter 3:** Mr. Yong Jin Lim assisted with tissue processing and histology (**Figure 3.1**), and created 3D coronary artery reconstructions as part of his 4<sup>th</sup> year undergraduate studies (**Figure 3.2**). Dr. Kambiz Norozi contributed to manuscript revision.

**Chapter 4:** Dr. Sharon Lu performed embryonic sample collection. Mr. Yuan Chen helped with immunohistochemistry as part of his 4th year undergraduate studies (Figure 4.4).

## Acknowledgments

It gives me great pleasure to sincerely express my gratitude to a number of individuals that played a pivotal role in my life, and without whom, this doctoral thesis would not have been possible. First and foremost, thank you to my supervisor and mentor, **Dr. Qingping Feng**. Thank you for your constant support, encouragement and guidance throughout these five years. Dr. Feng's expert knowledge and passion for research was truly inspiring, and the ideal environment for me to start my career. His patient and strategic mentorship challenged me, furthered my ambitions, and allowed me to recognize my potential. Thank you for having confidence in me, giving me room to develop my own ideas, but always making sure what we generated was of the highest quality and done the correct way. I greatly respect his regard for the scientific method, and deeply appreciate the opportunity to train as a scientist under him. The lessons I have learnt, skills I have developed, awards I have won, and manuscripts we have published under Dr. Feng's guidance will be forever cherished. I would also like to convey my genuine thanks to my advisory committee. Drs. Tom Drysdale, Stan Leung, and Tim Regnault provided valuable feedback and insightful comments, which strengthen this thesis, all while being incredibly encouraging and having a positive attitude. In addition, I must thank the faculty members of the Department of Physiology and Pharmacology for fostering a world-class graduate training program. Thank you, Dr. Doug Jones, for reviewing this thesis; Dr. Brad Urquhart, for collaborating with us; and Dr. Peter Stathopoulos, for giving me the opportunity to teach and lead a graduate-level course.

I am also extremely grateful for the numerous lab colleagues who have come and gone over these past five years. A constant force throughout this entire period was **Dr. Sharon Lu**. Thank you, Sharon, for teaching me every single experimental procedure

used in this thesis. This work would not have been possible without your expertise and immense technical knowledge. Sharon is a patient teacher, who can solve any problem or issue, without hesitation. I have learnt so much from you, and will especially value the surgical techniques you taught me. I feel lucky to have had you as a lab manager and friend, and will look fondly on all the stories and laughs shared throughout the years. Likewise, thank you to Ms. Murong Liu for her help with animal handling and my project when I first started in the lab. Thanks to all of the volunteers, co-op students, summer students, work-study students and 4<sup>th</sup> year thesis students who have been very helpful in the lab.

To my fellow graduate students in the Feng lab, I feel so fortunate to have spent time with each of you. You truly became my family away from home, and I could not have asked for better colleagues. Carmen Leung, thank you for taking me under your wing when I first started graduate school, you are the ultimate example. We instantly clicked, and I learnt so much from you. You are one of the most selfless people I know, and I am so happy with the brother-sister bond we have. Similarly, Jessica Blom, we started our grad school journeys together and I couldn't have asked for a better partner. We have had so many fun times, and the three years you were in the lab flew by because we were always up to something. I know you will thrive in residency and become a remarkable clinician scientist. Katherine Lee, thank you for guidance throughout graduate school, especially helping me with my role as Physiology and Pharmacology Graduate Council President. I learnt a lot from your shrewd advice, and I miss visiting every single restaurant in London with you. Tana Saiyin, you started as my lab volunteer and then became a great friend. I'm so proud of your success and I know you will be a great physician. Elizabeth Greco, the final two years of this PhD have been so memorable

because of you. Your one-of-a-kind personality and zest for life truly brought a lot of laughter to often gloomy times. Finally, thank you to Matt Novello and Carol Ma, I will always treasure the experiences we shared in the lab. Special thanks to two phenomenal undergraduate students, Mella Kim and MengQi Zhang. Mella, thank you for all your hard work on my projects. You are one of the kindest and most dedicated people I know, and I can't wait to see all the amazing things you accomplish. MengQi, thanks for the help, your ambition inspires me, and I'm so proud of your achievements.

The greatest takeaway from this grad school experience is the friendships I have made. I have had so many great times socializing with the graduate students in this department, and the bonds we've formed will last a life time. There are too many friends to name; however, the following have had a lasting impact and enriched my grad school experience: Melissa Fenech, Paxton Moon, Anusha Ratneswaran, Tom Velonosi, Jake Bedore, Sarah Woolsey, John-Mike Arpino, Lisa Choi, Melissa Crawford, Tyler Cooper, Laura Russel, Phyo Win, Victoria Deveau and Alexandra Pearce. The comradery in this department was unparalleled, and thank you to the original members of "PhysPhun" for starting the trend. To my two roommates who were with me for final years of grad school, Geoff Kerr and Brandon Baer, we've had countless fun times together, and I believe we were the life of this department. I will miss all of our exciting adventures, but we will forever revel in the memories. Best of luck on both of your PhD's, I know you both will do great things.

I would like to thank my family and my closest friends, who were instrumental parts of this process. Andrew Kucey and Adam Raffoul, I started this journey with you both as a roommate and a friend, and we ended it as brothers. Words can't describe what your friendship means to me, but thank you for always being there. Sometimes I think



you boys know me better than I know myself. You two always made me look at the bigger picture during the rough patches, making me realize my dreams were bigger than any obstacles I faced. We've had tons of fun together and will continue to do so, no matter how geographically separated we become. Thank you, Andrew, for the constant support, encouragement and life-chats. Thank you for your tireless help with the experiments in this thesis, I couldn't have asked for a better collaborator, and I know we will co-author many more manuscripts. Thank you, Adam, for bringing levity, laughter, and entertainment; you are a rockstar. From sunshine in San Diego to snow in London, we've been through it all. Great things are coming for you, and just know, I'm your number one fan.

Finally, thank you to my wonderful parents for giving me the opportunity to pursue higher education. Your unwavering love and support helped me every step of the way. You've sacrificed so much so that I could have everything I've ever desired. I am eternally grateful to you for providing me with the means to reach for the stars. You've instilled in me the fundamentals of a solid work ethic, and are the best role models. Thank you to my brother and sister-in-law, Neel and Anne Engineer, for the continuous encouragement, and thank you to my grandparents for inspiring me to live my life to the fullest.

*This thesis is dedicated to the loving memory of the late Dr. Neelam Engineer.*

# Table of Contents

Abstract.....	i
Lay Summary.....	iii
Co-Authorship Statement.....	iv
Acknowledgments.....	v
Table of Contents.....	x
List of Tables.....	xvi
List of Figures.....	xvii
List of Abbreviations.....	xx
Chapter 1.....	1
1 Introduction.....	1
1.1 Pregestational Diabetes.....	1
1.2 Heart Development.....	2
1.2.1 The First Heart Field.....	3
1.2.2 The Second Heart Field.....	4
1.2.3 Cardiac Looping and Endocardial Cushion Formation.....	6
1.2.4 Chamber Formation and Septation.....	6
1.2.5 Ventricular Myocardium Development.....	8
1.2.6 Outflow Tract Development.....	10
1.2.7 Cardiac Valve Development.....	11
1.2.8 Transcriptional Regulators of Heart Development.....	12
1.2.9 Proliferation and Apoptosis in Cardiogenesis.....	15
1.2.10 Fetal Cardiovascular Physiology.....	18
1.3 Coronary Artery Development.....	19
1.3.1 Epithelial-to-Mesenchymal Transition.....	22

1.3.2	Transcriptional Regulators of Coronary Artery Development .....	22
1.4	microRNA Regulation of Cardiovascular Development .....	23
1.4.1	microRNA Biogenesis, Structure and Function.....	24
1.4.2	microRNA in Cardiogenesis .....	27
1.4.3	microRNA-122 a novel player in CHD pathogenesis.....	29
1.5	Congenital Heart Disease.....	31
1.5.1	Types of Congenital Heart Defects.....	33
1.5.2	Epidemiology and Environmental Risk Factors of Congenital Heart Disease .....	37
1.6	Pregestational Diabetes and Congenital Heart Defects .....	38
1.6.1	Potential Mechanisms of Diabetic Embryopathy .....	40
1.7	Endothelial Nitric Oxide Synthase.....	42
1.7.1	Tetrahydrobiopterin .....	43
1.7.2	BH4 Cycling and eNOS Coupling; a Positive Feedback Loop .....	46
1.7.3	The role of eNOS in Cardiovascular Development .....	49
1.8	Rationale and Hypothesis .....	51
1.8.1	Aim 1: Sapropterin on Diabetes-Induced CHDs .....	52
1.8.2	Aim 2: Sapropterin on Diabetes-Induced CAMs.....	53
1.8.3	Aim 3: Role of microRNA-122 in Heart Development.....	54
1.9	References.....	56
Chapter 2	.....	84
2	Chapter 2 .....	85
2.1	Chapter Summary .....	85
2.2	Introduction.....	86
2.3	Methods.....	88
2.3.1	Animals.....	88

2.3.2	Induction of Diabetes and Sapropterin Treatment .....	88
2.3.3	Histological and Immunohistochemical Analysis .....	90
2.3.4	Lineage Tracing the Second Heart Field .....	91
2.3.5	Analysis of Superoxide Levels .....	92
2.3.6	Measurement of Cardiac Function.....	92
2.3.7	Western Blotting for eNOS Dimers and Monomers.....	93
2.3.8	Real-Time RT-PCR .....	93
2.3.9	Determination of Biopterin Levels .....	94
2.3.10	Statistical Analysis.....	95
2.4	Results.....	96
2.4.1	Effects of sapropterin on blood glucose, fertility, litter size and biopterin levels in pregestational diabetes.....	96
2.4.2	Sapropterin prevents CHDs induced by pregestational diabetes .....	98
2.4.3	Sapropterin prevents myocardial and valvular abnormalities induced by pregestational diabetes .....	103
2.4.4	Effects of sapropterin on outflow tract length and cell proliferation in the fetal heart .....	107
2.4.5	Fate-mapping of SHF derived cells in the fetal heart of diabetic mothers .....	109
2.4.6	Sapropterin prevents maternal diabetes-induced downregulation of regulators of heart development.....	111
2.4.7	Sapropterin decreases oxidative stress and improves eNOS dimerization in fetal hearts of pregestational diabetes .....	113
2.5	Discussion.....	115
2.6	Footnotes.....	121
2.7	References.....	122
Chapter 3	.....	127
3	Chapter 3 .....	128
3.1	Chapter Summary .....	128

3.2	Introduction.....	129
3.3	Methods.....	131
3.3.1	Animals.....	131
3.3.2	Induction of Diabetes and Sapropterin Treatment.....	131
3.3.3	Histological and Immunohistochemical Analysis.....	132
3.3.4	Analysis of 4-hydroxynonenal Levels.....	133
3.3.5	Assessment of Epicardial EMT using <i>ex vivo</i> Heart Explant Culture ....	133
3.3.6	Western Blotting for eNOS and Akt Phosphorylation.....	134
3.3.7	Real-time RT-PCR Analysis.....	134
3.3.8	Statistical Analysis.....	135
3.4	Results.....	136
3.4.1	Sapropterin prevents coronary artery malformations in offspring of diabetic mice without altering blood glucose levels.....	136
3.4.2	Sapropterin prevents diabetes-induced fetal hypoplastic coronary arteries and restores capillary density.....	137
3.4.3	Sapropterin regulates coronary artery progenitor proliferation and EMT.....	141
3.4.4	Tetrahydrobiopterin normalizes high glucose-impaired epicardial EMT <i>ex vivo</i> .....	143
3.4.5	Sapropterin restores expression of coronary vessel development and growth genes.....	144
3.4.6	Sapropterin inhibits oxidative stress and restores activity of the Akt/eNOS pathway.....	146
3.5	Discussion.....	148
3.6	Footnotes.....	153
3.7	References.....	154
	Chapter 4.....	158
4	Chapter 4.....	159
4.1	Chapter Summary.....	159

4.2	Introduction.....	160
4.3	Methods.....	163
4.3.1	Animals.....	163
4.3.2	Induction of Diabetes and AntimiR-122 Treatment.....	163
4.3.3	Histological Analysis.....	166
4.3.4	Embryonic Heart Explant Culture.....	166
4.3.5	<i>Ex vivo</i> Assessment of Epicardial EMT.....	167
4.3.6	Immunofluorescence.....	167
4.3.7	Real-time RT-PCR analysis.....	168
4.3.8	Fetal Echocardiography.....	170
4.3.9	Statistical Analysis.....	170
4.4	Results.....	171
4.4.1	miR-122 is upregulated in the fetal heart of pregestational diabetes.....	171
4.4.2	Gene targets of miR-122 in the embryonic heart.....	172
4.4.3	Role of miR-122 in Cell Proliferation and Apoptosis in the Embryonic Heart.....	175
4.4.4	Role of miR-122 in epicardial EMT.....	177
4.4.5	Effects of antimiR-122 on blood glucose, litter size, cardiac function and fetal liver.....	179
4.4.6	Anti-miR-122 administration reduces the incidence of diabetes-induced CHDs.....	182
4.5	Discussion.....	185
4.6	References.....	192
	Chapter 5.....	200
5	Chapter 5.....	200
5.1	Summary of Major Findings.....	200
5.2	Study Limitations.....	208

5.2.1	Justification of a Mouse Model of Pregestational Diabetes.....	208
5.2.2	Genetically Altered Mice.....	209
5.2.3	Use of <i>ex vivo</i> Organ Culture Systems .....	210
5.3	Suggestions for Future Studies .....	212
5.4	Conclusion .....	215
5.5	References.....	217
	Appendix.....	221
	Curriculum Vitae .....	223



## List of Tables

Table 2.1. Specific primer sequences used in real-time PCR analysis. ....	94
Table 2.2. The rate of congenital heart defects in the offspring of diabetic and control mothers with and without sapropterin (BH4) treatment. ....	100
Table 3.1. Specific primer sequences for real-time PCR analysis. ....	135
Table 3.2. Effects of sapropterin (BH4) on nonfasting maternal blood glucose levels and incidence of CAMs in E18.5 hearts during pregestational diabetes. ....	137
Table 4.1. Primer sequences for PCR analysis. ....	169
Table 4.2. The rate of congenital heart defects in the offspring of diabetic dams treated with anti-miR-122 or scramble LNA. ....	183

## List of Figures

Figure 1.1. Embryonic coronary artery development in the mouse.....	21
Figure 1.2. microRNA biosynthesis and function. ....	26
Figure 1.3. eNOS uncoupling and inactivation in states of oxidative stress.....	48
Figure 2.1. Experimental design to examine the effects of sapropterin (BH4) on congenital heart defects induced by pregestational diabetes. ....	90
Figure 2.2. Blood glucose levels of pregnant mice, percent successful plugs, litter size, fetal body weight and biopterin levels. ....	97
Figure 2.3. Effects of sapropterin (BH4) on congenital heart defects induced by pregestational diabetes. ....	102
Figure 2.4. Effects of sapropterin (BH4) on fetal heart wall thickness of pregestational diabetes at E18.5. ....	105
Figure 2.5. Effects of sapropterin (BH4) on aortic, pulmonary and mitral valve defects induced by pregestational diabetes at E18.5. ....	107
Figure 2.6. Effects of sapropterin (BH4) on outflow tract development and cell proliferation in E10.5 hearts of pregestational diabetes.....	108
Figure 2.7. Effects of pregestational diabetes on SHF progenitor contribution to E9.5 and E12.5 hearts.....	110
Figure 2.8. Effects of sapropterin (BH4) on molecular regulators of heart development at E12.5. ....	112
Figure 2.9. Effects of sapropterin (BH4) on superoxide production and eNOS dimer/monomer protein levels in E12.5 hearts. ....	114
Figure 2.10. Schematic summary of sapropterin on diabetes-induced CHDs . ....	116

Figure 3.1. Effects of sapropterin (BH4) on coronary artery malformations induced by pregestational diabetes. ....	139
Figure 3.2. Effects of sapropterin (BH4) on coronary artery volume at E18.5. ....	140
Figure 3.3. Effects of sapropterin (BH4) on epicardial cell proliferation and markers of EMT in E12.5 hearts. ....	142
Figure 3.4. Effects of BH4 on epicardial EMT ex vivo. ....	143
Figure 3.5. Effects of sapropterin (BH4) on gene expression of transcription and growth factors critical to coronary artery development in E12.5 hearts of offspring from diabetic and control dams. ....	146
Figure 3.6. Effects of sapropterin (BH4) on oxidative stress and Akt/eNOS phosphorylation in fetal hearts. ....	147
Figure 3.7. Schematic summary of sapropterin on diabetes-induced CAMs. ....	148
Figure 4.1. <i>Ex vivo</i> and <i>in vivo</i> approaches to examine the effects of miR-122 on heart development, and antimiR-122 on pregestational diabetes-induced CHDs. ....	165
Figure 4.2. Expression analysis of miR-122, Pri-miR-122 and GLD2. ....	172
Figure 4.3. Analysis of target gene expression of miR-122. ....	174
Figure 4.4. Effects of miR-122 and high glucose on cell proliferation and apoptosis in the embryonic heart. ....	177
Figure 4.5. Ex vivo assessment of epicardial EMT. ....	178
Figure 4.6. Outcomes of in vivo administration of antimiR-122 during diabetic pregnancy. ....	181
Figure 4.7. Effects of antimiR-122 on congenital heart defects induced by pregestational diabetes. ....	184

Figure 4.8. Schematic summary showing the effect of miR-122 on embryonic heart development.....186

Figure 5.1. The role of eNOS uncoupling/oxidative stress and miR-122 in the pathogenesis of pregestational diabetes-induced congenital heart defects. ....207

## List of Abbreviations

<b>Abbreviation</b>	<b>Full Name</b>
3D	Three Dimensional
ALDH1a2	Aldehyde Dehydrogenase 1 Family Member A2
Ao	Aorta
ASD	Atrial Septal Defect
AV	Atrioventricular
AVC	Atrioventricular Canal
AVSD	Atrioventricular Septal Defect
bFGF	Basic Fibroblast Growth Factor
BG	Blood Glucose
BH4	Tetrahydrobiopterin
BMP	Bone Morphogenic Protein
BrdU	Bromodeoxyuridine
CAM	Coronary Artery Malformation
CC3	Cleaved Caspase 3
cGMP	cyclic guanosine monophosphate
CHD	Congenital Heart Defect
CNC	Cardiac Neural Crest
DAB	3,3'-Diaminobenzidine
DHE	Dihydroethidium
DHFR	Dihydrofolate Reductase
DORV	Double Outlet Right Ventricle
DNA	Deoxyribonucleic Acid
E	Embryonic Day
EC	Endothelial Cell
ECC	Endocardial Cushion
ECM	Extracellular Matrix
eNOS	Endothelial Nitric Oxide Synthase
EMT	Epithelial-to-Mesenchymal Transition
EndMT	Endocardial-to-Mesenchymal Transition
EPDC	Epicardial-derived Cell
EPO	Erythropoietin
FGF	Fibroblast Growth Factor
FHF	First Heart Field
GAG	Glucoaminoglycan
GFP	Green Fluorescent Protein
GLD2	Germ Line Development 2
GTP	Guanosine Triphosphate

GTPCH1	GTP Cyclohydrase 1
HIF1	Hypoxia Inducible Factor 1
HNE	Hydroxynonenal
IP	Intraperitoneal
LA	Left Atrium
LNA	Locked Nucleic Acid
L-NAME	N( $\omega$ )-nitro-L-arginine methyl ester
LV	Left Ventricle
LVAWTd	Left Ventricle Anterior Wall Thickness diastole
LVAWTs	Left Ventricle Anterior Wall Thickness systole
Mef2c	Myocyte Enhancement Factor 2c
MHC	Myosin Heavy Chain
miR	microRNA
MMLV	Moloney Murine Leukemia Virus
mTmG	Membrane localized tomato membrane localized green
mRNA	messenger RNA
NAC	N-Acetylcysteine
NO	Nitric Oxide
OFT	Outflow Tract
P	Postnatal Day
PEO	Proepicardial Organ
pHH3	Phosphorylated Histone H3
PKU	Phenylketonuria
Pri-miR	Primary microRNA
RA	Right Atrium
Rac1	Ras-related C3 botulinum toxin substrate 1
RISC	RNA-Induced Silencing Complex
ROS	Reactive Oxygen Species
RV	Right Ventricle
RNA	Ribonucleic Acid
rRNA	Ribosomal RNA
SHF	Second Heart Field
SMA	Smooth Muscle Actin
SOD	Superoxide Dismutase
SRY	Sex-determining region Y
STZ	Streptozotocin
TBX	T-box
TGA	Transposition of the Great Arteries
TGF	Transforming Growth Factor
TOF	Tetralogy of Fallot

TNF	Tumor Necrosis Factor
Vegf	Vascular Endothelial Growth Factor
VSD	Ventricular Septal Defect
Wnt	Wingless type integration site
WT	Wilt Type
Wt1	Wilm's Tumor 1

## Chapter 1

### 1 Introduction

#### 1.1 Pregestational Diabetes

Diabetes is a major health problem, currently affecting 451 million people globally. The number of diabetic patients is estimated to reach 693 million by 2040.<sup>1</sup> In Canada, more than 11 million people are living with diabetes or prediabetes.<sup>2</sup> Diabetes has two subtypes. Type 1 diabetes (T1D) is also called juvenile or insulin-dependent diabetes. In T1D, pancreatic beta cells produce little or no insulin, the hormone that allows glucose to enter the cells, resulting in hyperglycemia. Type 2 diabetes (T2D) is often associated with obesity and peripheral insulin resistance. In T2D, hyperglycemia is present despite elevated blood levels of insulin or hyperinsulinemia. The prevalence of T2D among the adolescent population in the US has increased 31% between 2001 and 2009, with pre-diabetes rising from 9 to 23%.<sup>3</sup> It is well known that diabetes is an important risk factor for cardiovascular disease, such as congenital heart disease, stroke, peripheral artery disease and heart failure. In fact, about 80% of people with diabetes die as a result of heart disease or stroke.<sup>4</sup>

Importantly, the incidence of T2D is rapidly increasing in women at their childbearing age.<sup>1</sup> It is estimated that 1 in 5 women are overweight/obese during pregnancy.<sup>5</sup> Diabetes not only affects adult health but also puts developing embryos at risk in pregnant women as glucose can easily pass through the placenta and reach the fetal circulation. When these women have diabetes, not only is their own health affected, but their pregnancy is associated with a high risk of congenital malformations in the fetus. In addition, emerging longitudinal data suggests that adult metabolic and



cardiovascular disorders are in-part attributable to physiological insults in fetal life.<sup>6, 7</sup> Adverse uterine environments, including maternal obesity, diabetes, undernutrition and stress, can compromise embryonic development, reprogramming the epigenetic landscape.<sup>8</sup>

Pregestational diabetes (PGD) is the development of diabetes prior to conception either by T1D or T2D. The risk of major congenital malformations in the offspring of women with diabetes is 3 to 10-fold higher compared to the general population.<sup>9, 10</sup> In a recent population based study, similar rates of congenital malformations were reported between T1D and T2D (4.8% and 4.3%, respectively).<sup>11</sup> Although circulating insulin levels are elevated in T2D, maternal insulin does not cross the placenta. Thus, hyperglycaemia is likely the main cause of the congenital malformations in the offspring of diabetic women.

## 1.2 Heart Development

The heart is the first fully functional organ to form during embryogenesis, and its development is orchestrated by an interplay of conserved transcription factors that control growth, morphogenesis, and contractility of this ancient pump.<sup>12</sup> Cardiac development is a complex and intricate process that in essence involves the harmonic combination of 3 pools of progenitor cells, that when present in a specific spatial and temporal orientation together, form a self-excitable, four-chambered, vascular pump which only stops beating at the time of death.<sup>13</sup> Heart development commences at week 3 of human embryogenesis, corresponding to embryonic day 7.5 (E7.5) in the mouse,<sup>14</sup> with the formation of a cardiac crescent and subsequent heart tube from cells of the anterior lateral mesoderm. This first wave of cardiac progenitors has been termed the First Heart Field (FHF), and includes myoblasts forming the tube and endothelial cells lining the entire

structure.<sup>15</sup> The primitive heart tube is elongated at its poles by the addition of proliferative cells coming from the adjacent splanchnic pharyngeal mesoderm. This consecutive wave of myoblasts has been termed the Second Heart Field (SHF), and contributes to the rightward looping morphogenesis of the tube, whereby primitive chambers of the heart can be distinguished.<sup>15</sup> Chamber development by ballooning, muscularization and fusion of endocardial cushions, ventricular myocardialization and septation, outflow tract (OFT) and cardiac valve development are completed thereafter, with the addition of cardiac neural crest cells (CNCs) migrating from the dorsal neural tube.<sup>16</sup> Cardiac development is therefore an extremely complex spatiotemporal process, and a misstep in this orchestration could lead to a congenital heart defect (CHD). The sections to follow will detail the nature of these cardiac heart fields, the numerous steps involved in heart morphogenesis, as well as the transcriptional regulation that directs this entire process.

### 1.2.1 The First Heart Field

In embryology, a heart field is defined as a source of cardiac progenitor cells at a particular location that give rise to the heart.<sup>16</sup> Clonal analysis has revealed that the FHF segregates from the SHF early in gastrulation,<sup>17</sup> and the basic helix–loop–helix transcription factor *MESP1* marks this nascent cardiac mesoderm.<sup>18</sup> Following gastrulation, cardiac precursors of both lineages migrate to either sides of the embryo midline, below the head folds.<sup>19</sup> Here, cardiogenesis begins, with the formation of a cardiac crescent from cells of the anterior lateral mesoderm, at E7.5 in the mouse. These cells are known as the FHF and contribute to the establishment of a linear heart tube, which is formed by the joining of the edges of the cardiac crescent at the ventral

midline.<sup>20</sup> Here, the first evidence of a heart-beat is seen as calcium transients and peristaltic contractions commence through the heart tube at E8.0 in the mouse.<sup>21</sup> This heart tube is composed of a concentric inner layer of endocardial cells and outer layer of myocardial cells separated with extra-cellular matrix, also known as cardiac jelly.<sup>22</sup> The venous pole of this tube contains the cardiac inflow tract and the transient sinus venosus. This is connected via the atrioventricular canal to the primitive ventricle, which will develop into the left ventricle of the heart.<sup>15, 23</sup> The FHF-derived heart tube specifically contributes to parts of the atria and the left ventricle of the mature heart.

### 1.2.2 The Second Heart Field

The primitive heart tube is elongated with the addition of cells from a second subpopulation of progenitors, originating from the pharyngeal mesoderm. This group of cells was discovered after the FHF and has been termed the Second Heart Field (SHF), and is originally situated medial to the cardiac crescent and then dorsal to the primitive heart tube.<sup>24</sup> A distinct gene expression profile is noted in these cells before gastrulation in the early embryo. Lineage tracing experiments have revealed SHF-derived structures and precursors marked with the Mef2C transcription factor driven by an anterior heart field specific enhancer element. Activity of this enhancer is detectable as early as the late primitive streak stage in a subset of cells, prior to gastrulation,<sup>16</sup> suggesting that the regional contributions to the heart are specified before the onset of cardiogenesis. These cells elongate the heart tube by migrating to its arterial and venous poles, progressively adding new myocardium and endocardium to the outflow and inflow tracts, respectively. Accordingly, the cardiac outflow tract is derived from the anterior SHF whereas, the cardiac inflow tract, which will become the atria of the heart, is posterior SHF-derived.<sup>15</sup>

Posterior SHF progenitors can be further segmented into right and left regions, forming the right and left atria, by early expression of *Pitx2c* confined to the left.<sup>25</sup> The longitudinal growth of this tube brought about by the addition of the SHF is crucial for proper looping of heart onto itself. The linear tube undergoes a rightward looping morphogenesis, with the addition of the proliferative SHF progenitors between embryonic days 8.25 and 10.5.<sup>24</sup> Along with *Mef2C* marking the anterior SHF, the expression of *Fgf8* and *Fgf10* is noted in these cells beginning at the crescent stage.<sup>26</sup> These growth factors are a pro-proliferative signal for these progenitors, contributing to proper cardiac looping leading to the formation of the primitive chambers of the heart. While expression of these factors is restricted more anteriorly, *Isl1* expression extends into the posterior SHF, and is critical for both venous and arterial pole development. In fact, *Isl1*-mutant mice have defects in the atria and great arteries of the heart.<sup>27</sup> Additionally, ablation of *Hand2* in the SHF using the *Isl1*-Cre transgenic mouse resulted in high levels of apoptosis in the pharyngeal mesoderm, suggesting that *Hand2* is required for the survival of undifferentiated cardiac progenitors prior to their migration to the heart tube.<sup>28</sup> At the time of looping, another pro-proliferative signal for the SHF comes from the pharyngeal endoderm via sonic hedgehog (*Shh*). *Shh* signaling promotes SHF proliferation, survival and regulates migration of these progenitors into SHF-derived structures such as the atrial septum and pulmonary trunk.<sup>29, 30</sup> The canonical WNT pathway as well as Notch signaling also promote proliferation of the SHF. The progressive addition of the SHF to the looping heart tube contributes to the formation of endocardial, myocardial and smooth muscle cells of the outflow tract (OFT), the prospective right ventricle (RV), the atria and the interventricular septum.<sup>31</sup>

### 1.2.3 Cardiac Looping and Endocardial Cushion Formation

Bilateral asymmetry in the early embryo is first established with the looping of the primitive heart tube. Left-right patterning differences of gene expression and cell polarity govern the asymmetric morphological formation of the heart.<sup>32, 33</sup> Proper looping in a rightward fashion, commencing at E8.25, is critical for correct orientations of the atria and ventricles, establishing a circulatory system for the growing fetus.<sup>14</sup> The dextral looping results in an helical shape with an inner curvature between the outflow and inflow tracts.<sup>34</sup> Analysis of this morphogenesis using high-resolution episcopic microscopy has rendered a 3D computer simulated model of this morphogenesis. Le Garrec *et al.* show that the heart tube grows dorsally while remaining anchored at both ends. The length of the tube increases by over 4-fold, while the distance between the poles is fixed, resulting in a looped heart.<sup>32</sup> The highly proliferative nature of the SHF, discussed in the previous section, accounts for this elongation. Looping is followed by formation of endocardial cushions within the OFT and atrioventricular canal (AVC) eventually leading to a four chambered heart.<sup>35</sup> These OFT cushions form in the conotruncal region between the ventricle and aortic sac; and AVC cushions develop in the transition zone between the primitive atria and ventricle, both arising from the endocardium via epithelial-to-mesenchymal transition (EMT). The endocardial cushions transform into cardiac valves and aid in the septation of the mature heart, but function to shunt blood in the developing heart.<sup>36</sup>

### 1.2.4 Chamber Formation and Septation

The heart chambers grow outward from the heart tube in a process known as ballooning beginning at E9.5. The cardiomyocytes on the outer curvature of the tube begin

to proliferate acquiring a distinct transcription profile that facilitates their growth<sup>22</sup> as well as differentiates them into the cardiac myocardium, with an increased conduction velocity.<sup>37</sup> Cells along the inner curvature and AVC remain as undifferentiated myoblasts, which express transcriptional repressors to prevent differentiation, and resemble nodal myocardium.<sup>37</sup> Concurrent with ballooning growth at proliferative zones along the ventricle loop forming the right and left ventricle, trabeculae develop at proliferative zones on the luminal myocardium by Notch, BMP10 and Neuregulin1 signals coming from the endocardium.<sup>38, 39</sup> The trabeculae function to increase surface area for oxygen uptake prior to the establishment of the coronary vasculature. The atrial and ventricular septa are formed between E9.5 and E14.5 in mice. Multiple primordia contribute to a central mesenchymal mass, including the mesenchyme on the leading edge of the primary atrial septum, the atrioventricular endocardial cushions, and the cap of mesenchyme on the spina vestibule.<sup>40</sup> The membranous, primary atrial septum descends from the roof of the atrial segment of the heart tube, reaching the AV cushion. This structure is completely SHF derived, driven by the transcriptional activity of Gata4, initiating proliferative and cell cycle gene expression, such as Cyclin D2 and Cyclin-dependent kinase 4.<sup>41</sup> The primary atrial septum does not fully fuse with the endocardial cushion, instead creating the foramen primum, which allows for blood flow between the right and left atria until its closure at E12.5. At this point the foramen secundum forms on the primary atrial septum through apoptosis.<sup>42</sup> While this is occurring, a muscular septum, known as the septum secundum, grows downward parallel to the primary septum. An opening, termed the foramen ovale, exists between these two septa and allows for shunting of blood between the atria during gestation as oxygenated blood is not received from the fetal pulmonary circulation.<sup>43</sup> Similar to the atrial septum, the

ventricular septum has membranous and muscular components, however, they are fused together as one structure. Formation of the intraventricular septum begins with the invagination of muscular myocardium at the apical component of the heart tube during chamber ballooning around E10.5.<sup>44</sup> The muscular septum grows between the common ventricular superiorly toward the AV cushions located at the base of the heart.<sup>44</sup> The majority of the muscular septum is derived from proliferation of cardiomyocytes as well as compaction of the trabeculae; however, the epicardium also contributes to progenitors via EMT to form this structure.<sup>45</sup> The muscular septum fuses with the membranous component of the intraventricular septum that originates from the AV cushion and grows downwards. Lineage tracing with the anterior heart field specific *Mef2c* indicates that the interventricular septum is almost entirely SHF-derived. Moreover, experiments knocking out *Tbx5* and *Hand2* in the SHF result in atrial septal defects (ASDs) and ventricular septal defects (VSDs), respectively.<sup>16,24</sup>

### 1.2.5 Ventricular Myocardium Development

Maturation of the newly formed cardiac chambers occurs concurrently with ventricular septation and continues into the later stages of embryonic development, muscularizing the ventricles to meet the increased cardiac output demands of the embryo. At the onset of heart development, at E8.0, the volume of the myocardium constituting the linear heart tube is approximately 0.0014 mm<sup>3</sup>; by E17.5 the volume of the myocardium reaches 2 mm<sup>3</sup>.<sup>22</sup> This myocardial growth is achieved by hyperplasia of cardiomyocytes, estimated to be 1 million cells at birth.<sup>22</sup> About 30% of the cells forming the mature ventricle wall are cardiomyocytes, the rest being endothelial cells, vascular smooth muscle cells, fibroblasts, immune and epicardial cells.<sup>46</sup> Primitive

cardiomyocytes are spherical and mononuclear and begin to mature at E13.5 when they elongate and assume a rod shape.<sup>33</sup> Many signaling pathways regulate cardiomyocyte proliferation and maturation, including Hippo signaling.<sup>47</sup> Proliferation and apoptosis during normal cardiac development will be explored in a following section. Formation of the mature myocardial architecture of the ventricle wall begins with trabeculation, followed by compaction and growth. Prior to the development of the compact myocardium, which is primarily governed by epicardial-derived signals, endocardial-derived factors lead to the onset of trabecular development at E9.0.<sup>48</sup> The interplay of Notch and neuregulin/ErbB signals from the endocardium leads to rapid growth at the proliferative centers along the ventricle wall, forming protrusions known as trabeculae.<sup>49</sup> Individual trabecular units are formed from endocardial projections into the lumen resulting from Notch1-induced ECM degradation and neuregulin-induced ECM synthesis and rearrangement by the myocardium.<sup>48</sup> Since these trabeculations are established prior to coronary circulation, the increased surface area to volume ratio they provide enables sufficient oxygen uptake and nutrient exchange, facilitating growth of the myocardium.<sup>51</sup> These sponge-like structures of cardiomyocytes are also important for ventricular septation and papillary muscle development.<sup>52</sup> As the embryo develops, the muscle layer gradually thickens to compensate for the increased physiological load by cardiomyocyte proliferation and trabecular compaction, driven by FGF signaling from the epicardium. This process is concurrent with development of the coronary vasculature, and the spaces formed between compacted trabeculae become capillaries. Abnormalities in the formation of a multilayered myocardium, seen in cases of genetic perturbations of Notch



signaling components, disrupts chamber development, resulting in a noncompacted cardiomyopathy or ventricular hypoplasia.<sup>53, 54</sup>

### 1.2.6 Outflow Tract Development

Concurrent with chamber development and maturation, the arterial pole of the heart tube undergoes several remodeling steps to form the aorta and pulmonary artery. Prior to looping, the outflow tube of the heart is comprised of SHF-derived myocardial cells with an inner lumen lined by endocardial cells. Collectively known as the outflow tract, both arteries begin as a common arterial trunk connected to the right ventricle after looping. The OFT endocardial cushions and myocardium are anterior SHF-derived,<sup>55</sup> and these proliferative progenitors connect the ventricle to the aortic sac. The OFT must reorient and septate in order to establish proper connection of the aorta with the left ventricle and the pulmonary artery with the right ventricle. This re-positioning and counterclockwise rotation is accomplished by an asymmetric addition of SHF progenitors to the future pulmonary artery and primitive right ventricle regions, in a process termed the “pulmonary push.” This allows the pulmonary trunk and orifice to achieve a higher and more anterior orientation compared to the aorta.<sup>56</sup> Septation of the OFT is accomplished by the contribution of the cardiac neural crest cells. These multi-potential cells are a part of the cranial neural crest region of the dorsal neural tube from which progenitors delaminate and migrate to various regions of the embryo at E9.0. In the heart, the addition of these cells helps to separate the OFT, form the semilunar valves, and add parasympathetic innervation.<sup>57, 58</sup> Fusion of the OFT cushions with input from the CNC result in the formation of the aortopulmonary septum, which is complete by E14.0.<sup>59</sup> Abnormalities in the convergence of SHF and CNCs cells, or the improper wedging of

the OFT can cause major defects such as double outlet right ventricle (DORV) and transposition of great arteries (TGA), which will be discussed in following sections.

### 1.2.7 Cardiac Valve Development

The interfaces between the heart chambers and OFT house specialized structures that maintain unidirectional blood flow during a cardiac cycle. The semilunar valves exist at the junction between the ventricles and the great arteries, whereas the AV valves connect the atria to the ventricles. Both sets are comprised of a combination of connective tissue and valvular interstitial cells.<sup>60</sup> Valvulogenesis begins with the formation of endocardial cushions in the OFT and AV canal, in response to BMP2 signals from the myocardium, around E9.0.<sup>61</sup> These localized swellings of cardiac jelly, containing endocardial-derived mesenchyme and ECM components such as collagen and hyaluronic acid, initially act as valves in the primitive heart tube as they control the flow of blood.<sup>62-64</sup> TGF-beta, Notch and the canonical Wnt signalling pathways control the proliferation and expansion of the mesenchyme.<sup>65</sup> Endocardial cells then undergo endocardial-to-mesenchymal transition (EndMT), migrating and proliferating into the cushion causing its elongation. These mesenchymal cells differentiate into valvular interstitial cells, which extensively remodel the ECM and sculpt the valves.<sup>63</sup> The valve leaflet becomes thin and elongated, with the ECM becoming stratified, rich in elastin, fibrillar collagen and proteoglycans.<sup>66</sup> The mitral and tricuspid AV valves are derived from the endocardial cushion and epicardium, while the aortic and pulmonary semilunar valves are formed from endocardial cushion and cardiac neural crest cells.<sup>16, 35, 63</sup> Genetic tracing experiments using the Wt1-Cre transgenic mouse confirm that epicardial-derived cells differentiate into fibroblasts and contribute specifically to the mural leaflets of the AV valves.<sup>67</sup> Conversely, lineage tracing using the Cx43-lacZ,

Wnt1-Cre and Krox20-Cre mouse lines show a CNC contribution to the interleaflet region and insertion zone of the semilunar valves.<sup>68</sup>

## 1.2.8 Transcriptional Regulators of Heart Development

Recently, single cell RNA-sequencing to map the transcriptome of the developing human heart revealed that cardiomyocytes can be partitioned into 4-chamber specific clusters based on differential gene expression signatures as early as 5 weeks into embryogenesis.<sup>69</sup> A number of conserved transcription factors govern the complex process of cardiac development. Transcription factors are DNA binding elements that regulate the expression of downstream target genes. Through the use of genetic knockout mice, several transcriptional factors have been identified to be critical in the development of various cardiac structures. Mutations in GATA-4, Nkx2.5 and Tbx5 and MEF2 are associated with CHDs in humans.<sup>70-73</sup> Specific spatiotemporal interaction and crosstalk between these factors are essential to control cardiogenic gene programs driving normal heart development.<sup>74</sup>

### 1.2.8.1 Nkx2.5

*Nkx2.5* (homeobox protein NKX2-5) is an early cardiomyocyte marker and regulator of heart morphogenesis and function, conserved from *Drosophila* to humans.<sup>75</sup> Its expression begins at the cardiac crescent stage in the FHF, SHF and adjacent endoderm, controlling migration and differentiation of cardiac precursors.<sup>76, 77</sup> In the SHF, Nkx2.5 functions to maintain the proliferative progenitor cell pool.<sup>16</sup> Loss of *Nkx2.5* results in impaired cardiac development, as decreased myocardial growth and trabeculation are noted.<sup>78</sup> Nkx2.5 null mice die between E9 and 10.5 due to an underdeveloped heart.<sup>79</sup> Specifically, mesodermal expression of Nkx2.5 is required for

cardiogenesis, as its germ-layer specific deletion resulted in cardiac defects identical to null embryos, whereas endodermal expression is dispensable for heart formation.<sup>80</sup> Thus, *Nkx2.5* mutant mice have a spectrum of CHDs, including atrial septal defect (ASD), ventricular septal defect (VSD), tetralogy of Fallot (TOF), transposition of the great arteries (TGA) and double outlet right ventricle (DORV).<sup>81</sup> *Nkx2.5* is also implicated in familial CHDs in the human population, where a similar variety of malformations results.<sup>77</sup> As *Nkx2.5* is a dosage-sensitive regulator of cardiac development, haploinsufficiency and inherited point mutations cause CHDs in humans.<sup>82, 83</sup> *Nkx2.5* directly associates with *Gata4* early on in heart development to specify cardiac mesoderm.<sup>73</sup>

### 1.2.8.2 *Gata4*

Three isoforms of the GATA family of zinc finger transcription factors are cardiomyocyte specific. Specifically, *Gata4* is a master regulator of cardiac progenitor cell proliferation and differentiation, implicated in various facets of heart development and function.<sup>84</sup> Beginning its expression at E7.5, a number of cardiac transcriptional targets have been identified for this factor. The expression of the cardiomyocyte contractility protein  $\alpha$ -MHC, the SHF specific *Mef2c* and the cell cycle regulator *Cyclin D2* are all controlled by *Gata4*.<sup>41, 85</sup> In fact, a conserved enhancer element upstream of the *Mef2c* gene has two consensus GATA sites bound by *Gata4*, thereby dictating early OFT and right ventricle development in the anterior heart field.<sup>85</sup> *Gata4* also plays a pivotal, dose-sensitive role in cardiac septation through its interactions with Hedgehog signaling in the SHF.<sup>41</sup> Loss of *Gata4* is embryonically lethal in mice by E8.5 as a deregulation in lateral-to-ventral and rostral-to-caudal folding prevents the cardiac crescent from fusing

at the midline.<sup>86</sup> In humans, defects in the atrial and ventricular septum at birth, and dilated cardiomyopathy later in life, have been attributed to mutations in Gata4. This gene is considered hyper-mutable as 110 different genetic mutations have been identified.<sup>87, 72</sup> Interestingly, in a case of familial CHDs due to a Gata4 missense mutation, the physical interaction between Gata4 and Tbx5 was interrupted.<sup>72</sup> It has since been established that both these factors synergistically cooperate to activate cardiogenic gene expression.<sup>88</sup>

### 1.2.8.3 Tbx5

Tbx5 (T-box 5) is another transcription factor expressed in early cardiogenesis, beginning around E8.0.<sup>89</sup> Although Tbx5 marks the left ventricular myocardium, its expression is dynamic and even present in a subpopulation of the SHF.<sup>16, 90</sup> As such, Tbx5 is involved in the formation of the interventricular septum, but also plays a major role in the development and maintenance of the cardiac electro-physiological conduction system by regulating the expression of connexin 40.<sup>91</sup> *Tbx5* mutations affect cardiac septation, inflow tract development and result in left ventricular hypoplasia; leading to an arrest of cardiogenesis in null mice by E10.5.<sup>70, 90</sup> Holt-Oram syndrome affects patients with dominant mutations in Tbx5 and is characterized by septal and conduction defects in the heart, along with impaired anterior forelimb development.<sup>90, 92</sup> This factor not only activates cardiogenic genes, but also functions to repress transcription of incompatible gene programs by interacting with the nucleosome remodeling deacetylase complex (NuRD).<sup>93</sup> Tbx5 also interacts physically with Mef2c early on in heart development, leading to the activation of  $\alpha$ -cardiac myosin heavy chain, critical for cardiomyocyte differentiation.<sup>94</sup>

#### 1.2.8.4 Mef2C

Finally, *Mef2C* is a transcription factor expressed in the SHF precursors adjacent to the cardiac crescent and continues to the OFT and right ventricle of the mature heart from E7.5 to E11.5.<sup>95</sup> It is specified to the anterior SHF through independent enhancer elements, and controls myocyte differentiation.<sup>85</sup> The monocyte enhancer factor 2 (MEF2) family regulates muscle-specific genes, and *Mef2C* is essential for sarcomere contractile element expression, like  $\alpha$ -actin.<sup>96</sup> Absence of *Mef2C* results in a cardiac looping impairment, lack of a right ventricle and is embryonic lethal between E9.5 and E10.5.<sup>96, 97</sup> This germline knockout phenotype is recapitulated by deletion of *Mef2c* in early cardiac tissue using the *Nkx2.5-cre* transgenic mouse. However, deletion using the endothelial-specific *Etv2-cre* line results in viable offspring with no CHDs, suggesting that this factor is dispensable for endothelial progenitors, but is required for all myocardial cells.<sup>98</sup> Other SHF exclusive genes that distinguish this group of progenitors from the FHF include the growth factors *Fgf8* and *Fgf10* as well as the transcription factors *Tbx1* and *Isl1*.<sup>24</sup>

#### 1.2.9 Proliferation and Apoptosis in Cardiogenesis

Proliferation and apoptosis are key features of normal organ development. The adult heart is generally considered to be post-mitotic, as mouse cardiomyocytes lose their regenerative capacity after P7; unable to undergo cell division and instead increase in cell volume. The embryonic heart, however, depends on high amounts of proliferation. Multipotent cardiac progenitor cells of the FHF and SHF undergo proliferation followed by differentiation into cardiomyocytes, which in turn undergo further clonal expansion.<sup>50</sup> Specific regions of the heart tube undergo preferential proliferation resulting in chamber

ballooning, forming the left ventricle at E8.5.<sup>99</sup> The highest proliferation rates are observed at the base of the ventricles at E11, after which the increase in cardiomyocyte number declines.<sup>100</sup> Notch signaling, at the base of the trabecules, lining the ventricle wall, induces high rates of proliferation among less differentiated cardiomyocytes, resulting in trabecular elongation.<sup>39, 53</sup> Furthermore, mesodermal cells of the SHF are also highly proliferative, elongating the primitive heart tube and resulting in its rightward looping. These progenitors remain proliferative much after the FHF, and their capacity is mediated by canonical Wnt signaling.<sup>100, 101</sup>  $\beta$ -catenin was found to be essential for expansion of SHF cardiac progenitors through deletion of this Wnt pathway component using the *Isl1-cre* mouse line.<sup>101</sup> In addition, epicardial-derived growth factors induce myocardial proliferation, contributing to the expansion of the compact myocardium. These ligands include members of the Fgf, Igf and Wnt families (eg. Fgf-9, Igf-2 and Wnt9B), as well as retinoic acid, promoting proliferation of the myocardium.<sup>102-104</sup> The hippo kinase cascade also dictates embryonic cardiomyocyte proliferation. In fact, ablation of *Yap1*, the nuclear target of the hippo pathway, in vascular SMCs of the embryonic heart suppressed their expansion and enhanced expression of cell cycle arrest genes, leading to cardiac defects associated with decreased proliferation such as DORV and ventricle wall hypoplasia.<sup>105</sup> Deletion of *Yap1* in fetal cardiomyocytes is embryonic lethal by E16.5 due to decreased ventricle chamber size and cardiac hypoplasia, resulting in pericardial effusion and heart failure.<sup>106</sup> Conversely, overexpression of *Yap1* in cardiomyocytes increases heart size through elevated proliferation.<sup>106</sup> Furthermore, *Rac1*, a Rho GTPase and regulator of cellular structure, is required for anterior SHF progenitor cell proliferation and organization of the splanchnic mesoderm. Loss of *Rac1* signaling

decreases the proliferation rate of SHF progenitors, subsequently resulting in OFT and cardiac valve anomalies.<sup>107</sup> Finally, nitric oxide is intimately linked to cardiomyocyte proliferation. Postnatal eNOS knockout cardiomyocytes have lower levels of BrdU incorporation and fewer cells in culture compared to WT.<sup>108</sup> This decrease in proliferation is mediated in part by an increased TIMP-3 expression, as treatment with an anti-TIMP3 antibody increased proliferation of eNOS<sup>-/-</sup> cardiomyocytes.<sup>109</sup> In the embryonic heart eNOS deficiency decreased proliferation and growth of epicardial cells, by decreasing activity of cGMP-dependent protein kinase G signaling, thereby downregulating Gata4 and cardiac growth factor expression.<sup>110</sup> Along with promoting proliferation in the embryonic heart, nitric oxide promotes survival by protecting cardiac progenitors against apoptosis.<sup>110</sup>

Apoptosis, or programmed cell death, is an intricately regulated process involving cellular disintegration by cell shrinkage, cytoskeletal breakdown and DNA fragmentation, and is a normal part of an organism's development and life cycle. It is initiated and executed by the caspase family of proteinases, which systematically cleave proteins leading to blebbing and cell death.<sup>111</sup> This process is an integral part of embryonic development as it aids in the proper integration of cells into tissues, shaping the structure of an organ.<sup>112</sup> During cardiogenesis, apoptosis acts as a differentiation mechanism by inducing changes to nearby cells, contributing to the development of the OFT, cardiac valves, coronary vasculature and conduction system.<sup>113, 114</sup> Significant levels of apoptosis have been identified in the mesenchyme of the AV cushions, the trabeculae and compact zones of the ventricles, and the OFT.<sup>115</sup> Specifically, the cardiomyocytes of the OFT undergo apoptosis to facilitate shortening and rotation of the



myocardial conus, allowing for proper connection between the right ventricle and pulmonary artery.<sup>116</sup> In addition, high levels of programmed cell death have been observed in the CNCs, which may be involved in the process of myocardialization of the OFT.<sup>55</sup> Changes to the microenvironment induced by apoptosis of CNCs in the OFT cushion is thought to signal differentiation of the mesenchyme into myocardium.<sup>117</sup> Whole embryo knockout of FADD, the Fas-associated death domain protein, involved in the extrinsic pathway of programmed cell death, is lethal by E11.5 with a dilated cardiac phenotype. Similarly, mice with a deletion of the caspase-8 gene die in utero by E12.5 due to impaired cardiac muscle development leading to heart failure and edema.<sup>118</sup> Consistent with the proliferation defects, eNOS<sup>-/-</sup> hearts displayed elevated levels of cardiomyocyte apoptosis and myocardial cleaved caspase-3 at E12.5 and E15.5, compared to controls. Atrial and ventricular septal defects were found at a higher incidence in neonatal eNOS knockout hearts, in which increased apoptosis was maintained.<sup>119</sup> Interestingly, in neonatal cardiomyocytes, iNOS-derived nitric oxide production mediates the apoptotic effects of TNF- $\alpha$  stimulation.<sup>120</sup> Moreover, in cultured H9C2 myocytes, transduction of microRNA-122 increased caspase-3 activity and cell death.<sup>121</sup>

### 1.2.10 Fetal Cardiovascular Physiology

Circulation in the fetus shifts after birth as it becomes independent from the maternal circulation. Normally, in the postpartum heart, deoxygenated blood enters the right atrium from the venous inflow of the superior and inferior vena cavae. This blood fills the right ventricle which subsequently contracts and pumps venous blood to the pulmonary circulation through the pulmonary artery. Gas exchange occurs in the lungs,

and oxygenated blood returns back to the heart via the pulmonary veins, entering the left atrium. Once the left ventricle fills, oxygenated blood is pumped into the aorta and travels through the systemic circulation, allowing arteries and arterioles to perfuse tissues of the body.<sup>122</sup> In contrast, since the lungs are not functional in the fetus, gas exchange occurs via the placenta. Therefore, the fetal heart has structural adaptations, known as shunts, to facilitate blood flow throughout development.<sup>122</sup> The ductus arteriosus connects the pulmonary artery to the aorta. Oxygenated blood from the placenta flows into the inferior vena cava via the umbilical veins. This blood is pumped by the right ventricle, but, in this case, is shunted by the ductus arteriosus into the dorsal aorta because of the high-pressure resistance of the pulmonary artery. This shunt remains open throughout fetal development due to the high oxygen tension and prostaglandin secretion from the placenta.<sup>122</sup> Another feature of the fetal heart is the foramen ovale, which shunts oxygenated blood from the right to the left atria, following a pressure gradient. At birth, as the newborn's lungs inflate with air, the resistance in the pulmonary veins will decrease allowing for blood flow through the pulmonary circulation. This is followed by a closure of the foramen ovale by the septum secundum because of increased pressure in the left atrium.<sup>122</sup> Finally, hours to days after birth, the decline in prostaglandin levels in the newborn will cause the ductus arteriosus to close, completing the separation of pulmonary and systemic circulatory systems.<sup>123</sup>

### 1.3 Coronary Artery Development

The development of the coronary vasculature is distinct from the formation of the myocardium these vessels feed (Figure 1.1). Angiogenesis in the primitive heart begins at E9.5 in the proepicardial organ (PEO). The PEO is a transient structure adjacent to the

developing heart tube, located at the pericardial surface of the septum transversum close to the sinus venosus.<sup>124, 125</sup> It contains a heterogenous population of mesothelial cells expressing Wt1 and Tbx18, destined to migrate to the heart.<sup>126, 127</sup> Cells originating in the PEO migrate and proliferate to cover the surface of myocardium, forming an epicardium (Figure 1.1).<sup>16</sup> By E12.5 this epicardial layer is fully formed.<sup>124</sup> A subset of these epithelial cells undergo epithelial-to-mesenchymal transition (EMT) and become epicardial-derived cells (EPDCs).<sup>125</sup> These EPDCs migrate to the subepicardial space and myocardium where they differentiate into vascular smooth muscle cells, adventitial fibroblasts and endothelial cells (Figure 1.1).<sup>36</sup> These mesenchymal cells migrate throughout the developing myocardium and produce much of the coronary vasculature through a vasculogenic process. This immature vascular plexus initially develops without blood flow. The proximal ends of the coronary arteries connect to the ascending aorta through coronary orifices at the level of the left and right sinuses of the semilunar valves, initiating perfusion. This invasion occurs at the time of cardiac septation, following separation of the aorticopulmonary trunk, and involves apoptosis.<sup>128</sup> The establishment of blood flow is needed for subsequent remodelling and maturation of the vessels. Coronary veins connect to the right atrium via the coronary sinus.<sup>124, 125</sup> Other sources of coronary artery progenitors include the sinus venosus and the endocardium (Figure 1.1).<sup>36</sup> Similar to heart development, a complete coronary network is established by E15. Congenital abnormalities of the coronary arteries can impact heart function and are associated with coronary arteries diseases in adulthood.<sup>125, 129</sup>

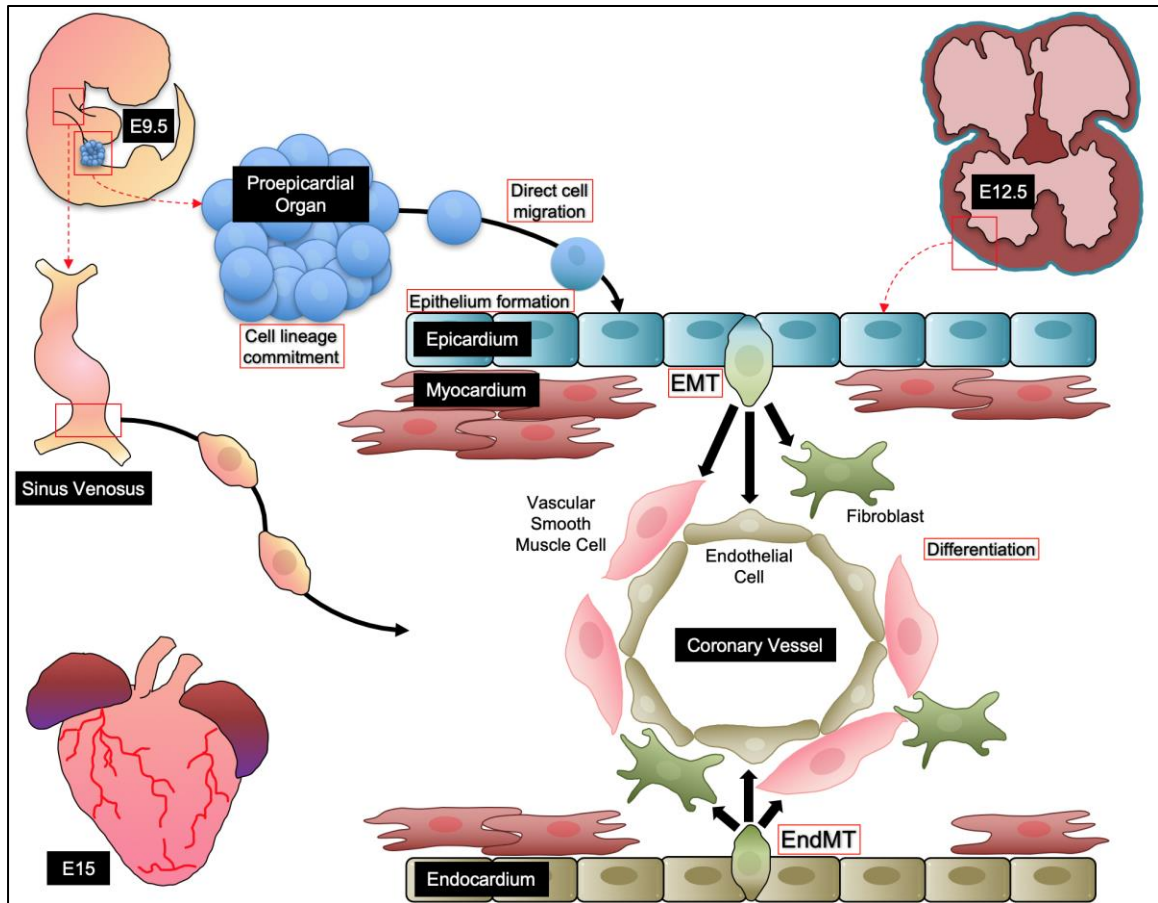


**Figure 1.1. Embryonic coronary artery development in the mouse.**

Coronary vessels arise from progenitors originating from three distinct sources, the proepicardial organ (PEO), sinus venosus and endocardium. Formation of these arteries involved epithelial-to-mesenchymal transition (EMT) followed by differentiation and growth. By E15 a fully formed vascular plexus supplies oxygen and nutrients to the heart. E: Embryonic Day, EMT: Epithelial-to-Mesenchymal Transition, EndMT: Endocardial-to-Mesenchymal Transition

### 1.3.1 Epithelial-to-Mesenchymal Transition

EMT is a transdifferentiation process of epithelial cells into motile mesenchymal cells by way of transcriptional reprogramming.<sup>130</sup> Cell polarity defines epithelial cells as they have luminal and basilar domains, connected to one another by adherence junctions, tight junctions, gap junctions and desmosomes. Delamination into a migratory cell type involves loss of this polarity, a dismantling of cell-to-cell connections and cytoskeletal rearrangement, all mediated via activating mesenchymal gene programs and repressing epithelial signatures. This switch in phenotype is carried out by local upregulations of EMT ligands and factors, as well as molecular signalling cascades initiated by receptor binding. In the cardiovascular system, transforming growth factor beta (TGF- $\beta$ ) and bFGF signalling induces the breakdown of the basement membrane, reorganizes actin filaments and allows for cell movement.<sup>36</sup> In addition, TGF- $\beta$  binding results in the upregulation of the transcription factors Snail and Slug, which further promote cell motility and repress epithelial genes, such as Cdh1 (E-cadherin).<sup>131</sup> A hallmark of EMT induction is cleavage and endocytosis of E-cadherin, a transmembrane protein that forms cell junction in the epithelium.<sup>132</sup> This is followed by the expression of N-cadherin, a mesenchymal protein, and together is known as the “cadherin switch.”<sup>130</sup> Furthermore, cell motility is enabled by actin reorganization and polymerization in the direction of migration, along with a degradation of ECM.<sup>133</sup> Following EMT and migration to the destination, the cells can re-differentiate into other cell types.

### 1.3.2 Transcriptional Regulators of Coronary Artery Development

Many transcription factors including Gata-4, Fog2, Wt1, VCAM-1 and  $\alpha$ -4 integrin play critical roles in the development of coronary arteries.<sup>134, 135</sup> The disruption of many

mediators of EMT have been implicated in the pathogenesis of coronary artery anomalies. For instance, the master regulator of EMT in the embryonic heart, Wt1, is required for coronary artery development and is indispensable for epicardial EMT.<sup>136</sup> Wt1 is a DNA binding protein, which directly regulates the expression of other mediators of EMT, such as Snail and Cdh1 (E-cadherin).<sup>137</sup> Mutation of Wt1 in the epicardium is embryonic lethal between E16.5 and E18.5 due to cardiovascular defects.<sup>137</sup> Additionally, Wt1 binds to the Raldh2 promoter in epicardial cells, thereby controlling retinoic acid signaling, essential for EPDC formation.<sup>138</sup> In fact, epicardium-specific mutation of the retinoic acid receptor reduced  $\beta$ -catenin and FGF2 expression, resulting in abnormal arterial branching in the embryonic heart.<sup>138</sup> In addition, genetic deletion of Gata-4 in mice impairs migration and EMT resulting in the absence of coronary arteries.<sup>125, 139, 140</sup> Coronary artery defects are also noted in Tbx18 knockout (Tbx18<sup>-/-</sup>) mouse models, as Tbx18 is a transcription factor highly expressed in the PEO, controlling early artery development. Moreover, coronary arteriogenesis is also dependent on  $\beta$ -catenin signaling, as ablation of this factor in the epicardium impaired epicardial expansion, invasion and differentiation; while specific deletion in the PEO was embryonic lethal.<sup>141</sup>

## 1.4 microRNA Regulation of Cardiovascular Development

MicroRNAs (miRNAs) are a class of endogenous, short (20-26 nucleotide), non-coding RNA molecules that post-transcriptionally regulate gene expression by degrading messenger RNA (mRNA) molecules or repressing their translation.<sup>142</sup> A single miRNA molecule does not require perfect sequence complementarity to bind the 3' untranslated region (UTR) of a target mRNA.<sup>142</sup> This means that one microRNA can target and modulate the expression of many mRNAs, and a particular mRNA molecule can be

controlled by many different miRNAs. The human genome encodes over 2000 miRNAs and it's predicted that one-third of all protein-coding genes are regulated by at least one miRNA.<sup>143</sup> Specifically, the human heart expresses over 700 miRNAs, which, in turn, fine tune the expression of 30% of the heart's protein coding genes.<sup>8</sup> In developmental biology, miRNAs act as molecular coordinators of gene expression, switching on and off transcription factors, activators and repressors, in complex regulatory circuits.<sup>144</sup> Regulation through miRNA suppression of gene expression has been shown to be vital for heart development.<sup>145</sup>

#### 1.4.1 microRNA Biogenesis, Structure and Function

miRNAs are transcribed in the nucleus by RNA Polymerase II or III.<sup>146</sup> They can reside in coding and non-coding regions of the genome and can be the result of alternative splicing. Expression of miRNAs is controlled in a cell-type specific manner by transcription factors, thereby creating unique expression profiles for each organ. Transcription results in a double-stranded RNA hairpin molecule with a 5' polyadenyl cap, known as a primary-miRNA (Figure 1.2).<sup>146</sup> About 40% of human miRNAs are transcribed together as clusters containing upwards of 8 distinct miRNA sequences.<sup>147</sup> Micro-processing and cleavage of this primary-miRNA by the nuclear Drosha enzyme-complex (an RNaseIII-type nuclease) and , DiGeorge syndrome critical region 8 protein (DGCR8) forms the ~70-nucleotide-long precursor-miRNA (pre-miRNA) molecule, which is transported to the cytosol via the Ran-GTP-dependent nuclear transport receptor Exportin5.<sup>148</sup> In the cytosol, the ribonuclease Dicer and transactivator RNA-binding proteins (TRBP) cleave the precursor-miRNA hairpin loop resulting in a short, ~22 nucleotide miRNA duplex of complementary strands.<sup>149</sup> The thermodynamically less

stable RNA strand is loaded into the RNA-induced silencing complex (RISC) and functions as the guide strand to mediate miRNA-RISC interactions (Figure 1.2).<sup>142-150</sup> The RISC loading complex is composed of Dicer, TRBPs, protein activator of PKR and Argonaute-2 (Ago2), the latter of which is the RISC effector protein mediating mRNA destabilization, decay or translational inhibition (Figure 1.2).<sup>151</sup> Specifically, the seed region of the mature miRNA, which usually spans from nucleotide 2 to 7 at the 5' end of the miRNA, participates in complementary base pairing at the 3' UTR of target mRNAs for mRNA repression.<sup>152</sup> Consequently, miRNAs are highly conserved between species, therefore having the same mRNA targets. Bioinformatic algorithms can predict the mRNA targets of different miRNAs.<sup>147</sup>



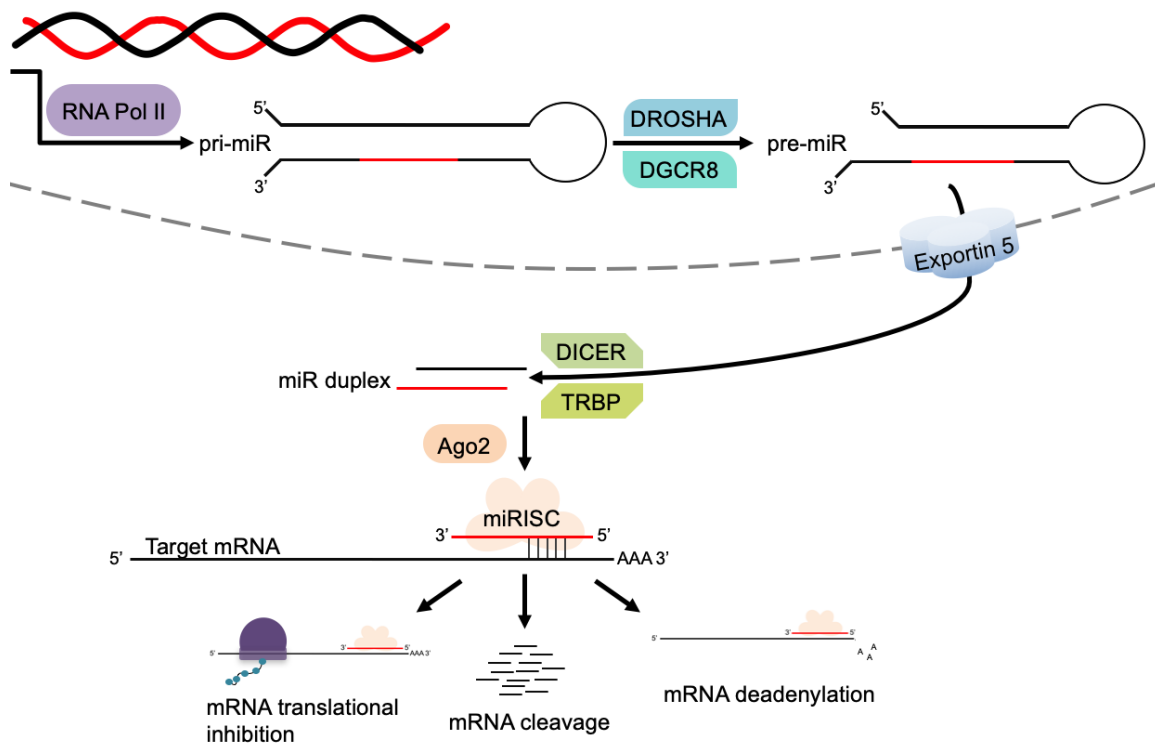


**Figure 1.2. microRNA biosynthesis and function.**

microRNAs are transcribed in the nucleus as a long precursor transcript with a hairpin loop, known as the primary microRNA (pri-miR). Processing steps occur in the nucleus by the enzymes DROSHA and DGCR8 to produce a shorter precursor miRNA (pre-miR), which is exported into the cytosol by Exportin 5. In the cytosol the precursor miRNA associated with the DICER, TRBP and Ago2 enzyme complex. The mature miRNA is loaded into the RNA-induced silencing complex (RISC) where it can execute its function and inhibit target mRNA expression via complementary binding to 3' UTRs. This leads to target mRNA translational inhibition, cleavage or destabilization.

## 1.4.2 microRNA in Cardiogenesis

In normal cardiogenesis, miRNAs control the expression of many critical genes involved in proliferation and differentiation, and play roles in regulating the stages of heart development.<sup>153</sup> The importance of miRNAs in heart development is illustrated in early cardiac progenitor-specific deletions of Dicer. Ablation of Dicer using Cre-recombinase under the control of the endogenous Nkx2.5 promoter in mice, is embryonic lethal due to cardiac failure by E12.5.<sup>154</sup> Deletion of Dicer in the CNC using the Wnt1-Cre transgenic mouse resulted in profound craniofacial defects and major CHDs, including VSD and DORV, stemming from impaired migration and patterning of this lineage.<sup>155</sup> Similarly, using the Gata5-Cre to conditionally knockout Dicer in the PEO and epicardium in mice led to complete mortality immediately after birth due to severe coronary vessel malformations stemming from impairments in EMT.<sup>156</sup> In addition, vascular smooth muscle-specific Dicer knockout, with the SM22 $\alpha$ -Cre, resulted in mutant mice having hypoplastic coronary arteries and diminished cardiac contractility, with embryonic lethality around E16.5.<sup>157</sup> These studies highlight the broad necessity of miRNAs for proper cardiac development as Dicer is required for their processing and function. Gain and loss-of-function experiments looking at specific miRNA families delineate the pivotal roles of particular miRNAs in cardiogenesis. In organ development, many miRNAs regulate the cell cycle and direct proliferation.<sup>158</sup> For instance, overexpression of miR-195 under control of the  $\beta$ -myosin heavy chain promoter in the embryonic heart results in VSD and ventricular hypoplasia in mice due to premature cell cycle arrest.<sup>159</sup> The same CHDs were seen when miR-133a is overexpressed by the  $\beta$ -myosin heavy chain promoter, along with reduced cardiac function and left ventricular

dysfunction.<sup>160</sup> Using the same promoter to overexpress miR-1-2 in mice, embryonic lethality occurs at E13.5 due to heart failure from ventricular hypoplasia, which is consistent with a significant decrease in proliferating cells and insufficient muscle mass.<sup>154</sup> Interestingly, deletion of miR-1-2 also results in an abnormal cardiac phenotype and 50% embryonic lethality. miR-1-2<sup>-/-</sup> mice have decreased heart rate, prolonged ventricular depolarization and VSDs.<sup>161</sup> These mice have greater heart-weight to body-weight ratios and larger ventricular cardiomyocytes. Combined deletion of the miR-133a-1-2 complex results in VSDs and is embryonic lethal in half of all double mutants. miR-1-2 modulates expression of genes involved in cell cycle progression and karyokinesis, but also downregulates Hand2 by targeting its 3'UTR.<sup>161</sup> Hand2 is a cardiogenic transcription factor, needed for cardiomyocyte expansion and proliferation.<sup>162</sup> Thus, the close regulation of Hand2 expression by miR-1-2 is vital for normal heart development. Taken together, the gain and loss-of-function studies on miR-1-2 exemplify the critical role miRNAs play in fine-tuning gene expression in the embryonic heart. Notably, studies on human congenital heart disease have revealed that some CHDs are associated with altered miRNA expression. miRNA profiling of human fetal single ventricle malformation identified 48 differentially expressed miRNAs in the heart, many of which target genes involved in cardiac development.<sup>163</sup> Moreover, in patients with Down Syndrome (Trisomy 21) who also presented with CHDs, 5 miRNAs (miR-99a, let-7c, miR-125b-2, miR-155 and miR-802) located on chromosome 21 were preferentially overexpressed in the heart.<sup>164</sup> Finally, case studies on infants with non-syndromic TOF revealed 61 miRNAs significantly altered in expression in the myocardium compared to normal subjects.<sup>165</sup> These animal models and clinical studies display the fundamental role

of miRNAs in fetal cardiovascular development, and the consequences of their dysregulation.

### 1.4.3 microRNA-122 a novel player in CHD pathogenesis

MiRNA-122 is a conserved, 22 nucleotide miRNA molecule that plays a critical role in liver development and homeostasis.<sup>166</sup> MiRNA-122 is encoded on human and mouse chromosome 18 and generates a ~4.5 kilobase primary-miR, which is processed to a 66 nucleotide pre-miR-122. The gene expression of miR-122 is regulated by circadian rhythms; however, miR-122 has a >24-hour half-life which maintains its constant levels.<sup>167</sup> The cytoplasmic poly(A) polymerase, GLD2, contributes to this stability by adding an adenosine tail to the mature transcript.<sup>168</sup> It is highly expressed in the adult liver, where it serves as a key regulator of cholesterol and fatty-acid metabolism, as well as blood alkaline phosphatase levels.<sup>166, 169</sup> In fact, just prior to birth, miR-122 copy numbers reach maximal levels (~50000 per cell) in the liver.<sup>170</sup> Mir-122 is also an important host factor for hepatitis C virus (HCV) replication as it binds to the 5' UTR of the viral genome, promoting HCV stability and accumulation, while protecting the RNA genome from degradation.<sup>171, 172</sup> In addition, miRNA-122 is regarded as a potent tumor suppressor. Liver-specific knockout of miR-122 results in hepatobiliary cysts leading to hepatocellular carcinoma (HCC).<sup>173</sup> MiR-122 is repressed in primary tumors in HCC patients, and its decreased levels are associated with poor prognosis and acquisition of an invasive, metastatic phenotype.<sup>174</sup> Interestingly, it has been shown *in vitro* that miRNA-122 inhibits the angiogenic potential of endothelial cells. Transfection of miRNA-122 to human dermal microvascular endothelial cells reduced their proliferation, motility, and ability to form interconnected tubes.<sup>175</sup> Correspondingly, it has been reported that

miRNA-122 is downregulated in many human cancers, which correlates with an increase in metastasis and EMT.<sup>174, 176-182</sup> In addition, miR-122 inhibition of the Wnt signaling pathways was confirmed by a dual luciferase reporter assay, showing its targeting of  $\beta$ -catenin.<sup>183</sup>

The molecular processes involved in cancer and angiogenesis are also critical components of cardiac development. Therefore, cardiac expression of miRNA-122 during embryogenesis could have deleterious effects by suppressing proliferation and EMT. Recently, however, studies have shown the presence of miRNA-122 in the adult heart following injury. In fact, miRNA-122 is regarded as a novel biomarker for cardiomyopathies. Elevated plasma levels of miRNA-122 are present in patients following myocardial infarction (MI),<sup>184</sup> and in patients with coronary artery disease,<sup>185</sup> with levels increasing linearly with the severity of atherosclerotic lesions.<sup>186</sup> In fact, plasma levels of miR-122 are also acutely increased in patients following cardiac arrest.<sup>187</sup> This elevation is noted in rat models of cardiac injury, as miRNA-122 is not only increased post-infarction in heart tissue, but also directly contributes to the apoptosis of cardiomyocytes.<sup>188</sup> Thus, along with the established roles of miRNA-122 in the liver and as a tumor suppressor, emerging evidence supports its involvement in cardiac pathophysiology, as a biomarker and possible contributor, which provides support for investigating this molecule in maladaptive cardiac development.

#### 1.4.3.1 microRNA Silencing *in vivo*: antimiR-122

In addition to having clinical value as a diagnostic marker, miRNA-122 is currently being tested as a therapeutic target in patients with chronic hepatitis C virus (HCV) infection.<sup>166, 189, 190</sup> MiRNA-122 specifically binds to two distinct sites in the 5'

non-coding region of the HCV genome and upregulates viral RNA levels, thereby facilitating viral replication.<sup>191, 192</sup> Therefore, targeting miRNA-122 presents an avenue for anti-viral intervention. AntimiRNAs are chemically modified antisense oligonucleotides that are designed to bind endogenous miRNAs with high affinity and decrease their expression levels. Accordingly, to combat HCV infection, clinicians utilize a locked nucleic acid (LNA) modulation of anti-miRNA-122 (Miravirsen, SPC3649), resistant to nuclease degradation *in vivo*.<sup>190, 193</sup> Miravirsen has sequence complementarity to human mature miRNA-122 allowing perfect hybridization, thereby blocking its interaction with the viral RNA genome. Moreover, Miravirsen has sequence complementarity with primary and precursor miRNA transcripts, and inhibits miRNA-122 biogenesis.<sup>189</sup> Currently in clinical trials, Miravirsen administration to patients with chronic hepatitis C infections results in a dose-dependent and prolonged reduction in plasma HCV RNA, without affecting the levels of other miRNAs.<sup>190</sup>

## 1.5 Congenital Heart Disease

CHDs arise from perturbations in complex cellular and molecular processes underlying embryonic heart development. Thus, because of the intricate nature of cardiac development, a misstep in the orchestration could lead to abnormalities. Alterations in cardiogenic gene expression, cell migration or proliferation can have implications for heart structure, and can result in CHDs. Congenital malformations of the heart are the most common birth defect, accounting for 1-5% of live births.<sup>194, 195</sup> Congenital heart disease is the leading cause of pediatric deaths in developed nations.<sup>196, 197</sup> Some congenital defects can go unnoticed at birth; however, as the child matures and is involved in increasing amounts of physical activity, the congenital malformations can

manifest themselves. A spectrum of congenital heart defects exist that span from minor anomalies such as an atrial septal defect (ASD) to major malformations including transposition of the great arteries (TGA).<sup>198</sup> Septal defects are holes in the ventricular or atrial septum, leading to a mixing of de-oxygenated and oxygenated blood. CHDs also affect sites distant to the actual myocardium such as the descending aorta, which can be narrowed resulting in coarctation. OFT defects such as persistent truncus arteriosus (PTA), and malformations in the valves of the heart contribute to the spectrum of defects of congenital heart disease and are a result of improper cardiogenesis. These defects compromise the function of the cardiovascular system as the ability of the heart to perfuse all tissues of the body with oxygenated blood is decreased. For instance, the inability of the endocardial cushions to complete the process of septation could result in a ventricular septal defect (VSD), which would allow for mixing of oxygenated and deoxygenated blood from the systemic and pulmonary circulations resulting in a decreased functional cardiac output. Congenital malformations can follow a pattern of incidence where multiple CHDs are present in the same heart. Tetralogy of Fallot (TOF) is an example of this phenomenon and is composed of a VSD, pulmonary stenosis, right ventricular hypertrophy and an overriding aorta.<sup>199, 200</sup> Genetic and environmental factors are associated with CHDs. Mutations causing cardiac abnormalities can either be sporadic or familial.<sup>77</sup> Teratogen exposure during gestation, such as polychlorinated biphenyls and pesticides, have been linked to CHDs, along with maternal alcohol consumption, smoking, anti-seizure medications and rubella infection.<sup>77</sup> Surgical procedures to correct congenital malformations of the heart do not always have high efficacy.<sup>201</sup> Individuals with CHDs commonly require multiple operations and drug

therapy, and are at an elevated risk for arrhythmias, bacterial endocarditis and heart failure, placing a large burden on the health care system.<sup>202</sup> Patients often have extra-cardiac co-morbidities, such as neurological deficits, which affect quality of life.<sup>203</sup> The prevalence of neurodevelopmental disabilities in the population of patients with CHDs ranges from 10% to over 50% depending on the severity of the lesion and whether pediatric surgery was required.<sup>204</sup> The spectrum of these abnormalities includes intellectual disability, autism spectrum disorder, and deficits in language, motor and social skills.<sup>205</sup> In fact, attention deficit hyperactivity disorder is 3 to 4 times more prevalent in children with a CHD.<sup>206</sup> Currently, an estimated 96,000 Canadian adults are living with a CHD,<sup>207</sup> making this disease a major cause of mortality and morbidity for both adults and infants. Therefore, it is vital that research be conducted into how and why these malformations develop, and more significantly, what remedies during pregnancy can prevent their occurrence.

### 1.5.1 Types of Congenital Heart Defects

The International Classification of Diseases (ICD-10) classifies 25 distinct types of anatomical or hemodynamic CHDs; however, due to varying nomenclature and the wide variety of cardiac lesions, some variation may exist.<sup>3</sup> CHDs can be categorized based on severity of the morphological lesions and functional consequences. Conventionally, CHDs are grouped into three categories: mild, moderate and severe. The majority of CHD cases can be considered mild. The cardiac defects in these patients would be largely asymptomatic, often undergoing spontaneous resolution.<sup>208</sup> Moderate CHDs are more complex and require expert care, but are less intensive than the severe cases. Severe CHDs include univentricular hearts, heterotaxy, conotruncal defects, and



atrioventricular canal defects, affecting one third of all patients with cardiac anomalies.<sup>209</sup> Expert cardiologic care and intervention are required for these patients in the first year of life. Accordingly, survival rate is dependent on the severity of the disease. This rate is estimated to be 98% for patients with a mild CHD, whereas only 56% for patients with a severe CHD.<sup>210</sup> CHD-related hospitalizations in the US have steadily risen with a financial burden of \$6.1 billion per annum.<sup>211</sup>

### 1.5.1.1 Septal Defects

Septal defects are the most common cardiac malformations in humans.<sup>71</sup> These manifest as hemodynamically significant shunts between the left and right chambers of the heart. ASDs involve a connection between the left and right atria, reducing heart function. These defects are considered mild lesions and are not cyanotic as the high pressure in the left atrium will cause oxygenated blood to partly shunt into the right atrium. There are three major types of ASDs: defects of the ostium primum, secundum or a common atrium, where the atrial septum is lacking completely.<sup>45</sup> Ostium primum defects are less common but more severe, and stem from incomplete growth of the primary atrial septum at the level of the inferior margin due to partial development of the endocardial cushions.<sup>212</sup> In comparison, ostium secundum defects arise from a failure in the proper formation of the primary or secondary atrial septum. The incidence of ASDs among patients with CHDs is approximately 11%, whereas the incidence of VSDs is upwards of 30%.<sup>45, 77</sup> VSDs are the most common congenital anomaly in children and the second most prevalent abnormality in adults.<sup>213</sup> Two types of VSDs exist, which differ in anatomic location and histologic variation, allow for shunting of blood between the left and right ventricle, and are functionally more severe than ASDs. A membranous VSD occurs more frequently, and is

usually a small shunt between the ventricles underneath the OFT, which is encircled by fibrous tissue. In contrast, muscular VSDs involve a shunt enclosed by a muscular border.<sup>45</sup> Accordingly, an open connection between all four chambers of the heart is considered an AVSD. The incidence of AVSD can be as high as 15% in patients with Down Syndrome.<sup>214</sup>

### 1.5.1.2 Outflow Tract Defects

OFT defects manifest in the aorta and/or pulmonary artery and result in a reduction of the functional cardiac output. Similar to septal defects, these malformations also involve a mixing of the systemic and pulmonary circulatory systems. A persistent truncus arteriosus, also referred to as a common arterial trunk (CAT), occurs as a result of improper development of the aortopulmonary septum, resulting in a shunt between both arteries. This defect is always accompanied by a subarterial VSD.<sup>45</sup> Mutations in the Pax3 or Semaphorin3 gene in CNC progenitor cells can lead to CAT.<sup>215, 216</sup> Next, as the name suggests, a DORV involves both arteries drawing blood from the right ventricle. In this case, the aorta is improperly connected to the right ventricle, thereby supplying the body with partially deoxygenated blood. Again, this defect occurs along with a VSD, compensating for the blood flow disruption.<sup>45</sup> Finally, an overriding aorta represent an alignment malformation instead of septation defect, and is linked to abnormal cardiac looping. This defect is also accompanied by a VSD. Together, the incidence of OFT defects is between 20 to 30% of total CHDs in humans at birth.<sup>3</sup>

### 1.5.1.3 Valvular Defects

Congenital valvular malformations can affect any of the four valves of the heart, and occurs in approximately 2% of the general population. These defects commonly have a genetic component as they tend to cluster in families.<sup>3</sup> The aortic semilunar valve

separates the aorta from the left ventricle, whereas the pulmonary semilunar valve separates the pulmonary artery from the right ventricle. The mitral valve exists between the left atrium and the left ventricle, and the tricuspid valve is between the right atria and ventricle. Congenital valvular defects occur most frequently at the aortic valve. In fact, a bicuspid aortic valve, in which only 2 out of 3 valve leaflets develop, is present in 1-2% of the general population.<sup>217</sup> Thickening of the aortic valve, also known as aortic valve sclerosis, is a common OFT obstruction and can be a consequence of abnormal valve remodeling *in utero*. The incidence of aortic valve sclerosis can be upwards of 25% in the aged population; however, calcification of the valve and rheumatic aortic valve disease, occurring later in life, can account for many cases.<sup>218</sup> Therefore, this disease represents a significant health problem, contributing to approximately 20,000 deaths annually.<sup>3</sup>

#### 1.5.1.4 Hypoplastic Coronary Artery Disease

Congenital under-development of the coronary arteries can result in hypoplastic coronary artery disease. This rare congenital abnormality is characterized by a marked decrease in luminal diameter, length or number of the coronary arteries.<sup>219</sup> This can occur in one or more of the major branches of the coronary artery tree, where no other compensatory collateral vessels exist. Hypoplastic coronary artery disease is usually asymptomatic at birth, but can manifest later in life under conditions of stress or physical exertion, possibly resulting in myocardial infarction or even sudden cardiac death.<sup>220</sup> Due to the asymptomatic nature of this disease, the incidence is estimated to be 1% in the general population.<sup>221, 222</sup> Post mortem analysis revealed hypoplastic coronary artery disease in 2.2% of cases with coronary artery anomalies.<sup>223</sup> Coronary angiography is the current tool to diagnose these congenital anomalies.

## 1.5.2 Epidemiology and Environmental Risk Factors of Congenital Heart Disease

In the general population, CHDs are the most common structural birth defect.<sup>3, 198, 224</sup> Congenital heart disease is the leading cause of pediatric deaths in developed nations.<sup>196</sup> It is estimated that 257,000 Canadians and about 2 million Americans are living with a CHD.<sup>207, 225</sup> Approximately 40,000 infants are diagnosed with a CHD each year in the US, and a quarter of these patients will need invasive treatment in the first year of life.<sup>3</sup> In the year 2000, the prevalence of CHDs in the province of Quebec was 14.75 per 1000 males and 17.22 per 1000 females.<sup>198</sup> This remained consistent with the rest of the country as 13.11 per 1000 children had a CHD in 2010.<sup>207</sup> In terms of specific cardiac malformations, the Centre for Disease Control reports that complex CHDs, such as TOF and AVSD are as common as 1 in 2518 and 1 in 2122, respectively.<sup>226</sup> Many epidemiologists have noted a steady increase in occurrence of CHDs over time. One study from metropolitan Atlanta states that from 1978 to 2005, malformations of the heart increased from 50.3 per 10,000 to 86.4 per 10,000.<sup>227</sup> This increase in proportion is alarming and calls for increased research to be conducted in order to elucidate the mechanisms behind potential insults to the developing heart. The variation in prevalence rates can be attributed to age of the patient when the defect is detected. Severe CHDs are usually cyanotic and can be diagnosed *in utero* or just after birth. Mild defects may not be identified until later in life or adulthood, making population prevalence difficult to estimate.<sup>3</sup> Nevertheless, prevalence rates are expected to increase over time due to improved screening techniques, such as fetal cardiac ultrasound by pulse oximetry.<sup>3</sup>

Both intrinsic and extrinsic risk factors are associated with the development of CHDs. Many of the intrinsic factors have been discussed in previous sections. These include mutations in key transcription factors, such as *NKX2.5*, that govern heart development, and chromosomal abnormalities, such as Trisomy 21.<sup>228, 229</sup> Extrinsic factors are non-genetic, and represent environmental insults during pregnancy that compromise developmental pathways in the embryo. These risk factors can include maternal smoking, nicotine exposure, alcohol consumption, obesity, chlamydia or rubella infections, preeclampsia and high altitude.<sup>230-238</sup> For instance, there was an exposure-response relationship between overweight, moderately obese and severely obese pregnant women with CHD incidence in the offspring. In fact, offspring of severely obese women were at a 1.94 times greater risk of having TOF.<sup>233</sup> Pregestational maternal diabetes is an established risk factor for offspring CHDs in both the clinic and experimental animal models, which will be described in the following sections.

## 1.6 Pregestational Diabetes and Congenital Heart Defects

Congenital malformations in the offspring of women with PGD include defects of the limb, neural tube and musculoskeletal systems. However, the predominant malformations are CHDs, which represent about 40% of the total malformations.<sup>9, 10</sup> PGD is an established risk factor for congenital heart disease,<sup>239</sup> and increases the risk of a CHD in the child by more than four-fold.<sup>194, 240-242</sup> This is a major concern as it is estimated that 451 million people are living with diabetes, and the incidence of this condition is increasing at a rate of 10 million people per year. It is projected that by the year 2040, approximately 693 million people will be affected.<sup>1</sup> In terms of the developmental origins of congenital heart defects, this increase in diabetes world-wide is alarming as

approximately 3 to 9 females in every 1000 pregnancies surveyed in Europe and North America are diabetic prior to conception of their child.<sup>243</sup> As this number increases with the increase in diabetes, more individuals will be born with congenital heart defects, inevitably placing a large burden on the healthcare system.

We recently demonstrated that pregestational diabetes induced by streptozotocin (STZ) in mice results in CHDs and coronary artery malformations (CAMs) in the offspring, which simulates diabetes-induced congenital heart disease in humans.<sup>200, 244</sup> In experimental animal models, the incidence of congenital malformations induced by pregestational diabetes has been successfully reduced by vitamin E, vitamin C, hydroxytoluene (BHT), superoxide dismutase-1 (SOD1) and N-acetylcysteine (NAC) treatment.<sup>244-249</sup> In the clinic, new-borns of pregestational diabetic women have an altered heart rate variability, fetal acidaemia and fetal glycaemia.<sup>250</sup> During development, a higher fetal heart rate has been reported by cardiotocographic analysis from the first to the third trimester in pregnancies complicated with pregestational diabetes.<sup>251, 252</sup> Accordingly, offspring of these women also have an altered QRS complex.<sup>253</sup> Although current prenatal care recommends tight glucose control before and during pregnancy, CHD incidence in the offspring of diabetic women remains unchanged, showing little improvement.<sup>240</sup> Insulin or other anti-diabetic medication, such as metformin for Type 2 diabetes, are currently prescribed for women with diabetes during pregnancy. Although these drugs are not teratogenic, their long-term effect on the offspring's health is not known. Compliance and maintenance are also major factors that can impact proper glycaemic control for diabetic women during pregnancy.<sup>254</sup> In addition, pregnancy can exacerbate and complicate diabetes management, usually requiring higher dosing of medication. Finally, the prevalence of diabetes is rapidly rising among low-

to-middle income populations, and access to proper prenatal care is often challenging.<sup>255</sup> Thus, research must be conducted to find alternate interventions that support current treatment practices, while being safe and accessible.

### 1.6.1 Potential Mechanisms of Diabetic Embryopathy

Maternal diet, nutrition and body composition have both short-term and long-term consequences for the offspring.<sup>256</sup> Uncontrolled maternal diabetes is not conducive to proper gestation. Specifically, the hyperglycemic environment to which the embryo is exposed is dangerous as increased serum glucose leads to oxidative stress in cells through numerous pathways. High levels of glucose will increase glycolysis in cells and will cause increased amounts of NADH and FADH<sub>2</sub>. These molecules act as electron sources for the mitochondrial electron transport chain, and higher levels of electrons flowing through this chain will lead to increased oxygen consumption and ATP formation.<sup>257</sup> Superoxide generation will accompany this energy production, resulting in a rise in ROS. Premature electron leak from the cytochrome chain occurs in pathological conditions, resulting in ROS. At several points during the oxidative phosphorylation process, electrons can react with oxygen, forming radicals.<sup>258</sup> Mitochondrial ROS can stimulate the production of cytosolic ROS through several mechanisms. Hydrogen peroxide can lead to the activation of cellular Src kinase, which promotes NADPH oxidase activity, producing superoxide.<sup>259</sup> These reactive molecules can damage DNA and proteins critical for organogenesis.<sup>260</sup> The developing heart is sensitive to changes in glucose availability. Early cardiac progenitors mainly rely on glycolysis for energy production; however, as cardiomyocytes terminally differentiate they switch to mitochondrial oxidative metabolism pathways.<sup>261</sup> In fact, the expression of glucose transporter 1 (GLUT1) is

upregulated in the embryonic heart in experimental models of maternal diabetes, facilitating the glucose overload.<sup>8</sup>

Consequently, recent murine studies are attempting to examine whether miRNA expression is altered in the embryonic heart under maternal pregestational diabetes. A global miRNA profiling study reported a differential expression pattern of 149 miRNAs in E12.5 hearts from diabetic dams compared to control.<sup>262</sup> Of these, 3,960 miRNA-mRNA complementary pairs were identified between 32 miRNAs and 2,111 mRNA transcripts; 284 of which are transcriptional regulators involved in cardiac hypertrophy, hypoplasia, and cardiomyocyte apoptosis.<sup>262</sup> In addition, pregestational diabetes-induced changes in miRNA expression in maternal exosomes can be relayed to the developing fetal heart. RNA sequencing revealed 186 upregulated and 92 downregulated miRNAs in maternal exosomes isolated from STZ-induced diabetic dams, compared to control.<sup>263</sup> In particular, levels of miRNA-122 are almost 3-fold higher in these diabetic exosomes.<sup>263</sup> Taken together, these changes in miRNA expression, especially the increase in miRNA-122, during fetal heart development in a diabetic environment warrant further investigation as these findings could provide new insights into the pathogenesis of diabetes-induced CHDs.

#### 1.6.1.1 ROS

Molecules containing one or more unpaired electrons in their valence orbital or unstable bonds are reactive. ROS can exist as neutral molecules, ions or radicals, such as hydrogen peroxide, the superoxide anion, or the hydroxyl radical, respectively.<sup>264</sup> These species oxidize other molecules by removing electrons in order to make themselves stable. For instance, the superoxide anion can react with nitric oxide forming the highly



reactive peroxyxynitrite.<sup>258</sup> Superoxide cannot readily cross plasma membranes, therefore having local, transient effects. This ion is spontaneously dismutated into hydrogen peroxide, which has long-lasting effects and is freely diffusible across membranes. This conversion can be catalyzed within cells by the enzyme superoxide dismutase.<sup>264</sup> Elevated concentrations of ROS can react with proteins, lipids, carbohydrates and nucleic acids causing non-specific damage and permanent functional changes. Along with mitochondrial ROS production, intracellular sources of ROS include peroxisomes, lysosomes, and the enzymes NADPH oxidase, xanthine oxidase and cytochrome p450.<sup>264</sup> A major contributor of ROS in endothelial cells is NADPH oxidases, which transfer electrons across membranes to an oxygen molecule.<sup>258</sup>

## 1.7 Endothelial Nitric Oxide Synthase

Nitric oxide (NO) is a lipophilic, small gaseous molecule that has numerous roles in biological signaling processes, and, most notably, serves as a potent vasodilator.<sup>265</sup> Nitric oxide production within the cell is accomplished by the enzyme nitric oxide synthase (NOS), which catalyzes the conversion of L-arginine into nitric oxide through a NADPH-dependent reaction. Three isoforms of this enzyme, neuronal (nNOS, NOS1), cytokine-inducible (iNOS, NOS2), and endothelial (eNOS, NOS3) are distinctly expressed in mammalian cells and produce NO in a tissue-specific manner.<sup>266</sup> nNOS is constitutively expressed in neurons of the central and peripheral nervous system, whereas iNOS is expressed in cells of the immune system and produces high levels of nitric oxide associated with inflammatory processes. eNOS is membrane bound and calcium-sensitive, expressed in endothelial and myocardial cells, located on chromosome 7 in humans.<sup>267</sup> They are homodimeric, haem-containing globular proteins, with a N-terminal

oxygenase domain and a C-terminal reductase domain, which are linked by a calmodulin binding sequence. The dimer produces NO in the coupled state, and requires  $\text{Ca}^{2+}$ /calmodulin, flavin adenine dinucleotide (FAD), flavin mononucleotide (FMN), and tetrahydrobiopterin (BH4) as cofactors.<sup>266</sup> Calcium-activated calmodulin initiates the electron transfer to produce nitric oxide, which, when produced, acts on soluble guanylyl cyclase to catalyze the formation of the second messenger, cyclic guanosine monophosphate (cGMP). Downstream targets of cGMP include protein kinases (PKGs), ion channels and cyclic nucleotide phosphodiesterases (PDEs).<sup>268</sup> Activation or inhibition of protein function via S-nitrosylation is also a downstream effect of nitric oxide. Interestingly, eNOS can be itself S-nitrosylated, reducing its activity.<sup>269</sup> Phosphorylation of eNOS at serine-1177 by Akt (protein kinase B) activates the enzyme, which itself is active when phosphorylated. Nitric oxide production via this PI3K/Akt/eNOS pathway represents a highly regulated biological process involved in endothelial cell permeability, vascular smooth muscle relaxation, calcium handling, immune regulation and neurotransmission.<sup>270</sup> The vital role of eNOS-derived NO in cardiovascular health and development will be explored in following sections.

### 1.7.1 Tetrahydrobiopterin

The pteridine (6R) 5,6,7,8-tetrahydrobiopterin (BH4) is an antioxidant and cofactor for many metabolic enzymes, involved in the production of neurotransmitters and nitric oxide. As a cofactor, its heterocyclic ring structure functions to facilitate complex chemical reactions in a wide variety of biological processes.<sup>271</sup> Aromatic amino acid hydroxylases utilize BH4 as a cofactor to produce monoamine neurotransmitters such as serotonin, melatonin, dopamine, norepinephrine and epinephrine. As stated

above, tetrahydrobiopterin is the principle co-factor for eNOS and can serve as an endogenous antioxidant as well. BH4 is essential for NOS-mediated nitric oxide synthesis, by all three isoforms, and serves both biochemical and structural functions.<sup>271</sup> It is required for eNOS homo-dimer stabilization and is an allosteric modulator of L-arginine binding to the active site.<sup>272</sup> BH4 participates in the biochemical formation of NO from O<sub>2</sub> by donating an electron for the conversion of L-arginine to L-citrulline.<sup>273</sup> It “couples” the haem reduction to nitric oxide synthesis, and acts as a sequential one-electron reductant and oxidant.<sup>266</sup> However, BH4 is not consumed in this process as it recaptures its electron from the iron-containing heme group, facilitating NO release.<sup>274</sup> BH4 biosynthesis within the cell is carried out via a three-step enzymatic process with the conversion of the nucleotide GTP into 7,8-dihydroneopterin triphosphate as the rate-limiting first step. The enzyme that catalyzes this conversion is GTP cyclohydrolase 1 (GTPCH-1). It is encoded by the gene *GHC1* on chromosome 14 in humans. The next steps are catalyzed by 6-pyruvoyl tetrahydropterin synthase and sepiapterin reductase.<sup>271</sup> GTPCH-1 expression and activity are tightly regulated at transcriptional, translational and post-translational levels. For example, a negative feedback loop exists whereby BH4 allosterically downregulates activity of GTPCH-1 when it is bound, in a dose-dependent manner, to the feedback regulatory protein, GFRP. Conversely, the interaction of GFRP with L-phenylalanine can reverse this effect, and increase GTPCH-1 activity and BH4 production.<sup>275</sup> Along with this *de novo* biosynthesis pathway, BH4 can also be recycled within the cell through a salvage pathway. The enzyme dihydrofolate reductase (DHFR) regenerates BH4 by reducing dihydrobiopterin (BH2), a byproduct of oxidation. DHFR is ubiquitously expressed and needed by eukaryotes and prokaryotes for normal cellular

metabolism. Apart from being involved in BH4 recycling, it also catalyzes the reduction of folate to tetrahydrofolate, which is required for many biological processes, such as amino acid biosynthesis.<sup>276</sup> Therefore, the cellular bioavailability of BH4 is balanced between its de novo synthesis, oxidation to BH2 and regeneration. Due to the critical role of nitric oxide in the cardiovascular system, BH4 administration has been tested for its clinical viability at improving endothelial function in many studies. Intravascular infusion of BH4 to chain smokers improved their endothelium-dependent vasodilation.<sup>277</sup> Similarly, in patients with hypercholesterolaemia, BH4 infusion improved coronary microvascular circulation.<sup>278</sup> In accordance, BH4 intra-arterial administration prevented ischemia reperfusion injury in the human forearm.<sup>279</sup>

#### 1.7.1.1 Sapropterin Dihydrochloride

Sapropterin dihydrochloride is an FDA-approved synthetic formulation of BH4, prescribed for the treatment of phenylketonuria.<sup>280</sup> Orally active and stable, this drug is marketed as Kuvan® and has been manufactured by Biomarin Pharmaceuticals since 2007.<sup>281</sup> Patients with PKU are unable to metabolize the amino acid phenylalanine, present in many food products, due to a mutation in the metabolizer phenylalanine hydroxylase (PAH).<sup>282</sup> This enzyme uses BH4 as a cofactor to oxidize phenylalanine to tyrosine. When mutated its activity is reduced leading to hyperphenylalaninemia, the toxic accumulation of phenylalanine in the blood. Complete phenylalanine restriction is recommended for patients with PKU; however, long-term compliance can be difficult, especially in youth and pregnant women. Treatment with sapropterin can activate the residual PAH enzyme, allowing for the metabolism of phenylalanine, thereby decreasing its levels in the blood. PKU patients administered sapropterin have increased

phenylalanine tolerance, thereby allowing a relaxation in dietary restrictions.<sup>282</sup> This drug has an acceptable safety profile and is prescribed as 100 mg tablets at a starting dose of 10 mg/kg/day.<sup>281</sup>

### 1.7.2 BH4 Cycling and eNOS Coupling; a Positive Feedback Loop

BH4 production, either through de novo synthesis or regeneration, promotes eNOS function, generating nitric oxide (Figure 1.3).<sup>283</sup> In fact, diminished levels of BH4 or depletion of L-arginine can uncouple the eNOS dimer, rendering it incapable of producing nitric oxide, instead generating oxygen derived free radicals.<sup>284</sup> Similarly, in states of oxidative stress, this process is insulted at many levels, sustaining the oxidative environment and leading to cellular dysfunction. The production of ROS is often amplified because of a positive-feedback loop; ROS generates more ROS. As mentioned above, GTPCH-1 is an enzyme involved in antioxidant biosynthesis. Specifically, it catalyzes the formation of BH4, an essential co-factor for eNOS.<sup>285</sup> Recently, a study has indicated that ROS causes the release of zinc from GTPCH-1, rendering it less functional (Figure 1.3).<sup>286</sup> Consequently, the intracellular levels of BH4 decline and eNOS is left without a cofactor, triggering its uncoupling. When eNOS is uncoupled, it cannot form nitric oxide, which has its own developmental implications, and instead generates ROS in the form of superoxide. This superoxide anion participates in a rapid reaction with low levels of NO in the cell and forms the peroxynitrite anion (ONOO<sup>-</sup>) (Figure 1.3).<sup>287</sup> This species is normally in equilibrium with peroxynitrous acid (ONOOH), which can decay and form ONOOH<sup>•</sup>, another reactive radical. Proteins are especially vulnerable to modification by the peroxynitrite system, as it incurs covalent changes to the amino acid residues cysteine, methionine, tryptophan, and tyrosine.<sup>288</sup> ONOO<sup>-</sup> specifically

inactivates GTPCH-1, decreasing de novo BH<sub>4</sub> synthesis, and the additional oxidative stress furthers the oxidation of BH<sub>4</sub> into BH<sub>2</sub>.<sup>286</sup> BH<sub>2</sub> is unable to couple eNOS, and competes with BH<sub>4</sub> for eNOS binding, exacerbating the superoxide production. Mice lacking GTPCH-1 in the endothelium display significantly decreased BH<sub>4</sub> levels, eNOS uncoupling and increased ROS production, resulting in loss of vasodilation.

Another enzyme inactivated by O<sub>2</sub><sup>-</sup> and ONOO<sup>-</sup> is dihydrofolate reductase (DHFR), responsible for the recycling of BH<sub>2</sub> back to BH<sub>4</sub>.<sup>273, 289</sup> Experiments done in *E. coli* demonstrate peroxynitrite-induced alterations to the catalytic site of DHFR, resulting in functional compromise.<sup>276</sup> Therefore, both the salvage and endogenous synthesis pathways are crippled due to ROS, furthering the oxidative environment (**Figure 1.3**). In states of oxidative stress, BH<sub>4</sub> levels decline, and eNOS function is impaired. Specifically, oxygen activation is functionally uncoupled to L-arginine oxygenation, resulting in decreased NO production.<sup>290</sup> Instead, activated O<sub>2</sub>, in the form of superoxide, is released from the enzyme, perpetuating the oxidative environment of the cell. The relationship between eNOS function and diabetes has been well established. Endothelial dysfunction is a common consequence of diabetes and is mediated by oxidative stress-induced eNOS uncoupling.<sup>291-293</sup> Previous studies indicate that dissolution of the eNOS dimer also occurs in aging vessels and in cardiovascular disease states, such as hypertension, ischemia-reperfusion injury and heart failure.<sup>294-296</sup> Treatment with BH<sub>4</sub> has been shown to recouple eNOS and improve vascular endothelial function in diabetes.<sup>271, 297</sup>

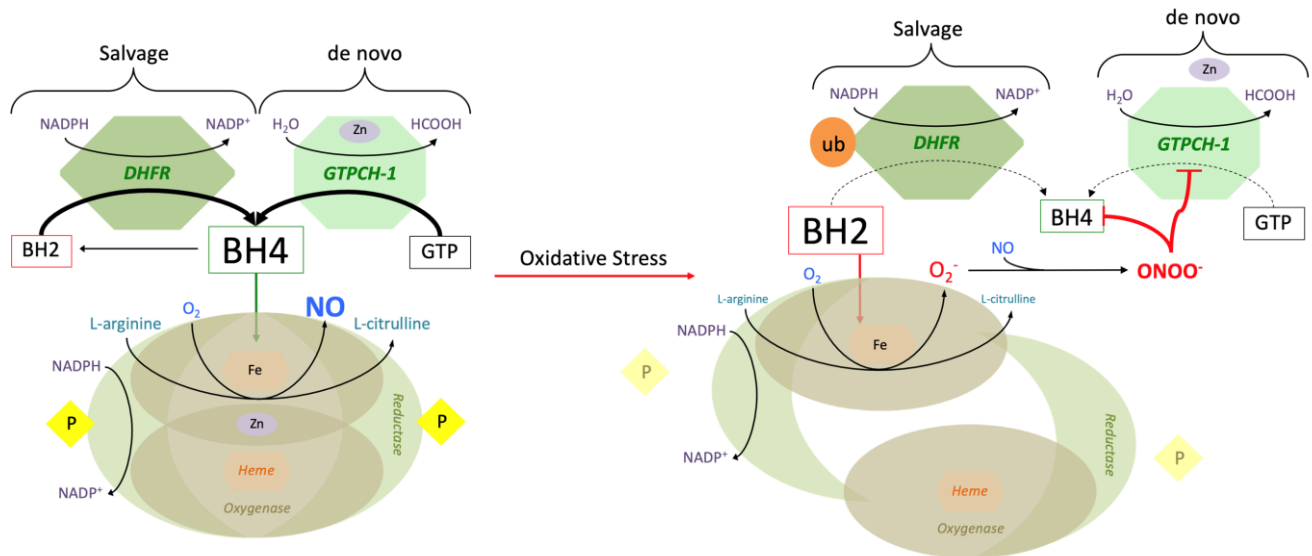


**Figure 1.3. eNOS uncoupling and inactivation in states of oxidative stress.**

The functional eNOS dimer, producing nitric oxide, is seen on the left. eNOS dysfunction, on the right, occurs in states of oxidative stress, where BH4 is oxidized, the dimer is uncoupled and eNOS is inactive. In this state, nitric oxide is no longer produced and instead superoxide radical is generated. The salvage and de novo BH4 biosynthesis pathways are actively producing BH4 in normal conditions, but are impaired by oxidative stress, specifically derived from eNOS uncoupling.

### 1.7.3 The role of eNOS in Cardiovascular Development

eNOS is vital for heart development. Expression of the synthase starts at E9.5 in the endothelium and cardiomyocyte precursors of the heart tube, and peaks at E13.5, after which it begins to decline, but remains detectable at birth and into postnatal development.<sup>270</sup> The lung, liver, gastrointestinal tract, reproductive organs and brain all express NOS3 during their organogenesis.<sup>298</sup> *In vitro* incubation of NOS inhibitors to embryonic stem cell-derived cardiomyocytes inhibited their maturation.<sup>298</sup> Interestingly, mouse embryonic stem cells exogenously treated with a NO donor or transfected with NOS promoted their differentiation into cardiomyocytes, inducing the expression of cardiac specific genes.<sup>299</sup> Induced pluripotent stem cells and E14.5 ventricular tissue both deficient in NOS3 show consistent transcriptome profiles, and particularly an up-regulation of glucose metabolism genes.<sup>300</sup> Gata4, a transcription factor needed for cardiomyocyte specification and heart development, can modulate and increase the expression of eNOS by binding to its promoter region.<sup>301</sup> The importance of eNOS in heart development has been showcased through the spectrum of cardiovascular anomalies seen in eNOS<sup>-/-</sup> mice. Embryonic deletion of nNOS or iNOS display normal cardiac phenotypes, however eNOS null mice have a high rate of CHDs, with a 75% incidence of septal malformations in the offspring. These mice have increased postnatal mortality, impaired heart function, and significant elevations in embryonic apoptosis in the heart.<sup>119</sup> In addition, these mice have severe valvular malformations, including bicuspid aortic valves (30 – 40% incidence), underdeveloped mitral and tricuspid valves, which have significant regurgitation during systole (analyzed using pulse-wave Doppler), along with aortic valve sclerosis and calcification.<sup>302-304</sup> During embryonic development, eNOS null



mice has less Snail<sup>+</sup> mesenchymal cells in the endocardial cushions, suggesting impaired EndMT. This was coupled with significantly lower mRNA levels of genes involved in valve formation, such as Tgf- $\beta$  and Bmp2.<sup>303</sup> Accordingly, patients with bicuspid aortic valve disease had lower eNOS protein expression in aortic endothelial cells compared with tricuspid aortic valves patient specimens.<sup>305</sup> eNOS-derived NO regulates cell growth and protects early cardiac progenitors against apoptosis.<sup>119</sup> This is accomplished through S-nitrosylation and inactivation of caspase-3.<sup>306</sup> Shear stress-induced NO production and up-regulation of superoxide dismutase also prevented endothelial cell death via inhibiting caspase-3 activity.<sup>307</sup> eNOS is also required for cardiomyocyte proliferation, as well as VEGF expression to form the capillary network supplying the muscle.<sup>108</sup> In fact, eNOS intimately controls coronary artery development in mice, as loss of this enzyme results in coronary artery hypoplasia and spontaneous postnatal myocardial infarction.<sup>110</sup> Key transcription factors that control EMT and vasculogenesis are downregulated in this model, including Gata4, Wt1, Vegf, bFGF and EPO, all of which are rescued by eNOS overexpression, restoring normal vasculature.<sup>110</sup> The congenital coronary artery anomalies and CHDs seen in eNOS knockout mice *in utero* and at birth impair heart function in adult mice. Adult eNOS<sup>-/-</sup> mice display heart failure, characterized by a molecular switch from  $\alpha$ - to  $\beta$ -myosin heavy chain expression as well as an increase in atrial natriuretic peptide levels.<sup>308</sup> Inhibition of eNOS function using L-NAME induces comparable levels of fibrosis to eNOS null mice, following transverse aortic constriction.<sup>309</sup> eNOS restoration in the heart of eNOS-deficient mice attenuates LV hypertrophy, cardiac dysfunction and protected against adverse myocardial remodeling after aortic banding.<sup>310</sup> Mechanistically, eNOS-derived NO signaling reduces cardiac

calcium currents, decreasing the sympathetic  $\beta$ -adrenergic response and arrhythmia incidence, protecting the heart. The same is true in the embryonic heart, as NO regulation of L-type calcium channels also promotes mouse embryonic stem cell differentiation into cardiomyocytes.<sup>311</sup> Thus, the indispensable role of eNOS in the development of the heart and coronary vascular means that any alterations to the NO balance could prove deleterious.

## 1.8 Rationale and Hypothesis

CHDs are the most common birth defect and the leading cause of death in the first year of infant life. Environmental, non-genetic factors are associated with the majority of CHDs seen in the clinic, while inherited genetic mutations only account for 15% of reported cases.<sup>195</sup> Pregestational diabetes is an important risk factor of CHDs, heightening the risk by 3 – 5 times.<sup>240</sup> While good glycemic control in diabetic mothers lowers the risk, the incident of CHDs in their children is still higher than in the general population.<sup>241</sup> The rapid increase of young adults with diabetes and pre-diabetes is alarming, and warrants further research to broaden our understanding of the pathogenesis of congenital cardiovascular malformations and their prevention. Due to of the critical roles of eNOS and miRNAs in heart development, **this thesis aims to study the effects of sapropterin and antimiR-122 on CHDs and coronary artery malformations in a mouse model of pregestational diabetes.**

**We hypothesized that:**

- (1) BH4 treatment during the full gestational term of pregnant female mice with pregestational diabetes will decrease the incidence of CHDs and CAMs in**

**fetal hearts, through changes in gene expression, cell migration and proliferation, ROS handling and eNOS coupling, and**

**(2) microRNA-122 is involved in pregestational diabetes-induced CHDs and CAMs, and antimiR-122 treatment will prevent these congenital cardiac abnormalities.**

### 1.8.1 Aim 1: Sapropterin on Diabetes-Induced CHDs

The first aim of this study was to determine if BH4 treatment during the full gestational term of female mice with pregestational diabetes could decrease the incidence of CHDs in fetal hearts by mitigating altered gene expression, cell proliferation, SHF development, ROS levels, and eNOS coupling. Previous animal studies, as well human clinical data, have suggested a strong association between diabetic pregnancy and CHD incidence. In addition, eNOS has been demonstrated to play a vital role in embryonic heart development.<sup>270</sup> The activity of this enzyme is compromised in diabetes, leading to endothelial dysfunction. Specifically, the eNOS dimer can be uncoupled, increasing the already high levels of oxidative stress brought on by hyperglycemia.<sup>312</sup> Sapropterin dihydrochloride (Kuvan®) is an orally active synthetic form of BH4 and an FDA approved drug for the treatment of phenylketonuria.<sup>281</sup> **We hypothesized that maternal diabetes-induced oxidative stress would lead to eNOS uncoupling in the developing myocardium, resulting in increased ROS, altered cardiogenic gene expression, decreased proliferation and development of SHF structures, and subsequent CHDs and damped cardiac function. We further hypothesized that exogenous sapropterin treatment would re-instate oxidative balance and recouple eNOS in the embryonic**

**heart, promote cell proliferation of cardiac progenitors and decrease the incidence of CHDs.**

Objectives:

1. Characterize the spectrum of CHDs induced by pregestational maternal diabetes, and test if sapropterin therapy can rescue the disease phenotype.
2. Utilize lineage tracing to determine the impact of maternal diabetes on the development of the SHF.
3. Determine if the eNOS dimer is uncoupled and if there is elevated ROS in the embryonic myocardium from diabetic dams, and assess if sapropterin treatment can recouple eNOS and reduce ROS.

### 1.8.2 Aim 2: Sapropterin on Diabetes-Induced CAMs

Congenital coronary artery malformations (CAMs) affect about 1% of the general population.<sup>221-223</sup> Hypoplastic coronary artery disease (HCAD) is a congenital abnormality characterized by marked decrease in luminal diameter and length of coronary vasculature.<sup>313</sup> HCAD usually is asymptomatic at birth, and can go unnoticed until the individual is older and/or subjected to increased physical exertion. Without intervention, this could lead to myocardial infarction and even sudden cardiac death.<sup>220</sup> As this disease is asymptomatic at birth and possibly for much of adulthood, it is pressing that preventative precautions be taken during gestational coronary artery development. The development of the coronary vasculature occurs in tandem with heart development, but is distinct in its cellular origin and molecular drivers. It involves coordinated EMT and differentiation, with eNOS again playing a major role. In fact, eNOS<sup>-/-</sup> mice display

hypoplastic coronary arteries and post-natal myocardial infarction.<sup>110</sup> Additionally, experiments in mice have indicated that hyperglycemia during pregnancy can induce coronary artery anomalies.<sup>200</sup> **Therefore, we hypothesized that pregestational diabetes would result in CAMs, akin to hypoplastic coronary artery disease, which would be a result of impaired EMT during embryonic development. Further, we hypothesized that sapropterin treatment would promote epicardial EMT and reduce the incidence of CAMs in offspring of pregestational diabetes.**

Objectives:

1. Analyze CAMs induced by pregestational diabetes, and determine if sapropterin treatment can reduce their incidence.
2. Determine if epicardial EMT is impaired by diabetic pregnancy, and if sapropterin can regulate the process under high glucose conditions.
3. Elucidate the impact of hyperglycemia during gestation on eNOS phosphorylation and oxidative stress in the fetal heart.

### 1.8.3 Aim 3: Role of microRNA-122 in Heart Development

MicroRNAs play an important role in cardiogenesis, often acting as temporal switches, turning on and off gene programs that govern developmental stages of the heart. miRs are short, non-coding RNA molecules that post-transcriptionally regulate gene expression by repressing mRNA.<sup>145</sup> These small RNA molecules can freely cross the placenta and enter fetal circulation. Patients with diabetes have a dysregulation in miRNA expression.<sup>314</sup> Diabetic pregnancy may illicit changes in the miRNA profile, in

either the mother or the fetus, contributing to the pathogenesis of CHDs. Our preliminary data confirms the finding of a differential miRNA transcriptome profile in embryonic hearts from diabetic dams. In our laboratory, using global microarray analysis, we found that miR-122 is upregulated 14-fold in E10.5 hearts from diabetic dams compared to control. miR-122 is required for liver homeostasis and acts as tumor suppressor, by inhibiting the expression of genes involved in proliferation and epithelial to mesenchymal transition (EMT); two processes critical to cardiogenesis. **Therefore, we hypothesized that miR-122 would be upregulated in fetal hearts from diabetic dams and would impair key developmental processes, such as cell proliferation, migration and apoptosis, in the heart. We further hypothesized that antimiR-122 treatment to diabetic dams would reduce the incidence of CHDs in the offspring.**

Objectives:

1. Validate the expression of miR-122 in embryonic hearts from diabetic dams, and determine if the expression of miR-122 targets is altered.
2. Determine the effects of miR-122 on cell proliferation, apoptosis and EMT in the embryonic heart.
3. Determine if in vivo administration of antimiR-122 could reduce the incidence of CHDs induced by pregestational diabetes.

## 1.9 References

1. Cho NH, Shaw JE, Karuranga S, Huang Y, da Rocha Fernandes JD, Ohlrogge AW and Malanda B. IDF Diabetes Atlas: Global estimates of diabetes prevalence for 2017 and projections for 2045. *Diabetes Res Clin Pract.* 2018;138:271-281.
2. Canadian Diabetes Association. <https://www.diabetes.ca/about-diabetes>. 2015.
3. Benjamin EJ, Virani SS, Callaway CW, Chamberlain AM, Chang AR, Cheng S, Chiuve SE, Cushman M, Delling FN, Deo R, de Ferranti SD, Ferguson JF, Fornage M, Gillespie C, Isasi CR, Jimenez MC, Jordan LC, Judd SE, Lackland D, Lichtman JH, Lisabeth L, Liu S, Longenecker CT, Lutsey PL, Mackey JS, Matchar DB, Matsushita K, Mussolino ME, Nasir K, O'Flaherty M, Palaniappan LP, Pandey A, Pandey DK, Reeves MJ, Ritchey MD, Rodriguez CJ, Roth GA, Rosamond WD, Sampson UKA, Satou GM, Shah SH, Spartano NL, Tirschwell DL, Tsao CW, Voeks JH, Willey JZ, Wilkins JT, Wu JH, Alger HM, Wong SS, Muntner P, American Heart Association Council on E, Prevention Statistics C and Stroke Statistics S. Heart Disease and Stroke Statistics-2018 Update: A Report From the American Heart Association. *Circulation.* 2018;137:e67-e492.
4. Lipscombe LL and Hux JE. Trends in diabetes prevalence, incidence, and mortality in Ontario, Canada 1995-2005: a population-based study. *Lancet.* 2007;369:750-6.
5. LaCoursiere DY, Bloebaum L, Duncan JD and Varner MW. Population-based trends and correlates of maternal overweight and obesity, Utah 1991-2001. *American journal of obstetrics and gynecology.* 2005;192:832-9.
6. Barker DJ. The developmental origins of adult disease. *J Am Coll Nutr.* 2004;23:588S-595S.
7. McMillen IC and Robinson JS. Developmental origins of the metabolic syndrome: prediction, plasticity, and programming. *Physiol Rev.* 2005;85:571-633.
8. Lock MC, Botting KJ, Tellam RL, Brooks D and Morrison JL. Adverse Intrauterine Environment and Cardiac miRNA Expression. *Int J Mol Sci.* 2017;18.
9. Casson IF, Clarke CA, Howard CV, McKendrick O, Pennycook S, Pharoah PO, Platt MJ, Stanisstreet M, van Velszen D and Walkinshaw S. Outcomes of pregnancy in insulin dependent diabetic women: results of a five year population cohort study. *Br Med J.* 1997;315:275-8.
10. Loffredo CA. Epidemiology of cardiovascular malformations: prevalence and risk factors. *Am J Med Genet.* 2000;97:319-25.
11. Macintosh MC, Fleming KM, Bailey JA, Doyle P, Modder J, Acolet D, Golightly S and Miller A. Perinatal mortality and congenital anomalies in babies of women

with type 1 or type 2 diabetes in England, Wales, and Northern Ireland: population based study. *Br Med J*. 2006;333:177.

12. DeRuiter MC, Poelmann RE, VanderPlas-de Vries I, Mentink MM and Gittenberger-de Groot AC. The development of the myocardium and endocardium in mouse embryos. Fusion of two heart tubes? *Anat Embryol (Berl)*. 1992;185:461-73.
13. Olson EN. Gene regulatory networks in the evolution and development of the heart. *Science*. 2006;313:1922-7.
14. Sizarov A, Ya J, de Boer BA, Lamers WH, Christoffels VM and Moorman AF. Formation of the building plan of the human heart: morphogenesis, growth, and differentiation. *Circulation*. 2011;123:1125-35.
15. Buckingham M, Meilhac S and Zaffran S. Building the mammalian heart from two sources of myocardial cells. *Nature reviews Genetics*. 2005;6:826-35.
16. Meilhac SM and Buckingham ME. The deployment of cell lineages that form the mammalian heart. *Nat Rev Cardiol*. 2018;15:705-724.
17. Meilhac SM, Lescroart F, Blanpain C and Buckingham ME. Cardiac cell lineages that form the heart. *Cold Spring Harb Perspect Med*. 2015;5:a026344.
18. Saga Y, Miyagawa-Tomita S, Takagi A, Kitajima S, Miyazaki J and Inoue T. MesP1 is expressed in the heart precursor cells and required for the formation of a single heart tube. *Development*. 1999;126:3437-47.
19. Ivanovitch K, Temino S and Torres M. Live imaging of heart tube development in mouse reveals alternating phases of cardiac differentiation and morphogenesis. *Elife*. 2017;6.
20. Srivastava D. Making or breaking the heart: from lineage determination to morphogenesis. *Cell*. 2006;126:1037-48.
21. Christoffels VM, Smits GJ, Kispert A and Moorman AF. Development of the pacemaker tissues of the heart. *Circulation research*. 2010;106:240-54.
22. de Boer BA, van den Berg G, de Boer PA, Moorman AF and Ruijter JM. Growth of the developing mouse heart: an interactive qualitative and quantitative 3D atlas. *Developmental biology*. 2012;368:203-13.
23. Nakajima Y, Sakabe M, Matsui H, Sakata H, Yanagawa N and Yamagishi T. Heart development before beating. *Anat Sci Int*. 2009;84:67-76.
24. Kelly RG. Molecular inroads into the anterior heart field. *Trends in cardiovascular medicine*. 2005;15:51-6.



25. Galli D, Dominguez JN, Zaffran S, Munk A, Brown NA and Buckingham ME. Atrial myocardium derives from the posterior region of the second heart field, which acquires left-right identity as Pitx2c is expressed. *Development*. 2008;135:1157-67.
26. Watanabe Y, Miyagawa-Tomita S, Vincent SD, Kelly RG, Moon AM and Buckingham ME. Role of mesodermal FGF8 and FGF10 overlaps in the development of the arterial pole of the heart and pharyngeal arch arteries. *Circulation research*. 2010;106:495-503.
27. Snarr BS, O'Neal JL, Chintalapudi MR, Wirrig EE, Phelps AL, Kubalak SW and Wessels A. Is11 expression at the venous pole identifies a novel role for the second heart field in cardiac development. *Circulation research*. 2007;101:971-4.
28. Tsuchihashi T, Maeda J, Shin CH, Ivey KN, Black BL, Olson EN, Yamagishi H and Srivastava D. Hand2 function in second heart field progenitors is essential for cardiogenesis. *Developmental biology*. 2011;351:62-9.
29. Goddeeris MM, Schwartz R, Klingensmith J and Meyers EN. Independent requirements for Hedgehog signaling by both the anterior heart field and neural crest cells for outflow tract development. *Development*. 2007;134:1593-604.
30. Lin L, Bu L, Cai CL, Zhang X and Evans S. Is11 is upstream of sonic hedgehog in a pathway required for cardiac morphogenesis. *Developmental biology*. 2006;295:756-63.
31. Moretti A, Caron L, Nakano A, Lam JT, Bernshausen A, Chen Y, Qyang Y, Bu L, Sasaki M, Martin-Puig S, Sun Y, Evans SM, Laugwitz KL and Chien KR. Multipotent embryonic is11+ progenitor cells lead to cardiac, smooth muscle, and endothelial cell diversification. *Cell*. 2006;127:1151-65.
32. Le Garrec JF, Dominguez JN, Desgrange A, Ivanovitch KD, Raphael E, Bangham JA, Torres M, Coen E, Mohun TJ and Meilhac SM. A predictive model of asymmetric morphogenesis from 3D reconstructions of mouse heart looping dynamics. *Elife*. 2017;6.
33. Leung C, Lu X, Liu M and Feng Q. Rac1 signaling is critical to cardiomyocyte polarity and embryonic heart development. *J Am Heart Assoc*. 2014;3:e001271.
34. Manner J. The anatomy of cardiac looping: a step towards the understanding of the morphogenesis of several forms of congenital cardiac malformations. *Clin Anat*. 2009;22:21-35.
35. Combs MD and Yutzey KE. Heart valve development: regulatory networks in development and disease. *Circulation research*. 2009;105:408-21.

36. von Gise A and Pu WT. Endocardial and epicardial epithelial to mesenchymal transitions in heart development and disease. *Circulation research*. 2012;110:1628-45.
37. van den Berg G and Moorman AF. Concepts of cardiac development in retrospect. *Pediatr Cardiol*. 2009;30:580-7.
38. Captur G, Wilson R, Bennett MF, Luxan G, Nasis A, de la Pompa JL, Moon JC and Mohun TJ. Morphogenesis of myocardial trabeculae in the mouse embryo. *J Anat*. 2016;229:314-25.
39. Luxan G, D'Amato G, MacGrogan D and de la Pompa JL. Endocardial Notch Signaling in Cardiac Development and Disease. *Circulation research*. 2016;118:e1-e18.
40. Webb S, Brown NA and Anderson RH. Formation of the atrioventricular septal structures in the normal mouse. *Circ Res*. 1998;82:645-56.
41. Zhou L, Liu J, Xiang M, Olson P, Guzzetta A, Zhang K, Moskowitz IP and Xie L. Gata4 potentiates second heart field proliferation and Hedgehog signaling for cardiac septation. *Proceedings of the National Academy of Sciences of the United States of America*. 2017;114:E1422-E1431.
42. Anderson RH, Spicer DE, Brown NA and Mohun TJ. The development of septation in the four-chambered heart. *Anatomical record*. 2014;297:1414-29.
43. Sylva M, van den Hoff MJ and Moorman AF. Development of the human heart. *Am J Med Genet A*. 2014;164A:1347-71.
44. Lin CJ, Lin CY, Chen CH, Zhou B and Chang CP. Partitioning the heart: mechanisms of cardiac septation and valve development. *Development*. 2012;139:3277-99.
45. Gittenberger-de Groot AC, Calkoen EE, Poelmann RE, Bartelings MM and Jongbloed MR. Morphogenesis and molecular considerations on congenital cardiac septal defects. *Ann Med*. 2014;46:640-52.
46. Pinto AR, Ilinykh A, Ivey MJ, Kuwabara JT, D'Antoni ML, Debuque R, Chandran A, Wang L, Arora K, Rosenthal NA and Tallquist MD. Revisiting Cardiac Cellular Composition. *Circulation research*. 2016;118:400-9.
47. Heallen T, Zhang M, Wang J, Bonilla-Claudio M, Klysik E, Johnson RL and Martin JF. Hippo pathway inhibits Wnt signaling to restrain cardiomyocyte proliferation and heart size. *Science*. 2011;332:458-61.
48. Del Monte-Nieto G, Ramialison M, Adam AAS, Wu B, Aharonov A, D'Uva G, Bourke LM, Pitulescu ME, Chen H, de la Pompa JL, Shou W, Adams RH, Harten SK, Tzahor E, Zhou B and Harvey RP. Control of cardiac jelly dynamics by

- NOTCH1 and NRG1 defines the building plan for trabeculation. *Nature*. 2018;557:439-445.
49. Peshkovsky C, Totong R and Yelon D. Dependence of cardiac trabeculation on neuregulin signaling and blood flow in zebrafish. *Developmental dynamics : an official publication of the American Association of Anatomists*. 2011;240:446-56.
  50. Kelly RG, Buckingham ME and Moorman AF. Heart fields and cardiac morphogenesis. *Cold Spring Harb Perspect Med*. 2014;4.
  51. Sedmera D and McQuinn T. Embryogenesis of the heart muscle. *Heart Fail Clin*. 2008;4:235-45.
  52. Moorman AF and Christoffels VM. Cardiac chamber formation: development, genes, and evolution. *Physiol Rev*. 2003;83:1223-67.
  53. D'Amato G, Luxan G, del Monte-Nieto G, Martinez-Poveda B, Torroja C, Walter W, Bochter MS, Benedito R, Cole S, Martinez F, Hadjantonakis AK, Uemura A, Jimenez-Borreguero LJ and de la Pompa JL. Sequential Notch activation regulates ventricular chamber development. *Nat Cell Biol*. 2016;18:7-20.
  54. Luxan G, Casanova JC, Martinez-Poveda B, Prados B, D'Amato G, MacGrogan D, Gonzalez-Rajal A, Dobarro D, Torroja C, Martinez F, Izquierdo-Garcia JL, Fernandez-Friera L, Sabater-Molina M, Kong YY, Pizarro G, Ibanez B, Medrano C, Garcia-Pavia P, Gimeno JR, Monserrat L, Jimenez-Borreguero LJ and de la Pompa JL. Mutations in the NOTCH pathway regulator MIB1 cause left ventricular noncompaction cardiomyopathy. *Nat Med*. 2013;19:193-201.
  55. Poelmann RE, Mikawa T and Gittenberger-de Groot AC. Neural crest cells in outflow tract septation of the embryonic chicken heart: differentiation and apoptosis. *Developmental dynamics : an official publication of the American Association of Anatomists*. 1998;212:373-84.
  56. Scherptong RW, Jongbloed MR, Wisse LJ, Vicente-Steijn R, Bartelings MM, Poelmann RE, Schalij MJ and Gittenberger-De Groot AC. Morphogenesis of outflow tract rotation during cardiac development: the pulmonary push concept. *Developmental dynamics : an official publication of the American Association of Anatomists*. 2012;241:1413-22.
  57. Hutson MR and Kirby ML. Model systems for the study of heart development and disease. Cardiac neural crest and conotruncal malformations. *Semin Cell Dev Biol*. 2007;18:101-10.
  58. Hildreth V, Webb S, Bradshaw L, Brown NA, Anderson RH and Henderson DJ. Cells migrating from the neural crest contribute to the innervation of the venous pole of the heart. *J Anat*. 2008;212:1-11.

59. Snider P, Olaopa M, Firulli AB and Conway SJ. Cardiovascular development and the colonizing cardiac neural crest lineage. *ScientificWorldJournal*. 2007;7:1090-113.
60. Schoen FJ. Evolving concepts of cardiac valve dynamics: the continuum of development, functional structure, pathobiology, and tissue engineering. *Circulation*. 2008;118:1864-80.
61. Ma L, Lu MF, Schwartz RJ and Martin JF. Bmp2 is essential for cardiac cushion epithelial-mesenchymal transition and myocardial patterning. *Development*. 2005;132:5601-11.
62. Butcher JT, McQuinn TC, Sedmera D, Turner D and Markwald RR. Transitions in early embryonic atrioventricular valvular function correspond with changes in cushion biomechanics that are predictable by tissue composition. *Circulation research*. 2007;100:1503-11.
63. Armstrong EJ and Bischoff J. Heart valve development: endothelial cell signaling and differentiation. *Circulation research*. 2004;95:459-70.
64. Person AD, Klewer SE and Runyan RB. Cell biology of cardiac cushion development. *Int Rev Cytol*. 2005;243:287-335.
65. Hinton RB and Yutzey KE. Heart valve structure and function in development and disease. *Annual review of physiology*. 2011;73:29-46.
66. Hinton RB, Jr., Lincoln J, Deutsch GH, Osinska H, Manning PB, Benson DW and Yutzey KE. Extracellular matrix remodeling and organization in developing and diseased aortic valves. *Circulation research*. 2006;98:1431-8.
67. Wessels A, van den Hoff MJ, Adamo RF, Phelps AL, Lockhart MM, Sauls K, Briggs LE, Norris RA, van Wijk B, Perez-Pomares JM, Dettman RW and Burch JB. Epicardially derived fibroblasts preferentially contribute to the parietal leaflets of the atrioventricular valves in the murine heart. *Developmental biology*. 2012;366:111-24.
68. Odelin G, Faure E, Culpier F, Di Bonito M, Bajolle F, Studer M, Avierinos JF, Charnay P, Topilko P and Zaffran S. Krox20 defines a subpopulation of cardiac neural crest cells contributing to arterial valves and bicuspid aortic valve. *Development*. 2018;145.
69. Cui Y, Zheng Y, Liu X, Yan L, Fan X, Yong J, Hu Y, Dong J, Li Q, Wu X, Gao S, Li J, Wen L, Qiao J and Tang F. Single-Cell Transcriptome Analysis Maps the Developmental Track of the Human Heart. *Cell Rep*. 2019;26:1934-1950 e5.
70. Bruneau BG. The developmental genetics of congenital heart disease. *Nature*. 2008;451:943-8.

71. Clark KL, Yutzey KE and Benson DW. Transcription factors and congenital heart defects. *Annu Rev Physiol.* 2006;68:97-121.
72. Garg V, Kathiriyia IS, Barnes R, Schluterman MK, King IN, Butler CA, Rothrock CR, Eapen RS, Hirayama-Yamada K, Joo K, Matsuoka R, Cohen JC and Srivastava D. GATA4 mutations cause human congenital heart defects and reveal an interaction with TBX5. *Nature.* 2003;424:443-7.
73. Zaidi S and Brueckner M. Genetics and Genomics of Congenital Heart Disease. *Circulation research.* 2017;120:923-940.
74. Durocher D, Charron F, Warren R, Schwartz RJ and Nemer M. The cardiac transcription factors Nkx2-5 and GATA-4 are mutual cofactors. *The EMBO journal.* 1997;16:5687-96.
75. Harvey RP, Lai D, Elliott D, Biben C, Solloway M, Prall O, Stennard F, Schindeler A, Groves N, Lavulo L, Hyun C, Yeoh T, Costa M, Furtado M and Kirk E. Homeodomain factor Nkx2-5 in heart development and disease. *Cold Spring Harb Symp Quant Biol.* 2002;67:107-14.
76. Schultheiss TM, Xydas S and Lassar AB. Induction of avian cardiac myogenesis by anterior endoderm. *Development.* 1995;121:4203-14.
77. Chung IM and Rajakumar G. Genetics of Congenital Heart Defects: The NKX2-5 Gene, a Key Player. *Genes (Basel).* 2016;7.
78. Yamagishi H, Yamagishi C, Nakagawa O, Harvey RP, Olson EN and Srivastava D. The combinatorial activities of Nkx2.5 and dHAND are essential for cardiac ventricle formation. *Developmental biology.* 2001;239:190-203.
79. Tanaka M, Chen Z, Bartunkova S, Yamasaki N and Izumo S. The cardiac homeobox gene Csx/Nkx2.5 lies genetically upstream of multiple genes essential for heart development. *Development.* 1999;126:1269-80.
80. Zhang L, Nomura-Kitabayashi A, Sultana N, Cai W, Cai X, Moon AM and Cai CL. Mesodermal Nkx2.5 is necessary and sufficient for early second heart field development. *Developmental biology.* 2014;390:68-79.
81. Benson DW, Silberbach GM, Kavanaugh-McHugh A, Cottrill C, Zhang Y, Riggs S, Smalls O, Johnson MC, Watson MS, Seidman JG, Seidman CE, Plowden J and Kugler JD. Mutations in the cardiac transcription factor NKX2.5 affect diverse cardiac developmental pathways. *The Journal of clinical investigation.* 1999;104:1567-73.
82. Pang S, Shan J, Qiao Y, Ma L, Qin X, Wanyan H, Xing Q, Wu G and Yan B. Genetic and functional analysis of the NKX2-5 gene promoter in patients with ventricular septal defects. *Pediatr Cardiol.* 2012;33:1355-61.

83. Schott JJ, Benson DW, Basson CT, Pease W, Silberbach GM, Moak JP, Maron BJ, Seidman CE and Seidman JG. Congenital heart disease caused by mutations in the transcription factor NKX2-5. *Science*. 1998;281:108-11.
84. Arceci RJ, King AA, Simon MC, Orkin SH and Wilson DB. Mouse GATA-4: a retinoic acid-inducible GATA-binding transcription factor expressed in endodermally derived tissues and heart. *Molecular and cellular biology*. 1993;13:2235-46.
85. Dodou E, Verzi MP, Anderson JP, Xu SM and Black BL. Mef2c is a direct transcriptional target of ISL1 and GATA factors in the anterior heart field during mouse embryonic development. *Development*. 2004;131:3931-42.
86. Kuo CT, Morrisey EE, Anandappa R, Sigrist K, Lu MM, Parmacek MS, Soudais C and Leiden JM. GATA4 transcription factor is required for ventral morphogenesis and heart tube formation. *Genes Dev*. 1997;11:1048-60.
87. Wang E, Sun S, Qiao B, Duan W, Huang G, An Y, Xu S, Zheng Y, Su Z, Gu X, Jin L and Wang H. Identification of functional mutations in GATA4 in patients with congenital heart disease. *PLoS one*. 2013;8:e62138.
88. Ang YS, Rivas RN, Ribeiro AJS, Srivas R, Rivera J, Stone NR, Pratt K, Mohamed TMA, Fu JD, Spencer CI, Tippens ND, Li M, Narasimha A, Radzinsky E, Moon-Grady AJ, Yu H, Pruitt BL, Snyder MP and Srivastava D. Disease Model of GATA4 Mutation Reveals Transcription Factor Cooperativity in Human Cardiogenesis. *Cell*. 2016;167:1734-1749 e22.
89. Steimle JD and Moskowitz IP. TBX5: A Key Regulator of Heart Development. *Curr Top Dev Biol*. 2017;122:195-221.
90. Bruneau BG, Logan M, Davis N, Levi T, Tabin CJ, Seidman JG and Seidman CE. Chamber-specific cardiac expression of Tbx5 and heart defects in Holt-Oram syndrome. *Developmental biology*. 1999;211:100-8.
91. Moskowitz IP, Pizard A, Patel VV, Bruneau BG, Kim JB, Kupersmidt S, Roden D, Berul CI, Seidman CE and Seidman JG. The T-Box transcription factor Tbx5 is required for the patterning and maturation of the murine cardiac conduction system. *Development*. 2004;131:4107-16.
92. Basson CT, Bachinsky DR, Lin RC, Levi T, Elkins JA, Soultis J, Grayzel D, Kroumpouzou E, Traill TA, Leblanc-Straceski J, Renault B, Kucherlapati R, Seidman JG and Seidman CE. Mutations in human TBX5 [corrected] cause limb and cardiac malformation in Holt-Oram syndrome. *Nat Genet*. 1997;15:30-5.
93. Waldron L, Steimle JD, Greco TM, Gomez NC, Dorr KM, Kweon J, Temple B, Yang XH, Wilczewski CM, Davis IJ, Cristea IM, Moskowitz IP and Conlon FL. The Cardiac TBX5 Interactome Reveals a Chromatin Remodeling Network Essential for Cardiac Septation. *Dev Cell*. 2016;36:262-75.

94. Ghosh TK, Song FF, Packham EA, Buxton S, Robinson TE, Ronksley J, Self T, Bonser AJ and Brook JD. Physical interaction between TBX5 and MEF2C is required for early heart development. *Molecular and cellular biology*. 2009;29:2205-18.
95. Edmondson DG, Lyons GE, Martin JF and Olson EN. Mef2 gene expression marks the cardiac and skeletal muscle lineages during mouse embryogenesis. *Development*. 1994;120:1251-63.
96. Potthoff MJ and Olson EN. MEF2: a central regulator of diverse developmental programs. *Development*. 2007;134:4131-40.
97. Lin Q, Schwarz J, Bucana C and Olson EN. Control of mouse cardiac morphogenesis and myogenesis by transcription factor MEF2C. *Science*. 1997;276:1404-7.
98. Materna SC, Sinha T, Barnes RM, Lammerts van Bueren K and Black BL. Cardiovascular development and survival require Mef2c function in the myocardial but not the endothelial lineage. *Developmental biology*. 2019;445:170-177.
99. Soufan AT, van den Berg G, Ruijter JM, de Boer PA, van den Hoff MJ and Moorman AF. Regionalized sequence of myocardial cell growth and proliferation characterizes early chamber formation. *Circulation research*. 2006;99:545-52.
100. Gunthel M, Barnett P and Christoffels VM. Development, Proliferation, and Growth of the Mammalian Heart. *Mol Ther*. 2018;26:1599-1609.
101. Kwon C, Arnold J, Hsiao EC, Taketo MM, Conklin BR and Srivastava D. Canonical Wnt signaling is a positive regulator of mammalian cardiac progenitors. *Proceedings of the National Academy of Sciences of the United States of America*. 2007;104:10894-9.
102. Sucov HM, Gu Y, Thomas S, Li P and Pashmforoush M. Epicardial control of myocardial proliferation and morphogenesis. *Pediatr Cardiol*. 2009;30:617-25.
103. Shen H, Cavallero S, Estrada KD, Sandovici I, Kumar SR, Makita T, Lien CL, Constanica M and Sucov HM. Extracardiac control of embryonic cardiomyocyte proliferation and ventricular wall expansion. *Cardiovascular research*. 2015;105:271-8.
104. Li P, Cavallero S, Gu Y, Chen TH, Hughes J, Hassan AB, Bruning JC, Pashmforoush M and Sucov HM. IGF signaling directs ventricular cardiomyocyte proliferation during embryonic heart development. *Development*. 2011;138:1795-805.
105. Wang Y, Hu G, Liu F, Wang X, Wu M, Schwarz JJ and Zhou J. Deletion of yes-associated protein (YAP) specifically in cardiac and vascular smooth muscle cells

- reveals a crucial role for YAP in mouse cardiovascular development. *Circulation research*. 2014;114:957-65.
106. von Gise A, Lin Z, Schlegelmilch K, Honor LB, Pan GM, Buck JN, Ma Q, Ishiwata T, Zhou B, Camargo FD and Pu WT. YAP1, the nuclear target of Hippo signaling, stimulates heart growth through cardiomyocyte proliferation but not hypertrophy. *Proceedings of the National Academy of Sciences of the United States of America*. 2012;109:2394-9.
  107. Leung C, Liu Y, Lu X, Kim M, Drysdale TA and Feng Q. Rac1 Signaling Is Required for Anterior Second Heart Field Cellular Organization and Cardiac Outflow Tract Development. *J Am Heart Assoc*. 2015;5.
  108. Lepic E, Burger D, Lu X, Song W and Feng Q. Lack of endothelial nitric oxide synthase decreases cardiomyocyte proliferation and delays cardiac maturation. *Am J Physiol Cell Physiol*. 2006;291:C1240-6.
  109. Hammoud L, Xiang F, Lu X, Brunner F, Leco K and Feng Q. Endothelial nitric oxide synthase promotes neonatal cardiomyocyte proliferation by inhibiting tissue inhibitor of metalloproteinase-3 expression. *Cardiovascular research*. 2007;75:359-68.
  110. Liu Y, Lu X, Xiang FL, Poelmann RE, Gittenberger-de Groot AC, Robbins J and Feng Q. Nitric oxide synthase-3 deficiency results in hypoplastic coronary arteries and postnatal myocardial infarction. *European heart journal*. 2014;35:920-31.
  111. McIlwain DR, Berger T and Mak TW. Caspase functions in cell death and disease. *Cold Spring Harb Perspect Biol*. 2013;5:a008656.
  112. Glucksmann A. Cell deaths in normal vertebrate ontogeny. *Biol Rev Camb Philos Soc*. 1951;26:59-86.
  113. Fisher SA, Langille BL and Srivastava D. Apoptosis during cardiovascular development. *Circulation research*. 2000;87:856-64.
  114. Poelmann RE and Gittenberger-de Groot AC. Apoptosis as an instrument in cardiovascular development. *Birth Defects Res C Embryo Today*. 2005;75:305-13.
  115. Zhao Z and Rivkees SA. Programmed cell death in the developing heart: regulation by BMP4 and FGF2. *Developmental dynamics : an official publication of the American Association of Anatomists*. 2000;217:388-400.
  116. Ya J, van den Hoff MJ, de Boer PA, Tesink-Taekema S, Franco D, Moorman AF and Lamers WH. Normal development of the outflow tract in the rat. *Circulation research*. 1998;82:464-72.



117. van den Hoff MJ, Moorman AF, Ruijter JM, Lamers WH, Bennington RW, Markwald RR and Wessels A. Myocardialization of the cardiac outflow tract. *Developmental biology*. 1999;212:477-90.
118. Varfolomeev EE, Schuchmann M, Luria V, Chiannikulchai N, Beckmann JS, Mett IL, Rebrikov D, Brodianski VM, Kemper OC, Kollet O, Lapidot T, Soffer D, Sobe T, Avraham KB, Goncharov T, Holtmann H, Lonai P and Wallach D. Targeted disruption of the mouse Caspase 8 gene ablates cell death induction by the TNF receptors, Fas/Apo1, and DR3 and is lethal prenatally. *Immunity*. 1998;9:267-76.
119. Feng Q, Song W, Lu X, Hamilton JA, Lei M, Peng T and Yee SP. Development of heart failure and congenital septal defects in mice lacking endothelial nitric oxide synthase. *Circulation*. 2002;106:873-9.
120. Song W, Lu X and Feng Q. Tumor necrosis factor-alpha induces apoptosis via inducible nitric oxide synthase in neonatal mouse cardiomyocytes. *Cardiovascular research*. 2000;45:595-602.
121. Huang X, Huang F, Yang D, Dong F, Shi X, Wang H, Zhou X, Wang S and Dai S. Expression of microRNA-122 contributes to apoptosis in H9C2 myocytes. *J Cell Mol Med*. 2012;16:2637-46.
122. Morton SU and Brodsky D. Fetal Physiology and the Transition to Extrauterine Life. *Clin Perinatol*. 2016;43:395-407.
123. Olley PM and Coceani F. Prostaglandins and the ductus arteriosus. *Annu Rev Med*. 1981;32:375-85.
124. Reese DE, Mikawa T and Bader DM. Development of the coronary vessel system. *Circ Res*. 2002;91:761-8.
125. Mu H, Ohashi R, Lin P, Yao Q and Chen C. Cellular and molecular mechanisms of coronary vessel development. *Vasc Med*. 2005;10:37-44.
126. Cai CL, Martin JC, Sun Y, Cui L, Wang L, Ouyang K, Yang L, Bu L, Liang X, Zhang X, Stallcup WB, Denton CP, McCulloch A, Chen J and Evans SM. A myocardial lineage derives from Tbx18 epicardial cells. *Nature*. 2008;454:104-8.
127. Vicente-Steijn R, Scherptong RW, Kruithof BP, Duim SN, Goumans MJ, Wisse LJ, Zhou B, Pu WT, Poelmann RE, Schaliq MJ, Tallquist MD, Gittenberger-de Groot AC and Jongbloed MR. Regional differences in WT-1 and Tcf21 expression during ventricular development: implications for myocardial compaction. *PloS one*. 2015;10:e0136025.
128. Eralp I, Lie-Venema H, DeRuiter MC, van den Akker NM, Bogers AJ, Mentink MM, Poelmann RE and Gittenberger-de Groot AC. Coronary artery and orifice development is associated with proper timing of epicardial outgrowth and

- correlated Fas-ligand-associated apoptosis patterns. *Circulation research*. 2005;96:526-34.
129. Barker DJ. Coronary heart disease: a disorder of growth. *Horm Res*. 2003;59 Suppl 1:35-41.
  130. Lamouille S, Xu J and Derynck R. Molecular mechanisms of epithelial-mesenchymal transition. *Nat Rev Mol Cell Biol*. 2014;15:178-96.
  131. Batlle E, Sancho E, Franci C, Dominguez D, Monfar M, Baulida J and Garcia De Herreros A. The transcription factor snail is a repressor of E-cadherin gene expression in epithelial tumour cells. *Nat Cell Biol*. 2000;2:84-9.
  132. Hartsock A and Nelson WJ. Adherens and tight junctions: structure, function and connections to the actin cytoskeleton. *Biochim Biophys Acta*. 2008;1778:660-9.
  133. Ridley AJ. Life at the leading edge. *Cell*. 2011;145:1012-22.
  134. Kwee L, Baldwin HS, Shen HM, Stewart CL, Buck C, Buck CA and Labow MA. Defective development of the embryonic and extraembryonic circulatory systems in vascular cell adhesion molecule (VCAM-1) deficient mice. *Development*. 1995;121:489-503.
  135. Yang JT, Rayburn H and Hynes RO. Cell adhesion events mediated by alpha 4 integrins are essential in placental and cardiac development. *Development*. 1995;121:549-60.
  136. Moore AW, McInnes L, Kreidberg J, Hastie ND and Schedl A. YAC complementation shows a requirement for Wt1 in the development of epicardium, adrenal gland and throughout nephrogenesis. *Development*. 1999;126:1845-57.
  137. Martinez-Estrada OM, Lettice LA, Essafi A, Guadix JA, Slight J, Velecela V, Hall E, Reichmann J, Devenney PS, Hohenstein P, Hosen N, Hill RE, Munoz-Chapuli R and Hastie ND. Wt1 is required for cardiovascular progenitor cell formation through transcriptional control of Snail and E-cadherin. *Nat Genet*. 2010;42:89-93.
  138. Guadix JA, Ruiz-Villalba A, Lettice L, Velecela V, Munoz-Chapuli R, Hastie ND, Perez-Pomares JM and Martinez-Estrada OM. Wt1 controls retinoic acid signalling in embryonic epicardium through transcriptional activation of Raldh2. *Development*. 2011;138:1093-7.
  139. Crispino JD, Lodish MB, Thurberg BL, Litovsky SH, Collins T, Molkentin JD and Orkin SH. Proper coronary vascular development and heart morphogenesis depend on interaction of GATA-4 with FOG cofactors. *Genes Dev*. 2001;15:839-44.

140. Moore AW, Schedl A, McInnes L, Doyle M, Hecksher-Sorensen J and Hastie ND. YAC transgenic analysis reveals Wilms' tumour 1 gene activity in the proliferating coelomic epithelium, developing diaphragm and limb. *Mech Dev.* 1998;79:169-84.
141. Zamora M, Manner J and Ruiz-Lozano P. Epicardium-derived progenitor cells require beta-catenin for coronary artery formation. *Proceedings of the National Academy of Sciences of the United States of America.* 2007;104:18109-14.
142. Winter J, Jung S, Keller S, Gregory RI and Diederichs S. Many roads to maturity: microRNA biogenesis pathways and their regulation. *Nat Cell Biol.* 2009;11:228-34.
143. Lewis BP, Burge CB and Bartel DP. Conserved seed pairing, often flanked by adenosines, indicates that thousands of human genes are microRNA targets. *Cell.* 2005;120:15-20.
144. Reinhart BJ, Slack FJ, Basson M, Pasquinelli AE, Bettinger JC, Rougvie AE, Horvitz HR and Ruvkun G. The 21-nucleotide let-7 RNA regulates developmental timing in *Caenorhabditis elegans*. *Nature.* 2000;403:901-6.
145. Cordes KR and Srivastava D. MicroRNA regulation of cardiovascular development. *Circ Res.* 2009;104:724-32.
146. Ha M and Kim VN. Regulation of microRNA biogenesis. *Nat Rev Mol Cell Biol.* 2014;15:509-24.
147. Kim VN, Han J and Siomi MC. Biogenesis of small RNAs in animals. *Nat Rev Mol Cell Biol.* 2009;10:126-39.
148. Lee Y, Ahn C, Han J, Choi H, Kim J, Yim J, Lee J, Provost P, Radmark O, Kim S and Kim VN. The nuclear RNase III Drosha initiates microRNA processing. *Nature.* 2003;425:415-9.
149. Flores-Jasso CF, Arenas-Huertero C, Reyes JL, Contreras-Cubas C, Covarrubias A and Vaca L. First step in pre-miRNAs processing by human Dicer. *Acta Pharmacol Sin.* 2009;30:1177-85.
150. Khvorova A, Reynolds A and Jayasena SD. Functional siRNAs and miRNAs exhibit strand bias. *Cell.* 2003;115:209-16.
151. Rand TA, Ginalski K, Grishin NV and Wang X. Biochemical identification of Argonaute 2 as the sole protein required for RNA-induced silencing complex activity. *Proc Natl Acad Sci U S A.* 2004;101:14385-9.
152. Kehl T, Backes C, Kern F, Fehlmann T, Ludwig N, Meese E, Lenhof HP and Keller A. About miRNAs, miRNA seeds, target genes and target pathways. *Oncotarget.* 2017;8:107167-107175.

153. Porrello ER. microRNAs in cardiac development and regeneration. *Clin Sci (Lond)*. 2013;125:151-66.
154. Zhao Y, Samal E and Srivastava D. Serum response factor regulates a muscle-specific microRNA that targets Hand2 during cardiogenesis. *Nature*. 2005;436:214-20.
155. Huang ZP, Chen JF, Regan JN, Maguire CT, Tang RH, Dong XR, Majesky MW and Wang DZ. Loss of microRNAs in neural crest leads to cardiovascular syndromes resembling human congenital heart defects. *Arteriosclerosis, thrombosis, and vascular biology*. 2010;30:2575-86.
156. Singh MK, Lu MM, Massera D and Epstein JA. MicroRNA-processing enzyme Dicer is required in epicardium for coronary vasculature development. *J Biol Chem*. 2011;286:41036-45.
157. Albinsson S, Suarez Y, Skoura A, Offermanns S, Miano JM and Sessa WC. MicroRNAs are necessary for vascular smooth muscle growth, differentiation, and function. *Arteriosclerosis, thrombosis, and vascular biology*. 2010;30:1118-26.
158. Ivey KN and Srivastava D. microRNAs as Developmental Regulators. *Cold Spring Harb Perspect Biol*. 2015;7:a008144.
159. Porrello ER, Johnson BA, Aurora AB, Simpson E, Nam YJ, Matkovich SJ, Dorn GW, 2nd, van Rooij E and Olson EN. MiR-15 family regulates postnatal mitotic arrest of cardiomyocytes. *Circ Res*. 2011;109:670-9.
160. Kim GH, Samant SA, Earley JU and Svensson EC. Translational control of FOG-2 expression in cardiomyocytes by microRNA-130a. *PLoS One*. 2009;4:e6161.
161. Zhao Y, Ransom JF, Li A, Vedantham V, von Drehle M, Muth AN, Tsuchihashi T, McManus MT, Schwartz RJ and Srivastava D. Dysregulation of cardiogenesis, cardiac conduction, and cell cycle in mice lacking miRNA-1-2. *Cell*. 2007;129:303-17.
162. McFadden DG, Barbosa AC, Richardson JA, Schneider MD, Srivastava D and Olson EN. The Hand1 and Hand2 transcription factors regulate expansion of the embryonic cardiac ventricles in a gene dosage-dependent manner. *Development*. 2005;132:189-201.
163. Yu ZB, Han SP, Bai YF, Zhu C, Pan Y and Guo XR. microRNA expression profiling in fetal single ventricle malformation identified by deep sequencing. *Int J Mol Med*. 2012;29:53-60.
164. Latronico MV, Catalucci D and Condorelli G. MicroRNA and cardiac pathologies. *Physiol Genomics*. 2008;34:239-42.

165. Bittel DC, Kibiryeveva N, Marshall JA and O'Brien JE. MicroRNA-421 Dysregulation is Associated with Tetralogy of Fallot. *Cells*. 2014;3:713-23.
166. Thakral S and Ghoshal K. miR-122 is a unique molecule with great potential in diagnosis, prognosis of liver disease, and therapy both as miRNA mimic and antimir. *Curr Gene Ther*. 2015;15:142-50.
167. Gatfield D, Le Martelot G, Vejnar CE, Gerlach D, Schaad O, Fleury-Olela F, Ruskeepaa AL, Oresic M, Esau CC, Zdobnov EM and Schibler U. Integration of microRNA miR-122 in hepatic circadian gene expression. *Genes Dev*. 2009;23:1313-26.
168. D'Ambrogio A, Gu W, Udagawa T, Mello CC and Richter JD. Specific miRNA stabilization by Gld2-catalyzed monoadenylation. *Cell Rep*. 2012;2:1537-45.
169. Esau C, Davis S, Murray SF, Yu XX, Pandey SK, Pear M, Watts L, Booten SL, Graham M, McKay R, Subramaniam A, Propp S, Lollo BA, Freier S, Bennett CF, Bhanot S and Monia BP. miR-122 regulation of lipid metabolism revealed by in vivo antisense targeting. *Cell Metab*. 2006;3:87-98.
170. Chang J, Nicolas E, Marks D, Sander C, Lerro A, Buendia MA, Xu C, Mason WS, Moloshok T, Bort R, Zaret KS and Taylor JM. miR-122, a mammalian liver-specific microRNA, is processed from hcr mRNA and may downregulate the high affinity cationic amino acid transporter CAT-1. *RNA Biol*. 2004;1:106-13.
171. Machlin ES, Sarnow P and Sagan SM. Masking the 5' terminal nucleotides of the hepatitis C virus genome by an unconventional microRNA-target RNA complex. *Proceedings of the National Academy of Sciences of the United States of America*. 2011;108:3193-8.
172. Schult P, Roth H, Adams RL, Mas C, Imbert L, Orlik C, Ruggieri A, Pyle AM and Lohmann V. microRNA-122 amplifies hepatitis C virus translation by shaping the structure of the internal ribosomal entry site. *Nat Commun*. 2018;9:2613.
173. Hsu SH, Wang B, Kutay H, Bid H, Shreve J, Zhang X, Costinean S, Bratasz A, Houghton P and Ghoshal K. Hepatic loss of miR-122 predisposes mice to hepatobiliary cyst and hepatocellular carcinoma upon diethylnitrosamine exposure. *Am J Pathol*. 2013;183:1719-1730.
174. Coulouarn C, Factor VM, Andersen JB, Durkin ME and Thorgeirsson SS. Loss of miR-122 expression in liver cancer correlates with suppression of the hepatic phenotype and gain of metastatic properties. *Oncogene*. 2009;28:3526-36.
175. Bai S, Nasser MW, Wang B, Hsu SH, Datta J, Kutay H, Yadav A, Nuovo G, Kumar P and Ghoshal K. MicroRNA-122 inhibits tumorigenic properties of hepatocellular carcinoma cells and sensitizes these cells to sorafenib. *J Biol Chem*. 2009;284:32015-27.

176. Wang B, Wang H and Yang Z. MiR-122 inhibits cell proliferation and tumorigenesis of breast cancer by targeting IGF1R. *PLoS One*. 2012;7:e47053.
177. Rao M, Zhu Y, Zhou Y, Cong X and Feng L. MicroRNA-122 inhibits proliferation and invasion in gastric cancer by targeting CREB1. *Am J Cancer Res*. 2017;7:323-333.
178. Qin H, Sha J, Jiang C, Gao X, Qu L, Yan H, Xu T, Jiang Q and Gao H. miR-122 inhibits metastasis and epithelial-mesenchymal transition of non-small-cell lung cancer cells. *Oncotargets Ther*. 2015;8:3175-84.
179. Wang Y, Xing QF, Liu XQ, Guo ZJ, Li CY and Sun G. MiR-122 targets VEGFC in bladder cancer to inhibit tumor growth and angiogenesis. *Am J Transl Res*. 2016;8:3056-66.
180. Barajas JM, Reyes R, Guerrero MJ, Jacob ST, Motiwala T and Ghoshal K. The role of miR-122 in the dysregulation of glucose-6-phosphate dehydrogenase (G6PD) expression in hepatocellular cancer. *Sci Rep*. 2018;8:9105.
181. Zhang Y and Tang L. Inhibition of breast cancer cell proliferation and tumorigenesis by long non-coding RNA RPPH1 down-regulation of miR-122 expression. *Cancer Cell Int*. 2017;17:109.
182. Wang W, Yang J, Yu F, Li W, Wang L, Zou H and Long X. MicroRNA-122-3p inhibits tumor cell proliferation and induces apoptosis by targeting Forkhead box O in A549 cells. *Oncol Lett*. 2018;15:2695-2699.
183. Cao F and Yin LX. miR-122 enhances sensitivity of hepatocellular carcinoma to oxaliplatin via inhibiting MDR1 by targeting Wnt/beta-catenin pathway. *Exp Mol Pathol*. 2019;106:34-43.
184. D'Alessandra Y, Devanna P, Limana F, Straino S, Di Carlo A, Brambilla PG, Rubino M, Carena MC, Spazzafumo L, De Simone M, Micheli B, Biglioli P, Achilli F, Martelli F, Maggiolini S, Marenzi G, Pompilio G and Capogrossi MC. Circulating microRNAs are new and sensitive biomarkers of myocardial infarction. *European heart journal*. 2010;31:2765-73.
185. Li XD, Yang YJ, Wang LY, Qiao SB, Lu XF, Wu YJ, Xu B, Li HF and Gu DF. Elevated plasma miRNA-122, -140-3p, -720, -2861, and -3149 during early period of acute coronary syndrome are derived from peripheral blood mononuclear cells. *PLoS One*. 2017;12:e0184256.
186. Wang YL and Yu W. Association of circulating microRNA-122 with presence and severity of atherosclerotic lesions. *PeerJ*. 2018;6:e5218.
187. Gilje P, Frydland M, Bro-Jeppesen J, Dankiewicz J, Friberg H, Rundgren M, Devaux Y, Stammet P, Al-Mashat M, Jogi J, Kjaergaard J, Hassager C and Erlinge D. The association between plasma miR-122-5p release pattern at

- admission and all-cause mortality or shock after out-of-hospital cardiac arrest. *Biomarkers*. 2019;24:29-35.
188. Liu X, Meng H, Jiang C, Yang S, Cui F and Yang P. Differential microRNA Expression and Regulation in the Rat Model of Post-Infarction Heart Failure. *PLoS One*. 2016;11:e0160920.
189. Gebert LF, Rebhan MA, Crivelli SE, Denzler R, Stoffel M and Hall J. Miravirsen (SPC3649) can inhibit the biogenesis of miR-122. *Nucleic Acids Res*. 2014;42:609-21.
190. van der Ree MH, van der Meer AJ, van Nuenen AC, de Bruijne J, Ottosen S, Janssen HL, Kootstra NA and Reesink HW. Miravirsen dosing in chronic hepatitis C patients results in decreased microRNA-122 levels without affecting other microRNAs in plasma. *Aliment Pharmacol Ther*. 2016;43:102-13.
191. Jopling CL, Yi M, Lancaster AM, Lemon SM and Sarnow P. Modulation of hepatitis C virus RNA abundance by a liver-specific MicroRNA. *Science*. 2005;309:1577-81.
192. Jopling CL, Schutz S and Sarnow P. Position-dependent function for a tandem microRNA miR-122-binding site located in the hepatitis C virus RNA genome. *Cell Host Microbe*. 2008;4:77-85.
193. Lanford RE, Hildebrandt-Eriksen ES, Petri A, Persson R, Lindow M, Munk ME, Kauppinen S and Orum H. Therapeutic silencing of microRNA-122 in primates with chronic hepatitis C virus infection. *Science*. 2010;327:198-201.
194. Jenkins KJ, Correa A, Feinstein JA, Botto L, Britt AE, Daniels SR, Elixson M, Warnes CA, Webb CL and American Heart Association Council on Cardiovascular Disease in the Y. Noninherited risk factors and congenital cardiovascular defects: current knowledge: a scientific statement from the American Heart Association Council on Cardiovascular Disease in the Young: endorsed by the American Academy of Pediatrics. *Circulation*. 2007;115:2995-3014.
195. van der Bom T, Zomer AC, Zwinderman AH, Meijboom FJ, Bouma BJ and Mulder BJ. The changing epidemiology of congenital heart disease. *Nat Rev Cardiol*. 2011;8:50-60.
196. Cleves MA, Ghaffar S, Zhao W, Mosley BS and Hobbs CA. First-year survival of infants born with congenital heart defects in Arkansas (1993-1998): a survival analysis using registry data. *Birth defects research Part A, Clinical and molecular teratology*. 2003;67:662-8.
197. Dolk H, Loane M and Garne E. The prevalence of congenital anomalies in Europe. *Adv Exp Med Biol*. 2010;686:349-64.

198. Gilboa SM, Devine OJ, Kucik JE, Oster ME, Riehle-Colarusso T, Nembhard WN, Xu P, Correa A, Jenkins K and Marelli AJ. Congenital Heart Defects in the United States: Estimating the Magnitude of the Affected Population in 2010. *Circulation*. 2016;134:101-9.
199. Fox D, Devendra GP, Hart SA and Krasuski RA. When 'blue babies' grow up: What you need to know about tetralogy of Fallot. *Cleve Clin J Med*. 2010;77:821-8.
200. Moazzen H, Lu X, Liu M and Feng Q. Pregestational diabetes induces fetal coronary artery malformation via reactive oxygen species signaling. *Diabetes*. 2015;64:1431-43.
201. Borghi A, Ciuffreda M, Quattrocioni M and Preda L. The grown-up congenital cardiac patient. *J Cardiovasc Med (Hagerstown)*. 2007;8:78-82.
202. Warnes CA. The adult with congenital heart disease: born to be bad? *J Am Coll Cardiol*. 2005;46:1-8.
203. Marelli A, Miller SP, Marino BS, Jefferson AL and Newburger JW. Brain in Congenital Heart Disease Across the Lifespan: The Cumulative Burden of Injury. *Circulation*. 2016;133:1951-62.
204. Egbe A, Lee S, Ho D, Uppu S and Srivastava S. Prevalence of congenital anomalies in newborns with congenital heart disease diagnosis. *Ann Pediatr Cardiol*. 2014;7:86-91.
205. Calderon J. Executive Function in Patients with Congenital Heart Disease: Only the Tip of the Iceberg? *J Pediatr*. 2016;173:7-9.
206. Marino BS, Lipkin PH, Newburger JW, Peacock G, Gerdes M, Gaynor JW, Mussatto KA, Uzark K, Goldberg CS, Johnson WH, Jr., Li J, Smith SE, Bellinger DC, Mahle WT, American Heart Association Congenital Heart Defects Committee CoCDitYCoCN and Stroke C. Neurodevelopmental outcomes in children with congenital heart disease: evaluation and management: a scientific statement from the American Heart Association. *Circulation*. 2012;126:1143-72.
207. Marelli AJ, Ionescu-Ittu R, Mackie AS, Guo L, Dendukuri N and Kaouache M. Lifetime prevalence of congenital heart disease in the general population from 2000 to 2010. *Circulation*. 2014;130:749-56.
208. Hoffman JI and Kaplan S. The incidence of congenital heart disease. *J Am Coll Cardiol*. 2002;39:1890-900.
209. Leirgul E, Fomina T, Brodwall K, Greve G, Holmstrom H, Vollset SE, Tell GS and Oyen N. Birth prevalence of congenital heart defects in Norway 1994-2009--a nationwide study. *Am Heart J*. 2014;168:956-64.



210. Bhatt AB, Foster E, Kuehl K, Alpert J, Brabeck S, Crumb S, Davidson WR, Jr., Earing MG, Ghoshhajra BB, Karamlou T, Mital S, Ting J, Tseng ZH and American Heart Association Council on Clinical C. Congenital heart disease in the older adult: a scientific statement from the American Heart Association. *Circulation*. 2015;131:1884-931.
211. Arth AC, Tinker SC, Simeone RM, Ailes EC, Cragan JD and Grosse SD. Inpatient Hospitalization Costs Associated with Birth Defects Among Persons of All Ages - United States, 2013. *MMWR Morb Mortal Wkly Rep*. 2017;66:41-46.
212. Jacobs JP, Burke RP, Quintessenza JA and Mavroudis C. Congenital Heart Surgery Nomenclature and Database Project: atrioventricular canal defect. *Ann Thorac Surg*. 2000;69:S36-43.
213. Dakkak W and Oliver TI. Ventricular Septal Defect *StatPearls* Treasure Island (FL); 2019.
214. Blom NA, Ottenkamp J, Wenink AG and Gittenberger-de Groot AC. Deficiency of the vestibular spine in atrioventricular septal defects in human fetuses with down syndrome. *Am J Cardiol*. 2003;91:180-4.
215. Conway SJ, Henderson DJ, Kirby ML, Anderson RH and Copp AJ. Development of a lethal congenital heart defect in the splotch (Pax3) mutant mouse. *Cardiovascular research*. 1997;36:163-73.
216. Kirby ML, Gale TF and Stewart DE. Neural crest cells contribute to normal aorticopulmonary septation. *Science*. 1983;220:1059-61.
217. Supino PG, Borer JS, Preibisz J and Bornstein A. The epidemiology of valvular heart disease: a growing public health problem. *Heart Fail Clin*. 2006;2:379-93.
218. Otto CM, Lind BK, Kitzman DW, Gersh BJ and Siscovick DS. Association of aortic-valve sclerosis with cardiovascular mortality and morbidity in the elderly. *N Engl J Med*. 1999;341:142-7.
219. De Giorgio F, Abbate A, Stigliano E, Capelli A and Arena V. Hypoplastic coronary artery disease causing sudden death. Report of two cases and review of the literature. *Cardiovasc Pathol*. 2010;19:e107-11.
220. Taylor AJ, Rogan KM and Virmani R. Sudden cardiac death associated with isolated congenital coronary artery anomalies. *J Am Coll Cardiol*. 1992;20:640-7.
221. Tuo G, Marasini M, Brunelli C, Zannini L and Balbi M. Incidence and clinical relevance of primary congenital anomalies of the coronary arteries in children and adults. *Cardiol Young*. 2013;23:381-6.
222. Yamanaka O and Hobbs RE. Coronary artery anomalies in 126,595 patients undergoing coronary arteriography. *Cathet Cardiovasc Diagn*. 1990;21:28-40.

223. Baltaxe HA and Wixson D. The incidence of congenital anomalies of the coronary arteries in the adult population. *Radiology*. 1977;122:47-52.
224. Pierpont ME, Basson CT, Benson DWJ, Gelb BD, Giglia TM, Goldmuntz E, McGee G, Sable CA, Srivastava D and Webb CL. Genetic basis for congenital heart defects: current knowledge: a scientific statement from the American Heart Association Congenital Cardiac Defects Committee, Council on Cardiovascular Disease in the Young: endorsed by the American Academy of Pediatrics. *Circulation*. 2007;115:3015-38.
225. CANADIAN CONGENITAL HEART ALLIANCE. 2016.
226. Parker SE, Mai CT, Canfield MA, Rickard R, Wang Y, Meyer RE, Anderson P, Mason CA, Collins JS, Kirby RS, Correa A and National Birth Defects Prevention N. Updated National Birth Prevalence estimates for selected birth defects in the United States, 2004-2006. *Birth defects research Part A, Clinical and molecular teratology*. 2010;88:1008-16.
227. Bjornard K, Riehle-Colarusso T, Gilboa SM and Correa A. Patterns in the prevalence of congenital heart defects, metropolitan Atlanta, 1978 to 2005. *Birth defects research Part A, Clinical and molecular teratology*. 2013;97:87-94.
228. McElhinney DB, Geiger E, Blinder J, Benson DW and Goldmuntz E. NKX2.5 mutations in patients with congenital heart disease. *J Am Coll Cardiol*. 2003;42:1650-5.
229. Paladini D, Tartaglione A, Agangi A, Teodoro A, Forleo F, Borghese A and Martinelli P. The association between congenital heart disease and Down syndrome in prenatal life. *Ultrasound Obstet Gynecol*. 2000;15:104-8.
230. Lee LJ and Lupo PJ. Maternal smoking during pregnancy and the risk of congenital heart defects in offspring: a systematic review and metaanalysis. *Pediatr Cardiol*. 2013;34:398-407.
231. Sullivan PM, Dervan LA, Reiger S, Buddhe S and Schwartz SM. Risk of congenital heart defects in the offspring of smoking mothers: a population-based study. *J Pediatr*. 2015;166:978-984 e2.
232. Baardman ME, Kerstjens-Frederikse WS, Corpeleijn E, de Walle HE, Hofstra RM, Berger RM and Bakker MK. Combined adverse effects of maternal smoking and high body mass index on heart development in offspring: evidence for interaction? *Heart*. 2012;98:474-9.
233. Cai GJ, Sun XX, Zhang L and Hong Q. Association between maternal body mass index and congenital heart defects in offspring: a systematic review. *American journal of obstetrics and gynecology*. 2014;211:91-117.

234. Waller DK, Shaw GM, Rasmussen SA, Hobbs CA, Canfield MA, Siega-Riz AM, Gallaway MS, Correa A and National Birth Defects Prevention S. Prepregnancy obesity as a risk factor for structural birth defects. *Arch Pediatr Adolesc Med.* 2007;161:745-50.
235. Auger N, Fraser WD, Healy-Profitos J and Arbour L. Association Between Preeclampsia and Congenital Heart Defects. *Jama.* 2015;314:1588-98.
236. Dong DY, Binongo JN and Kancherla V. Maternal Chlamydia Infection During Pregnancy and Risk of Cyanotic Congenital Heart Defects in the Offspring. *Matern Child Health J.* 2016;20:66-76.
237. Oster ME, Riehle-Colarusso T and Correa A. An update on cardiovascular malformations in congenital rubella syndrome. *Birth defects research Part A, Clinical and molecular teratology.* 2010;88:1-8.
238. Zheng JY, Tian HT, Zhu ZM, Li B, Han L, Jiang SL, Chen Y, Li DT, He JC, Zhao Z, Cao Y, Qiu YG and Li TC. Prevalence of symptomatic congenital heart disease in Tibetan school children. *Am J Cardiol.* 2013;112:1468-70.
239. Hoang TT, Marengo LK, Mitchell LE, Canfield MA and Agopian AJ. Original Findings and Updated Meta-Analysis for the Association Between Maternal Diabetes and Risk for Congenital Heart Disease Phenotypes. *Am J Epidemiol.* 2017;186:118-128.
240. Oyen N, Diaz LJ, Leirgul E, Boyd HA, Priest J, Mathiesen ER, Quertermous T, Wohlfahrt J and Melbye M. Prepregnancy Diabetes and Offspring Risk of Congenital Heart Disease: A Nationwide Cohort Study. *Circulation.* 2016;133:2243-53.
241. Liu S, Joseph KS, Lisonkova S, Rouleau J, Van den Hof M, Sauve R, Kramer MS and Canadian Perinatal Surveillance S. Association between maternal chronic conditions and congenital heart defects: a population-based cohort study. *Circulation.* 2013;128:583-9.
242. Loffredo CA, Wilson PD and Ferencz C. Maternal diabetes: an independent risk factor for major cardiovascular malformations with increased mortality of affected infants. *Teratology.* 2001;64:98-106.
243. Fong A, Serra A, Herrero T, Pan D and Ogunyemi D. Pre-gestational versus gestational diabetes: a population based study on clinical and demographic differences. *Journal of diabetes and its complications.* 2014;28:29-34.
244. Moazzen H, Lu X, Ma NL, Velenosi TJ, Urquhart BL, Wisse LJ, Gittenberger-de Groot AC and Feng Q. N-Acetylcysteine prevents congenital heart defects induced by pregestational diabetes. *Cardiovascular diabetology.* 2014;13:46.

245. Sivan E, Reece EA, Wu YK, Homko CJ, Polansky M and Borenstein M. Dietary vitamin E prophylaxis and diabetic embryopathy: morphologic and biochemical analysis. *American journal of obstetrics and gynecology*. 1996;175:793-9.
246. Siman CM and Eriksson UJ. Vitamin E decreases the occurrence of malformations in the offspring of diabetic rats. *Diabetes*. 1997;46:1054-61.
247. Siman CM and Eriksson UJ. Vitamin C supplementation of the maternal diet reduces the rate of malformation in the offspring of diabetic rats. *Diabetologia*. 1997;40:1416-24.
248. Sivan E, Lee YC, Wu YK and Reece EA. Free radical scavenging enzymes in fetal dysmorphogenesis among offspring of diabetic rats. *Teratology*. 1997;56:343-9.
249. Eriksson UJ and Siman CM. Pregnant diabetic rats fed the antioxidant butylated hydroxytoluene show decreased occurrence of malformations in offspring. *Diabetes*. 1996;45:1497-502.
250. Russell NE, Higgins MF, Kinsley BF, Foley ME and McAuliffe FM. Heart rate variability in neonates of type 1 diabetic pregnancy. *Early Hum Dev*. 2016;92:51-5.
251. Sirico A, Sarno L, Zullo F, Martinelli P and Maruotti GM. Pregestational diabetes and fetal heart rate in the first trimester of pregnancy. *Eur J Obstet Gynecol Reprod Biol*. 2019;232:30-32.
252. Tincello D, White S and Walkinshaw S. Computerised analysis of fetal heart rate recordings in maternal type I diabetes mellitus. *BJOG*. 2001;108:853-7.
253. Bacharova L, Krivosikova Z, Wsolova L and Gajdos M. Alterations in the QRS complex in the offspring of patients with metabolic syndrome and diabetes mellitus: early evidence of cardiovascular pathology. *J Electrocardiol*. 2012;45:244-51.
254. Kendrick JM, Wilson C, Elder RF and Smith CS. Reliability of reporting of self-monitoring of blood glucose in pregnant women. *J Obstet Gynecol Neonatal Nurs*. 2005;34:329-34.
255. Dunachie S and Chamnan P. The double burden of diabetes and global infection in low and middle-income countries. *Trans R Soc Trop Med Hyg*. 2019;113:56-64.
256. Phillips DI. External influences on the fetus and their long-term consequences. *Lupus*. 2006;15:794-800.
257. Brownlee M. Biochemistry and molecular cell biology of diabetic complications. *Nature*. 2001;414:813-20.

258. Brieger K, Schiavone S, Miller FJ, Jr. and Krause KH. Reactive oxygen species: from health to disease. *Swiss Med Wkly*. 2012;142:w13659.
259. Nazarewicz RR, Dikalova AE, Bikineyeva A and Dikalov SI. Nox2 as a potential target of mitochondrial superoxide and its role in endothelial oxidative stress. *American journal of physiology Heart and circulatory physiology*. 2013;305:H1131-40.
260. Takahashi M. Oxidative stress and redox regulation on in vitro development of mammalian embryos. *The Journal of reproduction and development*. 2012;58:1-9.
261. Lopaschuk GD and Jaswal JS. Energy metabolic phenotype of the cardiomyocyte during development, differentiation, and postnatal maturation. *J Cardiovasc Pharmacol*. 2010;56:130-40.
262. Dong D, Zhang Y, Reece EA, Wang L, Harman CR and Yang P. microRNA expression profiling and functional annotation analysis of their targets modulated by oxidative stress during embryonic heart development in diabetic mice. *Reproductive toxicology*. 2016;65:365-374.
263. Shi R, Zhao L, Cai W, Wei M, Zhou X, Yang G and Yuan L. Maternal exosomes in diabetes contribute to the cardiac development deficiency. *Biochem Biophys Res Commun*. 2017;483:602-608.
264. Aldosari S, Awad M, Harrington EO, Sellke FW and Abid MR. Subcellular Reactive Oxygen Species (ROS) in Cardiovascular Pathophysiology. *Antioxidants (Basel)*. 2018;7.
265. Ignarro LJ. Nitric oxide is not just blowing in the wind. *Br J Pharmacol*. 2019;176:131-134.
266. Stuehr DJ and Haque MM. Nitric oxide synthase enzymology in the 20 years after the Nobel Prize. *Br J Pharmacol*. 2019;176:177-188.
267. Knowles RG and Moncada S. Nitric oxide synthases in mammals. *The Biochemical journal*. 1994;298 ( Pt 2):249-58.
268. Francis SH, Busch JL, Corbin JD and Sibley D. cGMP-dependent protein kinases and cGMP phosphodiesterases in nitric oxide and cGMP action. *Pharmacol Rev*. 2010;62:525-63.
269. Erwin PA, Lin AJ, Golan DE and Michel T. Receptor-regulated dynamic S-nitrosylation of endothelial nitric-oxide synthase in vascular endothelial cells. *J Biol Chem*. 2005;280:19888-94.
270. Liu Y and Feng Q. NOing the heart: role of nitric oxide synthase-3 in heart development. *Differentiation; research in biological diversity*. 2012;84:54-61.

271. Bendall JK, Douglas G, McNeill E, Channon KM and Crabtree MJ. Tetrahydrobiopterin in cardiovascular health and disease. *Antioxidants & redox signaling*. 2014;20:3040-77.
272. Werner ER, Blau N and Thony B. Tetrahydrobiopterin: biochemistry and pathophysiology. *The Biochemical journal*. 2011;438:397-414.
273. Sugiyama T, Levy BD and Michel T. Tetrahydrobiopterin recycling, a key determinant of endothelial nitric-oxide synthase-dependent signaling pathways in cultured vascular endothelial cells. *J Biol Chem*. 2009;284:12691-700.
274. Wei CC, Wang ZQ, Tejero J, Yang YP, Hemann C, Hille R and Stuehr DJ. Catalytic reduction of a tetrahydrobiopterin radical within nitric-oxide synthase. *J Biol Chem*. 2008;283:11734-42.
275. Hussein D, Starr A, Heikal L, McNeill E, Channon KM, Brown PR, Sutton BJ, McDonnell JM and Nandi M. Validating the GTP-cyclohydrolase 1-feedback regulatory complex as a therapeutic target using biophysical and in vivo approaches. *Br J Pharmacol*. 2015;172:4146-57.
276. Pucciarelli S, Spina M, Montecchia F, Lupidi G, Eleuteri AM, Fioretti E and Angeletti M. Peroxynitrite-mediated oxidation of the C85S/C152E mutant of dihydrofolate reductase from *Escherichia coli*: functional and structural effects. *Arch Biochem Biophys*. 2005;434:221-31.
277. Heitzer T, Brockhoff C, Mayer B, Warnholtz A, Mollnau H, Henne S, Meinertz T and Munzel T. Tetrahydrobiopterin improves endothelium-dependent vasodilation in chronic smokers : evidence for a dysfunctional nitric oxide synthase. *Circulation research*. 2000;86:E36-41.
278. Wyss CA, Koepfli P, Namdar M, Siegrist PT, Luscher TF, Camici PG and Kaufmann PA. Tetrahydrobiopterin restores impaired coronary microvascular dysfunction in hypercholesterolaemia. *Eur J Nucl Med Mol Imaging*. 2005;32:84-91.
279. Mayahi L, Heales S, Owen D, Casas JP, Harris J, MacAllister RJ and Hingorani AD. (6R)-5,6,7,8-tetrahydro-L-biopterin and its stereoisomer prevent ischemia reperfusion injury in human forearm. *Arterioscler Thromb Vasc Biol*. 2007;27:1334-9.
280. Qu J, Yang T, Wang E, Li M, Chen C, Ma L, Zhou Y and Cui Y. Efficacy and safety of sapropterin dihydrochloride in patients with phenylketonuria: A meta-analysis of randomized controlled trials. *Br J Clin Pharmacol*. 2019;85:893-899.
281. *Pharmacoeconomic Review Report: Sapropterin dihydrochloride (Kuvan)* Ottawa (ON); 2017.

282. Vockley J, Andersson HC, Antshel KM, Braverman NE, Burton BK, Frazier DM, Mitchell J, Smith WE, Thompson BH, Berry SA, American College of Medical G and Genomics Therapeutics C. Phenylalanine hydroxylase deficiency: diagnosis and management guideline. *Genet Med*. 2014;16:188-200.
283. Chuaiphichai S, Crabtree MJ, McNeill E, Hale AB, Trelfa L, Channon KM and Douglas G. A key role for tetrahydrobiopterin-dependent endothelial NOS regulation in resistance arteries: studies in endothelial cell tetrahydrobiopterin-deficient mice. *Br J Pharmacol*. 2017;174:657-671.
284. Forstermann U and Sessa WC. Nitric oxide synthases: regulation and function. *European heart journal*. 2012;33:829-37, 837a-837d.
285. Tayeh MA and Marletta MA. Macrophage oxidation of L-arginine to nitric oxide, nitrite, and nitrate. Tetrahydrobiopterin is required as a cofactor. *J Biol Chem*. 1989;264:19654-8.
286. Zhao Y, Wu J, Zhu H, Song P and Zou MH. Peroxynitrite-dependent zinc release and inactivation of guanosine 5'-triphosphate cyclohydrolase 1 instigate its ubiquitination in diabetes. *Diabetes*. 2013;62:4247-56.
287. Beckman JS, Beckman TW, Chen J, Marshall PA and Freeman BA. Apparent hydroxyl radical production by peroxynitrite: implications for endothelial injury from nitric oxide and superoxide. *Proceedings of the National Academy of Sciences of the United States of America*. 1990;87:1620-4.
288. Ischiropoulos H and al-Mehdi AB. Peroxynitrite-mediated oxidative protein modifications. *FEBS Lett*. 1995;364:279-82.
289. Chalupsky K and Cai H. Endothelial dihydrofolate reductase: critical for nitric oxide bioavailability and role in angiotensin II uncoupling of endothelial nitric oxide synthase. *Proceedings of the National Academy of Sciences of the United States of America*. 2005;102:9056-61.
290. Vasquez-Vivar J, Kalyanaraman B and Martasek P. The role of tetrahydrobiopterin in superoxide generation from eNOS: enzymology and physiological implications. *Free radical research*. 2003;37:121-7.
291. Youn JY, Zhou J and Cai H. Bone Morphogenic Protein 4 Mediates NOX1-Dependent eNOS Uncoupling, Endothelial Dysfunction, and COX2 Induction in Type 2 Diabetes Mellitus. *Mol Endocrinol*. 2015;29:1123-33.
292. Yamamoto E, Nakamura T, Kataoka K, Tokutomi Y, Dong YF, Fukuda M, Nako H, Yasuda O, Ogawa H and Kim-Mitsuyama S. Nifedipine prevents vascular endothelial dysfunction in a mouse model of obesity and type 2 diabetes, by improving eNOS dysfunction and dephosphorylation. *Biochem Biophys Res Commun*. 2010;403:258-63.

293. Cassuto J, Dou H, Czikora I, Szabo A, Patel VS, Kamath V, Belin de Chantemele E, Feher A, Romero MJ and Bagi Z. Peroxynitrite disrupts endothelial caveolae leading to eNOS uncoupling and diminished flow-mediated dilation in coronary arterioles of diabetic patients. *Diabetes*. 2014;63:1381-93.
294. Yang YM, Huang A, Kaley G and Sun D. eNOS uncoupling and endothelial dysfunction in aged vessels. *American journal of physiology Heart and circulatory physiology*. 2009;297:H1829-36.
295. Perkins KA, Pershad S, Chen Q, McGraw S, Adams JS, Zambrano C, Krass S, Emrich J, Bell B, Iyamu M, Prince C, Kay H, Teng JC and Young LH. The effects of modulating eNOS activity and coupling in ischemia/reperfusion (I/R). *Naunyn Schmiedebergs Arch Pharmacol*. 2012;385:27-38.
296. Takimoto E, Champion HC, Li M, Ren S, Rodriguez ER, Tavazzi B, Lazzarino G, Paolocci N, Gabrielson KL, Wang Y and Kass DA. Oxidant stress from nitric oxide synthase-3 uncoupling stimulates cardiac pathologic remodeling from chronic pressure load. *The Journal of clinical investigation*. 2005;115:1221-31.
297. Alp NJ, Mussa S, Khoo J, Cai S, Guzik T, Jefferson A, Goh N, Rockett KA and Channon KM. Tetrahydrobiopterin-dependent preservation of nitric oxide-mediated endothelial function in diabetes by targeted transgenic GTP-cyclohydrolase I overexpression. *The Journal of clinical investigation*. 2003;112:725-35.
298. Bloch W, Fleischmann BK, Lorke DE, Andressen C, Hops B, Hescheler J and Addicks K. Nitric oxide synthase expression and role during cardiomyogenesis. *Cardiovascular research*. 1999;43:675-84.
299. Kanno S, Kim PK, Sallam K, Lei J, Billiar TR and Shears LL, 2nd. Nitric oxide facilitates cardiomyogenesis in mouse embryonic stem cells. *Proceedings of the National Academy of Sciences of the United States of America*. 2004;101:12277-81.
300. Campbell KA, Li X, Biendarra SM, Terzic A and Nelson TJ. Nos3<sup>-/-</sup> iPSCs model concordant signatures of in utero cardiac pathogenesis. *J Mol Cell Cardiol*. 2015;87:228-36.
301. Nadeau M, Georges RO, Laforest B, Yamak A, Lefebvre C, Beaugard J, Paradis P, Bruneau BG, Andelfinger G and Nemer M. An endocardial pathway involving Tbx5, Gata4, and Nos3 required for atrial septum formation. *Proceedings of the National Academy of Sciences of the United States of America*. 2010;107:19356-61.
302. Lee TC, Zhao YD, Courtman DW and Stewart DJ. Abnormal aortic valve development in mice lacking endothelial nitric oxide synthase. *Circulation*. 2000;101:2345-8.



303. Liu Y, Lu X, Xiang FL, Lu M and Feng Q. Nitric oxide synthase-3 promotes embryonic development of atrioventricular valves. *PLoS one*. 2013;8:e77611.
304. El Accaoui RN, Gould ST, Hajj GP, Chu Y, Davis MK, Kraft DC, Lund DD, Brooks RM, Doshi H, Zimmerman KA, Kutschke W, Anseth KS, Heistad DD and Weiss RM. Aortic valve sclerosis in mice deficient in endothelial nitric oxide synthase. *American journal of physiology Heart and circulatory physiology*. 2014;306:H1302-13.
305. Aicher D, Urbich C, Zeiher A, Dimmeler S and Schafers HJ. Endothelial nitric oxide synthase in bicuspid aortic valve disease. *Ann Thorac Surg*. 2007;83:1290-4.
306. Razavi HM, Hamilton JA and Feng Q. Modulation of apoptosis by nitric oxide: implications in myocardial ischemia and heart failure. *Pharmacol Ther*. 2005;106:147-62.
307. Dimmeler S, Hermann C, Galle J and Zeiher AM. Upregulation of superoxide dismutase and nitric oxide synthase mediates the apoptosis-suppressive effects of shear stress on endothelial cells. *Arterioscler Thromb Vasc Biol*. 1999;19:656-64.
308. Ojaimi C, Li W, Kinugawa S, Post H, Csiszar A, Pacher P, Kaley G and Hintze TH. Transcriptional basis for exercise limitation in male eNOS-knockout mice with age: heart failure and the fetal phenotype. *American journal of physiology Heart and circulatory physiology*. 2005;289:H1399-407.
309. Kazakov A, Hall R, Jagoda P, Bachelier K, Muller-Best P, Semenov A, Lammert F, Bohm M and Laufs U. Inhibition of endothelial nitric oxide synthase induces and enhances myocardial fibrosis. *Cardiovascular research*. 2013;100:211-21.
310. Buys ES, Raheer MJ, Blake SL, Neilan TG, Graveline AR, Passeri JJ, Llano M, Perez-Sanz TM, Ichinose F, Janssens S, Zapol WM, Picard MH, Bloch KD and Scherrer-Crosbie M. Cardiomyocyte-restricted restoration of nitric oxide synthase 3 attenuates left ventricular remodeling after chronic pressure overload. *American journal of physiology Heart and circulatory physiology*. 2007;293:H620-7.
311. Ji GJ, Fleischmann BK, Bloch W, Feelisch M, Andressen C, Addicks K and Hescheler J. Regulation of the L-type Ca<sup>2+</sup> channel during cardiomyogenesis: switch from NO to adenylyl cyclase-mediated inhibition. *FASEB J*. 1999;13:313-24.
312. Thum T, Fraccarollo D, Schultheiss M, Froese S, Galuppo P, Widder JD, Tsikas D, Ertl G and Bauersachs J. Endothelial nitric oxide synthase uncoupling impairs endothelial progenitor cell mobilization and function in diabetes. *Diabetes*. 2007;56:666-74.

313. Zugibe FT, Zugibe FT, Jr., Costello JT and Breithaupt MK. Hypoplastic coronary artery disease within the spectrum of sudden unexpected death in young and middle age adults. *Am J Forensic Med Pathol.* 1993;14:276-83.
314. Assmann TS, Recamonde-Mendoza M, De Souza BM and Crispim D. MicroRNA expression profiles and type 1 diabetes mellitus: systematic review and bioinformatic analysis. *Endocr Connect.* 2017;6:773-790.

## Chapter 2

### **Sapropterin Treatment Prevents Congenital Heart Defects Induced by Pregestational Diabetes in Mice**

A version of this chapter has been published in *Journal of the American Heart Association*. 2018 Nov 6;7(21):e009624

Anish Engineer <sup>1</sup>, Tana Saiyin <sup>1</sup>, Xiangru Lu <sup>1</sup>, Andrew S. Kucey <sup>1</sup>, Brad L. Urquhart <sup>1</sup>,  
Thomas A. Drysdale <sup>1,2,4</sup>, Kambiz Norozi <sup>2,4-6</sup>, Qingping Feng <sup>1,3,4</sup>.

<sup>1</sup> Department of Physiology and Pharmacology, <sup>2</sup> Department of Pediatrics, <sup>3</sup> Department of Medicine, Schulich School of Medicine and Dentistry, Western University, <sup>4</sup> Children's Health Research Institute, London, Ontario, Canada

<sup>5</sup> Department of Paediatric Cardiology and Intensive Care Medicine, Medical School Hannover, Germany; <sup>6</sup> Department of Paediatric Cardiology and Intensive Care Medicine, University of Goettingen, Germany

“Sapropterin Treatment Prevents Congenital Heart Defects Induced by Pregestational Diabetes in Mice”

## 2 Chapter 2

### 2.1 Chapter Summary

Tetrahydrobiopterin (BH4) is a co-factor of endothelial nitric oxide synthase (eNOS), which is critical to embryonic heart development. We aimed to study the effects of sapropterin (Kuvan®), an orally active synthetic form of BH4 on eNOS uncoupling and congenital heart defects (CHDs) induced by pregestational diabetes in mice. Adult female mice were induced to pregestational diabetes by streptozotocin and bred with normal males to produce offspring. Pregnant mice were treated with sapropterin or vehicle during gestation. CHDs were identified by histological analysis. Cell proliferation, eNOS dimerization and reactive oxygen species (ROS) production were assessed in the fetal heart. Pregestational diabetes results in a spectrum of CHDs in their offspring. Oral treatment with sapropterin in the diabetic dams significantly decreased the incidence of CHDs from 59% to 27% and major abnormalities, such as atrioventricular septal defect and double outlet right ventricle were absent in the sapropterin treated group. Lineage tracing revealed that pregestational diabetes resulted in decreased commitment of second heart field progenitors to the outflow tract, endocardial cushions, and ventricular myocardium of the fetal heart. Notably, decreased cell proliferation and cardiac transcription factor expression induced by maternal diabetes were normalized with sapropterin treatment. Furthermore, sapropterin administration in the diabetic dams increased eNOS dimerization and lowered ROS levels in the fetal heart. Sapropterin treatment in the diabetic mothers improves eNOS coupling, increases cell proliferation and prevents the development of CHDs in the offspring. Thus, sapropterin may have therapeutic potential in preventing CHDs in pregestational diabetes.

## 2.2 Introduction

Congenital heart defects (CHDs) are the most common structural birth defect, occurring in 1-5% of live births, making them the leading cause of death in the first year of infant life.<sup>1, 2</sup> The prevalence of CHDs has been rapidly increasing,<sup>3</sup> and it is estimated that approximately 2.4 million Americans, including 1 million children, are living with a congenital malformation of the heart.<sup>2</sup> CHDs are formed when complex cellular and molecular processes underlying embryonic heart development are disturbed. The heart is developed from three pools of progenitor cells: the first heart field (FHF), the second heart field (SHF) and cardiac neural crest (CNC).<sup>4</sup> The FHF progenitors initially form the primary heart tube. SHF cells are then added to the heart tube to form the right ventricle, give rise to myocardial and endothelial cells of the outflow tract and semilunar valves, as well as the vascular smooth muscle cells at the base of the aorta and pulmonary trunk. The CNC cells contribute to septation of the outflow tract and remodeling of semilunar valves, while the left ventricle is mainly formed from FHF progenitors. The SHF is particularly significant to CHDs as many common cardiac abnormalities including atrial and ventricular septal defects, cardiac valve malformation, double outlet right ventricle and truncus arteriosus, are caused by defects in SHF progenitors.<sup>4</sup>

Pregestational diabetes (type 1 or 2) in the mother increases the risk of a CHD in the child by more than four-fold.<sup>5, 6</sup> While good glycemic control in diabetic mothers lowers the risk, the incident of CHDs in their children is still higher than the general population.<sup>7, 8</sup> The prevalence of pregestational diabetes has nearly doubled from 0.58% to 1.06% from 1996 to 2014 in Northern California,<sup>9</sup> and has reached 4.3% in Saudi Arabia.<sup>10</sup> As the prevalence of pregestational diabetes further increases in women during

their reproductive age, more individuals will be born with CHDs, inevitably placing a large burden on the healthcare system.<sup>11, 12</sup>

Uncontrolled maternal diabetes is not conducive to proper gestation. Hyperglycemia leads to cellular oxidative stress through numerous pathways,<sup>13</sup> which include increased electron transport chain flow resulting in mitochondrial dysfunction, non-enzymatic protein glycosylation and glucose auto-oxidation all contributing to reactive oxygen species (ROS) generation.<sup>14, 15</sup> Increased oxidative stress can lead to the inactivation of many molecules and proteins necessary for proper heart development. Endothelial nitric oxide synthase (eNOS) is intimately regulated by redox balance within the cell and is vital for cardiogenesis.<sup>16</sup> eNOS expression in the embryonic heart regulates cell growth and protects early cardiac progenitors against apoptosis.<sup>17</sup> The importance of eNOS in heart development has been demonstrated in eNOS<sup>-/-</sup> mice by a spectrum of cardiovascular anomalies such as ventricular septal defects (VSDs), valvular malformations and hypoplastic coronary arteries.<sup>17-19</sup>

Tetrahydrobiopterin (BH4) has antioxidant properties and is a critical co-factor for eNOS function.<sup>20</sup> It is required for eNOS dimer stabilization and is an allosteric modulator of arginine binding to the active site.<sup>21</sup> In states of oxidative stress, BH4 levels decline, and eNOS is uncoupled, resulting in decreased NO synthesis and increased superoxide production, perpetuating the oxidative environment of the cell.<sup>22</sup> The production of ROS is amplified by this feedback loop, further inducing eNOS uncoupling. Treatment with BH4 has been shown to recouple eNOS and improve vascular endothelial function in diabetes.<sup>23, 24</sup> However, the potential of BH4 to reduce the severity and incidence of CHDs is not known. Sapropterin dihydrochloride (Kuvan®) is an orally-active, synthetic

form of BH4 and an FDA approved drug for the treatment of phenylketonuria.<sup>25</sup> The present study was aimed to examine the effects of sapropterin in mice with pregestational diabetes. We hypothesized that sapropterin treatment during gestation re-couples eNOS, improves cell proliferation in SHF derived cells, and reduces CHD incidence in the offspring of mice with pregestational diabetes.

## 2.3 Methods

### 2.3.1 Animals

All procedures were performed in accordance with the Canadian Council on Animal Care guidelines and approved by the Animal Care Committee at Western University. C57BL/6 wild type and *Rosa26<sup>mTmG</sup>* mice were purchased from Jackson Laboratory (Bar Harbor, Maine). *Mef2c<sup>cre/+</sup>* embryos were obtained from Mutant Mouse Regional Resource Center (Chapel Hill, NC) and rederived. All animals were housed in a 12-hour light/dark cycle and given ad libitum access to standard chow and water. A breeding program was established to generate embryonic, fetal and post-natal mice.

### 2.3.2 Induction of Diabetes and Sapropterin Treatment

A study flow chart in **Figure 2.1** illustrates timelines of saline or streptozotocin (STZ) injection, breeding, sapropterin or insulin treatment and assessments of fetal hearts in 5 groups of mice. Female C57BL/6 mice, 8 to 10 weeks old were made diabetic through five consecutive daily injections of STZ (50 mg/kg body weight, IP, Sigma) freshly dissolved in sterile saline. Mice were randomly assigned to STZ (n=37) or saline treatment (n=19) groups. One week following the last STZ injection, non-fasting blood glucose levels were measured with a tail snip procedure using a glucose meter (One Touch Ultra2, LifeScan, Burnaby, BC). Mice were categorized as diabetic if blood

glucose measurements exceeded 11 mmol/L, and were subsequently bred to 10 to 12 week old C57BL/6 male mice. In the morning when a vaginal plug was observed indicating embryonic day 0.5 (E0.5), the female diabetic mouse was placed in a separate cage with littermates. A cohort of diabetic and control female mice were treated with sapropterin dihydrochloride (Kuvan®, BioMarin Pharmaceutical Inc.) at a dose of 10 mg/kg body weight per day during gestation. Sapropterin was dissolved in water and mixed with a small amount peanut butter in a weigh boat, ensuring it was fully consumed by the mouse. At the time of feeding, mice were separated and individually housed in cages for about 15 min until the sapropterin or vehicle containing peanut butter mixture was fully consumed under an investigator's watch. All mice were fed in the morning, once per day. Non-fasting blood glucose levels were monitored throughout pregnancy. To prevent hyperglycemia, a long acting form of insulin (Lantus®, Sanofi Aventis) was administered subcutaneously to a cohort diabetic dams (n=3) at a dose of 0.5 units/day.



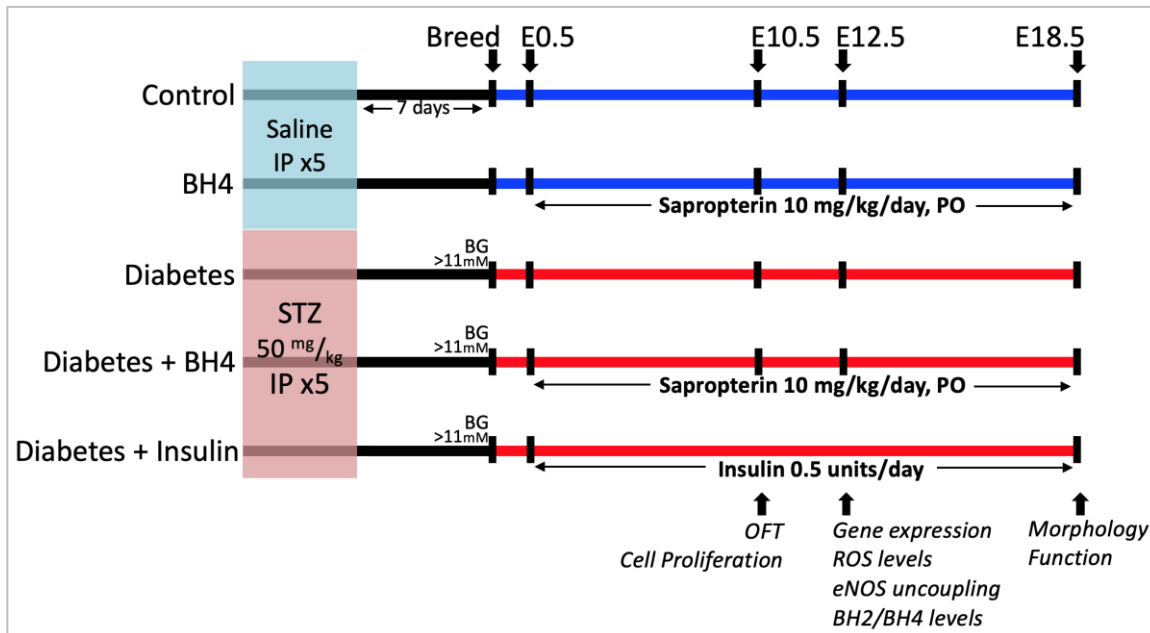


**Figure 2.1. Experimental design to examine the effects of sapropterin (BH4) on congenital heart defects induced by pregestational diabetes.**

A study flow chart illustrates timelines of saline or STZ injection, breeding, sapropterin or insulin treatment and assessments of fetal hearts in 5 groups of mice. IP indicates intraperitoneal injection; PO, oral administration; STZ, streptozotocin. BG, blood glucose; E, embryonic day; eNOS, endothelial NO synthase; OFT, outflow tract; ROS, reactive oxygen species.

### 2.3.3 Histological and Immunohistochemical Analysis

Fetal samples were harvested at E10.5, E12.5 and E18.5 for histological and immunohistochemical analysis. To diagnose CHDs in E18.5 hearts, fetuses were decapitated and the isolated thorax was fixed overnight in 4% paraformaldehyde, dehydrated in ethanol and paraffin embedded. Samples were sectioned in 5  $\mu\text{m}$  slices and hematoxylin/eosin (H&E) or toluidine blue stained to visualize morphology. Images were taken and analyzed using a light microscope (Observer D1, Zeiss, Germany). Embryonic samples at E10.5 and E12.5 were fixed in 4% paraformaldehyde for 1 and 2 hours,

respectively, and processed as described above. Immunostaining to analyze cell proliferation at E10.5 using anti-phosphohistone H3 (pHH3) antibody (1:1000, Abcam), and sex determination at E18.5 using anti-sex-determining region Y protein antibody (1:200, Santa Cruz) were performed after antigen retrieval in citrate buffer (10 mmol/L, pH 6). This was followed by incubation with biotinylated goat anti-mouse IgG (1:300, Vector Laboratories) secondary antibody. The signal was amplified by the ABC reagent (Vector Laboratories) allowing for visualization through 3-3'-di-aminobenzidine tetrahydrochloride (DAB, Sigma) with hematoxylin as a counterstain. Blinded pHH3<sup>+</sup> cell counts within the outflow tract (OFT) were taken from at least 3 heart sections per heart and normalized to OFT length.

#### 2.3.4 Lineage Tracing the Second Heart Field

Fate mapping of SHF progenitors was performed using the SHF specific *Mef2c*<sup>cre/+</sup> transgenic mouse and the global double fluorescent *Cre* reporter line *Rosa26*<sup>mTmG</sup> that has *LoxP* sites on either side of a tomato-red fluorescence membrane protein (mT) cassette, which is preceded by a green fluorescence protein (GFP, mG) cassette. In the *Mef2c*<sup>Cre/+</sup> transgenic line with C57BL/6 background, elements of the *Mef2c* promoter drives *Cre* recombinase expression in all SHF derived cells. When crossed with the *Rosa26*<sup>mTmG</sup> mice this results in a GFP signal that is detected in all SHF derived cells.<sup>26, 27</sup> In all other tissues, the absence of the *Cre* results in mT expression and red fluorescence. Diabetes was induced in homozygous *Rosa26*<sup>mTmG</sup> females (8 to 10 weeks old) by STZ as described above. Hyperglycemic *Rosa26*<sup>mTmG</sup> female mice were crossed with *Mef2c*<sup>cre/+</sup>; *Rosa26*<sup>mTmG</sup> males to generate E9.5 and E12.5 *Mef2c*<sup>cre/+</sup>; *Rosa26*<sup>mTmG</sup> embryos, which were fixed, embedded and sectioned in the same

manner as above. Immunostaining for membrane bound GFP was conducted using an anti-GFP (1:500, Abcam) primary antibody, followed by biotinylated goat anti-rabbit IgG (1:300, Vector Laboratories) secondary antibody using DAB for visualization. The SHF derived cells, which are GFP<sup>+</sup>, were blindly quantified and compared between control and diabetic groups.

### 2.3.5 Analysis of Superoxide Levels

Hearts collected from E12.5 fetuses from all four groups were cryo-sectioned (CM1950, Leica, Germany) into 8  $\mu\text{m}$  thick slices and placed onto slides. A subset of cryo-sectioned embryonic hearts from untreated and sapropterin-treated diabetic dams were incubated with either 300  $\mu\text{M}$  L-NAME (Sigma), a nitric oxide synthase inhibitor, or 100 units/mL superoxide dismutase (SOD, Sigma), recombinant antioxidant enzyme for 30 minutes. Samples were then probed with 2  $\mu\text{M}$  dihydroethidium (DHE) (Invitrogen Life Technologies, Burlington, Canada) for 30 minutes in a dark humidity chamber at 37 °C. After cover glass was mounted, DHE fluorescence signals were visualized using a fluorescence microscope (Observer D1, Zeiss, Germany). Five – 8 images from each sample were captured at fixed exposure times for all groups and the fluorescence intensity per myocardial area was blindly quantified using AxioVision software.

### 2.3.6 Measurement of Cardiac Function

Pregnant dams were anesthetized and M-mode echocardiography images of E18.5 embryonic hearts were recorded using the Vevo 2100 ultrasound imaging system with a MS 700 transducer (VisualSonics, Toronto, Canada) as previously described.<sup>18, 19</sup> Briefly, an incision was made to the abdominal wall of the pregnant dam to expose the uterine

sacs containing the E18.5 fetuses. The transducer was aligned to the uterine sac to obtain a short-axis view of the fetal heart. The end diastolic left ventricular internal diameter and end systolic left ventricular internal diameter were measured from the short-axis M-mode images to calculate LV ejection fraction and fractional shortening.

### 2.3.7 Western Blotting for eNOS Dimers and Monomers

Ventricular myocardial tissues from E12.5 hearts were dissected in PBS and used for measurement of eNOS dimerization. In order to not disrupt the dimer, proteins were isolated from three pooled hearts from each group via sonication using a non-reducing lysis buffer, on ice.<sup>28</sup> Protein lysates without boiling were run on an 8% SDS-PAGE at 4 °C followed by transferring to a nitrocellulose membrane and immunoblotted with anti-eNOS polyclonal antibody (1:3000, Santa Cruz). This technique resulted in two distinct bands at 260 and 130 kDa, representing the eNOS dimer and monomer, respectively.<sup>28</sup> Proteins isolated from cultured coronary artery microvascular endothelial cells was boiled and separated with the sample, acting as an eNOS monomer size control.

### 2.3.8 Real-Time RT-PCR

Total RNA was isolated from E12.5 hearts using TRIzol reagent (Invitrogen). 200 nanograms of RNA were synthesized into cDNA with Moloney murine leukemia virus reverse transcriptase and random primers. Real-time PCR was conducted on cDNA using Evagreen qPCR MasterMix (Applied Biological Systems, Vancouver, BC). Primers were designed for Gata4, Gata5, Nkx2.5, Tbx5, Notch1, GCH1, DHFR using the Primer3 software v 4.1.0. The primer sequences are listed in **Table 2.1**. Eppendorf Realplex (Eppendorf, Hamburg) was used to amplify samples for 35 cycles. Values were

normalized to 28S ribosomal RNA, and mRNA levels were extrapolated through a comparative  $C_T$  method.<sup>19</sup>

**Table 2.1. Specific primer sequences used in real-time PCR analysis.**

Gene	Accession no.	Product Size	Primer Sequence
<i>Gata4</i>	NM_008092.3	134	F: GCCTGCGATGTCTGAGTGAC R: CACTATGGGCACAGCAGCTC
<i>Gata5</i>	NM_008093.2	167	F: ACCCCACAACCTACCCAGCA R: GCCCTCACCAGGGAACCTCCT
<i>Nkx2.5</i>	NM_008700.2	162	F: GACAGCGGCAGGACCAGACT R: CGTTGTAGCCATAGGCATTG
<i>Tbx5</i>	NM_011537.3	103	F: AGGAGCACAGTGAGGCACAA R: GGGCCAGAGACACCATTCTC
<i>Notch1</i>	NM_008714.3	142	F: CAGCTTGCACAACCAGACAGA R: TAACGGAGTACGGCCCATGT
<i>Gch1</i>	NM_008102.3	117	F: TCAAGAGCGCCTCACCAAAC R: TTCTGCACGCCTCGCATTAC
<i>Dhfr</i>	NM_010049.3	153	F: GAATCAACCAGGCCACCTCA R: TTGATGCCTTTTTCTCCTG
28S	NR_003279.1	178	F: GGGCCACTTTTGGTAAGCAG R: TTGATTCGGCAGGTGAGTTG

F: forward primer; R: reverse primer

### 2.3.9 Determination of Biopterin Levels

Tissue and plasma biopterin levels were determined using ultra-performance liquid chromatography (UPLC) coupled to mass spectrometry. Briefly, dams were anesthetized with an intraperitoneal injection of ketamine and xylazine cocktail at E12.5. Whole embryos were harvested followed by blood collections from the dams for (UPLC) analysis. About 1 mL of blood was collected via cardiac puncture using a 23-gauge heparinized needle inserted into the beating left ventricle of the dam. Plasma samples were then diluted 1:4 with 150  $\mu$ l of acetonitrile containing internal standard (100  $\mu$ M aminopimilic acid and 2.5  $\mu$ M chlorpromazine) before injection into the UPLC

instrument. Total BH4 and BH2 levels were assessed using a Waters Acuity I Class UPLC system coupled to a XEVO G2-S quadrupole time-of-flight mass spectrometer (Waters Corporation: Milford, Massachusetts) as previously described.<sup>29</sup>

### 2.3.10 Statistical Analysis

Data are presented as the mean  $\pm$  SEM. Statistical analysis was performed using GraphPad Prism (Version 5, GraphPad Software, La Jolla, CA, USA). For comparisons between two groups, unpaired Student's t-test was used. Multiple group comparisons between diabetic and control dams with and without sapropterin treatment, and their interactions were conducted using two-way analysis of variance (ANOVA) followed by the Bonferroni post-hoc test. Two-way repeated measures ANOVA followed by Bonferroni post-hoc test was used to analyze blood glucose differences over time between control and diabetic dams with or without sapropterin treatment. The incidence of CHDs was assessed with Fisher's exact test. Differences were deemed significant with  $P < 0.05$ .

## 2.4 Results

### 2.4.1 Effects of sapropterin on blood glucose, fertility, litter size and biopterin levels in pregestational diabetes

This study was conducted in the same pregestational diabetes model we recently employed.<sup>30, 31</sup> One week following the final administration of STZ, female mice with random blood glucose levels >11 mmol/L were bred with normal adult males. During gestation, blood glucose levels in the diabetic dams were progressively increased from E0.5-18.5 compared to both sapropterin treated and untreated control mice (Fig. 2.2A). Treatment with insulin but not sapropterin in the diabetic mice restored blood glucose to normal levels. Diabetic dams had a significant lower fertility rate (38%) compared to controls (82%,  $P<0.05$ ), which was improved to 64% by sapropterin treatment (Fig. 2.2B).

Diabetic dams had a significantly smaller litter size ( $P<0.01$ ), which was improved by sapropterin treatment (Fig. 2.2C). Indeed, absorbed or dead fetuses were more commonly seen in utero in diabetic dams. Fetal body weight was significantly lower from diabetic dams than controls ( $P<0.001$ ), and was restored to normal weight with sapropterin ( $P<0.001$ , Fig. 2.2D). To assess biopterin levels following oral sapropterin administration, maternal blood and embryos were collected at E12.5. Our data show that sapropterin treatment significantly increased plasma BH2 levels in the diabetic mothers ( $P<0.01$ , Fig. 2.2E). BH2 levels in E12.5 embryos from sapropterin-treated dams were elevated by 91.3% ( $P=0.0537$ , Fig. 2.2F), and BH4 levels in E12.5 embryos of diabetic dams were significantly increased ( $P=0.0433$ , Fig. 2.2G).

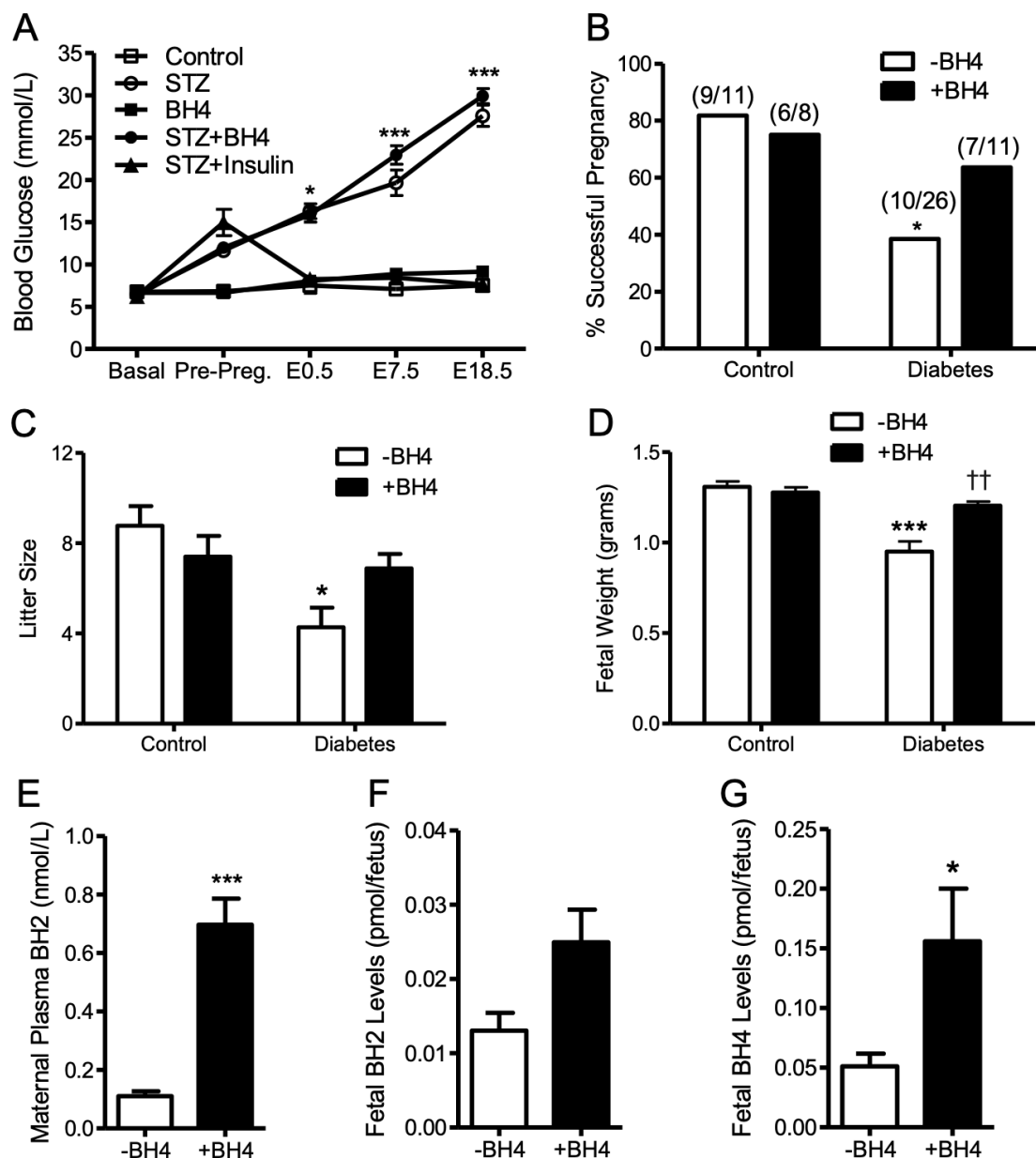


**Figure 2.2. Blood glucose levels of pregnant mice, percent successful plugs, litter size, fetal body weight and bipterin levels.**

(A) Non-fasting blood glucose levels from before mating (basal) to E18.5 during pregnancy in STZ-treated and control female mice with and without sapropterin (BH4) administration (n = 4-8 mice per group). (B) The percent of successful pregnancy. The numbers in the brackets indicate the number of successful pregnancy at the day of fetus harvest to total plugs. (C) The offspring litter size measured at the day of fetus harvest (n = 5-11 litters per group). (D) Fetal body weight at E18.5 (n = 5-8 fetuses per group). (E-G) Levels of BH2 in maternal plasma, and fetal BH2 and BH4 levels at E12.5 with or



without BH4 treatment in the diabetic dams (n = 3-9 mice per group). Two-way repeated measures ANOVA (A) or two-way ANOVA (C-D) followed by Bonferroni post-hoc test was used. B was analyzed by Fisher's exact test. E-G were analyzed by unpaired Student's t test. \* $P < 0.05$ , \*\*\* $P < 0.001$  vs. corresponding controls, and †† $P < 0.001$  vs. untreated diabetes. Data are means  $\pm$  SEM in A, C-G.

#### 2.4.2 Sapropterin prevents CHDs induced by pregestational diabetes

CHDs were observed in 59.4% of offspring from diabetic dams (Table 2.2 and Fig. 2.3). Normal control heart sections are shown in Fig. 2.3A-C. Septal defects constituted a large proportion of the anomalies with 47.4% atrial septal defects (ASD, Fig. 2.3D) and 37.8% ventricular septal defects (VSD, Fig. 2.3E). The diagnosis of ASD was based on a complete or partial absence of the septum secundum and/or primum in multiple serial heart sections. Hypoplastic left heart was seen in 21.1% of offspring from diabetic dams. In particular, 2 of these hearts displayed the characteristics of hypoplastic left heart syndrome, with an underdeveloped left ventricle, a small ascending aorta, ASD and abnormal mitral valve. Whereas, 6 hearts had an isolated hypoplastic left ventricle. One fetus had an atrioventricular septal defect (AVSD). Outflow tract (OFT) defects were also common in offspring from diabetic mothers. A double outlet right ventricle (DORV) was present in one of the offspring (Fig. 2.3F) and truncus arteriosus was seen in another fetus (Fig. 2.3G). Maternal diabetes also resulted in cardiac valve defects with 37.8% thickened aortic valves (Fig. 2.3H) and 29.7% thickened pulmonary valves (Fig. 2.3I). Finally, 24.3% of hearts from diabetic mothers displayed a narrowing aorta (Fig. 2.3H vs. B). Treatment with sapropterin to diabetic dams during pregnancy significantly decreased the overall incidence of CHDs to 26.5% (Table 2.2). Specifically, offspring from sapropterin-treated diabetic mothers show a significantly lower incidence of ASD and thickened aortic valves, and did not display any VSD, AVSD, truncus arteriosus,

DORV or hypoplastic left heart (Table 2.2, Fig. 2.3J-O). Cardiac anomalies were seen in all litters from diabetic dams, and every dam in the sapropterin treatment group had at least one offspring with a CHD. No CHDs were seen in diabetic dams who received a daily dose of insulin to maintain normal blood glucose levels, indicating that CHDs seen in the diabetic offspring were induced through hyperglycemia (Table 2.2, Fig. 2.3P-R). The incidence of CHDs was significantly higher in males than females (65% vs. 47%,  $P<0.05$ ). Furthermore, sapropterin treatment was more effective in reducing the incidence of CHDs to 16% in females compared to 35% in males ( $P<0.05$ , Fig. 2.3S). Cardiac function of E18.5 fetuses was assessed through echocardiography. LV fractional shortening and ejection fraction were significantly decreased in offspring of diabetic dams, and were recovered by sapropterin treatment ( $P<0.001$ , Fig. 2.3T and U). In addition, anterior wall thickness of the fetal heart during systole and diastole was reduced in offspring of diabetic dams, which was restored following sapropterin treatment ( $P<0.01$ , Fig. 2.3V and W). Pregestational diabetes also induced neural tube defects (NTD) in our model. A case of exencephaly in the offspring of mother with pregestational diabetes is shown in Fig. 2.3X.

**Table 2.2. The rate of congenital heart defects in the offspring of diabetic and control mothers with and without sapropterin (BH4) treatment.**

	<b>Control</b>		<b>STZ</b>		<b>BH4</b>		<b>STZ+BH4</b>		<b>STZ+Insulin</b>	
	N	dams	N	dams	N	dams	N	dams	N	dams
	n	%	n	%	n	%	n	%	n	%
Normal	14	100	16	40.6**	23	100	25	73.5††	20	100
Abnormal	0	0	22	59.4**	0	0	9	26.5††	0	0
ASD	0	0	18	47.4**	0	0	9	26.5	0	0
VSD	0	0	14	37.8*	0	0	0	0.0††	0	0
Truncus Arteriosus	0	0	1	2.7	0	0	0	0.0	0	0
AVSD	0	0	2	5.4	0	0	0	0.0	0	0
DORV	0	0	1	2.7	0	0	0	0.0	0	0
Pulmonary Valve Stenosis	0	0	14	37.8*	0	0	0	0.0††	0	0
Aortic Valve Stenosis	0	0	11	29.7*	0	0	1	2.9††	0	0
RV Hypertrophy	0	0	9	24.3	0	0	0	0.0††	0	0
Hypoplastic Left Heart	0	0	8	21.1	0	0	0	0.0††	0	0
Narrowing of the Aorta	0	0	9	24.3	0	0	0	0.0††	0	0

Data was analyzed using Fisher's exact test. \* $P < 0.05$ , \*\* $P < 0.001$  vs. untreated control, † $P < 0.05$ , †† $P < 0.001$  vs. STZ. ASD: atrial septal defect, VSD: ventricular septal defect, AVSD: atrioventricular septal defect, DORV: double outlet right ventricle. N indicates total number of fetuses, dams are litter numbers.

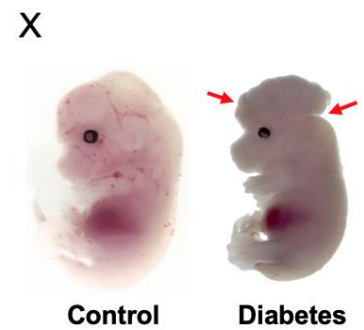
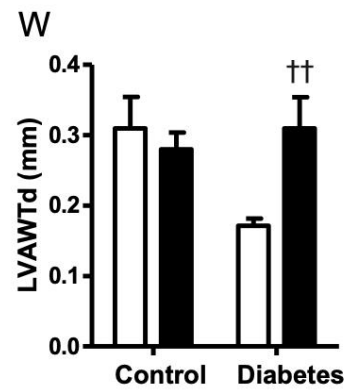
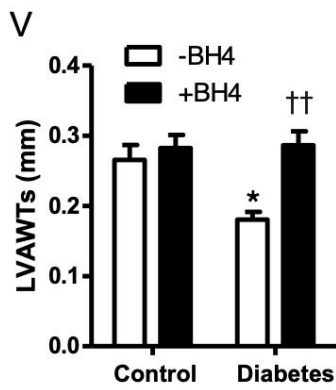
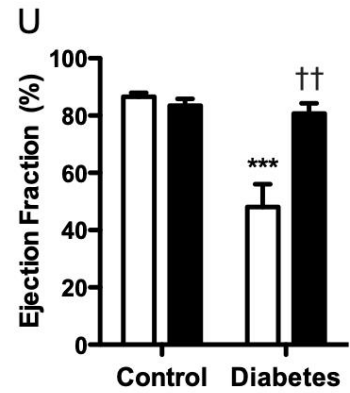
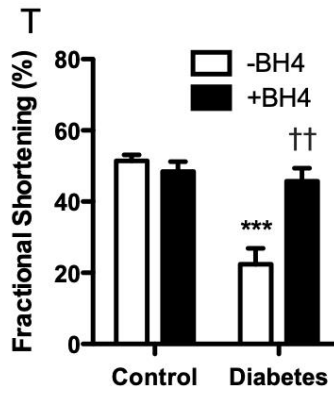
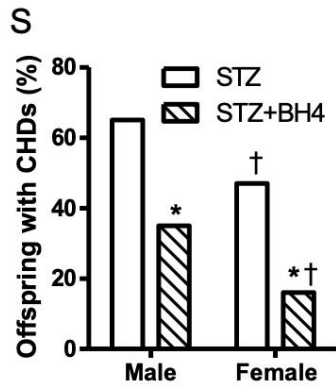
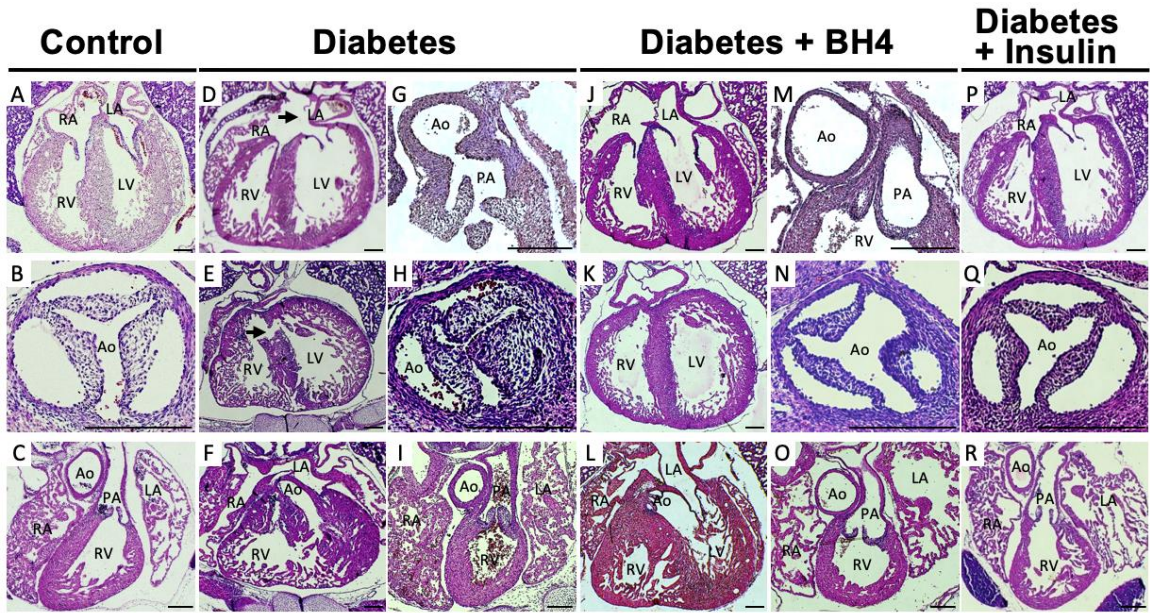


**Figure 2.3. Effects of sapropterin (BH4) on congenital heart defects induced by pregestational diabetes.**

Representative histological sections of E18.5 hearts from offspring of diabetic mothers with and without BH4 treatment. (A-C) show hearts sections from controls. Pregestational diabetes resulted in atrial septal defect (D), ventricular septal defect (E), double outlet right ventricle (F), truncus arteriosus (G), thickened aortic (H) and pulmonary (I) valves. BH4 treatment in diabetic dams shows normal heart morphology (J-O). Diabetic dams on insulin therapy to control blood glucose levels show normal fetal heart morphology (P-R). Scale bars are 200  $\mu\text{m}$ . (S) Incidence of CHDs as percent of offspring separated by sex at E18.5 from diabetic dams with or without BH4 treatment. \* $P < 0.05$  vs. STZ group of corresponding sex; † $P < 0.05$  vs. corresponding males. (T-W) LV fractional shortening and ejection fraction, anterior wall thickness during systole (LVAWTs) and diastole (LVAWTd) assessed by echocardiography in E18.5 offspring (n = 5-7 fetuses per group). \* $P < 0.05$ , \*\*\* $P < 0.001$  vs. corresponding controls, and †† $P < 0.001$  vs. untreated diabetes. (X) An exencephaly was seen in the offspring of mother with pregestational diabetes. A normal control fetus is shown on the right panel. Fetuses are harvested at E13.5. S-W were analyzed by two-way ANOVA followed by Bonferroni post-hoc test. Data are means  $\pm$  SEM in T-W. Ao indicates aorta; LA, left atrium; LV, left ventricle; PA, pulmonary artery; RA, right atrium, RV, right ventricle.

### 2.4.3 Sapropterin prevents myocardial and valvular abnormalities induced by pregestational diabetes

The free walls of the right and left ventricle at E18.5 were measured at the mid-ventricular region (Fig. 2.4A). The RV and LV myocardium was thinner in the offspring of diabetic mothers compared to those of control offspring, which was prevented by sapropterin treatment ( $P<0.001$ , Fig. 2.4B and C). Additionally, since valve leaflets were thickened (Fig. 2.3H and I), we assessed glycosaminoglycans, a component of extracellular matrix in the cardiac valves using toluidine blue staining. Our data show that glycosaminoglycans occupied a greater space in the leaflets of aortic and pulmonary valves (light purple color) from E18.5 fetal hearts of diabetic mothers compared to controls (Fig. 2.5A and B). Treatment with sapropterin decreased these extracellular polysaccharides in both aortic and pulmonary valves ( $P<0.01$ , Fig. 2.5D and E). There was no significant difference in glycosaminoglycan content in the mitral valve, however the distal tip of mitral valve was thicker in the offspring of diabetic dams ( $P<0.01$ , Fig. 2.5F). Notably, the area of aortic orifice and diameter of pulmonary artery were significantly smaller in hearts from diabetic mothers compared to controls ( $P<0.01$ , Fig. 2.5G and H).



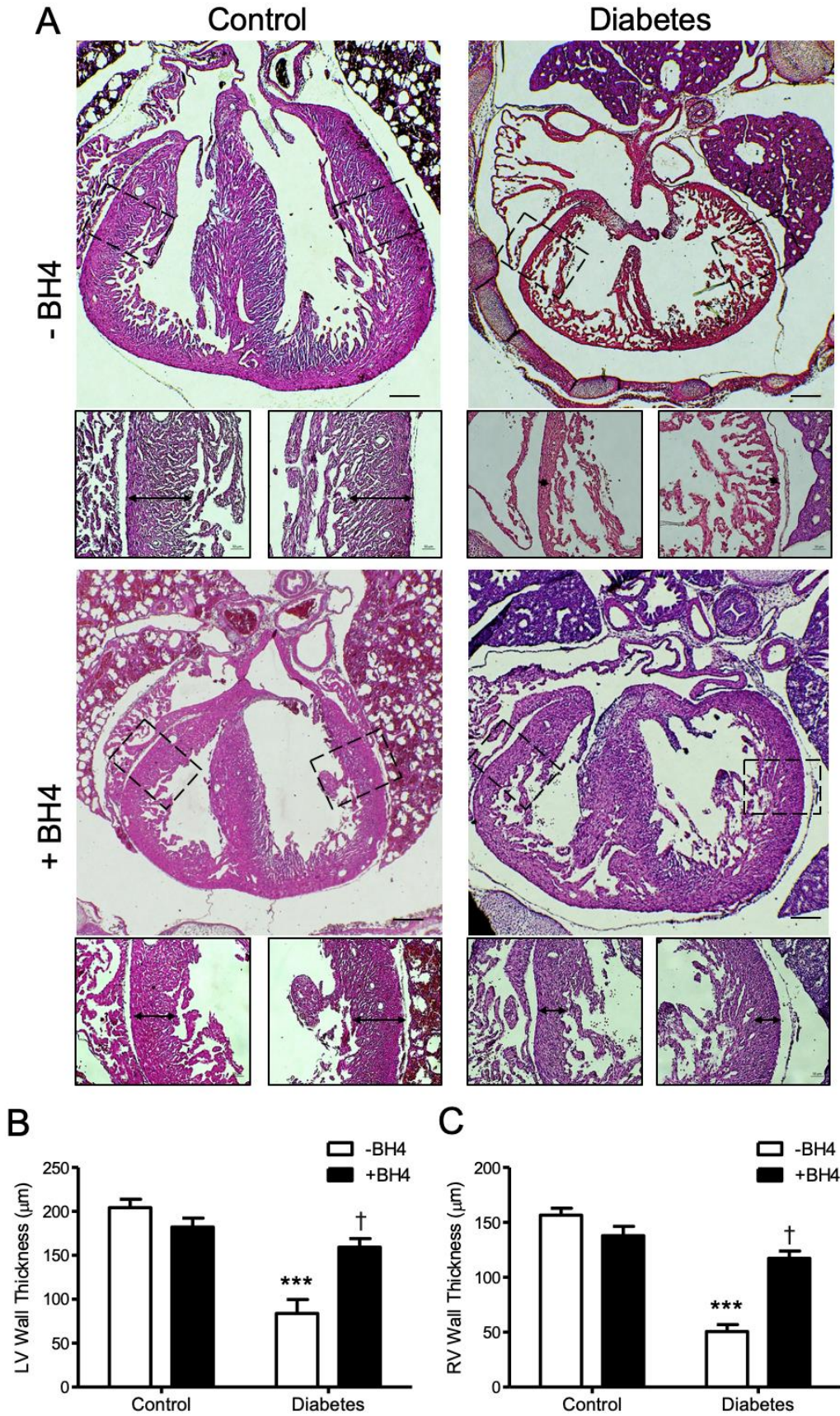


**Figure 2.4. Effects of sapropterin (BH4) on fetal heart wall thickness of pregestational diabetes at E18.5.**

(A) Representative images of myocardial wall thickness in control and pregestational diabetes with and without BH4 treatment. Arrows indicate compact myocardium boundary from which measurements were obtained. (B-C) Quantification of right and left ventricular myocardial thickness, respectively.  $n = 6$  per group from 3 – 6 litters, \*\*\* $P < 0.01$  vs. untreated control, † $P < 0.01$  vs. untreated diabetes. Data are means  $\pm$  SEM in B-C and analyzed using two-way ANOVA followed by Bonferroni post-hoc test. Scale bars are 200  $\mu\text{m}$ . LV indicates left ventricle; RV, right ventricle.



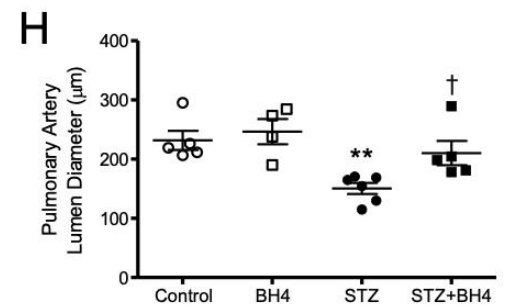
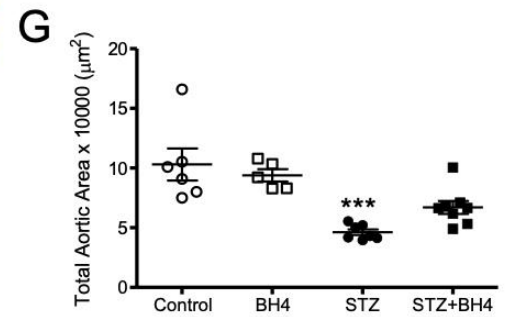
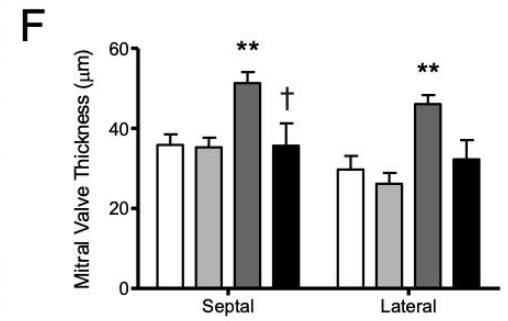
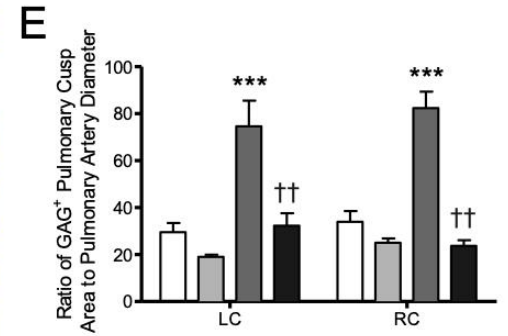
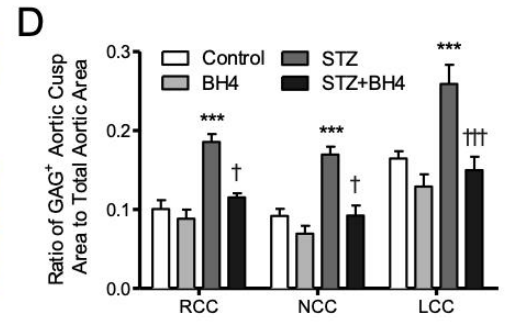
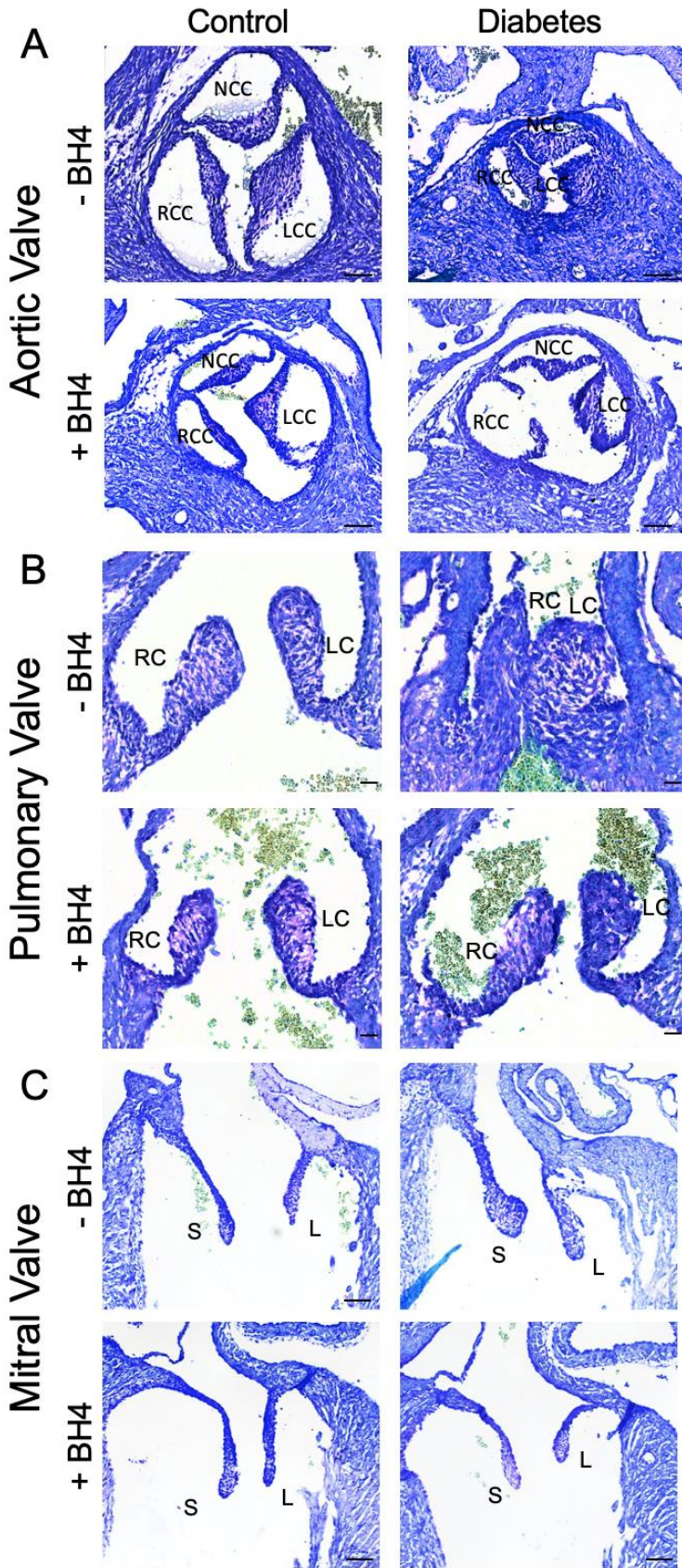


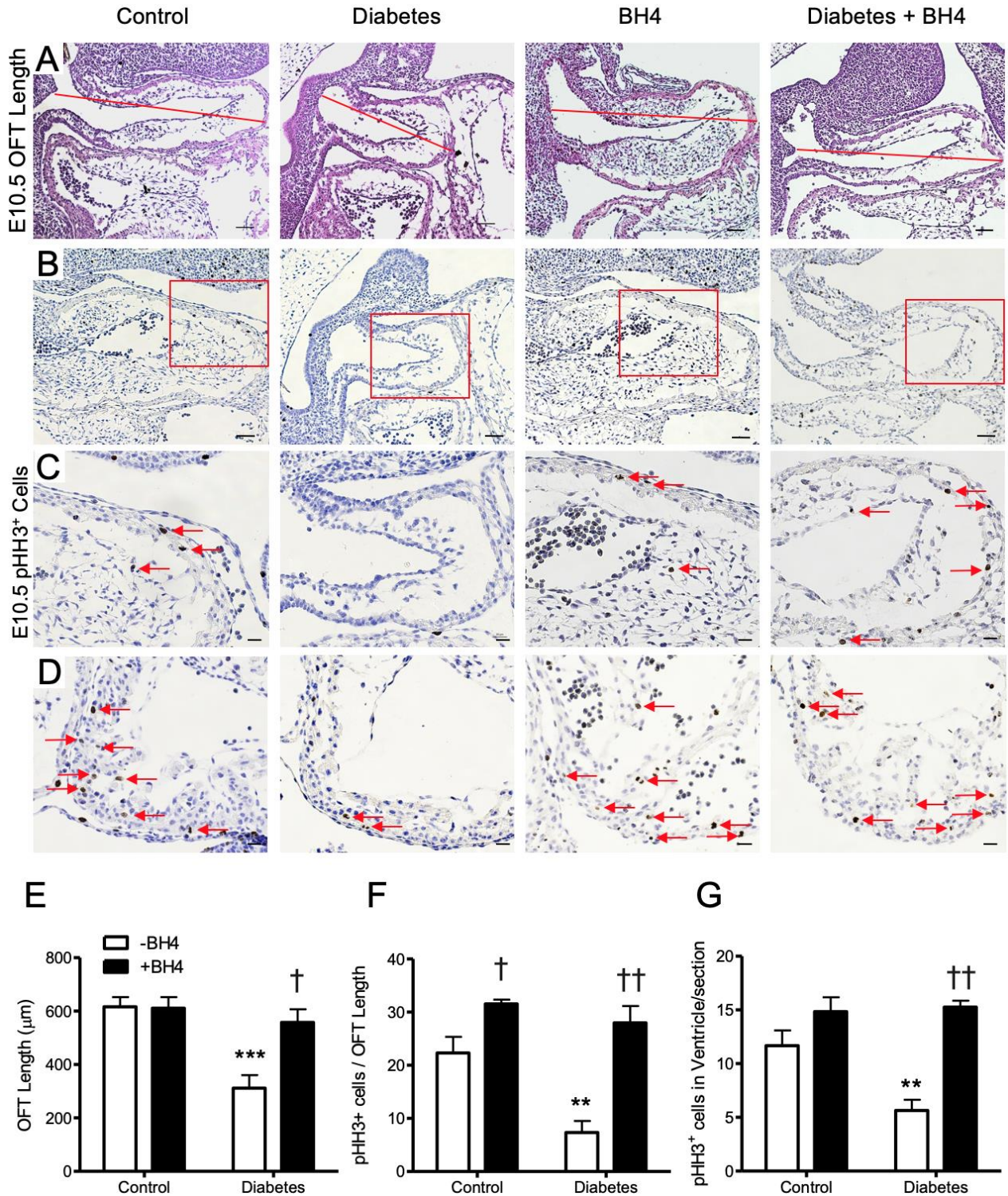
**Figure 2.5. Effects of sapropterin (BH4) on aortic, pulmonary and mitral valve defects induced by pregestational diabetes at E18.5.**

(A-C) Representative images of toluidine blue staining of glycosaminoglycans (GAG) in aortic, pulmonary, and mitral valves in E18.5 hearts. (D) The ratio of GAG<sup>+</sup> area to total valve leaflet area. (E) Pulmonary valve leaflet thickness. (F) Mitral valve leaflet thickness. (G) Total aortic orifice area. (H) Pulmonary artery luminal diameter at the base of the orifice. LCC, left coronary cusp; NCC, noncoronary cusp; RCC, right coronary cusp; RC, right cusp; LC, left cusp; S, septal; L, lateral. Scale bars are 50, 20 and 20  $\mu\text{m}$  in A, B and C, respectively. \* $P < 0.05$ , \*\* $P < 0.01$  vs. controls. † $P < 0.01$ , †† $P < 0.01$  vs. untreated diabetes.  $n = 4-7$  hearts per group from 3 – 4 litters. Data are means  $\pm$  SEM in B-C and analyzed using two-way ANOVA followed by Bonferroni post-hoc test.

#### 2.4.4 Effects of sapropterin on outflow tract length and cell proliferation in the fetal heart

Since offspring of diabetic mothers show OFT defects, we aimed to investigate changes in cell proliferation at a critical stage in OFT formation. At E10.5 sagittal sections of whole embryos reveal a shortened OFT in hearts from diabetic mothers compared to control ( $P < 0.001$ , Fig. 2.6A), which was restored with sapropterin treatment ( $P < 0.05$ , Fig. 2.6E). To further analyze this change, phosphorylated histone H3, a marker for the mitotic phase of cell division, was used to compare the levels of proliferating cells in the OFT at E10.5 using the same hearts (Fig. 2.6B-D). Embryos from mice with pregestational diabetes had a significantly lower number of proliferating cells in the OFT ( $P < 0.01$ , Fig. 2.6F-G). Sapropterin treatment was able to prevent impaired cell proliferation in the OFT in hearts from diabetic dams ( $P < 0.001$ , Fig. 2.6F-G).





(A) Length of the OFT was measured via sagittal sections according to the line. (B-D) Immunostaining for phosphorylated histone H3 marking proliferating cells in the OFT (B-C) and ventricular myocardium (D). Panel C is the magnification of boxed area in panel B. (E) Quantification of OFT length. (F) Quantification of pHH3<sup>+</sup> cells in the OFT. (G) Quantification of pHH3<sup>+</sup> cells in the ventricle. n = 3-6 hearts per group from 2 – 4 litters, \*\* $P < 0.01$  vs. untreated control, † $P < 0.05$  vs. untreated control, †† $P < 0.01$  vs. untreated diabetes. Data are means  $\pm$  SEM in E-G and analyzed using two-way ANOVA followed by Bonferroni post-hoc test. Scale bars are 50  $\mu$ m and 20  $\mu$ m, respectively. OFT indicates outflow tract; pHH3, phosphorylated histone H3.

#### 2.4.5 Fate-mapping of SHF derived cells in the fetal heart of diabetic mothers

In order to better understand the spectrum of malformations induced by maternal diabetes seen at birth, embryonic lineage tracing of the SHF was carried out. Fate mapping using *Mef2c-Cre* and the global double fluorescent Cre reporter line *Rosa26<sup>mTmG</sup>* identified all SHF derived cells as GFP<sup>+</sup>. At E9.5, the number of GFP<sup>+</sup> SHF cells and total number of cells in the heart were significantly less than control ( $P < 0.01$ , Fig. 2.7A, D and E). Furthermore, significantly less GFP<sup>+</sup> SHF cells were infiltrated into the endocardial cushion at E12.5 in diabetic embryos compared to control ( $P = 0.0476$ , Fig. 2.7B and F). Additionally, E12.5 hearts from diabetic mothers had thinner ventricular walls with significantly less myocardial cell layers than controls ( $P < 0.01$ , Fig. 2.7C and G).



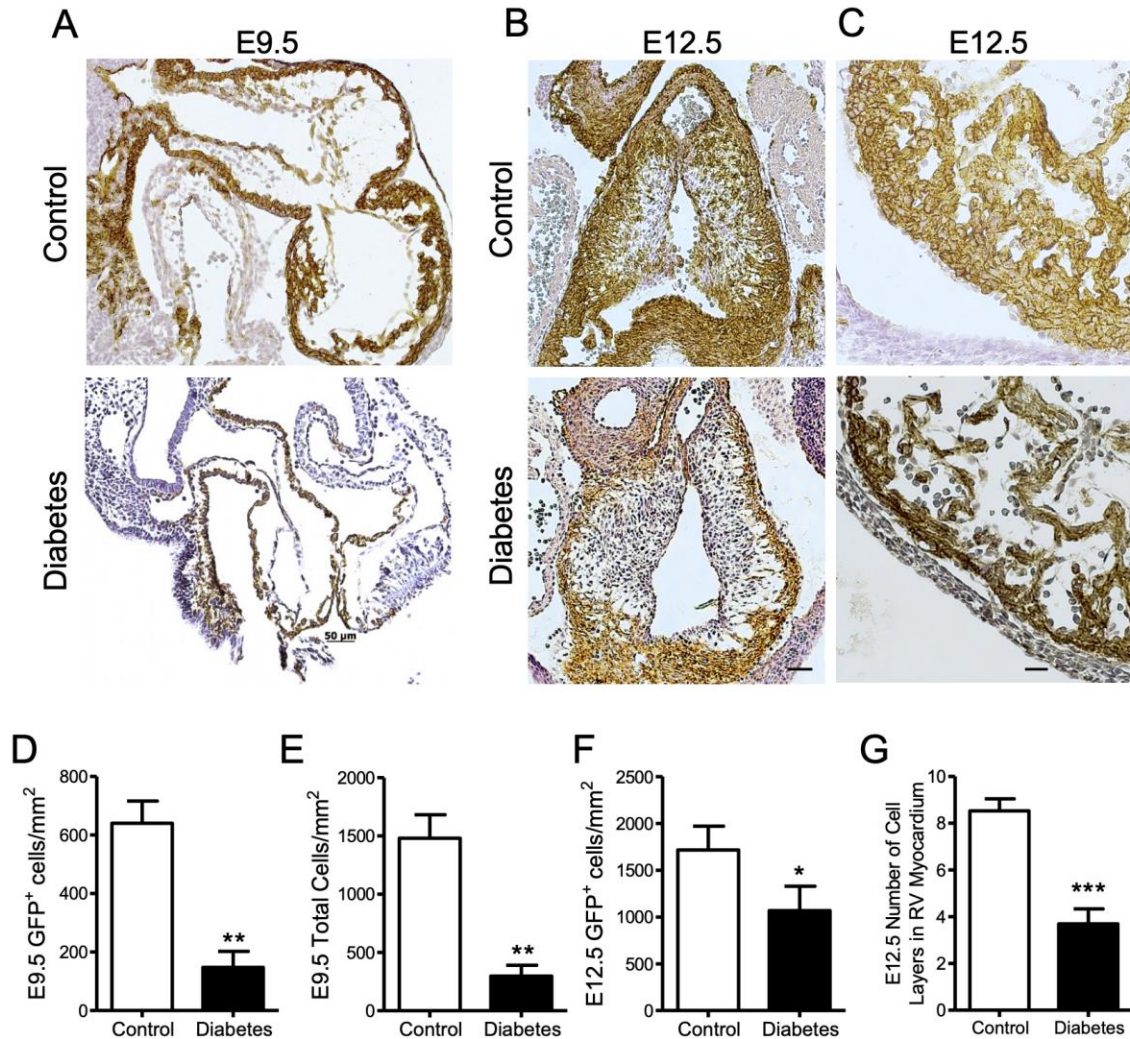


**Figure 2.7. Effects of pregestational diabetes on SHF progenitor contribution to E9.5 and E12.5 hearts.**

Fate mapping using the *mT/mG* reporter showing GFP<sup>+</sup> cells expressing Cre recombinase under the control of the anterior heart field specific *Mef2c* transcription factor. Representative sections of OFT of E9.5 (A) and E12.5 (B) hearts from control and diabetic mothers. (C) Representative sections showing the cell layers of the RV myocardium from E12.5 hearts. Quantification of SHF GFP<sup>+</sup> cells (D) and total number of cells (E) in the OFT cushions at E9.5. Quantification of SHF GFP<sup>+</sup> cells in the OFT cushions (F) and number of cell layers in the RV myocardium (G) at E12.5. N = 3 per group from 2 litters in D and E. N = 5 per group in F and G from 2 – 4 litters. \* $P < 0.05$ , \*\* $P < 0.01$ , \*\*\* $P < 0.001$  vs. control. Data are means  $\pm$  SEM in D-G and analyzed using unpaired Student's t test. Scale bars are 50  $\mu\text{m}$ . GFP indicates green fluorescent protein; RV, right ventricle.

#### 2.4.6 Sapropterin prevents maternal diabetes-induced downregulation of regulators of heart development

Pregestational diabetes induces changes in gene expression in the developing heart.<sup>32</sup> To determine if key transcriptional regulators of heart development were altered under maternal diabetes and with sapropterin treatment, qPCR analysis was performed from E12.5 hearts. Our data show that the mRNA levels of *Gata4*, *Tbx5*, *Nkx2.5*, *Gata5*, *Bmp10* and *Notch1* were significantly lower compared to controls ( $P < 0.05$ , Fig. 2.8A-F). Treatment with sapropterin significantly improved mRNA levels of these transcription factors ( $P < 0.001$ , Fig. 2.8A-F). Additionally, gene expression of BH4 biosynthesis enzymes including *GTP cyclohydrolase 1* (*Gch1*) and *dihydrofolate reductase* (*Dhfr*) was significantly decreased in embryonic hearts from diabetic mothers ( $P < 0.05$ , Fig. 2.8G and H). Of note, sapropterin treatment completely recovered the expression of *Dhfr* ( $P < 0.001$ , Fig. 2.8H).

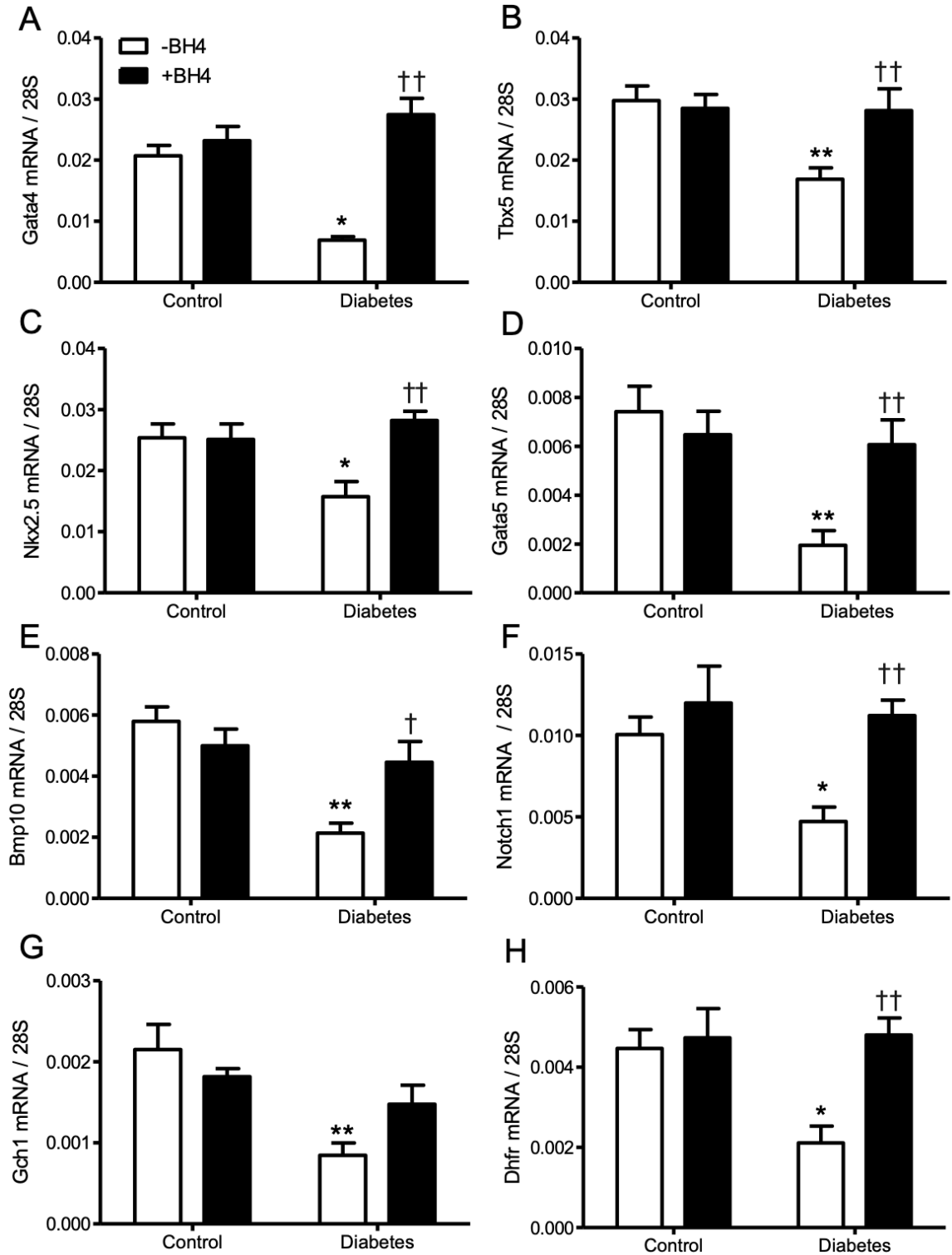


**Figure 2.8. Effects of sapropterin (BH4) on molecular regulators of heart development at E12.5.**

Real-time RT-PCR of cardiac transcription factors and regulators in E12.5 hearts of offspring from control and diabetic mothers. (A-F) The expression of Gata4, Tbx5, Nkx2.5, Gata5, Bmp10 and Notch1 were significantly decreased under maternal diabetes and restored with BH4 treatment. (G-H) The expression of Gch1 and Dhfr was significantly decreased with maternal diabetes. BH4 treatment rescues expression of DHFR. n = 4 – 7 hearts per group. \* $P < 0.05$ , \*\* $P < 0.01$  vs. untreated control, and † $P < 0.05$ , †† $P < 0.01$  vs. untreated diabetes. Data are means  $\pm$  SEM and analyzed using two-way ANOVA followed by Bonferroni post-hoc test.

#### 2.4.7 Sapropterin decreases oxidative stress and improves eNOS dimerization in fetal hearts of pregestational diabetes

To examine the effects of sapropterin on ROS in the developing heart, DHE probe was used to label the oxygen radical. Quantification of red fluorescence intensity indicates that superoxide generation was significantly elevated in embryonic hearts from mice with pregestational diabetes compared to control ( $P < 0.05$ , Fig. 2.9A and 2.B). Sapropterin treatment significantly reduced myocardial ROS levels to basal conditions ( $P < 0.05$  Fig. 2.9B). Pre-treatment with L-NAME, a NOS inhibitor, and SOD, an antioxidant enzyme, significantly decreased DHE fluorescence in embryonic hearts from diabetic dams indicating eNOS uncoupling and superoxide generation, respectively ( $P < 0.05$  Fig. 2.9B). Finally, eNOS uncoupling has been implicated as a mechanism for endothelial dysfunction in diabetes.<sup>23</sup> To assess the effects of sapropterin on eNOS coupling, eNOS dimerization was analyzed using Western blotting in non-reducing conditions, which yields two bands at 260 and 130 kDa, representing the intact dimer and monomer of eNOS, respectively. Figure 2.9C shows a representative blot of the dimer and monomer of eNOS. In control conditions, there was a higher level of eNOS dimers than monomers, indicating a functional eNOS enzyme. However, embryonic hearts from



diabetic dams show a significant decrease of dimer/monomer ratios compared to controls ( $P < 0.05$ , Fig. 2.9D), which was restored by sapropterin treatment ( $P < 0.01$ , Fig. 2.9D).

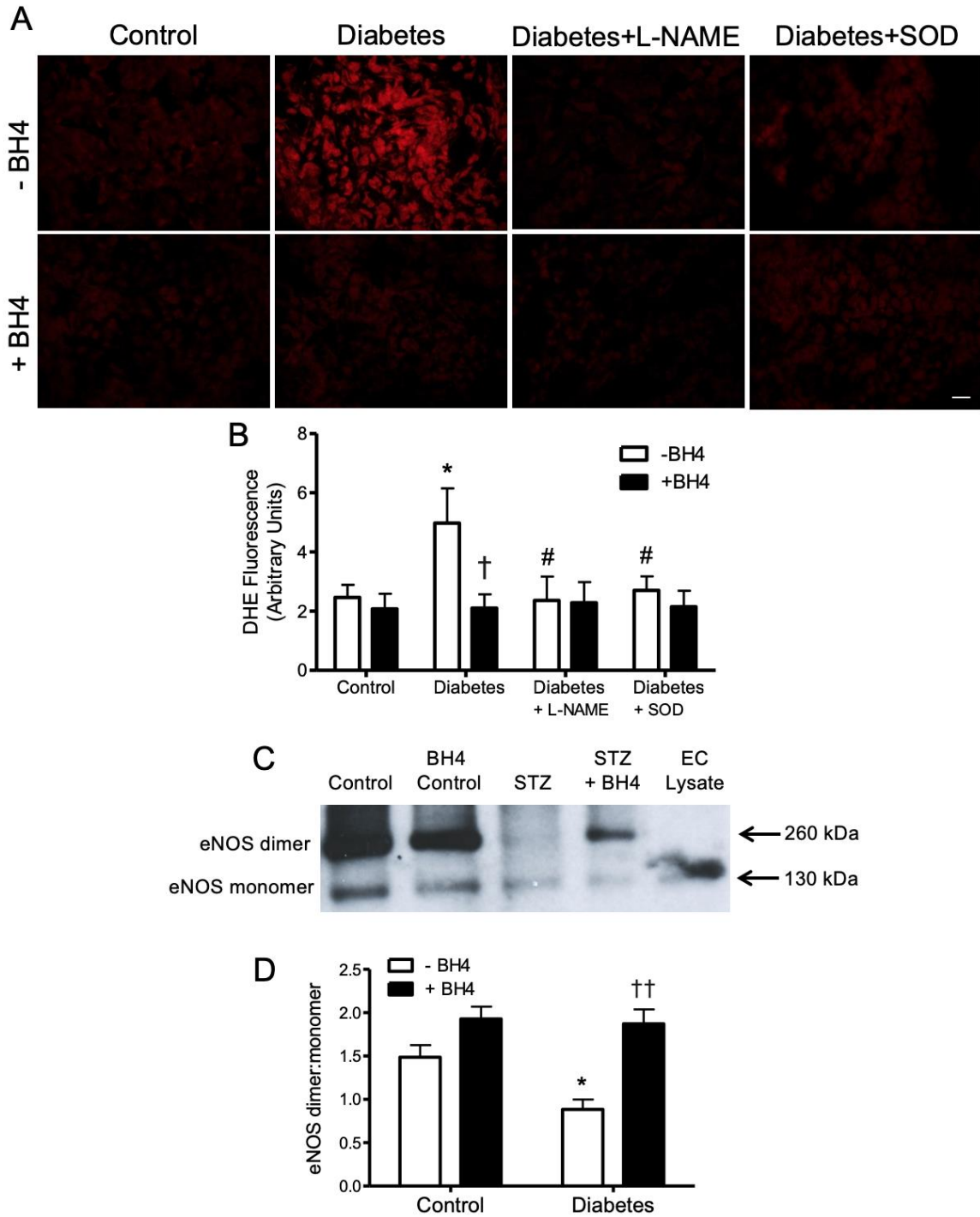


**Figure 2.9. Effects of sapropterin (BH4) on superoxide production and eNOS dimer/monomer protein levels in E12.5 hearts.**

(A) Representative images of DHE staining in the ventricular myocardium of E12.5 hearts from control and diabetic dams with and without BH4 administration. A subset of heart sections from diabetic dams were pre-treated with L-NAME (300  $\mu$ M) or SOD (100 units/mL) for 30 minutes prior to DHE probing. (B) Quantification of DHE fluorescence signals. (C) Representative Western blotting showing eNOS dimer and monomer bands of E12.5 hearts from control and diabetic dams with and without BH4 treatment. Denatured endothelial cell lysate validates the size of the eNOS monomer band. (D) Densitometric analysis of eNOS dimer/monomer ratios.  $n = 5 - 6$  hearts per group from 2 - 4 litters. \* $P < 0.05$  vs. untreated control, †† $P < 0.01$  vs. untreated diabetes, # $P < 0.05$  vs. untreated diabetes. Data are means  $\pm$ SEM in B and D, and analyzed using two-way ANOVA followed by Bonferroni post-hoc test. DHE indicates dihydroethidium; EC, endothelial cell; L-NAME, N $\omega$ -Nitro-L-arginine methyl ester; SOD, superoxide dismutase.

## 2.5 Discussion

The present study utilized a clinically relevant model of CHDs induced by pregestational diabetes we recently established.<sup>30, 31</sup> Consistent with our previous studies, a spectrum of CHDs were observed in the offspring of diabetic mothers. The CHDs range from ASD, VSD and valve thickening, to major malformations including AVSD, DORV, truncus arteriosus and hypoplastic left heart, as clinically categorized by Hoffman *et al.*<sup>33</sup> Sapropterin treatment was able to prevent all major defects and significantly reduce the overall level of defects induced by pregestational diabetes. Other changes in the fetal heart such as thinner ventricular myocardium, thickened valves, stenosis of the aorta and pulmonary artery, impaired cardiac function along with decreased cell proliferation and gene expression induced by maternal diabetes, were normalized with sapropterin treatment. Furthermore, sapropterin administration in the diabetic dams increased eNOS dimerization and decreased ROS levels in the fetal heart. Our study suggests that sapropterin improves eNOS coupling and prevents CHDs in pregestational diabetes in mice (Fig. 2.10).

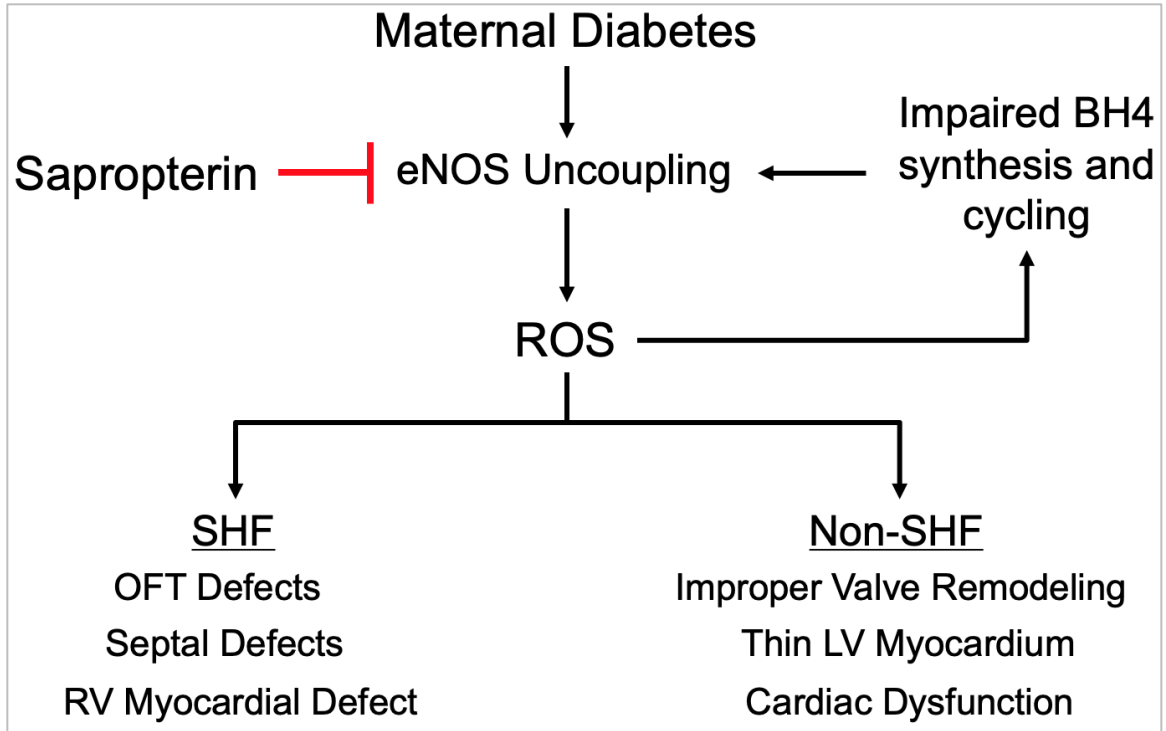


**Figure 2.10. Schematic summary of sapropterin on diabetes-induced CHDs .**

eNOS uncoupling and CHDs induced by pregestational diabetes and the inhibitory effects by sapropterin treatment. Abnormalities of both second heart field (SHF) and non-SHF derived structures are prevented by sapropterin treatment. LV indicates left ventricle; OFT, outflow tract; ROS, reactive oxygen species; RV, right ventricle.

In this model, STZ was used to induce hyperglycemia in female mice at least 7 days before they were bred with normal healthy males. Since STZ has a short plasma half-life of 10 minutes in rodents,<sup>34</sup> it is unlikely that STZ would cause any teratogenic effects in the fetus. To confirm that hyperglycemia is the cause of CHD in this model, a group of mice were treated with insulin to lower glucose levels in diabetic dams. Our data show that insulin treatment abrogated CHDs in pregestational diabetes, which is consistent with clinical studies that good glycemic control in women with pregestational diabetes lowers the incidence of CHDs.<sup>7</sup> It should be noted that the incidence of CHDs found in the diabetic groups with or without sapropterin treatment at E18.5 may be an

underestimate as fetuses may have been absorbed in utero at around E12.5. To study the effects of sapropterin on maternal diabetes, blood glucose levels were assessed during pregnancy. Our data show that sapropterin treatment in the diabetic dams had no effect on the hyperglycemic state of the animal, suggesting that the beneficial effects of sapropterin on fertility (or percent successful pregnancy), litter size, and heart development under pregestational diabetes are independent of blood glucose levels. In humans, sex-related differences in the prevalence of CHDs have been reported. In a recent large cohort study with 9,727 cases of CHDs, the male to female ratio was 55% to 45%, indicating a significant predisposition of CHDs in the male sex.<sup>35</sup> In agreement with clinical studies, our data show a male dominance of CHDs in the offspring of diabetic mothers. Notably, sapropterin treatment appears to be more effective in preventing CHDs in females than in males.

We have recently shown that defects in SHF signaling results in thin myocardium, septal defects and OFT defects.<sup>26, 36</sup> The defective SHF progenitor contribution may explain the majority of heart malformations in the OFT, cardiac septum and cardiac valves induced by pregestational diabetes. Since sapropterin treatment significantly prevented these CHDs in the offspring of diabetic dams, it is likely that impairment in SHF progenitors will be diminished by maternal sapropterin treatment, which still needs to be confirmed in future studies. Considering the presence of hypoplastic left heart and OFT septation defect (truncus arteriosus), it is possible that pregestational diabetes also impairs FHF and CNC cells in our model. Notably, these defects were all prevented in diabetic dams treated with sapropterin. These findings are consistent with previous studies showing that oxidative stress during diabetic pregnancy disrupts CNC migration

and causes OFT defects in rodents,<sup>37, 38</sup> which are prevented by treatment with vitamin E, an antioxidant.<sup>39</sup> Our results suggest that sapropterin treatment improves the function of both SHF and non-SHF (FHF and CNC) progenitors in pregestational diabetes (Fig. 2.10).

Cell proliferation is critical to cardiac morphogenesis and the growth of the fetal heart.<sup>40</sup> Decreased cell proliferation results in shortening of OFT length, thin myocardium and CHDs.<sup>36, 41</sup> In the present study, E10.5 hearts show less cell proliferation and a shorter OFT in embryos from diabetic dams. Furthermore, E18.5 hearts from diabetic dams are notably smaller and their ventricular walls are significantly thinner than control hearts. These abnormalities were all prevented by sapropterin treatment. Previous studies have shown that BH4 increases DNA synthesis and cell proliferation in erythroid cells.<sup>42</sup> Additionally, BH4 mediates the proliferative effects of epidermal growth factor and nerve growth factor in PC12 cells.<sup>43</sup> We have previously shown that eNOS promotes cardiomyocyte proliferation.<sup>17, 44</sup> Since BH4 increases eNOS coupling as shown by higher dimer/monomer ratios in our study, it is possible that a normalized eNOS signaling may contribute to the improved cell proliferation by sapropterin treatment. Increases in cell apoptosis may also contribute to CHDs. However, we have previously shown that the incidence of cell apoptosis in fetal hearts of diabetic offspring is low (about 1%) and was not affected by anti-oxidant treatment, suggesting an insignificant role of apoptosis in our model.<sup>31</sup> We therefore did not assess cell apoptosis in the present study.

Cardiac transcription factors including Gata4, Gata5, Nkx2.5 and Tbx5 are critical to normal heart development, and genetic mutations of these transcription factors result in

CHDs in humans.<sup>45</sup> Interestingly, both eNOS and ROS can alter the expression of these transcription factors.<sup>16, 31</sup> For example, deficiency in eNOS decreases the expression of cardiac transcription factors including *Gata4* during embryonic heart development.<sup>19</sup> Additionally, the expression of cardiac transcription factors was downregulated in the fetal heart of offspring of diabetic mothers, which was restored by treatment with an antioxidant, N-acetylcysteine.<sup>31</sup> In agreement with our previous studies, we showed a downregulation of *Gata4*, *Gata5*, *Nkx2.5* and *Tbx5* in fetal hearts of offspring from diabetic mothers in the present study. Decreased expression was also seen in *Bmp10*, essential in cardiac growth and chamber maturation.<sup>46</sup> Importantly, sapropterin administration to diabetic dams restored the expression profile of these factors to normal levels. We also assessed the expression of *Gch1* and *Dhfr*, which are enzymes responsible for de novo BH<sub>4</sub> biosynthesis and recycling of BH<sub>2</sub> back to BH<sub>4</sub>, respectively. Both GCH1 and DHFR are sensitive to oxidative stress and NO signaling.<sup>21, 47</sup> Of note, NO has been shown to stabilize DHFR protein from ubiquitination and degradation by S-nitrosylation.<sup>48</sup> During pregestational diabetes, GCH1 and DHFR transcript levels in the fetal heart were downregulated, which was normalized by sapropterin treatment. Our findings indicate a possible gene regulatory mechanism governing DHFR expression. Recent studies show a strong interaction between eNOS and Notch1 promoting semilunar valve and outflow tract development.<sup>49</sup> Here we show that Notch1 mRNA is decreased in embryonic hearts from diabetic dams, which is rescued with sapropterin treatment. Our results indicate a perturbed NO-Notch1 signaling pathway in the fetal hearts of diabetic dams. Together, these effects are consistent with the ability of sapropterin treatment to recouple eNOS and restore ROS balance in the

embryonic heart of diabetic dams. It should be noted that nNOS and iNOS are dispensable for heart development since nNOS<sup>-/-</sup> and iNOS<sup>-/-</sup> mice do not exhibit any developmental abnormalities of the heart.<sup>16</sup>

A major non-cardiac malformation induced by pregestational diabetes is NTD such as anencephaly, exencephaly and spina bifida.<sup>50</sup> It has been reported that 25-40% offspring of diabetic dams have NTDs when the fetuses are examined at E10.5.<sup>51, 52</sup> To analyze cardiac malformation, we examined the fetuses at E18.5 and may have missed most of the NTDs, which are likely absorbed beyond E10.5. This may be the reason that we only observed one exencephaly in the present study and a low incidence of NTDs (4.8%) in our previous study.<sup>31</sup> Additionally, BH4 biosynthesis is important to neural tube development. Inhibition of GCH1 activity, a rate limiting enzyme in the biosynthesis of BH4, interrupts neural tube closure, which can be prevented by BH4 treatment in chick embryos.<sup>53</sup> Furthermore, *GCHI* haplotypes are significantly associated with a higher risk of NTD in infants.<sup>54</sup> It is possible that sapropterin treatment may prevent NTD induced by pregestational diabetes, a hypothesis that needs to be tested in future studies. Surprisingly, the GCH1 knockout mice die at E13.5 due to bradycardia without any structural anomalies.<sup>55</sup> Apart from being a cofactor of eNOS, BH4 is also a substrate for aromatic amino acid hydroxylases.<sup>56</sup> BH4 treatment at postnatal day 14 elevated dopamine levels in the brain and fully restored the loss of tyrosine hydroxylase protein caused by the BH4 deficiency in infant mice,<sup>57</sup> indicating an important role of BH4 in dopaminergic function of the brain. The effects of pregestational diabetes and sapropterin treatment on tyrosine hydroxylase expression and dopamine levels in the fetal brain are beyond the scope of the present investigation.

In summary, the present study demonstrates that treatment with sapropterin (Kuvan®), an orally active synthetic form of BH4 during gestation improves eNOS coupling, reduces ROS and increases cell proliferation in the embryonic heart of offspring of diabetic mothers. Notably, sapropterin treatment prevents the development of major CHDs induced by pregestational diabetes. Sapropterin is an FDA approved drug to treat phenylketonuria (PKU), a genetic disorder due to mutations of phenylalanine hydroxylase (PAH) gene leading to low levels of phenylalanine hydroxylase.<sup>25</sup> Our study suggests that sapropterin may also have therapeutic potential in preventing CHDs in offspring of women with pregestational diabetes.

## 2.6 Footnotes

This study was funded in part by grants from the Canadian Institutes of Health Research (CIHR) to Qingping Feng and Tom Drysdale, and the Children's Health Foundation in London, Ontario, Canada to Kambiz Norozi, Tom Drysdale and Qingping Feng. We thank Dr. Ben Rubin, Western University for his advice on statistical analysis. Qingping Feng is a Richard and Jean Ivy Chair in Molecular Toxicology at University of Western Ontario.



## 2.7 References

1. Pierpont ME, Basson CT, Benson DW, Jr., Gelb BD, Giglia TM, Goldmuntz E, McGee G, Sable CA, Srivastava D, Webb CL, American Heart Association Congenital Cardiac Defects Committee CoCDitY. Genetic basis for congenital heart defects: current knowledge: a scientific statement from the American Heart Association Congenital Cardiac Defects Committee, Council on Cardiovascular Disease in the Young: endorsed by the American Academy of Pediatrics. *Circulation*. 2007;115:3015-38
2. Gilboa SM, Devine OJ, Kucik JE, Oster ME, Riehle-Colarusso T, Nembhard WN, Xu P, Correa A, Jenkins K, Marelli AJ. Congenital heart defects in the United States: Estimating the magnitude of the affected population in 2010. *Circulation*. 2016;134:101-9
3. Marelli AJ, Ionescu-Ittu R, Mackie AS, Guo L, Dendukuri N, Kaouache M. Lifetime prevalence of congenital heart disease in the general population from 2000 to 2010. *Circulation*. 2014;130:749-56
4. Meilhac SM, Lescroart F, Blanpain C, Buckingham ME. Cardiac cell lineages that form the heart. *Cold Spring Harb Perspect Med*. 2014;4:a013888
5. Oyen N, Diaz LJ, Leirgul E, Boyd HA, Priest J, Mathiesen ER, Quertermous T, Wohlfahrt J, Melbye M. Prepregnancy diabetes and offspring risk of congenital heart disease: A nationwide cohort study. *Circulation*. 2016;133:2243-53
6. Liu S, Joseph KS, Lisonkova S, Rouleau J, Van den Hof M, Sauve R, Kramer MS, Canadian Perinatal Surveillance S. Association between maternal chronic conditions and congenital heart defects: a population-based cohort study. *Circulation*. 2013;128:583-9
7. Starikov R, Bohrer J, Goh W, Kuwahara M, Chien EK, Lopes V, Coustan D. Hemoglobin A1c in pregestational diabetic gravidas and the risk of congenital heart disease in the fetus. *Pediatr Cardiol*. 2013;34:1716-22
8. Eriksen NB, Damm P, Mathiesen ER, Ringholm L. The prevalence of congenital malformations is still higher in pregnant women with pregestational diabetes despite near-normal HbA1c: a literature review. *J Matern Fetal Neonatal Med*. 2017:1-5
9. Peng TY, Ehrlich SF, Crites Y, Kitzmiller JL, Kuzniewicz MW, Hedderson MM, Ferrara A. Trends and racial and ethnic disparities in the prevalence of pregestational type 1 and type 2 diabetes in Northern California: 1996-2014. *Am J Obstet Gynecol*. 2017;216:177.e1-177.e8
10. Wahabi H, Fayed A, Esmaeil S, Mamdouh H, Kotb R. Prevalence and Complications of Pregestational and Gestational Diabetes in Saudi Women:

Analysis from Riyadh Mother and Baby Cohort Study (RAHMA). *Biomed Res Int.* 2017;2017:6878263

11. Agarwal S, Sud K, Menon V. Nationwide hospitalization trends in adult congenital heart disease across 2003-2012. *J Am Heart Assoc.* 2016;5:e002330
12. Opotowsky AR, Siddiqi OK, Webb GD. Trends in hospitalizations for adults with congenital heart disease in the U.S. *J Am Coll Cardiol.* 2009;54:460-7
13. Ornoy A. Embryonic oxidative stress as a mechanism of teratogenesis with special emphasis on diabetic embryopathy. *Reprod Toxicol.* 2007;24:31-41
14. Eriksson UJ, Borg LA. Diabetes and embryonic malformations. Role of substrate-induced free-oxygen radical production for dysmorphogenesis in cultured rat embryos. *Diabetes.* 1993;42:411-9
15. Zangen SW, Yaffe P, Shechtman S, Zangen DH, Ornoy A. The role of reactive oxygen species in diabetes-induced anomalies in embryos of Cohen diabetic rats. *Int J Exp Diabetes Res.* 2002;3:247-55
16. Liu Y, Feng Q. NOing the heart: role of nitric oxide synthase-3 in heart development. *Differentiation.* 2012;84:54-61
17. Feng Q, Song W, Lu X, Hamilton JA, Lei M, Peng T, Yee SP. Development of heart failure and congenital septal defects in mice lacking endothelial nitric oxide synthase. *Circulation.* 2002;106:873-9
18. Liu Y, Lu X, Xiang FL, Lu M, Feng Q. Nitric oxide synthase-3 promotes embryonic development of atrioventricular valves. *PLoS One.* 2013;8:e77611
19. Liu Y, Lu X, Xiang FL, Poelmann RE, Gittenberger-de Groot AC, Robbins J, Feng Q. Nitric oxide synthase-3 deficiency results in hypoplastic coronary arteries and postnatal myocardial infarction. *Eur Heart J.* 2014;35:920-31
20. Werner ER, Blau N, Thony B. Tetrahydrobiopterin: biochemistry and pathophysiology. *Biochem J.* 2011;438:397-414
21. Bendall JK, Douglas G, McNeill E, Channon KM, Crabtree MJ. Tetrahydrobiopterin in cardiovascular health and disease. *Antioxid Redox Signal.* 2014;20:3040-77
22. Ma S, Ma CC. Recent developments in the effects of nitric oxide-donating statins on cardiovascular disease through regulation of tetrahydrobiopterin and nitric oxide. *Vascul Pharmacol.* 2014;63:63-70
23. Cai S, Khoo J, Mussa S, Alp NJ, Channon KM. Endothelial nitric oxide synthase dysfunction in diabetic mice: importance of tetrahydrobiopterin in eNOS dimerisation. *Diabetologia.* 2005;48:1933-40

24. Heitzer T, Krohn K, Albers S, Meinertz T. Tetrahydrobiopterin improves endothelium-dependent vasodilation by increasing nitric oxide activity in patients with type II diabetes mellitus. *Diabetologia*. 2000;43:1435-8
25. Burnett JR. Sapropterin dihydrochloride (Kuvan/phenoptin), an orally active synthetic form of BH4 for the treatment of phenylketonuria. *IDrugs*. 2007;10:805-13
26. Leung C, Lu X, Liu M, Feng Q. Rac1 signaling is critical to cardiomyocyte polarity and embryonic heart development. *J Am Heart Assoc*. 2014;3:e001271
27. Verzi MP, McCulley DJ, De Val S, Dodou E, Black BL. The right ventricle, outflow tract, and ventricular septum comprise a restricted expression domain within the secondary/anterior heart field. *Dev Biol*. 2005;287:134-45
28. Zou MH, Shi C, Cohen RA. Oxidation of the zinc-thiolate complex and uncoupling of endothelial nitric oxide synthase by peroxynitrite. *J Clin Invest*. 2002;109:817-26
29. Fukushima T, Nixon JC. Analysis of reduced forms of biopterin in biological tissues and fluids. *Anal Biochem*. 1980;102:176-88
30. Moazzen H, Lu X, Liu M, Feng Q. Pregestational diabetes induces fetal coronary artery malformation via reactive oxygen species signaling. *Diabetes*. 2015;64:1431-43
31. Moazzen H, Lu X, Ma NL, Velenosi TJ, Urquhart BL, Wisse LJ, Gittenberger-de Groot AC, Feng Q. N-Acetylcysteine prevents congenital heart defects induced by pregestational diabetes. *Cardiovasc Diabetol*. 2014;13:46
32. Vijaya M, Manikandan J, Parakalan R, Dheen ST, Kumar SD, Tay SS. Differential gene expression profiles during embryonic heart development in diabetic mice pregnancy. *Gene*. 2013;516:218-27
33. Hoffman JI, Kaplan S, Liberthson RR. Prevalence of congenital heart disease. *Am Heart J*. 2004;147:425-39
34. Schein PS, Loftus S. Streptozotocin: depression of mouse liver pyridine nucleotides. *Cancer Res*. 1968;28:1501-6
35. Hoang TT, Goldmuntz E, Roberts AE, Chung WK, Kline JK, Deanfield JE, Gardini A, Aleman A, Gelb BD, Mac Neal M, Porter GA, Jr., Kim R, Brueckner M, Lifton RP, Edman S, Woyciechowski S, Mitchell LE, Agopian AJ. The Congenital Heart Disease Genetic Network Study: Cohort description. *PLoS One*. 2018;13:e0191319

36. Leung C, Liu Y, Lu X, Kim M, Drysdale TA, Feng Q. Rac1 signaling is required for anterior second heart field cellular organization and cardiac outflow tract development. *J Am Heart Assoc.* 2016;5:e002508
37. Morgan SC, Relaix F, Sandell LL, Loeken MR. Oxidative stress during diabetic pregnancy disrupts cardiac neural crest migration and causes outflow tract defects. *Birth Defects Res A Clin Mol Teratol.* 2008;82:453-63
38. Molin DG, Roest PA, Nordstrand H, Wisse LJ, Poelmann RE, Eriksson UJ, Gittenberger-De Groot AC. Disturbed morphogenesis of cardiac outflow tract and increased rate of aortic arch anomalies in the offspring of diabetic rats. *Birth Defects Res A Clin Mol Teratol.* 2004;70:927-38
39. Siman CM, Gittenberger-De Groot AC, Wisse B, Eriksson UJ. Malformations in offspring of diabetic rats: morphometric analysis of neural crest-derived organs and effects of maternal vitamin E treatment. *Teratology.* 2000;61:355-67
40. Sedmera D, Thompson RP. Myocyte proliferation in the developing heart. *Dev Dyn.* 2011;240:1322-34
41. Roux M, Laforest B, Capecchi M, Bertrand N, Zaffran S. Hoxb1 regulates proliferation and differentiation of second heart field progenitors in pharyngeal mesoderm and genetically interacts with Hoxa1 during cardiac outflow tract development. *Dev Biol.* 2015;406:247-58
42. Tanaka K, Kaufman S, Milstien S. Tetrahydrobiopterin, the cofactor for aromatic amino acid hydroxylases, is synthesized by and regulates proliferation of erythroid cells. *Proc Natl Acad Sci U S A.* 1989;86:5864-7
43. Anastasiadis PZ, Bezin L, Imerman BA, Kuhn DM, Louie MC, Levine RA. Tetrahydrobiopterin as a mediator of PC12 cell proliferation induced by EGF and NGF. *Eur J Neurosci.* 1997;9:1831-7
44. Lepic E, Burger D, Lu X, Song W, Feng Q. Lack of endothelial nitric oxide synthase decreases cardiomyocyte proliferation and delays cardiac maturation. *Am J Physiol Cell Physiol.* 2006;291:C1240-6
45. McCulley DJ, Black BL. Transcription factor pathways and congenital heart disease. *Curr Top Dev Biol.* 2012;100:253-77
46. Chen H, Shi S, Acosta L, Li W, Lu J, Bao S, Chen Z, Yang Z, Schneider MD, Chien KR, Conway SJ, Yoder MC, Haneline LS, Franco D, Shou W. BMP10 is essential for maintaining cardiac growth during murine cardiogenesis. *Development.* 2004;131:2219-31
47. Li H, Forstermann U. Pharmacological prevention of eNOS uncoupling. *Curr Pharm Des.* 2014;20:3595-606

48. Cai Z, Lu Q, Ding Y, Wang Q, Xiao L, Song P, Zou MH. Endothelial Nitric Oxide Synthase-Derived Nitric Oxide Prevents Dihydrofolate Reductase Degradation via Promoting S-Nitrosylation. *Arterioscler Thromb Vasc Biol.* 2015;35:2366-73
49. Koenig SN, Bosse K, Majumdar U, Bonachea EM, Radtke F, Garg V. Endothelial Notch1 Is Required for Proper Development of the Semilunar Valves and Cardiac Outflow Tract. *J Am Heart Assoc.* 2016;5:e003075
50. Correa A, Gilboa SM, Besser LM, Botto LD, Moore CA, Hobbs CA, Cleves MA, Riehle-Colarusso TJ, Waller DK, Reece EA. Diabetes mellitus and birth defects. *Am J Obstet Gynecol.* 2008;199:237 e1-9
51. Yang P, Li X, Xu C, Eckert RL, Reece EA, Zielke HR, Wang F. Maternal hyperglycemia activates an ASK1-FoxO3a-caspase 8 pathway that leads to embryonic neural tube defects. *Sci Signal.* 2013;6:ra74
52. Yang P, Zhao Z, Reece EA. Activation of oxidative stress signaling that is implicated in apoptosis with a mouse model of diabetic embryopathy. *Am J Obstet Gynecol.* 2008;198:130.e1
53. Nachmany A, Gold V, Tsur A, Arad D, Weil M. Neural tube closure depends on nitric oxide synthase activity. *J Neurochem.* 2006;96:247-53
54. Lupo PJ, Chapa C, Noursome D, Duhon C, Canfield MA, Shaw GM, Finnell RH, Zhu H, National Birth Defects Prevention S. A GCH1 haplotype and risk of neural tube defects in the National Birth Defects Prevention Study. *Mol Genet Metab.* 2012;107:592-5
55. Douglas G, Hale AB, Crabtree MJ, Ryan BJ, Hansler A, Watschinger K, Gross SS, Lygate CA, Alp NJ, Channon KM. A requirement for Gch1 and tetrahydrobiopterin in embryonic development. *Dev Biol.* 2015;399:129-138
56. Fitzpatrick PF. The aromatic amino acid hydroxylases. *Adv Enzymol Relat Areas Mol Biol.* 2000;74:235-94
57. Homma D, Katoh S, Tokuoka H, Ichinose H. The role of tetrahydrobiopterin and catecholamines in the developmental regulation of tyrosine hydroxylase level in the brain. *J Neurochem.* 2013;126:70-81

## Chapter 3

### **Sapropterin Reduces Coronary Artery Malformation in Offspring of Pregestational Diabetes Mice**

A version of this chapter has been submitted to *Nitric Oxide*.

Anish Engineer <sup>1</sup>, Yong Jin Lim <sup>1</sup>, Xiangru Lu <sup>1</sup>, Kambiz Norozi <sup>3,4,5,6</sup>, and Qingping Feng <sup>1,2,3</sup>.

<sup>1</sup> Department of Physiology and Pharmacology, <sup>2</sup> Department of Medicine, Schulich School of Medicine and Dentistry, Western University, <sup>3</sup> Children's Health Research Institute, London, Ontario, Canada.

<sup>4</sup> Department of Paediatrics, Western University, London, Ontario, Canada; <sup>5</sup> Department of Paediatric Cardiology and Intensive Care Medicine, Medical School Hannover, Germany; <sup>6</sup> Department of Paediatric Cardiology and Intensive Care Medicine, University of Goettingen, Germany

“Sapropterin Reduces Coronary Artery Malformation in Offspring of Pregestational Diabetes Mice”

## 3 Chapter 3

### 3.1 Chapter Summary

Endothelial nitric oxide synthase (eNOS) and oxidative stress are critical to embryonic coronary artery development. Maternal diabetes increases oxidative stress and reduces eNOS activity in the fetal heart. Sapropterin (Kuvan®) is an orally active, synthetic form of tetrahydrobiopterin (BH4) and a co-factor for eNOS with antioxidant properties. The aim of the present study was to examine the effects of sapropterin on embryonic coronary artery development during pregestational diabetes in mice. Diabetes was induced by streptozotocin to adult female C57BL/6 mice. Sapropterin (10 mg/kg/day) was orally administered to pregnant mice from E0.5 to E18.5. Fetal hearts were collected at E18.5 for coronary artery morphological analysis. Sapropterin treatment to diabetic dams reduced the incidence of coronary artery malformation in offspring from 50.0% to 20.6%. Decreases in coronary artery luminal diameter, volume and abundance in hearts from diabetic mothers, were prevented by sapropterin treatment. Maternal diabetes reduced epicardial epithelial-to-mesenchymal transition (EMT) and expression of transcription and growth factors critical to coronary artery development including hypoxia-inducible factor 1a (*Hif1a*), *Snail1*, *Slug*,  $\beta$ -*catenin*, retinaldehyde dehydrogenase 2 (*Aldh1a2*) and basic fibroblast growth factor (*bFGF*) in E12.5 hearts. Additionally, eNOS phosphorylation was lower while oxidative stress was higher in E12.5 hearts from maternal diabetes. Notably, these abnormalities were all restored to normal levels after sapropterin treatment. In conclusion, sapropterin treatment increases eNOS activity, reduces oxidative stress and prevents coronary artery malformation in

offspring of pregestational diabetes. Sapropterin may have therapeutic potential in the prevention of coronary artery malformation in pregestational diabetes.

## 3.2 Introduction

Diabetes is a global health concern. In 2013, approximately 21.4 million pregnancies worldwide were affected by diabetes, of which 16% were pregestational diabetes.<sup>1</sup> Women with pregestational diabetes are at an increased risk of having a child with a congenital heart defect (CHD).<sup>2</sup> Hypoplastic coronary artery disease (HCAD) is a congenital abnormality characterized by a marked decrease in luminal diameter and length of one or more major branches of coronary arteries.<sup>3-6</sup> HCAD can be asymptomatic at birth but are often associated with myocardial infarction and sudden cardiac death under physical exertion later in life.<sup>7, 8</sup> In the clinic, newborns are screened for many forms of CHDs, however, coronary artery branches are not reliably imaged using non-invasive tools perinatally.<sup>9</sup> HCAD is a rare form of congenital coronary artery malformations (CAMs) including anomalous origins of the left and right coronary arteries, single coronary artery, and coronary artery fistula, which collectively affect ~1% of the general population.<sup>10, 11</sup> While the clinical etiology of congenital coronary artery anomalies is undefined, we have recently shown that pregestational diabetes results in CAMs in the fetal heart of offspring in mice.<sup>12</sup>

The heart is the first functional organ to form during embryogenesis, and vascularization in the primitive heart initiates at E9.5 in the proepicardial organ.<sup>13, 14</sup> Cells from this primitive structure migrate to cover the surface of myocardium, forming an epicardium, which is fully formed by E12.5. These cells then undergo coordinated epithelial-to-mesenchymal transition (EMT) and become epicardial-derived cells



(EPDCs).<sup>14</sup> EPDCs migrate to the subepicardial space and differentiate into vascular smooth muscle cells, endothelial cells and adventitial fibroblasts, all which are needed to form coronary vessels.<sup>14</sup> The endocardium and sinus venosus also contribute to this coronary plexus, and a complete coronary network is established by E15.<sup>15, 16</sup> A misstep in any of these processes including alterations in gene expression, cell proliferation and epicardial EMT may result in coronary artery malformations.

Hyperglycemia-induced reactive oxygen species (ROS) is not conducive to heart and coronary artery development as it oxidizes cardiogenic and angiogenic molecules. Endothelial nitric oxide synthase (eNOS) is critical to embryonic heart development as nitric oxide (NO) regulates transcription factor expression, progenitor cell growth and EMT.<sup>17</sup> In fact, eNOS<sup>-/-</sup> mice display hypoplastic coronary arteries and postnatal myocardial infarction.<sup>18</sup> Tetrahydrobiopterin (BH4) is a co-factor for eNOS, and an antioxidant. It stabilizes the enzyme dimer and allows arginine binding.<sup>19</sup> Under oxidative stress, BH4 levels decline and eNOS is uncoupled and unable to form NO, instead generates superoxide.<sup>20</sup> BH4 improve eNOS coupling and vascular endothelial function in diabetes.<sup>21</sup> However, the ability of BH4 to regulate coronary artery development in the fetal heart is not known. The FDA-approved drug, sapropterin dihydrochloride (Kuvan®), is a stable, orally active, synthetic form of BH4. In the present study, we aim to determine the effects of sapropterin on coronary artery development under pregestational diabetes in mice. Our hypothesis was that sapropterin treatment improves epicardial EMT and prevents CAMs during pregestational diabetes.

### 3.3 Methods

#### 3.3.1 Animals

C57BL/6 wild-type mice were purchased from Jackson Laboratory (Bar Harbour, Maine), and a breeding program was implemented to generate postnatal and fetal mice. All animals used in this study were handled according to the National Institute of Health Guide for the Care and Use of Laboratory Animals (8<sup>th</sup> edition, 2011). All procedures were approved by the Animal Care Committee at Western University, following the Canadian Council on Animal Care guidelines.

#### 3.3.2 Induction of Diabetes and Sapropterin Treatment

Diabetes was induced to six to eight-week old female C57BL/6 mice by streptozotocin (STZ, 50 mg/kg body weight, I.P.) injections for five consecutive days, as previously described.<sup>22, 23</sup> STZ was dissolved in a sterile saline solution at the time of administration, with sterile saline as vehicle controls. Non-fasting blood glucose levels were measured one week following the last injection using a glucose meter (One Touch Ultra2, LifeScan Canada, Burnaby, BC). Mice with blood glucose levels above 11.0 mmol/L were considered to be diabetic and subsequently bred with adult wild-type male mice. A vaginal plug indicated embryonic day 0.5 (E0.5) and the pregnant female mice were placed in a cage with littermates. A subset of the diabetic dams received a 10 mg/kg per body weight oral dose of sapropterin dihydrochloride (Kuvan®, BioMarin Pharmaceutical Inc., Novato, CA, USA) each day of gestation. Sapropterin dihydrochloride was dissolved in water and combined with a small amount of peanut butter. Blood glucose levels, food and water intake were monitored throughout pregnancy.

### 3.3.3 Histological and Immunohistochemical Analysis

To analyze coronary artery development and resulting vasculature, embryos were harvested at E12.5 and E18.5 for morphological and immunohistochemical analyses. Briefly, the thoraces of embryos were isolated and fixed in 4% paraformaldehyde overnight. The samples were dehydrated, paraffin embedded and subsequently serial sectioned into 5- $\mu$ m sections. Prior to immunostaining, antigen retrieval was conducted in citric acid buffer (0.01 mol/L, pH 6.0) for 12 minutes at 94°C using a microwave (BP-111; Microwave Research & Applications, Inc., Carol Stream, IL). The following primary antibodies were applied and incubated overnight; anti- $\alpha$ -smooth muscle actin (1:3,000, mus monoclonal, Sigma-Aldrich A2547, Lot 032M4822), biotinylated lectin-1 (1:250, *Bandeiraea Simplicifolia*, Sigma-Aldrich L2380, Lot 054M4086V), anti-sex-determining region Y protein antibody (1:200, mus monoclonal, Santa Cruz SC-398567, Lot J1316), anti-Wt1 (1:300, rb polyclonal, Santa Cruz SC-192, Lot F0513), anti-E-cadherin (1:200, goat polyclonal, Santa Cruz SC-31020, Lot D2413), and anti-phosphohistone H3 (pHH3) (1:500, rb polyclonal, Abcam ab5176, Lot GR72823-1), followed by either biotinylated goat anti-rabbit IgG (1:500) or biotinylated donkey anti-goat IgG (1:500), for one hour. Signals were amplified through the ABC reagent (Vector Laboratories), which enabled visualization by 3-3' diaminobenzidine tetrahydrochloride (DAB, Sigma). Counterstaining was performed with Mayer's Hematoxylin (Thermo Scientific, Waltham, MA), and images were captured with a light microscope (Observer D1, Zeiss). To analyze coronary artery volume and branching, the AMIRA software (FEI Visualization Sciences Group) was used to create three-dimensional reconstructions of  $\alpha$ -smooth muscle actin stained sections 25- $\mu$ m apart. A ratio of coronary artery to

myocardial volume was obtained using the AMIRA software. Counts of coronary arteries, capillaries, and coronary progenitor cells were taken from a minimum of three heart sections and normalized to the myocardium.

### 3.3.4 Analysis of 4-hydroxynonenal Levels

To analyze lipid peroxidation as an indication of oxidative stress in embryonic hearts, E12.5 ventricles from all four groups were harvested and embedded in FSC22 frozen section media (Leica). Samples were cryosectioned (CM1950, Leica) into 8  $\mu\text{m}$  thick sections, and immunostained with 4-hydroxynonenal (4-HNE) antibody (1:300, goat polyclonal, ABM Y072093, Lot AP1217). This was followed by CY3-conjugated anti-goat IgG secondary antibody (1:1000; Jackson ImmunoResearch). Signals were detected using fluorescence microscopy (Observer D1, Zeiss, Oberkochen, Germany). Using a fixed exposure time, a minimum of 4 images were captured per heart, and fluorescence intensity per area of myocardium were measured using AxioVision Software (Zeiss, Oberkochen, Germany).

### 3.3.5 Assessment of Epicardial EMT using *ex vivo* Heart Explant Culture

To assess epicardial EMT, ventricles of E12.5 embryonic hearts from non-diabetic dams were harvested and cultured on a collagen gel matrix for 96 hours. To prepare the collagen matrix, 1 mg/mL type I rat tail collagen (BD Bioscience) was added to 2x M199 media (M5017; Sigma) containing 5 mM D-glucose or 30mM D-glucose in a 24-well plate. The casted collagen wells were hydrated with 500  $\mu\text{L}$  1x M199 media plus 10% FBS and insulin-transferrin-selenium, with or without 0.1 mM BH4 (Sigma), and 5 mM or 30 mM D-glucose. E12.5 ventricles were isolated in sterile saline, placed centrally in a

well containing the set collagen matrix and media, and incubated at 37°C for 4 days. Images were captured with a phase contrast microscope (Zeiss, Oberkochen, Germany), and spindle-shaped cell outgrowth distance was quantified.

### 3.3.6 Western Blotting for eNOS and Akt Phosphorylation

Ventricular myocardial tissue from E14.5 hearts, isolated in PBS, was used to analyze eNOS and Akt activity. Briefly, 30 µg of protein from isolated ventricular tissue was separated via 10% SDS-PAGE and transferred to a nitrocellulose membrane. Blots were probed with antibodies against p-NOS3 (Ser1177; 1:1000, rb polyclonal, Cell Signaling 9571S, Lot 7), NOS3 (1:1000, rb polyclonal, Santa Cruz SC-654, Lot G2414), p-Akt (Ser473; 1:5000, rb polyclonal, Cell Signaling 9271, Lot 19), Akt (1:5000, rb polyclonal, Cell Signaling 9272, Lot 22), and  $\alpha$ -actinin (1:5000, mus monoclonal, Sigma-Aldrich A7811, Lot 029K4844). Washed blots were probed with horseradish peroxidase–conjugated secondary antibodies (1:2500; Bio-Rad). The signal was detected using enhanced chemiluminescence and quantified by densitometry.

### 3.3.7 Real-time RT-PCR Analysis

Total RNA was extracted from E12.5 hearts using TRIzol reagent (Invitrogen). 200 nanograms of RNA was reverse transcribed using the Maloney murine leukemia virus reverse transcriptase and random primers. Evergreen qPCR MasterMix (Applied Biological Systems, Vancouver, BC) was used to conduct Real-time PCR on cDNA. Primers were designed for HIF-1 $\alpha$ , Aldh1a2,  $\beta$ -catenin, bFGF, Slug, Snail1, and Tbx18 using the Primer3 software v 4.1.0 (Table 3.1). Samples were amplified for 35 cycles using the Eppendorf Realplex (Hamburg, Germany). mRNA levels were extrapolated using a comparative C<sub>T</sub> method by normalizing to 28S-Ribosomal RNA.

**Table 3.1. Specific primer sequences for real-time PCR analysis.**

Gene	Accession no.	Product Size	Primer Sequence
Hif1- $\alpha$	NM_001313919	237	F: CAGCCTCACCAGACAGAGCA R: GTGCACAGTCACCTGGTTGC
Snail1	NM_011427.3	133	F: CACACGCTGCCTTGTGTCT R: GGTCAGCAAAAGCACGGTT
Slug	NM_011415.2	161	F: CAACGCCTCCAAGAAGCCCA R: GAGCTGCCGACGATGTCCAT
Aldh1a2	NM_009022.4	219	F: GGCAGCAATCGCTTCTCACA R: CAGCACTGGCCTTGGTTGAA
$\beta$ -catenin	NM_001165902.1	178	F: CTTGGCTGAACCATCACAGAT R: AGCTTCCTTTTTGGAAAGCTG
bFgf	NM_008006.2	174	F: CAAGGGAGTGTGTGCCAACC R: TGCCCAGTTCGTTTCAGTGC
Tbx18	NM_023814.4	199	F: GAGCAGCAACCCGTCTGTGA R: GGGACTGTGCAATCGGAAGG
28S	NR_003279.1	178	F: GGGCCACTTTTGTAAGCAG R: TTGATTTCGGCAGGTGAGTTG

F: forward primer; R: reverse primer

### 3.3.8 Statistical Analysis

Data are shown as mean  $\pm$  SEM. A two-way analysis of variance (ANOVA) was used for multiple group comparisons between diabetic and control dams with and without sapropterin treatment, and their interactions, followed by the Bonferroni post-hoc test (Version 5, GraphPad Software, La Jolla, CA, USA). The incidence of coronary artery malformations was assessed with Chi-square test. Differences were regarded significant with  $P < 0.05$ .

## 3.4 Results

### 3.4.1 Sapropterin prevents coronary artery malformations in offspring of diabetic mice without altering blood glucose levels

The present study was conducted using the same model of pregestational diabetes previously employed.<sup>12, 22, 23</sup> A week following STZ administration, diabetes was confirmed by measuring non-fasting blood glucose levels. Female mice with >11 mmol/L blood glucose were considered diabetic and bred with normal males. The glycemic state of the diabetic dam steadily increased from  $15.9 \pm 4.9$  mmol/L at E0.5 to  $25.1 \pm 4.4$  mmol/L by E18.5 (Table 3.2). The diabetic dams fed with sapropterin during gestation displayed a similar increase in hyperglycemia, gradually reaching  $26.9 \pm 5.2$  mmol/L at the end of pregnancy. Of note, treatment with sapropterin did not affect blood glucose levels in either the control or diabetic groups. A daily dose of insulin was administered to a cohort of diabetic dams throughout gestation, which normalized their elevated blood glucose levels (Table 3.2).

Half of all fetuses from untreated diabetic dams examined at E18.5 displayed CAM. This ratio was significantly reduced to 20.6% with sapropterin treatment (Table 3.2). Furthermore, 36.8% of fetal hearts presented with both CHD and CAM. Sapropterin effectively prevented the dual defect occurrence, as no hearts from the offspring of sapropterin-treated diabetic dams had both CHD and CAM. No CAMs or CHDs were found in either of the control groups or the insulin treatment groups, indicating that any vascular abnormalities seen were induced by diabetes and not a teratogenic effect of STZ. Finally, CAM incidence or the effectiveness of sapropterin treatment did not show any bias towards the male or female sex (Table 3.2).

**Table 3.2. Effects of sapropterin (BH4) on nonfasting maternal blood glucose levels and incidence of CAMs in E18.5 hearts during pregestational diabetes.**

	Control	Diabetes	BH4	Diabetes + BH4	Diabetes + Insulin
Litters (n)	3	9	4	5	3
Blood glucose at E0.5 (mmol/L)	7.5 ± 1.8	15.9 ± 4.9*	8.0 ± 0.6	16.8 ± 4.2†	6.2 ± 0.8
Blood glucose at E18.5 (mmol/L)	7.5 ± 0.6	25.1 ± 4.4**	9.1 ± 1.0	26.9 ± 5.2††	7.6 ± 0.7
CAM/total fetuses (n)	0/14	19/38*	0/23	7/34†	0/20
Males: CAM/total fetuses (n)	0/14	9/38*	0/23	3/34	0/20
Females: CAM/total fetuses (n)	0/14	10/38*	0/23	4/34	0/20
CAMs (%)	0.0	50.0	0.0	20.6	0.0

### 3.4.2 Sapropterin prevents diabetes-induced fetal hypoplastic coronary arteries and restores capillary density

Hearts with hypoplastic coronary arteries have marked decreases in vessel number and luminal diameter.<sup>12</sup> Immunostaining with  $\alpha$ -smooth muscle actin and biotinylated lectin-1 was used to identify hypoplastic coronary arteries and capillaries, respectively in E18.5 hearts. The left coronary artery originating from the aortic orifice in fetuses from diabetic dams was significantly smaller in luminal diameter than control ( $P < 0.01$ , Fig. 3.1A and E). Similarly, the diameter of the right ventricular coronary artery in offspring from diabetic dams was also smaller than control ( $P < 0.001$ , Fig. 3.1B and F). Sapropterin treatment prevented this diabetes-induced reduction in luminal diameter of the left and right coronary arteries ( $P < 0.05$ , Fig. 3.1A, B, E and F). Sapropterin treatment also rescued a maternal diabetes-induced decrease in coronary artery abundance within the ventricular myocardium ( $P < 0.01$ , Fig 3.1C and G). Interestingly, strong  $\alpha$ -smooth muscle



actin staining was noted in hearts from diabetic dams throughout the myocardium at E18.5, suggesting a delayed maturation of cardiomyocytes. Finally, immunostaining of lectin-1 marking endothelial cells revealed a reduced capillary density in the ventricular myocardium of E18.5 hearts from diabetic dams compared to controls, which was restored to normal with sapropterin treatment ( $P < 0.05$ , Fig. 3.1D and H). Coronary arteries were reconstructed in 3-dimensions to illustrate branching and extrapolate volume measurements. Figure 2A shows a notable decrease of coronary artery arborisation in E18.5 hearts from diabetic dams. The typical branching patterns were restored in offspring from diabetic mothers treated with sapropterin, resulting in normalization of the coronary artery volume to myocardial volume ratio ( $P < 0.01$ , Fig. 3.2B).

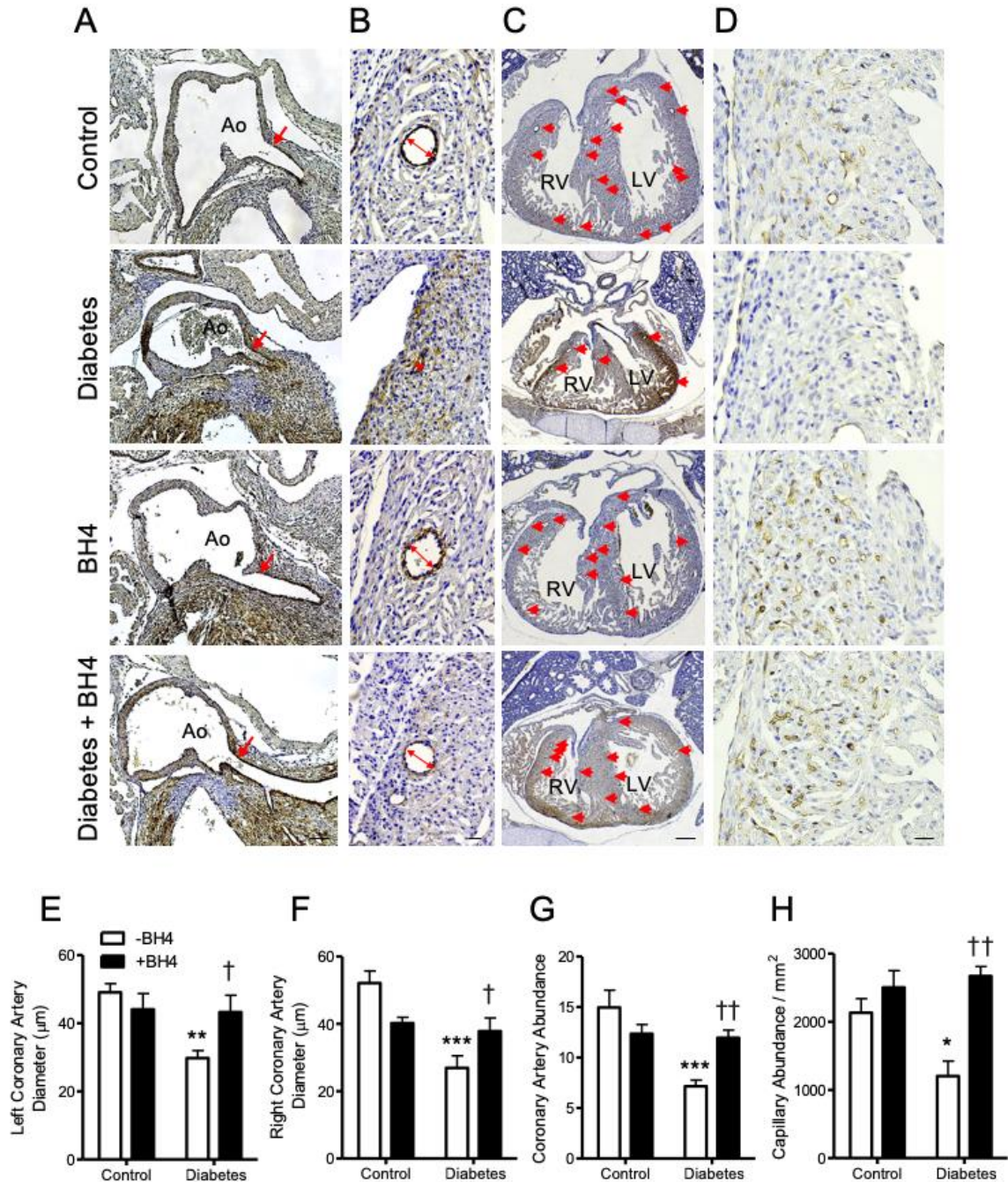


**Figure 3.1. Effects of sapropterin (BH4) on coronary artery malformations induced by pregestational diabetes.**

Representative histological sections of E18.5 hearts from offspring of control and diabetic dams with and without BH4 treatment.  $\alpha$ -smooth muscle actin staining of vascular smooth muscle cells specifying the left (A) and right (B) coronary artery, with arrows indicating diameter of the artery lumen measurements. (C)  $\alpha$ -smooth muscle actin

staining for total number of coronary arteries throughout the ventricular and septal myocardium. (D) Biotinylated lectin-1 immunostaining marking endothelial cells forming myocardial capillaries in the right ventricle. (E-H) Analysis of left (E) and right (F) coronary artery diameter, coronary artery abundance (G) and capillary density (H).  $n = 7 - 9$  per group,  $*P < 0.05$ ,  $**P < 0.01$  and  $***P < 0.001$  vs. untreated control,  $\dagger P < 0.05$  and  $\dagger\dagger P < 0.01$  vs. untreated diabetes. Scale bars represent 50, 20, 200 and 20  $\mu\text{m}$  in A, B, C and D, respectively.

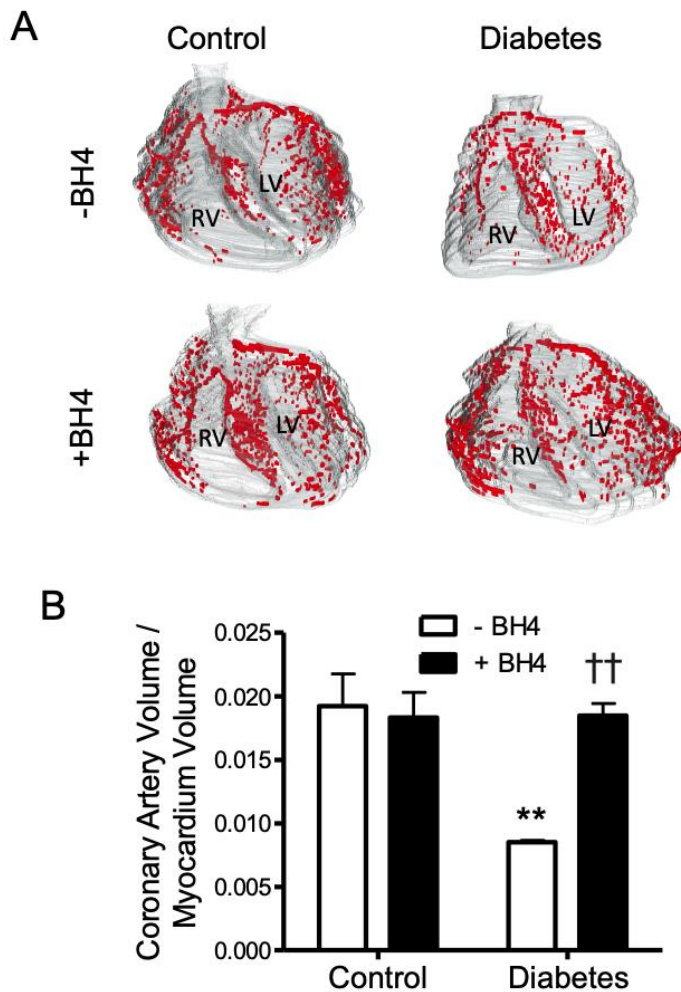


**Figure 3.2. Effects of sapropterin (BH4) on coronary artery volume at E18.5.**

(A) Frontal views of 3D reconstructions of the coronary arteries with superimposed myocardium. (B) Total coronary artery volume normalized to myocardial volume.  $n = 4$  hearts per group.  $**P < 0.01$  vs. untreated control,  $\dagger\dagger P < 0.01$  vs. untreated diabetes.

### 3.4.3 Sapropterin regulates coronary artery progenitor proliferation and EMT

To determine if diabetes-induced perturbations in coronary artery formation could give rise to the hypoplastic phenotype seen at E18.5, and whether sapropterin affected coronary artery precursors, epicardial proliferation and EMT were examined at E12.5. The epicardium is the source of coronary artery progenitors, which migrate from this epithelial layer via EMT into the myocardium.<sup>24</sup> Immunostaining for phosphorylated histone H3 (pHH3), marking cells undergoing division, revealed less proliferation, reduced cell density, a loosely attached epicardium in hearts from diabetic dams compared to controls ( $P < 0.01$ , Fig. 3.3A and D). Sapropterin treatment restored the number of pHH3<sup>+</sup> cells to almost control levels and rescued epicardial detachment (Fig. 3.3A). Concurrent with these changes in proliferation, a significantly greater number of E-cadherin<sup>+</sup> epicardial cells were found in embryonic hearts from diabetic dams, which was abrogated by sapropterin treatment ( $P < 0.01$ , Fig. 3.3B and E). To determine the number of cells actively going through the process of EMT, immunostaining for the transcription factor Wt1 was conducted and showed significantly fewer positive cells in the epicardium and subepicardium in E12.5 hearts from diabetic dams compared to controls ( $P < 0.05$ , Fig. 3.3D). These abnormalities were also prevented by sapropterin treatment ( $P < 0.05$ , Fig. 3.3D, F-G).



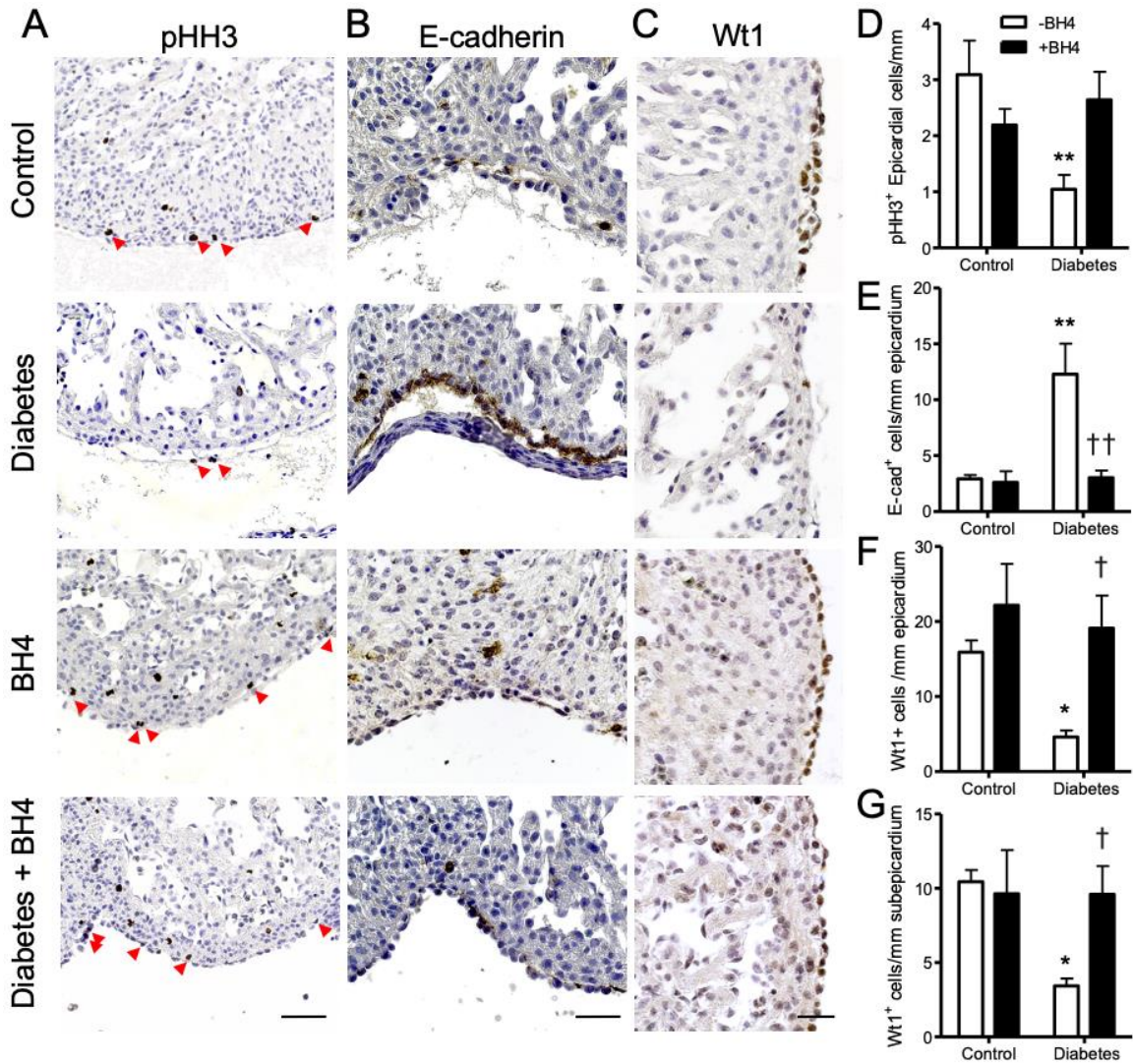


**Figure 3.3. Effects of sapropterin (BH4) on epicardial cell proliferation and markers of EMT in E12.5 hearts.**

(A) Representative images of immunostaining for phosphorylated histone H3 marking proliferating cells (red arrows), (B) E-cadherin (brown staining) representing cell-to-cell adhesion, and (C) Wt1<sup>+</sup> cells (brown staining) indicating EMT. Quantification of pHH3<sup>+</sup> cells (D), E-cadherin<sup>+</sup> cells (E) in the epicardium, and Wt1<sup>+</sup> cells in the epicardium (F) and subepicardium (G).  $n = 3 - 6$  hearts per group, \* $P < 0.05$ , \*\* $P < 0.01$  vs. untreated control, † $P < 0.05$ , †† $P < 0.01$  vs. untreated diabetes. Scale bars are 20  $\mu\text{m}$ .

### 3.4.4 Tetrahydrobiopterin normalizes high glucose-impaired epicardial EMT *ex vivo*

To further investigate the ability of sapropterin to restore epicardial EMT and thereby prevent diabetes-induced CAMs, effects of BH4 on EPDC migration was studied *ex vivo* under high glucose conditions. The ventricular myocardium of E12.5 hearts from control dams was isolated and cultured on collagen gel in both high glucose (30 mmol/L) and normal glucose (5 mmol/L) conditions for 4 days (Fig. 3.4A). The outgrowth radius of spindle shaped cells from the explanted heart tissue was measured. The data shows that high glucose impaired EPDC migration through the collagen matrix with significantly shorter outgrowth distance compared to normal glucose ( $P < 0.01$ , Fig. 3.4A). The addition of 0.1 mmol/L BH4 restored the distance travelled by the spindle-shaped EPDCs to normal levels ( $P < 0.05$ , Fig. 3.4A and B).

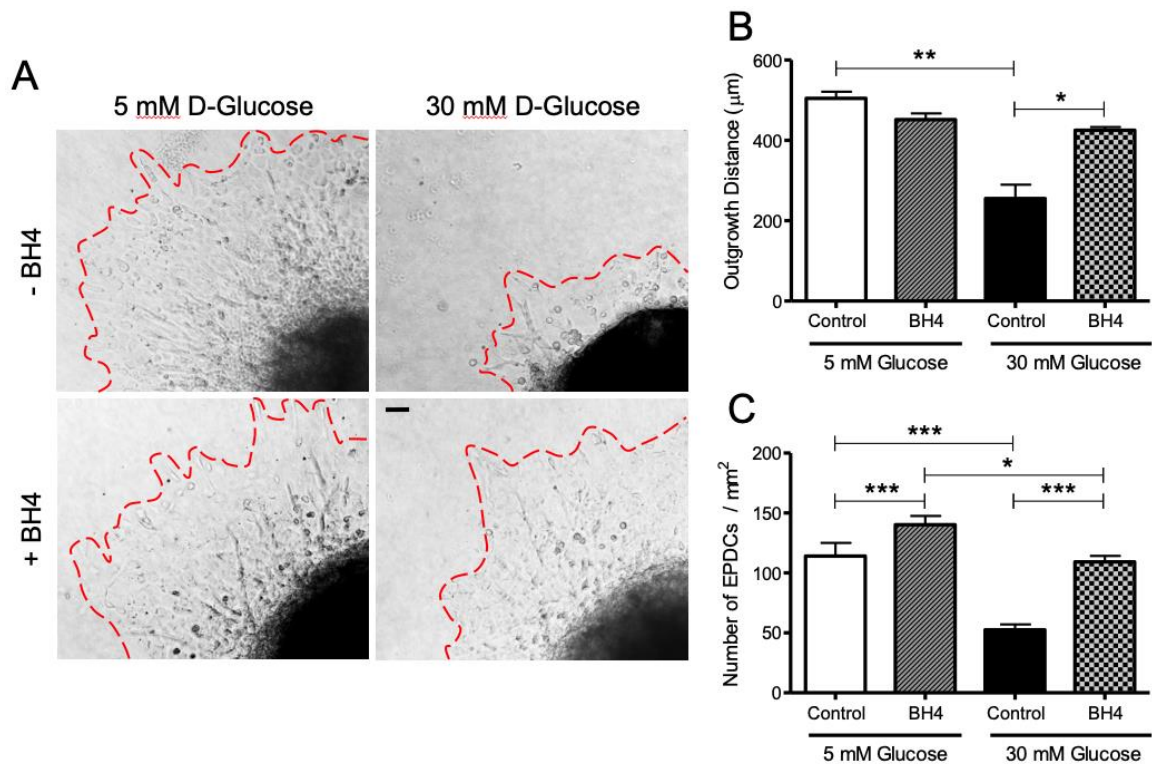


**Figure 3.4. Effects of BH4 on epicardial EMT *ex vivo*.**

(A) Representative images of epicardial cell outgrowth and EMT from E12.5 heart explants grown on a collagen matrix in normal (5 mM) and high (30 mM) glucose conditions with and without BH4 (0.1 mM). Dashed line indicated the border of the migrated cells. (B) Measurements of the average distance traveled by epicardial cells. (C) Quantification of spindle shaped cells (epicardial-derived cells, EPDCs) that have undergone EMT. \* $P < 0.05$ , \*\* $P < 0.01$ .  $n = 3-5$  explants per group from five litters.

### 3.4.5 Sapropterin restores expression of coronary vessel development and growth genes

Pregestational diabetes has been shown to alter gene expression in the developing heart.<sup>12, 22, 25</sup> To determine if the expression of key transcriptional regulators and signaling molecules responsible for epicardial EMT, angiogenesis, differentiation and growth were affected by maternal diabetes and sapropterin treatment, qPCR analysis was performed on E12.5 hearts. The mRNA levels of *Hif-1 $\alpha$* , *Snail1*, *Slug*, *Aldh1a2*,  $\beta$ -*catenin*, *bFGF*, and *Tbx18* were significantly lower in hearts from diabetic dams compared to controls ( $P < 0.05$ , Fig. 3.5A-G). Treatment with sapropterin significantly improved the expression levels of *Hif-1 $\alpha$* , *Snail1*, *Aldh1a2*,  $\beta$ -*catenin* and *bFGF* ( $P < 0.05$ , Fig. 3.5A-G).

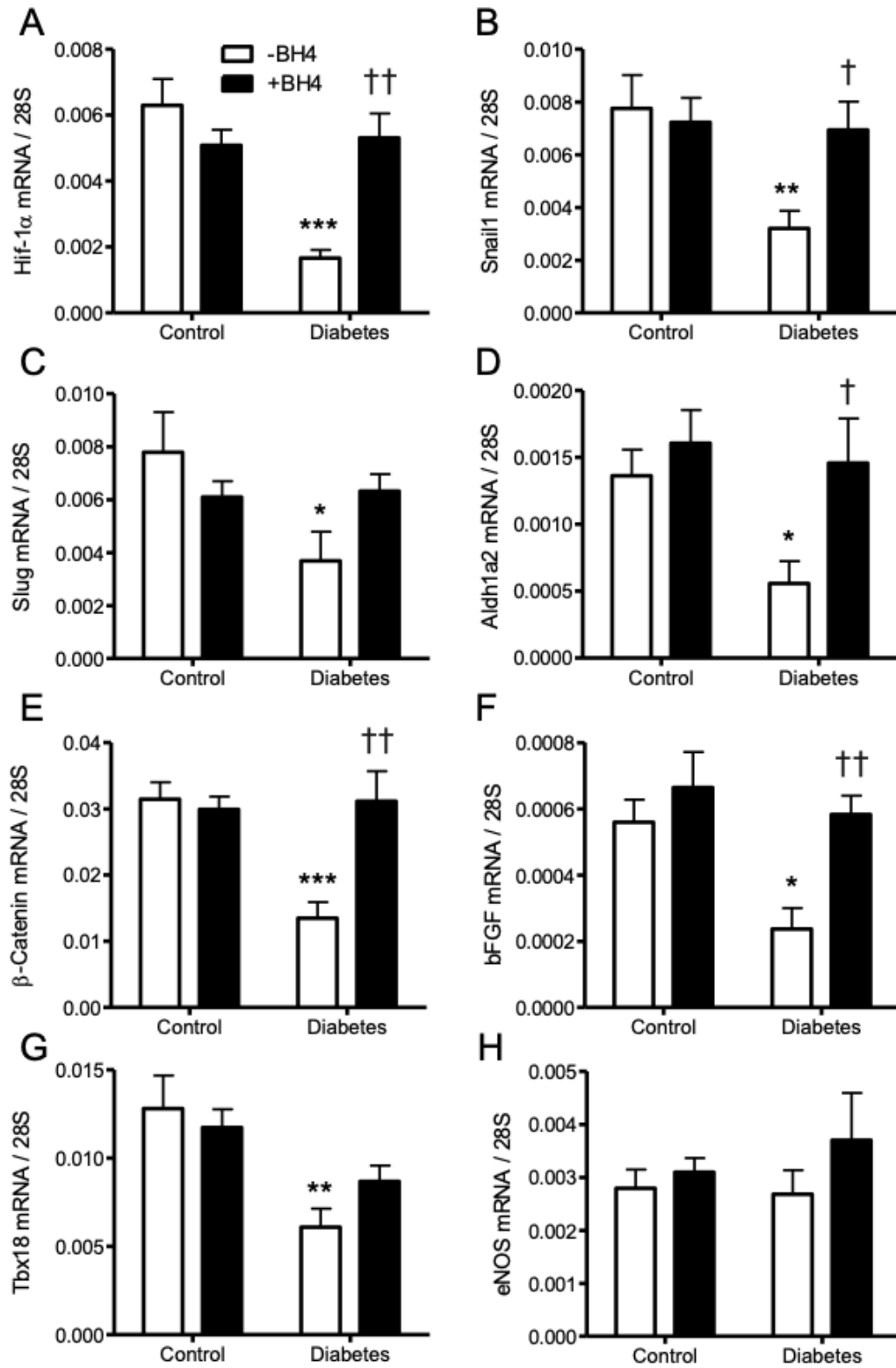




**Figure 3.5. Effects of sapropterin (BH4) on gene expression of transcription and growth factors critical to coronary artery development in E12.5 hearts of offspring from diabetic and control dams.**

mRNA levels were analyzed by qPCR. (A-G) The expression of *Hif-1 $\alpha$* , *Snail1*, *Slug*, *Aldh1a2*,  $\beta$ -*catenin*, *bFGF*, and *Tbx18* were significantly decreased under maternal diabetes. All (A, B, D-F) were restored to control levels by BH4 treatment except *Slug* and *Tbx18* (C and G). (H) eNOS expression was not significantly changed. n = 4 – 7 hearts per group. \* $P < 0.05$ , \*\* $P < 0.01$  vs. untreated control, and † $P < 0.05$ , †† $P < 0.01$  vs. untreated diabetes.

### 3.4.6 Sapropterin inhibits oxidative stress and restores activity of the Akt/eNOS pathway

To assess levels of oxidative stress in the developing myocardium, immunofluorescent staining of 4-hydroxynonenal (4-HNE), a product of lipid peroxidation, was conducted on E12.5 hearts. Quantification of red fluorescence intensity indicated higher levels of myocardial 4-HNE in offspring from diabetic dams compared to controls ( $P < 0.05$ , Fig. 3.6A and B). Sapropterin administration to diabetic dams significantly reduced lipid peroxidation ( $P < 0.05$ , Fig. 3.6B). Next, we assessed the effects of pregestational diabetes on Akt and eNOS activity in E14.5 hearts. Western blotting was used to analyze the phosphorylated and total amounts of Akt and eNOS (Fig. 3.6C). Fetal hearts from diabetic dams had significantly lower levels of p-Akt and p-eNOS compared to controls, without any major changes in total protein levels ( $P < 0.001$ , Fig. 3.6C-E). Phosphorylation of both enzymes was recovered to control levels with sapropterin treatment ( $P < 0.05$ , Fig. 3.6C-E).

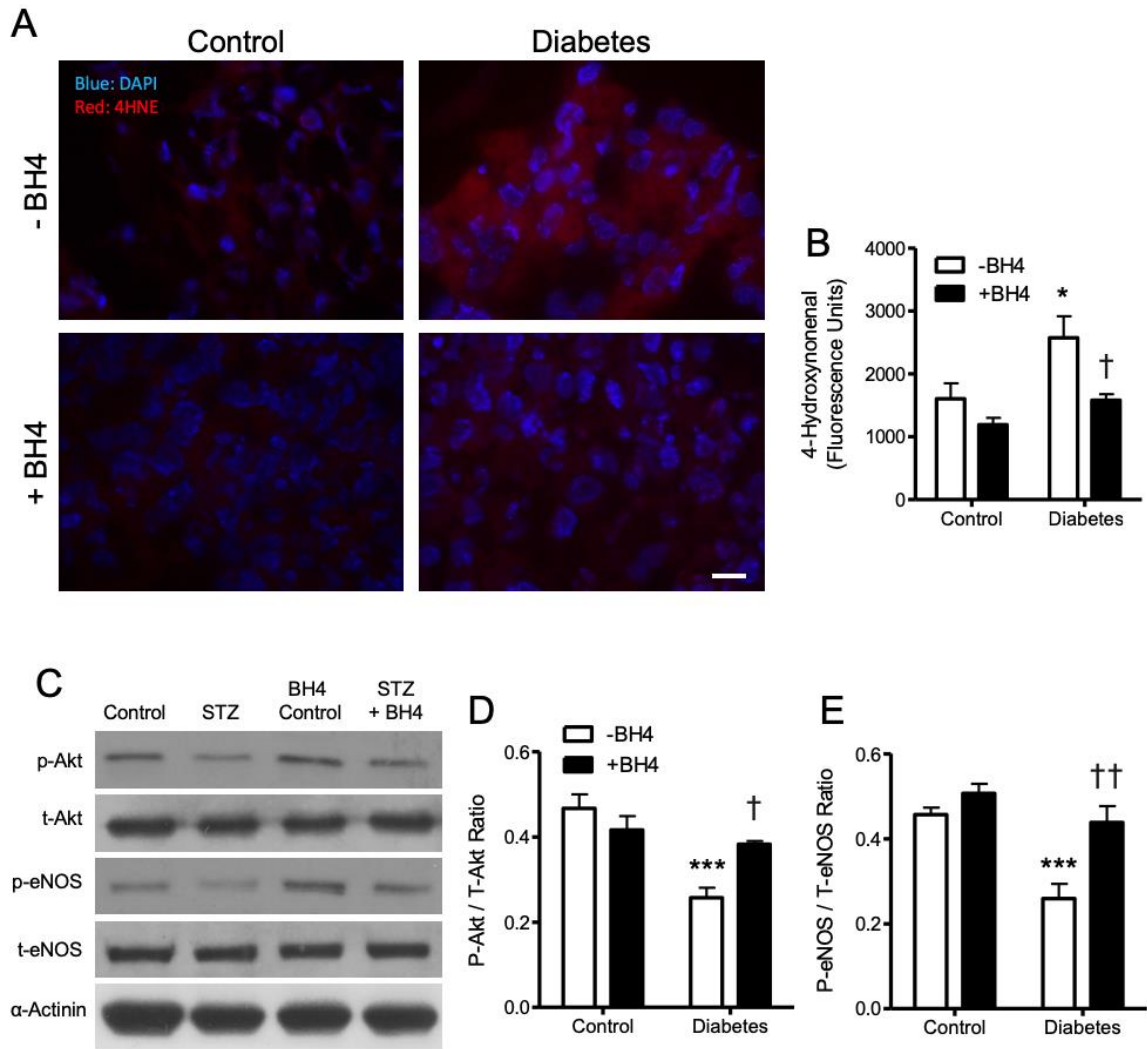


**Figure 3.6. Effects of sapropterin (BH4) on oxidative stress and Akt/eNOS phosphorylation in fetal hearts.**

(A) Representative immunofluorescence images of 4-hydroxynonenal staining for lipid peroxidation in the ventricular myocardium at E12.5. (B) Quantification of 4-HNE red immunofluorescence signal. (C) Representative Western blots for phosphorylated and total levels of Akt and eNOS with  $\alpha$ -actinin as a loading control in E14.5 hearts. (D and E) Densitometric analysis of phosphorylated to total protein levels of Akt (D) and eNOS (E).  $n = 4$  hearts per group.  $***P < 0.001$  vs. untreated control,  $\dagger P < 0.05$  and  $\dagger\dagger P < 0.01$  vs. untreated diabetes.

### 3.5 Discussion

The current study displays the efficacy of the FDA-approved drug sapropterin dihydrochloride (Kuvan®) in preventing congenital malformations of coronary arteries induced by a clinically relevant model of pregestational diabetes (Figure 3.7). In accordance with our previous studies,<sup>12</sup> CAMs were observed in the offspring of diabetic female mice. These CAMs manifest as hypoplastic coronary arteries, with marked decreases in luminal diameter and abundance, which translates to an overall reduction in the volume of coronary vasculature. We show that daily sapropterin administration to diabetic dams prevents hypoplastic coronary arteries, restores myocardial coronary arborisation and increases capillary density. Additionally, sapropterin decreases oxidative stress, improves Akt/eNOS activity and epicardial EMT, leading to normal coronary artery development.

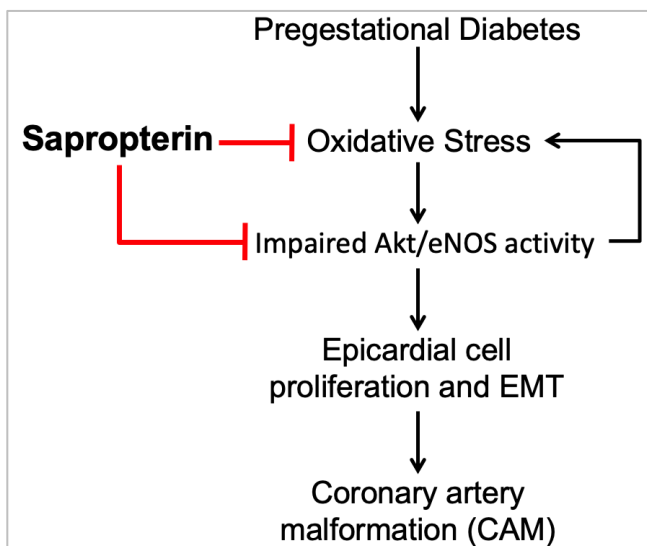


**Figure 3.7. Schematic summary of sapropterin on diabetes-induced CAMs.**

Oral sapropterin (Kuvan®) treatment inhibits oxidative stress, improves Akt/eNOS activity, and prevents coronary artery malformation (CAM) during pregestational diabetes.

Recently, we have shown the effectiveness of sapropterin in preventing CHDs in the offspring of diabetic mice.<sup>23</sup> Sapropterin treatment throughout gestation to diabetic dams decreased the incidence of CHDs in their offspring from 59.4% to 26.5%, despite dams having a comparable hyperglycemic status.<sup>23</sup> No major CHDs were reported in the treatment group, and insulin administration completely prevented the presence of malformations.<sup>23</sup> Correspondingly, our previous work show that N-acetylcysteine (NAC) treatment in the same model of pregestational diabetes, significantly reduced the incidence of CHDs and CAMs from 58.1% to 16.3% and from 46.6% to 6.0%, respectively.<sup>12, 22</sup> In fact, only 3% of fetal hearts from diabetic dams treated with NAC showed dual congenital heart and coronary artery anomalies.<sup>12</sup> In the present study, sapropterin treatment completely prevented the presence of both a CHD and CAM within the same heart, and significantly reduced CAM incidence from 50.0% to 20.6%. Whether sapropterin and NAC have an additive or synergistic effect in preventing CHDs and CAMs remains to be determined in future studies.

STZ is commonly used in animal models of diabetes to induce congenital malformations.<sup>12, 22, 23, 25</sup> Following STZ administration in our study, the glycemic levels of female mice steadily rose throughout pregnancy. Daily insulin treatment, the clinical gold-standard for controlling hyperglycemia in diabetes,<sup>26</sup> to a cohort of these diabetic mice normalized blood glucose levels. Interestingly, no CAMs were seen with insulin treatment, indicating that STZ does not have teratogenic effects on coronary artery development, and the defects seen in non-insulin treated STZ cohort are due to hyperglycemia. Unlike insulin, sapropterin did not affect blood glucose levels of the diabetic dam, suggesting that its beneficial effects are independent of maternal glucose

levels. Clinically, a male predominance of coronary artery anomalies has been reported.<sup>27</sup>,<sup>28</sup>. In the present study, the incidence of pregestational diabetes-induced CAMs did not show a sex bias and sapropterin treatment was equally effective in both females and males. Of note, in dams with blood glucose exceeding 30 mmol/L, fetuses harvested at E18.5 were 69% females, suggesting that more males with CAMs may have succumbed to maternal diabetes, which may explain a lack of sex difference in the incidence of CAMs in our study.

The epicardium is a major source of coronary arteries during embryonic heart development. Between E11.5 and E12.5 many cells in the epicardium undergo EMT and delaminate, forming EPDCs.<sup>14, 29</sup> These EPDCs migrate into the myocardium and differentiate into vascular smooth muscle cells, endothelial cells and perivascular fibroblasts, and form coronary arteries.<sup>13</sup> Wt1 is the master regulator of epicardial EMT, and transcriptionally controls the expression of many mediators of EMT such as Snail1, Aldh1a2 and E-cadherin.<sup>30, 31</sup> In mice deficient of Wt1, epicardial cells fail to undergo EMT, resulting in null coronary artery formation.<sup>32</sup> In the present study, consistent with our previous work,<sup>12</sup> pregestational diabetes decreased epicardial and subepicardial expression of Wt1, and inhibited epicardial cell proliferation and EMT in the developing heart. We also showed lower mRNA levels of many drivers of EMT including, Snail1, Slug, and Aldh1a2, and increased expression of E-cadherin. Notably these changes were restored to control levels with sapropterin treatment. Interestingly, BH4 has been shown to increase cell proliferation in retinal microvascular endothelial cells, mesangial (smooth muscle) cells of the kidney, and human vascular endothelial cells (HUVECs), and promote cell migration and tubulogenesis.<sup>33-35</sup> Consistent with these studies, we showed a

pro-angiogenic effect of sapropterin in the fetal heart of diabetic pregnancies in the present study.

Akt and eNOS are critical for proper heart development. In fact, Akt1/3 double knockout mice exhibit CHDs and early neonatal lethality.<sup>36</sup> We have previously shown that eNOS-deficient mice display major cardiac defects including ASD, VSD and hypoplastic coronary arteries.<sup>18, 37, 38</sup> Diabetes impairs eNOS function. For example, eNOS Ser1177 phosphorylation is decreased in the heart of diabetic patients<sup>39</sup> and eNOS is uncoupled in E12.5 hearts from diabetic dams.<sup>23</sup> In the present study, maternal diabetes induces a significant reduction in Akt and eNOS phosphorylation in E14.5 hearts, which was restored by sapropterin treatment. eNOS-derived NO is a key signaling molecule involved in proliferation, differentiation, EMT and ROS handling.<sup>17</sup> High levels of 4-hydroxynonenal, a marker of lipid peroxidation, reduces eNOS phosphorylation in bovine aortic endothelial cells by decreasing cellular BH4 bioavailability.<sup>40</sup> In our study, sapropterin treatment in diabetic dams significantly reduced ROS and 4-hydroxynonenal levels in fetal hearts. These findings suggest that sapropterin prevents hyperglycemia-induced oxidative stress and maintains redox balance and eNOS function in the developing heart.

A notable observation from immunohistochemical analysis is  $\alpha$ -SMA positive staining in cardiomyocytes in addition to coronary arteries in E18.5 hearts of offspring from diabetic mothers. During early cardiogenesis, immature cardiomyocytes express  $\alpha$ -SMA and as cardiac development progresses,  $\alpha$ -SMA is eventually replaced by cardiac actin isoforms.<sup>41, 42</sup> The persistent  $\alpha$ -SMA expression in cardiomyocytes and smaller

heart size at E18.5 in offspring of pregestational diabetes suggest that maternal diabetes delays fetal heart maturation, which is also prevented by sapropterin treatment.

The present study is limited to simulate type 1 diabetes. In pregnant women, the prevalence of pregestational type 2 diabetes is rapidly increasing in recent years.<sup>43</sup> The effects of type 2 diabetes on CAMs remain to be investigated in future studies. Additionally, coronary arteries are formed from at least 3 sources of progenitors, the epicardium, endothelial cells of sinus venosus and the endocardium.<sup>14-16</sup> The present study examined the changes of epicardial progenitors, which is considered a major contributor to coronary arteries.<sup>14</sup> Whether the other two sources of coronary progenitors are affected by pregestational diabetes and/or sapropterin requires further investigation.

In conclusion, oral treatment with the FDA-approved drug sapropterin dihydrochloride (Kuvan®), a stable, synthetic form of BH<sub>4</sub>, prevents the development of CAMs induced by maternal diabetes in mice. Sapropterin increases Akt and eNOS phosphorylation, decreases oxidative stress in the developing heart, and promotes cell proliferation, EMT and growth of coronary artery progenitors. Sapropterin did not negatively affect litter size, fetal weight or heart development in our studies,<sup>23</sup> suggesting an excellent safety profile in normal mouse pregnancies. Currently sapropterin is prescribed as a phenylalanine hydroxylase activator for patients with phenylketonuria (PKU), a genetic disorder. The potential of sapropterin as a treatment to prevent CHDs and CAMs in the offspring of women with pregestational diabetes needs to be tested in clinical trials.

### 3.6 Footnotes

This study was funded in part by grants from the Canadian Institutes of Health Research (CIHR) to Qingping Feng, and the Children's Health Foundation in London, Ontario, Canada to Kambiz Norozi, and Qingping Feng. Qingping Feng is a Richard and Jean Ivy Chair in Molecular Toxicology at Western University.



### 3.7 References

1. Guariguata L, Linnenkamp U, Beagley J, Whiting DR and Cho NH. Global estimates of the prevalence of hyperglycaemia in pregnancy. *Diabetes Res Clin Pract.* 2014;103:176-85.
2. Oyen N, Diaz LJ, Leirgul E, Boyd HA, Priest J, Mathiesen ER, Quertermous T, Wohlfahrt J and Melbye M. Prepregnancy Diabetes and Offspring Risk of Congenital Heart Disease: A Nationwide Cohort Study. *Circulation.* 2016;133:2243-53.
3. Zugibe FT, Zugibe FT, Jr., Costello JT and Breithaupt MK. Hypoplastic coronary artery disease within the spectrum of sudden unexpected death in young and middle age adults. *Am J Forensic Med Pathol.* 1993;14:276-83.
4. Roberts WC and Glick BN. Congenital hypoplasia of both right and left circumflex coronary arteries. *Am J Cardiol.* 1992;70:121-3.
5. Amabile N, Fraisse A and Quilici J. Hypoplastic coronary artery disease: report of one case. *Heart.* 2005;91:e12.
6. McFarland C, Swamy RS and Shah A. Hypoplastic coronary artery disease: A rare cause of sudden cardiac death and its treatment with an implantable defibrillator. *J Cardiol Cases.* 2011;4:e148-e151.
7. Basso C, Maron BJ, Corrado D and Thiene G. Clinical profile of congenital coronary artery anomalies with origin from the wrong aortic sinus leading to sudden death in young competitive athletes. *J Am Coll Cardiol.* 2000;35:1493-501.
8. Taylor AJ, Rogan KM and Virmani R. Sudden cardiac death associated with isolated congenital coronary artery anomalies. *J Am Coll Cardiol.* 1992;20:640-7.
9. Goo HW. Coronary artery imaging in children. *Korean J Radiol.* 2015;16:239-50.
10. Yamanaka O and Hobbs RE. Coronary artery anomalies in 126,595 patients undergoing coronary arteriography. *Cathet Cardiovasc Diagn.* 1990;21:28-40.
11. Tuo G, Marasini M, Brunelli C, Zannini L and Balbi M. Incidence and clinical relevance of primary congenital anomalies of the coronary arteries in children and adults. *Cardiol Young.* 2013;23:381-6.
12. Moazzen H, Lu X, Liu M and Feng Q. Pregestational diabetes induces fetal coronary artery malformation via reactive oxygen species signaling. *Diabetes.* 2015;64:1431-43.
13. Reese DE, Mikawa T and Bader DM. Development of the coronary vessel system. *Circ Res.* 2002;91:761-8.

14. Gittenberger-de Groot AC, Winter EM, Bartelings MM, Goumans MJ, DeRuiter MC and Poelmann RE. The arterial and cardiac epicardium in development, disease and repair. *Differentiation*. 2012;84:41-53.
15. Wu B, Zhang Z, Lui W, Chen X, Wang Y, Chamberlain AA, Moreno-Rodriguez RA, Markwald RR, O'Rourke BP, Sharp DJ, Zheng D, Lenz J, Baldwin HS, Chang CP and Zhou B. Endocardial cells form the coronary arteries by angiogenesis through myocardial-endocardial VEGF signaling. *Cell*. 2012;151:1083-96.
16. Red-Horse K, Ueno H, Weissman IL and Krasnow MA. Coronary arteries form by developmental reprogramming of venous cells. *Nature*. 2010;464:549-53.
17. Liu Y and Feng Q. NOing the heart: role of nitric oxide synthase-3 in heart development. *Differentiation*. 2012;84:54-61.
18. Liu Y, Lu X, Xiang FL, Poelmann RE, Gittenberger-de Groot AC, Robbins J and Feng Q. Nitric oxide synthase-3 deficiency results in hypoplastic coronary arteries and postnatal myocardial infarction. *Euro Heart J*. 2014;35:920-31.
19. Werner ER, Blau N and Thony B. Tetrahydrobiopterin: biochemistry and pathophysiology. *Biochem J*. 2011;438:397-414.
20. Cai S, Khoo J, Mussa S, Alp NJ and Channon KM. Endothelial nitric oxide synthase dysfunction in diabetic mice: importance of tetrahydrobiopterin in eNOS dimerisation. *Diabetologia*. 2005;48:1933-40.
21. Heitzer T, Krohn K, Albers S and Meinertz T. Tetrahydrobiopterin improves endothelium-dependent vasodilation by increasing nitric oxide activity in patients with Type II diabetes mellitus. *Diabetologia*. 2000;43:1435-8.
22. Moazzen H, Lu X, Ma NL, Velenosi TJ, Urquhart BL, Wisse LJ, Gittenberger-de Groot AC and Feng Q. N-Acetylcysteine prevents congenital heart defects induced by pregestational diabetes. *Cardiovasc Diabetol*. 2014;13:46.
23. Engineer A, Saiyin T, Lu X, Kucey AS, Urquhart BL, Drysdale TA, Norozi K and Feng Q. Sapropterin Treatment Prevents Congenital Heart Defects Induced by Pregestational Diabetes Mellitus in Mice. *J Am Heart Assoc*. 2018;7:e009624.
24. Gittenberger-de Groot AC, Winter EM and Poelmann RE. Epicardium-derived cells (EPDCs) in development, cardiac disease and repair of ischemia. *J Cell Mol Med*. 2010;14:1056-60.
25. Kumar SD, Dheen ST and Tay SS. Maternal diabetes induces congenital heart defects in mice by altering the expression of genes involved in cardiovascular development. *Cardiovasc Diabetol*. 2007;6:34.

26. Starikov R, Bohrer J, Goh W, Kuwahara M, Chien EK, Lopes V and Coustan D. Hemoglobin A1c in pregestational diabetic gravidas and the risk of congenital heart disease in the fetus. *Pediatr Cardiol.* 2013;34:1716-22.
27. Tongut A, Ozyedek Z, Cerezci I, Erenturk S and Hatemi AC. Prevalence of congenital coronary artery anomalies as shown by multi-slice computed tomography coronary angiography: a single-centre study from Turkey. *J Int Med Res.* 2016;44:1492-1505.
28. De Giorgio F, Abbate A, Stigliano E, Capelli A and Arena V. Hypoplastic coronary artery disease causing sudden death. Report of two cases and review of the literature. *Cardiovasc Pathol.* 2010;19:e107-11.
29. Cai CL, Martin JC, Sun Y, Cui L, Wang L, Ouyang K, Yang L, Bu L, Liang X, Zhang X, Stallcup WB, Denton CP, McCulloch A, Chen J and Evans SM. A myocardial lineage derives from Tbx18 epicardial cells. *Nature.* 2008;454:104-8.
30. Martinez-Estrada OM, Lettice LA, Essafi A, Guadix JA, Slight J, Velegela V, Hall E, Reichmann J, Devenney PS, Hohenstein P, Hosen N, Hill RE, Munoz-Chapuli R and Hastie ND. Wt1 is required for cardiovascular progenitor cell formation through transcriptional control of Snail and E-cadherin. *Nat Genet.* 2010;42:89-93.
31. Vicente-Steijn R, Scherptong RW, Kruithof BP, Duim SN, Goumans MJ, Wisse LJ, Zhou B, Pu WT, Poelmann RE, Schalijs MJ, Tallquist MD, Gittenberger-de Groot AC and Jongbloed MR. Regional differences in WT-1 and Tcf21 expression during ventricular development: implications for myocardial compaction. *PloS one.* 2015;10:e0136025.
32. von Gise A, Zhou B, Honor LB, Ma Q, Petryk A and Pu WT. WT1 regulates epicardial epithelial to mesenchymal transition through beta-catenin and retinoic acid signaling pathways. *Dev Biol.* 2011;356:421-31.
33. Edgar KS, Galvin OM, Collins A, Katusic ZS and McDonald DM. BH4-Mediated Enhancement of Endothelial Nitric Oxide Synthase Activity Reduces Hyperoxia-Induced Endothelial Damage and Preserves Vascular Integrity in the Neonate. *Invest Ophthalmol Vis Sci.* 2017;58:230-241.
34. Wang J, Yang Q, Nie Y, Guo H, Zhang F, Zhou X and Yin X. Tetrahydrobiopterin contributes to the proliferation of mesangial cells and accumulation of extracellular matrix in early-stage diabetic nephropathy. *J Pharm Pharmacol.* 2017;69:182-190.
35. Chen L, Zeng X, Wang J, Briggs SS, O'Neill E, Li J, Leek R, Kerr DJ, Harris AL and Cai S. Roles of tetrahydrobiopterin in promoting tumor angiogenesis. *Am J Pathol.* 2010;177:2671-80.

36. Yang ZZ, Tschopp O, Di-Poi N, Bruder E, Baudry A, Dummler B, Wahli W and Hemmings BA. Dosage-dependent effects of Akt1/protein kinase Balpha (PKBalpha) and Akt3/PKBgamma on thymus, skin, and cardiovascular and nervous system development in mice. *Mol Cell Biol*. 2005;25:10407-18.
37. Feng Q, Song W, Lu X, Hamilton JA, Lei M, Peng T and Yee SP. Development of heart failure and congenital septal defects in mice lacking endothelial nitric oxide synthase. *Circulation*. 2002;106:873-9.
38. Liu Y, Lu X, Xiang FL, Lu M and Feng Q. Nitric oxide synthase-3 promotes embryonic development of atrioventricular valves. *PloS one*. 2013;8:e77611.
39. Streit U, Reuter H, Bloch W, Wahlers T, Schwinger RH and Brixius K. Phosphorylation of myocardial eNOS is altered in patients suffering from type 2 diabetes. *J Appl Physiol*. 2013;114:1366-74.
40. Whitsett J, Picklo MJ, Sr. and Vasquez-Vivar J. 4-Hydroxy-2-nonenal increases superoxide anion radical in endothelial cells via stimulated GTP cyclohydrolase proteasomal degradation. *Arterioscler Thromb Vasc Biol*. 2007;27:2340-7.
41. Woodcock-Mitchell J, Mitchell JJ, Low RB, Kieny M, Sengel P, Rubbia L, Skalli O, Jackson B and Gabbiani G. Alpha-smooth muscle actin is transiently expressed in embryonic rat cardiac and skeletal muscles. *Differentiation*. 1988;39:161-6.
42. Marinas ID, Marinas R, Pirici I and Mogoanta L. Vascular and mesenchymal factors during heart development: a chronological study. *Rom J Morphol Embryol*. 2012;53:135-42.
43. Coton SJ, Nazareth I and Petersen I. A cohort study of trends in the prevalence of pregestational diabetes in pregnancy recorded in UK general practice between 1995 and 2012. *BMJ Open*. 2016;6:e009494.

## Chapter 4

### **The Role of microRNA-122 in Pathogenesis of Congenital Heart Defects during Pregestational Diabetes**

A version of this chapter is in preparation for submission.

Anish Engineer <sup>1</sup>, Xiangru Lu <sup>1</sup>, Qingping Feng <sup>1,2,3</sup>.

<sup>1</sup> Department of Physiology and Pharmacology, <sup>2</sup> Department of Medicine, Schulich School of Medicine and Dentistry, Western University, <sup>3</sup> Children's Health Research Institute, London, Ontario, Canada.

## 4 Chapter 4

### 4.1 Chapter Summary

Pregestational maternal diabetes increases the risk for congenital heart defects (CHDs) in infants by over four times. Diabetes may alter maternal/fetal microRNA (miRNA) profiles leading to the pathogenesis of CHDs. An elevation of miR-122 has recently been reported in patients with impaired glucose tolerance, insulin resistance and obesity. miR-122 is highly abundant in the liver and acts as tumor suppressor. The aim of the present study was to determine if miR-122 is elevated in embryonic hearts from diabetic female mice, and to examine the effects of antimiR-122 on pathogenesis of CHDs during pregestational diabetes. Diabetes was induced by streptozotocin (50 mg/kg, IP x5) to adult female C57BL/6 mice. Diabetic females were treated with a locked nucleic acid (LNA) antimiR-122 or scramble LNA control (10 mg/kg, SC x2), and their offspring's hearts were examined at E18.5 for morphology and function. RT-qPCR analysis showed that miR-122 was upregulated in E12.5 hearts of offspring from diabetic dams. In cultured E12.5 hearts, treatment with miR-122 or high glucose inhibited cell proliferation and epicardial EMT, and increased apoptosis. These effects of miR-122 and high glucose were abrogated by antimiR-122 transfection. Downregulation of genes critical to cell cycle progression, angiogenesis, and heart development, such as Cyclin D1, Snail1, Gata4 and Hand2 under high glucose conditions, was also prevented by antimiR-122 transfection. Furthermore, *in vivo* antimiR-122 treatment to diabetic dams decreased the incidence of CHDs and improved cardiac function of fetuses compared to scramble LNA controls. The current study reveals for the first time a critical role of miR-

122 in CHD pathogenesis, and may have therapeutic implications in preventing CHDs during pregestational diabetes.

## 4.2 Introduction

Congenital heart defects (CHDs) are the most prevalent birth defect, accounting for 1 to 5% of live births, and represent the leading, non-infectious cause of pediatric mortality and morbidity worldwide.<sup>1-4</sup> These defects result from perturbations in complex molecular and cellular processes underlying normal embryonic heart development, compromising cardiac structure and function at birth. Adverse genetic and environmental factors impair cardiogenesis and increase the likelihood of CHDs. Pregestational maternal diabetes increases the incidence of CHDs in children by more than four-fold.<sup>5-8</sup> Importantly, the incidence of both type 1 (insulin-dependent) and type 2 (insulin resistant) diabetes (T1D and T2D) is rapidly increasing in women of childbearing age and youth aged 10 -19 years.<sup>9-11</sup> In fact, between 2000 and 2010, there was a 37% rise in pregnancies affected by pregestational diabetes in the U.S.<sup>12</sup> Despite glycemic control, congenital malformations occur at higher rates from pregnancies with pregestational diabetes.<sup>13</sup> With the rising number of women with pregestational diabetes, more children are predicted to be born with CHDs, conferring a greater burden on the healthcare system as this pediatric population enters into adulthood.<sup>14</sup>

The heart is the first functional organ to arise during mammalian embryogenesis, and involves the combination of three pools of progenitor cells in a spatiotemporal specific manner, reliant upon regulated cell proliferation, apoptosis and epithelial-to-mesenchymal transition (EMT).<sup>15</sup> First and second heart field-derived (FHF and SHF) multipotent cardiac progenitors undergo proliferation followed by differentiation into

cardiomyocytes, which further clonally expand resulting in chamber ballooning and formation of the left and right ventricles.<sup>16,17</sup> The canonical Wnt/ $\beta$ -catenin signaling pathway directs proliferation of the SHF allowing for cardiac looping and outflow tract (OFT) development.<sup>18</sup> Conversely, a basal level of apoptosis is necessary for proper heart development, as it induces changes in both the endocardial cushions and myocardial microenvironment, signaling differentiation and development of cardiac valves, OFT, coronary vasculature and conduction system.<sup>19</sup> Additionally, EMT is required for coronary artery formation, causing a delamination and migration of epicardial cells into the myocardium, whereby they differentiate into smooth muscle cells, fibroblasts and endothelial cells, forming the vasculature. This trans-differentiation process is mediated by upregulations of EMT factors, such as Wt1 and Snail1/2, which promote cell motility.<sup>20,21</sup> Thus, an insult to any of these coordinated cellular processes could result in a misstep in heart development and lead to a CHD.

miRNAs are short, single-stranded RNA molecules that post-transcriptionally modulate gene expression by targeting mRNA transcripts at the 3' UTR and repressing their expression.<sup>22</sup> These endogenous, non-coding nucleic acids are key players in the pathogenesis of diabetes and its cardiovascular comorbidities, and are recently being recognized for their diagnostic potential, serving as biomarkers for disease progression, and therapeutic targets.<sup>23</sup> miRNAs are expressed in the embryonic heart and their levels of expression are critical to heart development. For example, targeted deletion of miR-1-2 causes ventricular septal defects and 50% mortality at late gestation while overexpression of miR-1 in the embryonic heart under the control of  $\beta$ -myosin heavy chain results in



lethality at E13.5.<sup>24</sup> Maternal diabetes changes maternal and fetal miRNA profiles which may contribute to the pathogenesis of CHDs.<sup>25-27</sup>

miR-122 is a conserved, 22 nucleotide molecule that plays a critical role in liver development and homeostasis. It regulates lipid and cholesterol metabolism, and serves as a tumor suppressor, protecting against hepatocellular carcinoma (HCC) by inhibiting proliferation and angiogenesis.<sup>28-30</sup> In patients with impaired glucose tolerance, insulin resistance, obesity, metabolic syndrome or T2D, elevated levels of circulating miRNA-122 (miR-122) have been reported.<sup>31-35</sup> Upregulation of plasma miR-122 was demonstrated in T2D rodent models on a high-fat, high-sucrose diet.<sup>32,36</sup> However, the role of miR-122 in pathogenesis of CHDs during pregestational maternal diabetes is unknown. RNA sequencing of maternal exosomes from STZ-induced diabetic and control dams noted significant alterations in plasma miRNAs, with a 3-fold increase in miR-122.<sup>27</sup> Using a global miRNA microarray we found a 14-fold upregulation in miR-122 in E10.5 hearts from diabetic dams compared to control. The present study aimed to assess miR-122 expression in embryonic hearts from maternal diabetes, and delineate its role in CHD pathogenesis during pregestational diabetes using anti-miR-122 treatment in mice. We hypothesized that miR-122 will be upregulated in embryonic hearts from mice with pregestational diabetes, which will decrease cell proliferation and epicardial EMT, and increase apoptosis in the developing heart, contributing to the pathogenesis of CHDs. In addition, anti-miR-122 treatment will reduce the incidence of CHDs induced by pregestational diabetes.

## 4.3 Methods

### 4.3.1 Animals

All procedures on mice in this study were performed in accordance with the Canadian Council on Animal Care guidelines and approved by the Animal Care Committee at Western University. C57BL/6 wild-type mice were purchased from Jackson Laboratory (Bar Harbor, Maine), and a breeding program was implemented to harvest fetal mice. Animals were housed in a 12-hour light/dark cycle and given *ad libitum* access to normal chow and water. All animals used in this study were handled according to the National Institute of Health Guide for the Care and Use of Laboratory Animals (8<sup>th</sup> edition, 2011).

### 4.3.2 Induction of Diabetes and AntimiR-122 Treatment

The *in vivo* and *ex vivo* experimental approach in Figure 4.1 illustrating timelines for saline or streptozotocin injection, breeding, anti-miR-122 or scramble LNA administration, organ culture conditions, and assessment of fetal hearts in 6 randomly assigned groups of mice. Female C57BL/6 mice, 8 to 10 weeks old were made diabetic through five consecutive, daily injections of streptozotocin (STZ, 50 mg/kg body weight, IP, Sigma), as we previously described.<sup>37</sup> STZ was dissolved in sterile saline (0.9% NaCl) at time of administration; sterile saline served as vehicle control. One week following the last STZ injection, non-fasting blood glucose levels were measured with a tail snip procedure using a glucose meter (One Touch Ultra2, LifeScan Canada, Burnaby, BC). Mice were categorized as diabetic if blood glucose measurements exceeded 11 mmol/L, and were subsequently injected with locked nucleic acid (LNA) oligos for anti-miR-122 or scramble control at a dose of 10 mg/kg, dissolved in sterile saline,

subcutaneously. A LNA oligo is a modified nucleic acid with a phosphothiate backbone and methylene bridge connecting the 2' oxygen and 4' carbon, enhancing stability and uptake *in vivo* (Exiqon, Qiagen). Mice were then bred with 10 to 12-week-old C57BL/6 male mice, and E0.5 was confirmed with presence of a vaginal plug after which pregnant dams were placed in a cage with littermates. At E7.5, the dams received another 10 mg/kg dose of anti-miR-122 or scramble LNA control, subcutaneously. This dose was determined based on the manufacturer's *in vivo* guidelines (Exiqon, Qiagen). Food and water intake, as well as non-fasting blood glucose levels were monitored throughout pregnancy. Fetal samples were collected at E18.5 for morphological and gene expression analysis, following *in utero* echocardiography. E12.5 embryonic hearts were isolated from a cohort of LNA-untreated control and STZ-induced diabetic dams for gene expression analysis. E10.5 and E12.5 hearts were collected under sterile conditions for organ culture from non-diabetic dams.

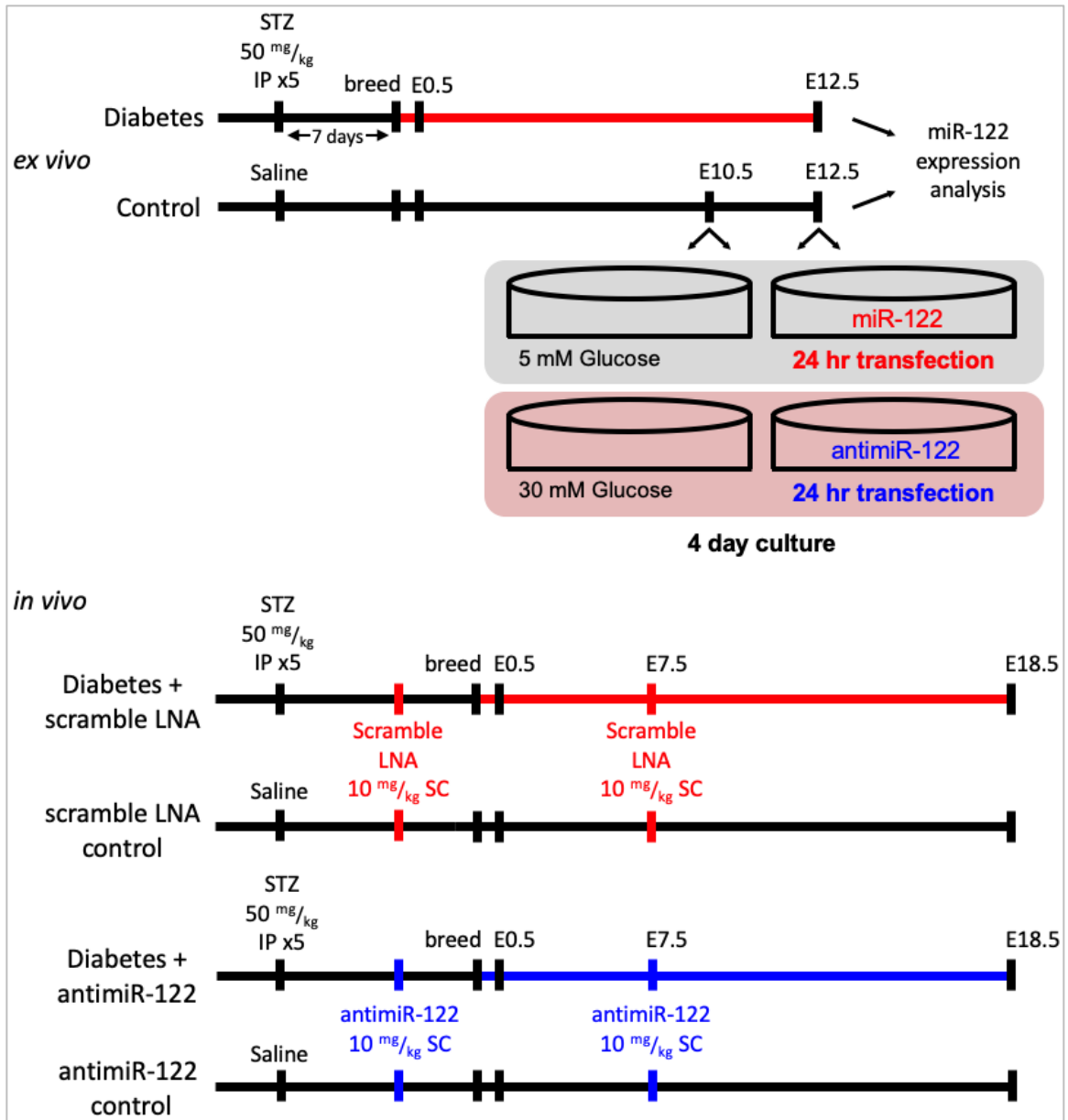


**Figure 4.1.** *Ex vivo* and *in vivo* approaches to examine the effects of miR-122 on heart development, and antimiR-122 on pregestational diabetes-induced CHDs.

Flow charts illustrate timelines of saline or streptozocin injection, breeding, embryonic heart harvest and culture, anti-miR-122 administration and assessment of fetal hearts for gene expression at E12.5, and cardiac morphology and function at E18.5. To determine miR-122 levels in the embryonic heart, E12.5 hearts from control and STZ-induced diabetic dams were collected for RNA isolation and gene expression analysis. In order to determine the effects of miR-122 on heart development, E10.5 and E12.5 hearts from control dams were cultured *ex vivo* for 4 days in normal or high glucose media, with miR-122 or antimiR-122 transfection for 24 hours. Two *in vivo* doses of anti-miR-122 or

scramble LNA to control and diabetic dams were administered according to this timeline to determine their effects on the fetal heart.

### 4.3.3 Histological Analysis

Fetal cardiac and liver samples were collected at E18.5 for histological analysis from control and diabetic dams treated with anti-miR-122 or scramble LNA. Morphological analysis of cardiac structures in order to diagnose CHDs was performed at E18.5 by first decapitating the fetuses and isolating the thorax in PBS. After removing skin and fascia, samples were fixed in 4% paraformaldehyde overnight at 4 °C, after which samples were dehydrated in ethanol and embedded in paraffin. The hearts were serial sectioned into 5 µm slices using a Leica RM2255 microtome, and mounted onto positively charged albumin/glycerin-coated slides. Following dewaxing of the slides, they were stained with hematoxylin/eosin (Thermo Scientific, Waltham, MA) to visualize morphology under a light microscope (Observer D1; Zeiss, Germany). Fetal liver samples were processed, sectioned and stained in the same manner.

### 4.3.4 Embryonic Heart Explant Culture

Figure 1 depicts the *ex vivo* organ culture system used to assess the effects of miR-122 and its antagonist, anti-miR-122, on gene expression, proliferation, apoptosis and EMT in heart development. E10.5 hearts from control, untreated dams were isolated in sterile saline and placed individually in wells of a 24-well plate with 500 µL of M199 cardiomyocyte media (with 10% FBS and 1% penicillin/streptomycin) containing either 5 or 30 mM D-glucose per well. JetPrime transfection reagent and buffer system (Polypus Transfection, Illkirch, France) was used to transfect miR-122 to a cohort of explants in normal (5 mM) D-glucose media, or anti-miR-122 to a subset of explants in high (30

mM) D-glucose media for 24 hours, according to the manufacturer's protocol. After 4 days of culture at 37°C in 5% CO<sub>2</sub>, the media was removed and the hearts were either cryosectioned or used for gene expression analysis.

#### 4.3.5 *Ex vivo* Assessment of Epicardial EMT

To investigate the effects of miR-122 on epicardial EMT during cardiogenesis, E12.5 hearts from control, non-diabetic dams were harvested in sterile conditions, dissected into small pieces in sterile saline, and placed on a collagen matrix. The collagen matrix was prepared using 1 mg/mL type I rat tail collagen (BD Bioscience) diluted with 2x M199 cardiomyocyte media (M5017; Sigma) containing either 5 or 30 mM D-glucose in a 24-well plate. The casted wells were then hydrated with 500 µL 1x M199 media plus 10% FBS, 1% penicillin/streptomycin and insulin-transferrin-selenium, with either, 5 or 30 mM D-glucose, matching the collagen layer. The pieces of E12.5 ventricles were placed centrally in the well on top of the matrix, and the JetPrime transfection reagent and buffer system (Polypus Transfection, Illkirch, France) was used to deliver miR-122 to a cohort of explants in the 5 mM D-glucose condition, or anti-miR-122 to a subset of explants in the 30 mM D-glucose group. The transfection was removed after 24 hours, and explants were again incubated at 37°C in 5% CO<sub>2</sub> for 72 hours. After culture, images were captured by phase contrast microscopy (Observer D1; Zeiss, Germany), and spindle-shaped EPDCs, which are epicardial cells that have undergone EMT, were quantified and normalized to the area of the explant.

#### 4.3.6 Immunofluorescence

To determine the effects of miR-122 on proliferation and apoptosis during cardiac development, E10.5 heart explants from all 4 groups were aspirated and embedded in

FSC22 frozen section media (Leica) following 4 days of culture. Samples were cryosectioned into 8 µm thick sections using the CM1950 cryostat (Leica), and mounted on glass slides. Immunostaining for proliferation and apoptosis markers was performed using anti-phosphohistone H3 antibody (1:1000; Abcam) and anti-cleaved caspase 3 antibody (1:1000; Cell Signaling), respectively. After 2 hours of primary antibody incubation, CY3-conjugated anti-goat IgG fluorescent secondary antibody (1:1000; Jackson ImmunoResearch) was aliquoted onto the slides for 1 hour, followed by Hoechst 33342 (Invitrogen). Fluorescence microscopy (Observer D1, Zeiss, Oberkochen, Germany) was used to detect signals and capture images from which positive cells were counted and normalized to myocardial area using the AxioVision Software (Zeiss).

#### 4.3.7 Real-time RT-PCR analysis

Total RNA from individual E12.5 hearts, E10.5 heart explants and E18.5 livers was isolated using miRNeasy Mini Kit (Qiagen, Burlington, Ontario, Canada). Stem-loop pulsed reverse transcription was performed by using Moloney Murine Leukemia Virus (MMLV) reverse transcriptase to synthesize cDNA from 800 nanograms of total RNA with specific primers for miR-122, snord-47, as previously described.<sup>38</sup> RT using random primer was also conducted. Primers were specifically designed using the Primer3 software v 4.1.0 (Table 4.1) for *miR-122*, *snord-47*, *28S*, *GLD2*, *Gata4*, *Hand2*, *EPO*, *Cyclin D1*, *Wnt1*, *Snail1*, and *Slug*. Real-time PCR analysis was performed using EvaGreen qPCR MasterMix (Applied Biological Material, Vancouver, British Columbia, Canada). Sample amplification was set for 35 cycles via the usage of Eppendorf Realplex (Eppendorf, Hamburg, Germany). Transcript levels were normalized with snord-47 miRNA or 28S, and extrapolated through the approach of comparative CT method.<sup>39</sup>

**Table 4.1. Primer sequences for PCR analysis.**

<b>Gene Name</b>	<b>Accession Number</b>	<b>Product Size</b>	<b>Primer Sequence (5' → 3')</b>
<i>miR-122</i>	NR_029600.1	56	RT: GTCGTATGCAGAGCAGGGTCCGAGG TATTCGCACTGCATACGACCAAACA Forward: AGGCTGGAGTGTGACAATG Reverse: GAGCAGGGTCCGAGGT
<i>Snord-47</i>	NR_028543.1	70	RT: GTCGTATGCAGAGCAGGGTCCGAGG TATTCGCACTGCATACGACAACCTC Forward: ATCACTGTAAAACCGTTCCA Reverse: GAGCAGGGTCCGAGGT
<i>28S</i>	NR_003279.1	178	Forward: GGGCCACTTTTGGTAAGCAG Reverse: TTGATTCGGCAGGTGAGTTG
<i>GLD2</i>	BC016629.1	236	Forward: CCGTTGTTTCACACGCACTAT Reverse: AGTCTGCTTTGTGGGAAGAGC
<i>Pri-miR-122</i>	NR_029600.1	141	Forward: AAAGCCTGAGCAAAACTGGA Reverse: TGGCTTACCATAGCCACTCC
<i>Gata4</i>	NM_008092.4	137	Forward: CACTATGGGCACAGCAGCTC Reverse: GCCTGCGATGTCTGAGTGAC
<i>Hand2</i>	NM_010402.4.1	159	Forward: GCTACATCGCCTACCTCATGGAT Reverse: TCTTGTCGTTGCTGCTCACTGT
<i>Cyclin D1</i>	NM_007631.2	155	Forward: CTGACACCAATCTCCTCAACG Reverse: CTCACAGACCTCCAGCATCCA
<i>Snail1</i>	NM_011427.3	133	Forward: CACACGCTGCCTTGTGTCT Reverse: GGTCAGCAAAGCACGGT
<i>Slug</i>	NM_011415.2	161	Forward: CAACGCCTCCAAGAAGCCA Reverse: GAGCTGCCGACGATGTCAT
<i>Wt1</i>	NM_144783.2	214	Forward: GATGTGCGGCGTGTATCTGG Reverse: GCTGGTCTGAGCGAGAAAACCT
<i>Wnt1</i>	NM_021279	241	Forward: CTGGAAGTGCCTTGTGTCT Reverse: GCCAAAGAGGCGACCAAAAT
<i>EPO</i>	NM_007942.2	165	Forward: GGAATTGATGTCGCCTCCAG Reverse: GCAGCAGCATGTACCTGTC

RT: Reverse Transcription



#### 4.3.8 Fetal Echocardiography

To assess the effects of anti-miR-122 treatment on cardiac function, *in utero* fetal echocardiography using the Vevo 2100 ultrasound imaging system was conducted. Dams were anesthetized and an incision was made to the abdomen to expose the uterine sacs containing the E18.5 fetuses. A MS 700 transducer (VisualSonics, Toronto, ON, Canada) was positioned to obtain a short-axis view of the fetal heart, and M-mode echocardiography images of fetal hearts were recorded with, as previously described.<sup>39,40</sup> LV ejection fraction and fractional shortening were calculated by measuring the end-diastolic LV internal diameter and end-systolic LV internal diameter from the short-axis M-mode images.

#### 4.3.9 Statistical Analysis

Statistical analysis was performed using GraphPad Prism, Version 5 (GraphPad Software, La Jolla, CA) and data are presented as mean  $\pm$  SEM. An unpaired Student t test was used for comparisons between 2 groups. For multiple group comparisons between normal and high glucose conditions with miR-122 or anti-miR-122 treatment, a one-way ANOVA, followed by the Tukey's post hoc test was conducted. CHD incidence was statistically assessed via a Chi-square test. Differences were deemed significant with  $P < 0.05$ .

## 4.4 Results

### 4.4.1 miR-122 is upregulated in the fetal heart of pregestational diabetes

Since miR-122 is highly expressed in the liver, we first assessed miR-122 levels in the adult liver. RT-qPCR analysis shows that miR-122 was abundantly expressed in the liver compared to the LV myocardium of the adult mice ( $P < 0.001$ , Figure 4.2A). Subsequent analysis revealed that significantly higher levels of miR-122 were present in E12.5 hearts from diabetic dams compared to control ( $P < 0.05$ , Figure 4.2B). To verify that miR-122 is expressed in the fetal heart, the levels of primary-miR-122, a longer precursor transcript, existing only in the nucleus was analyzed. Pri-miR-122 was significantly increased in E12.5 hearts from diabetic dams compared to control ( $P < 0.05$ , Figure 4.2C). Once in the cytoplasm, mature miRNA transcripts are processed by cytoplasmic poly(A) polymerases, which confer stability to the RNA molecules. miR-122 is stabilized by GLD2,<sup>41</sup> and we found it to be significantly elevated in E12.5 hearts from diabetic dams compared to control ( $P < 0.001$ , Figure 4.2D). Taken together, these results show, for the first time, that a significantly higher level of miR-122 is expressed in hearts from diabetic dams.

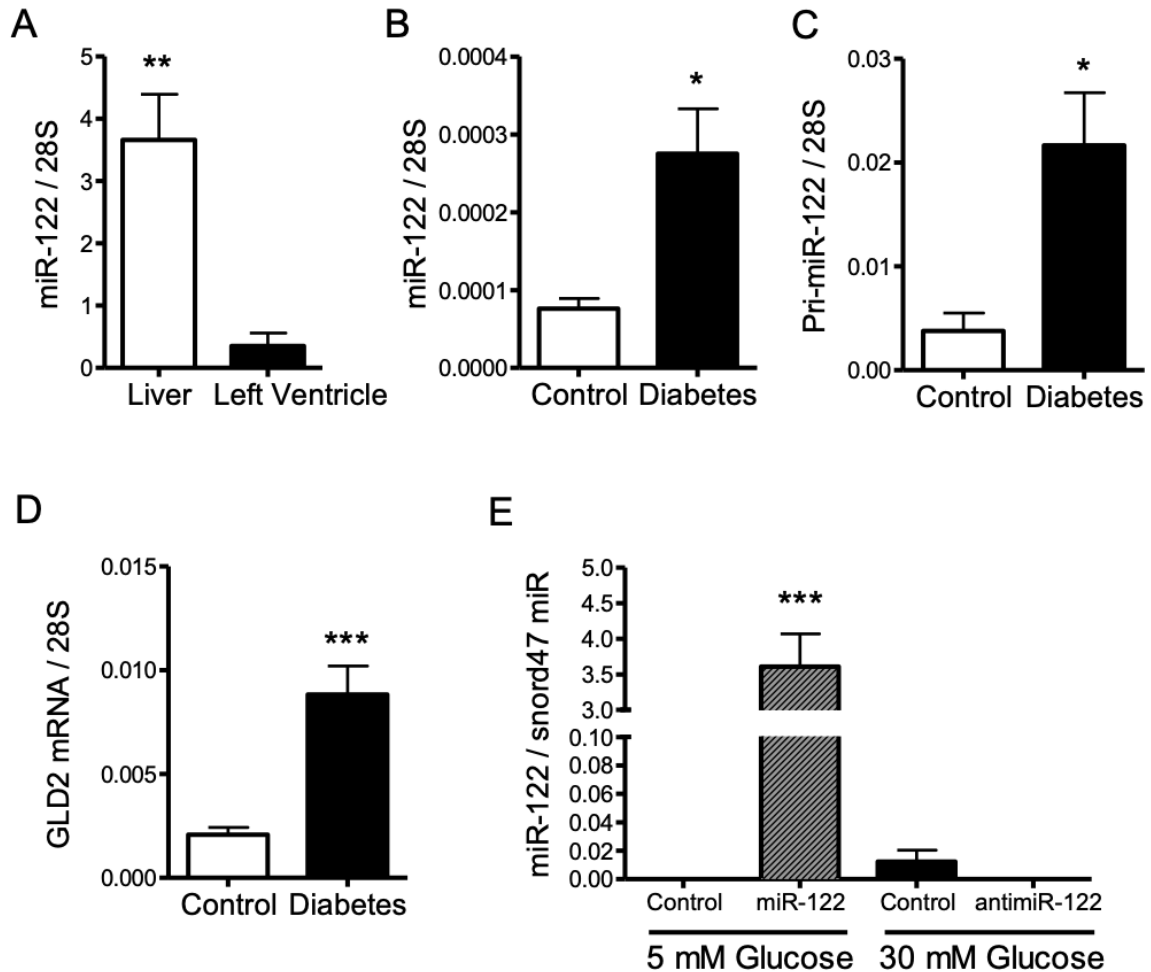


**Figure 4.2. Expression analysis of miR-122, Pri-miR-122 and GLD2.**

(A) Real-time qPCR of miR-122 in the liver and left ventricle of adult mice. Gene expression analysis of E12.5 hearts from control or diabetic dams for miR-122 (B), pri-miR-122 (C) and GLD2 (D). (E) miR-122 expression analysis from E10.5 explanted hearts following four days of culture in normal (5 mM) or high (30 mM) D-glucose conditions transfected with either miR-122 or anti-miR-122.  $n = 3$  to 6 hearts per group. Data are mean  $\pm$  SEM. \* $P < 0.05$ , \*\* $P < 0.01$  and \*\*\* $P < 0.001$  vs. respective controls.

#### 4.4.2 Gene targets of miR-122 in the embryonic heart

To identify 3' UTR mRNA targets of genes critical to embryonic heart development that are affected by miR-122, the miRbase and TargetScan online databases were used. Over 200 genes were predicted to be the targets of miR-122, however direct

targets that have an active role in embryonic heart development include, *Gata4*, *Hand2*, *EPO*, *Cyclin D1*, *Wnt1*, *Snail1*, and *Slug* (Figure 4.3B-H), which are critical to cell cycle progression, angiogenesis and cardiogenesis. An *ex vivo* embryonic heart culture was used to further assess the effects of miR-122 and anti-miR-122 on the expression of these genes in E10.5 hearts under normal or high glucose conditions. Transfection of miR-122 significantly elevated its levels in the cultured hearts, compared to control, whereas miR-122 was not detectable in anti-miR-122 transfected hearts ( $P < 0.001$ , Figure 4.2D). Hearts exposed to high glucose media showed a slight elevation in miR-122 levels, however this change was not statistically significant. Hyperglycemia is known to alter gene expression in the embryonic heart.<sup>37,42,43</sup> In agreement with this notion, mRNA levels of *Gata4*, *Hand2*, *Cyclin D1*, *Wnt1* and *EPO* were significantly reduced in the high glucose (30 mM) compared to the normal glucose (5 mM) conditions ( $P < 0.05$ , Figure 4.3A-D, G). Strikingly, in normal glucose conditions miR-122 transfection significantly lowered the expression of these genes in the cultured hearts compared to control ( $P < 0.05$ , Figure 4.3A-C, E-F). Treatment with anti-miR-122 in the high glucose conditions was effective in restoring expression back to normal levels for all 6 genes ( $P < 0.05$ , Figure 4.3A -F). In addition, anti-miR-122 treatment significantly elevated *Gata4*, *Hand2*, *Cyclin D1*, and *Snail1* levels back to normal when compared to miR-122 administration ( $P < 0.05$ , Figure 4.3A-C, E). Taken together, these results demonstrate that miR-122 and high glucose independently inhibit the expression of genes required for heart development, and the changes can be reversed by anti-miR-122.

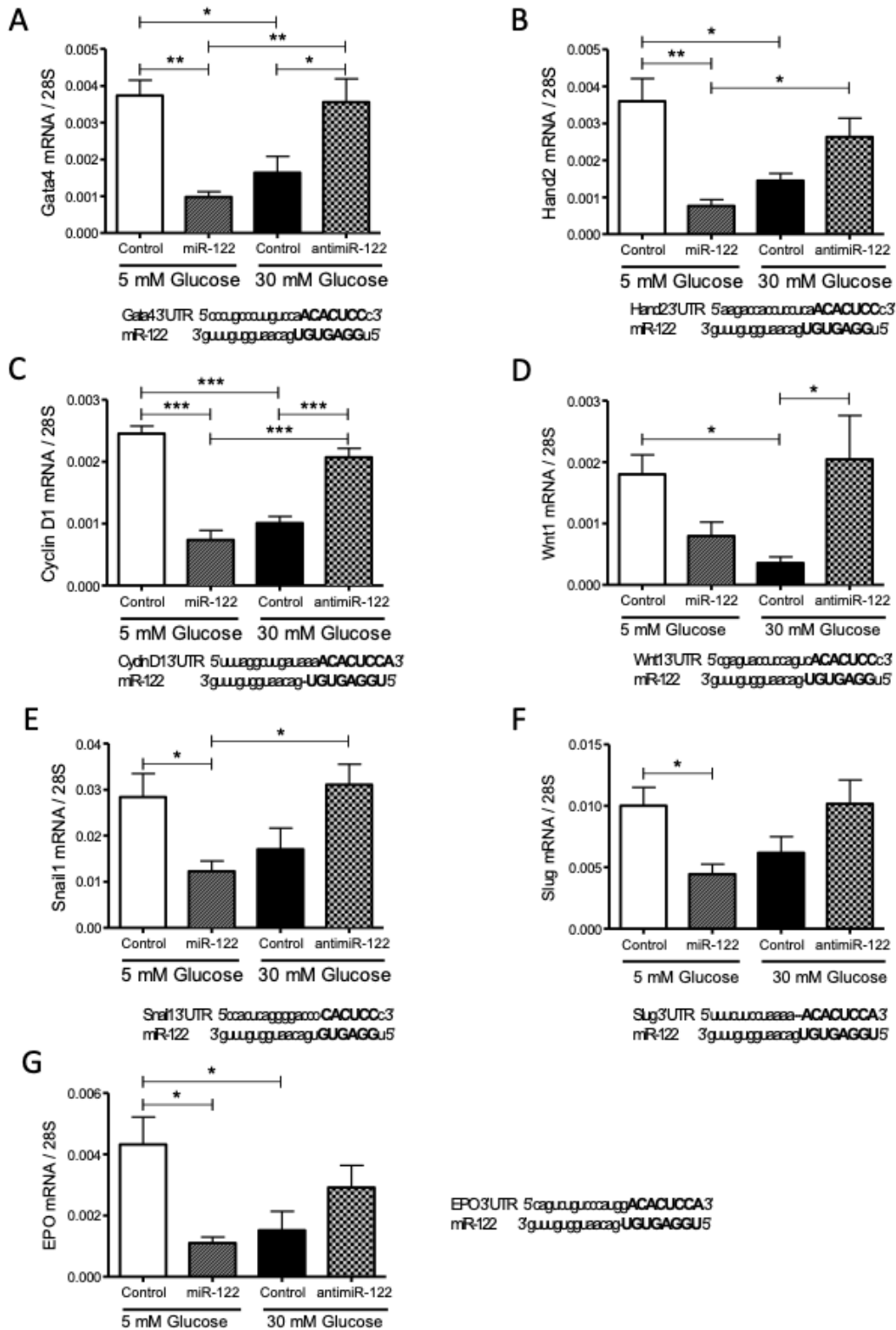
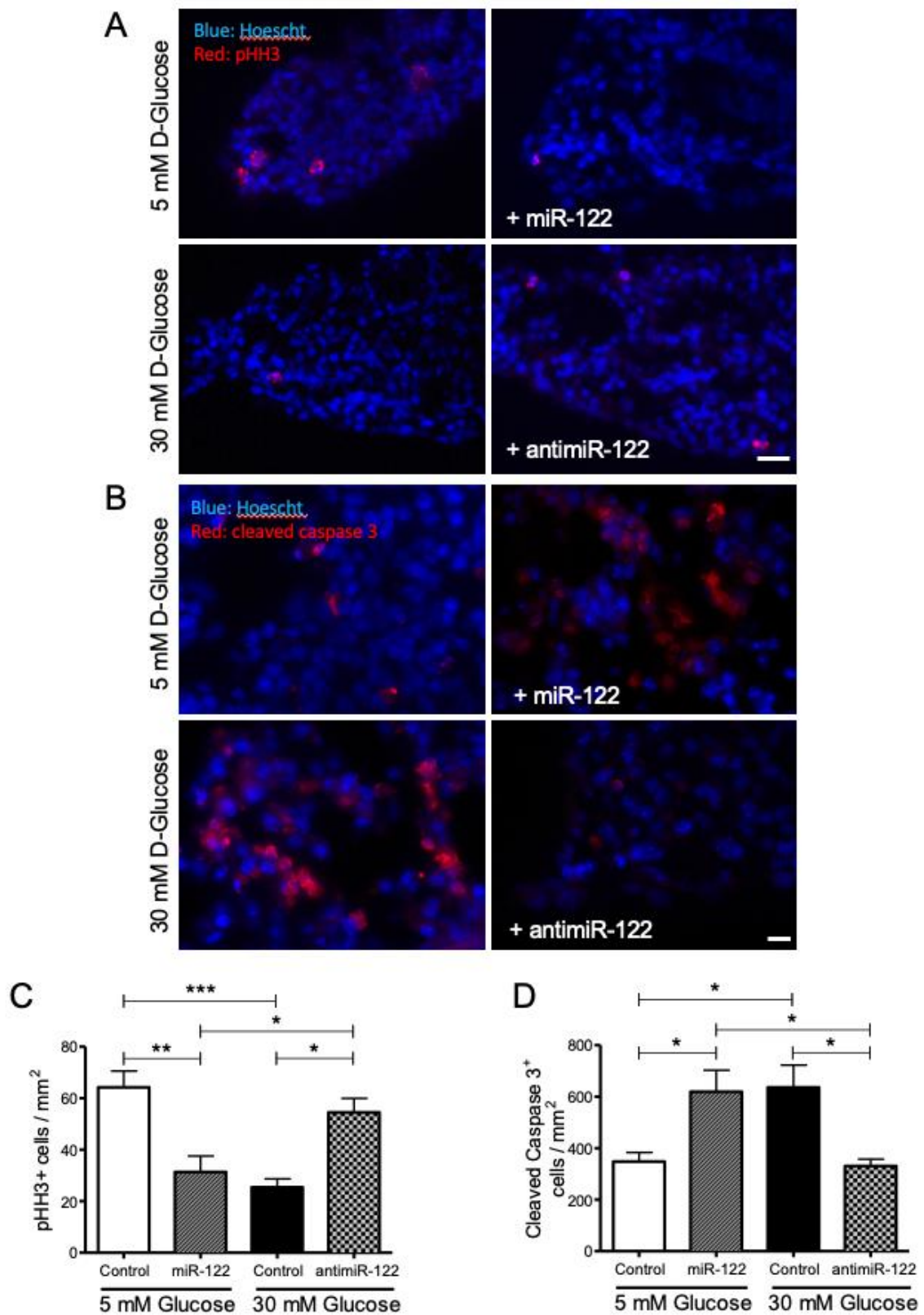


Figure 4.3. Analysis of target gene expression of miR-122.

mRNA isolated from E10.5 hearts and analyzed by RT-qPCR. Values are normalized to reference gene 28S. (A) Gata4, (B) Hand2, (C) Cyclin D1, (D) Wnt1, (E) Snail1, (F) Slug, (G) EPO. miR-122 to 3' UTR sequence complementarity prediction was performed using online databases (miRbase, TargetScan). n=4-5 per group from three litters. Data are mean  $\pm$  SEM. \* $P$ <0.05, \*\* $P$ <0.01, \*\*\* $P$ <0.001.

#### 4.4.3 Role of miR-122 in Cell Proliferation and Apoptosis in the Embryonic Heart

MiR-122 is a tumor suppressor and many studies have shown its ability to inhibit cell proliferation and increase apoptosis.<sup>44-46</sup> These two processes are integral to embryonic heart development.<sup>47,48</sup> E10.5 explanted hearts were cultured for four days in normal or high glucose conditions. A subset of hearts cultured in normal glucose were transfected with miR-122, and a cohort of hearts grown in high glucose were transfected with antimiR-122. Cell proliferation was analyzed using immunostaining for phosphorylated histone H3 (pHH3). Results show that high glucose or miR-122 transfection significantly lowered pHH3<sup>+</sup> cells in E10.5 hearts compared to normal glucose control ( $P$ <0.001, Figure 4A and C). Transfection with antimiR-122 under high glucose conditions restored cell proliferation to normal control levels ( $P$ <0.05, Figure 4.4A and C). Conversely, cell apoptosis as assessed by immunostaining of cleaved caspase 3 revealed a significant higher level of cell death under high glucose conditions as well as miR-122 transfection ( $P$ <0.05, Figure 4.4B and D). Notably, antimiR-122 transfection in explants grown under high glucose conditions significantly lowered the number of cleaved caspase 3 positive cells to basal levels ( $P$ <0.05, Figure 4.4D).



**Figure 4.4. Effects of miR-122 and high glucose on cell proliferation and apoptosis in the embryonic heart.**

Representative images of immunohistological staining of pHH3 (A) and cleaved caspase 3 (B). E10.5 hearts isolated from normal dams were used for *ex vivo* heart explant cultures. Explants cultured in 5 mM D-glucose were transfected with miR-122; whereas those exposed to 30 mM D-glucose received antimiR-122 for 24 hours. Heart sections were incubated with rhodamine phalloidin and DAPI to stain for pHH3<sup>+</sup> or cleaved caspase 3<sup>+</sup> cells and nuclei, respectively. Quantification of pHH3<sup>+</sup> (C) and cleaved caspase 3<sup>+</sup> cells (D). n = 5-6 hearts per group. Data are mean ± SEM. \**P*<0.05, \*\**P*<0.01, \*\*\**P*<0.001; Scale bar is 20 μm.

#### 4.4.4 Role of miR-122 in epicardial EMT

In addition to inhibiting cell proliferation, miR-122 has been shown to impede EMT in tumorigenesis.<sup>45,49,50</sup> High glucose has been previously shown to impair epicardial EMT *ex vivo*.<sup>42</sup> To study the role of miR-122 on epicardial EMT in the developing heart, an *ex vivo* EMT assay was performed by culturing E12.5 hearts on a collagen matrix for 4 days. The number of spindle like cells, which are epicardial-derived cells (EPDCs) that underwent EMT and migrated into the collagen matrix was counted and their migration distance was measured (Figure 4.5A). The data indicates that, after 4 days of culture, the number of EPDCs was significantly lowered by miR-122 transfection and by high glucose compared to normal glucose control (*P*<0.01, Figure 4.5C). However, treatment with antimiR-122 to the high glucose cultures restored the number of EPDCs back to control levels (*P*<0.001, Figure 4.5C). During EMT, mesenchymal cells migrate away from the explant to form the outgrowth area. The outgrowth distance, which is the distance from the edge of the explant to the edge of the outgrowth area, was quantified (Figure 4.5A-B). The data demonstrates that outgrowth distance was significantly reduced in the presence of miR-122 and under high glucose conditions compared to the



normal glucose control ( $P < 0.001$ , Figure 4.5B). Finally, anti-miR-122 transfection under high glucose conditions restored the outgrowth distance to normal glucose levels ( $P < 0.001$ , Figure 5B).

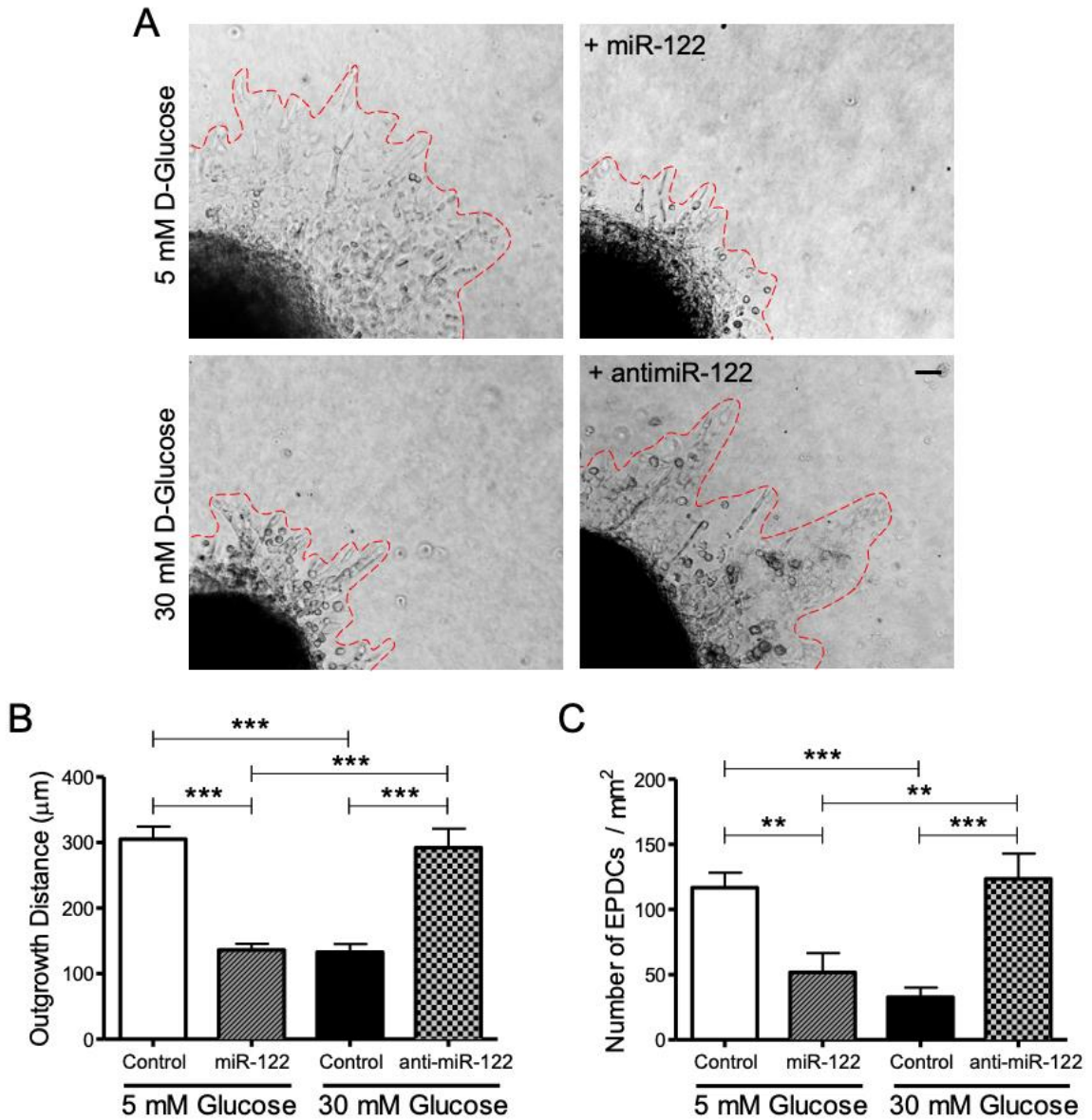


**Figure 4.5. Ex vivo assessment of epicardial EMT.**

(A) Representative images of E12.5 heart explant cultures grown on collagen matrix. Dashed lines outline the edge of the EPDC outgrowth area. (B) Quantification of the number of spindle shaped EPDCs normalized to the total explant area. (C) Quantification of outgrowth distance from the cultured heart explants. Values are measured from the edge of the explant to the edge of EPDC outgrowth area.  $n = 5 - 8$  explants per group from four litters. Data are mean  $\pm$  SEM. \* $P < 0.05$ , \*\* $P < 0.01$ , \*\*\* $P < 0.001$ . Scale bar is 50  $\mu\text{m}$ .

#### 4.4.5 Effects of anti-miR-122 on blood glucose, litter size, cardiac function and fetal liver

To study the role of miR-122 in heart development *in vivo*, a stable, a locked nucleic acid (LNA) version of anti-miR-122 was formulated. STZ-induced diabetic female mice received two subcutaneous 10 mg/kg doses of either anti-miR-122 or scramble LNA control, one prior to pregnancy and one during pregnancy. Figure 4.6A shows the blood glucose profile of female mice before pregnancy to fetal harvest with progressive increases throughout gestation, which were not affected by anti-miR-122 or scramble LNA control. While CHDs were present in an equal number of male and female offspring from diabetic dams administered scramble LNA, anti-miR-122 treatment was more effective in preventing CHDs in males compared to females ( $P < 0.05$ , Figure 4.6B). No significant changes in offspring litter size was noted between the two groups (Figure 4.6C). Next, cardiac function of E18.5 fetuses was measured using M-Mode echocardiography. Left ventricle ejection fraction (Figure 4.6D) and fractional shortening (Figure 4.6E) were significantly higher in offspring of diabetic dams treated with anti-miR-122 compared to scramble LNA ( $P < 0.001$ ). Finally, fetal livers were analyzed at E18.5 to determine whether the anti-miR-122 treatment had any adverse consequences on normal development *in vivo*. As anti-miR-122 treatment is expected to decrease the abundance of miR-122, the levels of miR-122 in the fetal liver were analyzed.<sup>51</sup> Indeed,

qPCR results indicate that antimiR-122 treatment significantly reduced miR-122 levels in the fetal liver in offspring of control and diabetic dams compared to scramble LNA administration ( $P < 0.01$ , Figure 4.6F). This result indicates that antimiR-122 treatment decreases miR-122 levels in mice. To determine whether antimiR-122 treatment had any effect on the fetal liver, hepatic histology was examined. No significant differences were seen in the average number of nuclei per liver section, or the ratio of sinusoid area to total hepatic area between anti-miR-122 and scramble LNA treated groups (Figure 4.6G-I).

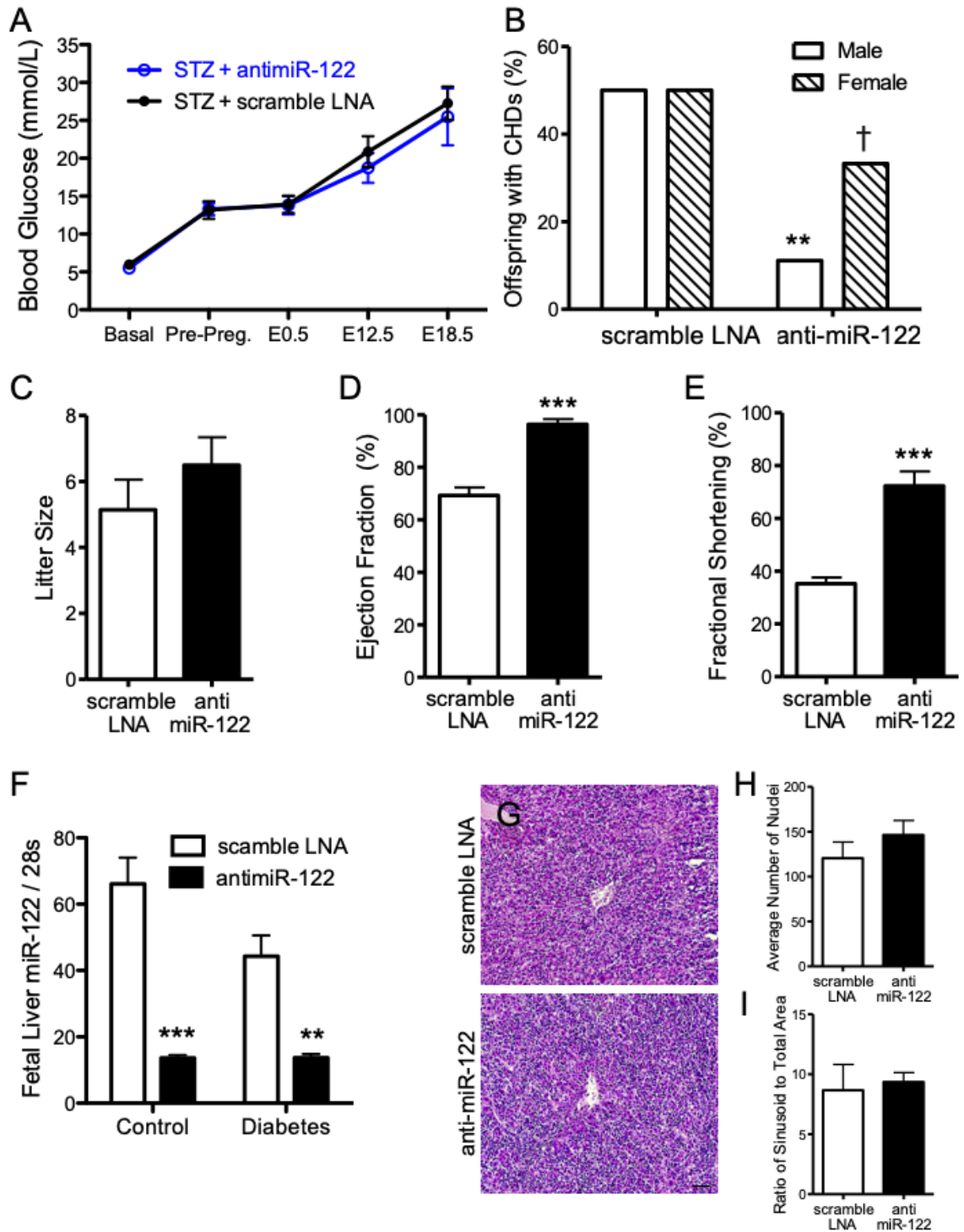


**Figure 4.6. Outcomes of in vivo administration of anti-miR-122 during diabetic pregnancy.**

(A) Blood glucose profile of diabetic dams administered with antimiR-122 (n=4) or scramble LNA control (n=5-6). (B) Sex differences in CHDs incidence in the offspring of diabetic dams administered with antimiR-122 or scramble LNA. (C) The offspring litter size measured at the day of fetus harvest (n=6-7 per group). (D) Ejection fraction and (E) fractional shortening measured through fetal echocardiography (n=4 per group). (F) E18.5 fetal liver miR-122 levels in offspring of control and diabetic dams treated with scramble LNA or anti-miR-122 (n=4 per group). (G) Effects of antimiR-122 on fetal liver morphology at E18.5. Representative histological sections of E18.5 liver samples from dams administered with scramble LNA or antimir-122. Scale bar is 100  $\mu$ m. (H) Average number of nuclei per fetal liver section and (I) ratio of sinusoid area to total fetal hepatic area (n=4 per group). Data are mean  $\pm$  SEM except B. \* $P$ <0.05, \*\* $P$ <0.01, \*\*\* $P$ <0.001 vs. respective controls.

#### 4.4.6 Anti-miR-122 administration reduces the incidence of diabetes-induced CHDs

CHDs were observed in 55.6% of offspring from diabetic dams treated with scramble LNA. This ratio was significantly reduced to 23.0% with antimiR-122 treatment (Table 4.2). Congenital malformations of the heart were present in all litters from scramble LNA-treated diabetic dams, and every dam in the antimiR-122 treatment group had at least one offspring with a CHD. Septal defects were commonly found in both groups. Atrial septal defects (ASD, Figure 4.7A) were observed in similar proportions. Diabetic dams treated with scramble LNA had 22.2% of offspring with a ventricular septal defect (VSD, Figure 4.7B), which was reduced to 4.2% with antimiR-122 treatment (Figure 4.7E). Two fetal hearts with double outlet right ventricles (DORV) were present in the scramble LNA group (Figure 4.7C), whereas normal aortic connections were maintained with antimiR-122 treatment (Figure 4.7F). Other severe CHDs of the outflow tract, such as truncus arteriosus and a vascular ring constricting the esophagus and trachea were only present in fetuses from diabetic dams treated with scramble LNA. Valvular defects were also prevalent in offspring of diabetic dams given

scramble LNA. Thicker pulmonary (13.9%, Figure 4.7G) and aortic (19.4%, Figure 4.7H) valves were more common in hearts from scramble-treated diabetic dams compared to anti-miR-122-treated diabetic dams (2.6% and 7.4%, Figure 4.7J-K, respectively). Finally, non-compaction of the ventricular myocardium was more prevalent in the right ventricle of offspring from scramble-treated diabetic dams (8.3%, Figure 4.7I). No such defect was seen in offspring of diabetic dams administered with anti-miR-122 (Figure 4.7L).

**Table 4.2. The rate of congenital heart defects in the offspring of diabetic dams treated with anti-miR-122 or scramble LNA.**

	STZ + Scramble LNA		STZ + anti-miR-122		Control Scramble LNA		Control anti-miR-122	
	N	dams	N	dams	N	dams	N	dams
	n	%	n	%	n	%	n	%
Normal	16	44.4**	30	76.9††	24	100.0	17	100.0
Abnormal	20	55.6**	9	23.0††	0	0.0	0	0.0
ASD	7	19.4*	6	18.5	0	0.0	0	0.0
VSD	8	22.2*	2	4.2†	0	0.0	0	0.0
AVSD	2	5.6	0	0.0	0	0.0	0	0.0
DORV	2	5.6	0	0.0	0	0.0	0	0.0
TGA	1	2.8	0	0.0	0	0.0	0	0.0
Truncus Arteriosus	1	2.8	0	0.0	0	0.0	0	0.0
OA	1	2.8	0	0.0	0	0.0	0	0.0
Vascular Ring	1	2.8	0	0.0	0	0.0	0	0.0
PA Stenosis	1	2.8	0	0.0	0	0.0	0	0.0
Thick PV	5	13.9	1	2.6	0	0.0	0	0.0
Thick AV	7	19.4*	4	7.4	0	0.0	0	0.0
NCVM	3	8.3	0	0.0	0	0.0	0	0.0

Morphological analysis was performed on E18.5 hearts. Data was analyzed using the Chi-square test. \* $P < 0.05$ , \*\* $P < 0.001$  vs. scramble control, † $P < 0.05$ , †† $P < 0.001$  vs. scramble diabetes. ASD: atrial septal defect, VSD: ventricular septal defect, AVSD: atrioventricular septal defect, DORV: double outlet right ventricle, PA: pulmonary artery, OA: overriding aorta, PV: pulmonary valve, AV: aortic valve, NCVM: Non-compaction of the ventricular myocardium. N indicates total number of fetuses, dams are litter numbers.



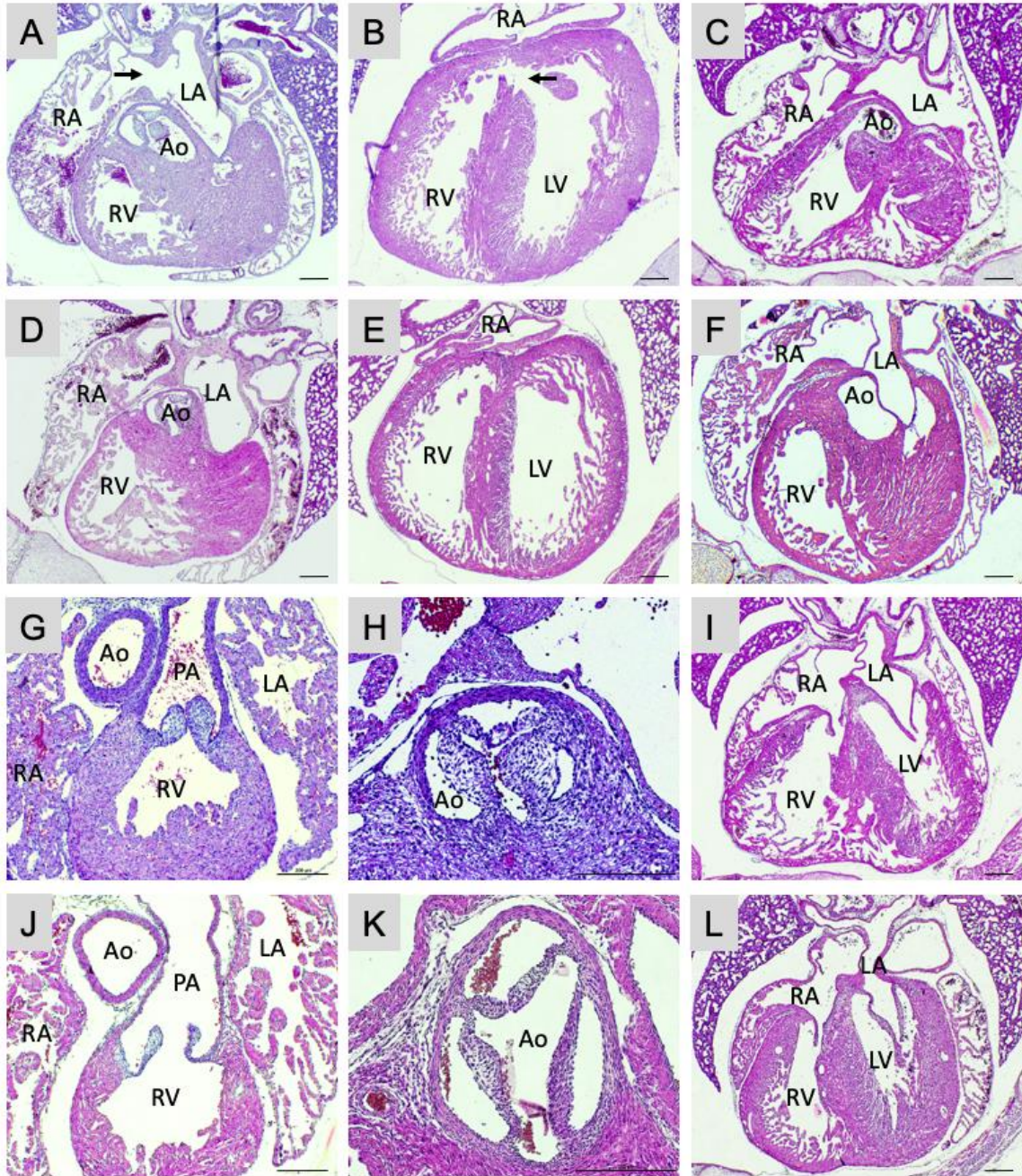


**Figure 4.7. Effects of anti-miR-122 on congenital heart defects induced by pregestational diabetes.**

Representative histological sections of E18.5 hearts from offspring of diabetic mothers either administered with anti-miR-122 or scramble LNA during gestation. Scramble LNA administered to diabetic dams resulted in offspring with atrial septal defect (A), ventricular septal defect (B), double outlet right ventricle (C), thickened pulmonary (G) and aortic (H) valves, and noncompaction of the myocardium (I). Anti-miR-122 treatment

reduced or fully prevented the incidence of these defects: intact atrial septum (D), intact ventricular septum (E), normal aortic connections (F), normal pulmonary (J) and aortic valves (K), and normal compact myocardium (L). Scale bars are 200  $\mu\text{m}$ .

## 4.5 Discussion

Pregestational diabetes is an established risk factor for CHDs, and increases the risk in infants by 3 to 5 times.<sup>5,7</sup> The molecular mechanisms behind the pathogenesis of diabetes-induced cardiac malformations require further understanding, and effective preventative measures need to be elucidated. Here, we employ an *ex vivo* and *in vivo* approach to delineate the effects of miR-122 upregulation in embryonic heart development, and test the efficacy of antimiR-122 treatment in a clinically relevant model of diabetes-induced CHDs in mice. The results of this study demonstrate that pregestational diabetes results in a high incidence of offspring CHDs and impaired cardiac function, which are rescued by maternal antimiR-122 treatment. This study also shows an upregulation of miR-122 in embryonic hearts from diabetic dams, and experimentally verified its target genes critical to heart development. miR-122 decreases the proliferative capacity of the developing heart, increases apoptosis, and inhibits epicardial EMT, leading to CHDs during pregestational diabetes (Figure 4.8).



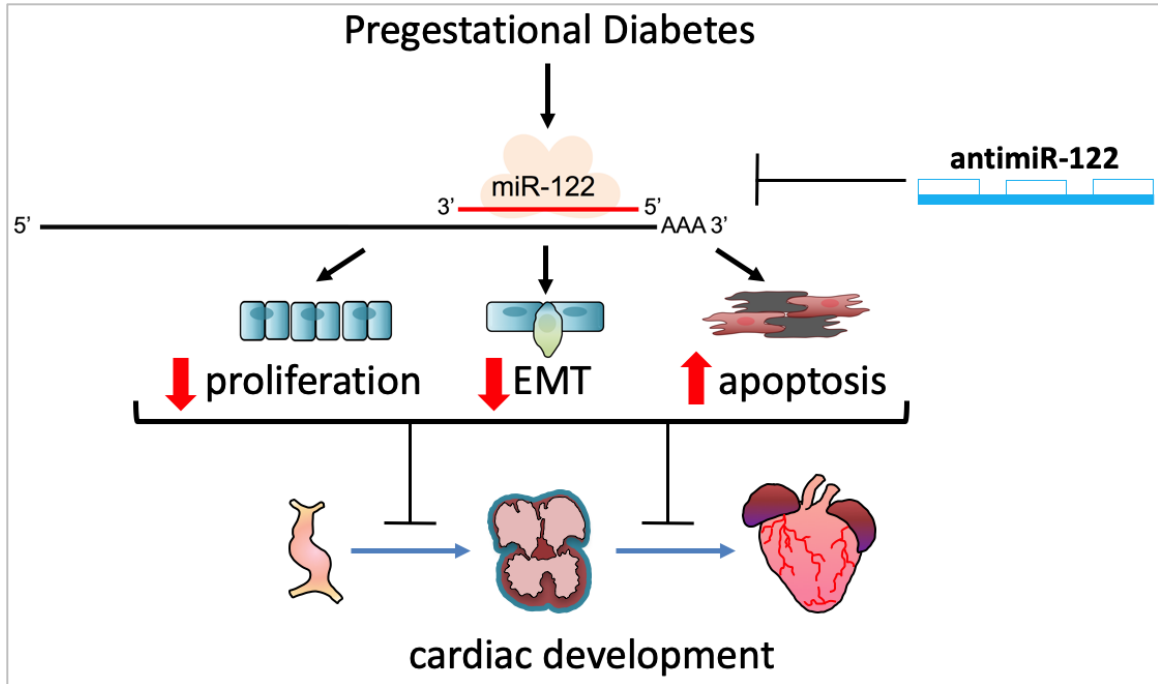


**Figure 4.8. Schematic summary showing the effect of miR-122 on embryonic heart development.**

Our findings suggest that pregestational diabetes induces cardiac expression of miR-122 in the early heart tube, which negatively affects heart development. miR-122 alters the expression of key genes involved in cell proliferation, apoptosis and epicardial EMT, processes crucial to proper cardiogenesis. AntimiR-122 administration to diabetic dams during gestation reduces the incidence of congenital heart defects in their offspring.

We recently demonstrated, using the same model of pregestational diabetes, the efficacy of the drug sapropterin dihydrochloride (Kuvan®) at reducing the incidence of CHDs from 59.4 to 26.5% in E18.5 fetal mice.<sup>37</sup> Accordingly, our previous work testing N-acetylcysteine treatment in this model prevented these cardiac malformations in a comparable fashion from 58.1 to 16.3%.<sup>43</sup> In a similar manner, maternal exercise also abrogated the effects of diabetes on the fetal heart by reducing the rate of CHDs from 56.8 to 25.0%.<sup>52</sup> These studies, as well as others, all focus on mitigating the damaging consequences of hyperglycemia-induced oxidative stress on the embryonic heart.<sup>53-55</sup>

However, in the present study we show that antimiR-122 treatment to diabetic dams significantly reduces offspring CHD incidence from 55.6 to 23.0%, specifically decreasing the VSD rate from 22.2 to 4.2%, via a potential epigenetic mechanism. By controlling aberrant miR-122 upregulation during diabetic pregnancy, the incidence of offspring cardiac malformations is reduced, and normal cardiac function is restored. Since antimiR-122 or antioxidant treatment alone does not completely prevent diabetes-induced CHDs, further studies are required to investigate whether the combination of antimiR-122 and N-acetylcysteine has a synergistic effect in preventing these malformations.

miRNAs play an indispensable role in cardiogenesis, acting as molecular switches, turning on and off gene programs controlling different stages of heart development.<sup>56</sup> In fact, cardiac progenitor-specific deletion of Dicer, a cytosolic RNase essential for miRNA maturation, results in major CHDs, such as VSD and DORV, and can be embryonic lethal depending on progenitor lineage.<sup>57-59</sup> Here we show a 3-fold increase in both miR-122 and pri-miR-122 in E12.5 hearts from diabetic dams. During embryonic development, miR-122 expression is normally limited to the developing liver, where it maintains hepatic transcriptome signatures, and has been shown to direct differentiation of mouse embryonic stem cells into hepatocytes.<sup>60,61</sup> miR-122 is also regarded as a tumor suppressor, and miR-122 null mice spontaneously develop hepatocellular carcinoma.<sup>30</sup> In the present study, we noted high miR-122 abundance in the fetal liver. Our novel finding is that miR-122 expression was elevated in embryonic hearts from diabetic dams. Expression of primary and precursor miR-122 transcripts follows circadian rhythm regulation, with expression fluctuating diurnally.<sup>62</sup> However,

the mature miRNA is sustained at constant levels in the cytosol due to the cytoplasmic poly(A) polymerase, GLD2, which confers stability and prolongs the half-life of miR-122 by adding a 3' adenosine cap.<sup>41</sup> In the present study, mRNA levels of GLD2 were significantly elevated in embryonic hearts from diabetic dams, suggesting miR-122 stabilization is a possible cause of its higher levels in our model. To identify miR-122 target genes critical to embryonic heart development, E10.5 and E12.5 heart explant culture was employed. Downregulations of *Gata4* and *Hand2* were seen with miR-122 transfection. *Gata4* is involved in SHF progenitor proliferation and differentiation, necessary for atrioventricular septation and OFT formation.<sup>63</sup> Similarly, deletion of *Hand2* in the cardiac neural crest results in VSD and DORVs, and in the SHF, *Hand2* protects the pharyngeal mesoderm against apoptosis.<sup>64,65</sup> Accordingly, in the present study, miR-122 transfection to E10.5 hearts induced high levels of apoptosis. This data agrees with previous findings that transduction of miR-122 promoted cell apoptosis in H9C2 cultured cardiomyocytes, and that its knockdown enhanced cell survival.<sup>44</sup> The increase in apoptosis could be due to miR-122 targeting the X-linked inhibitor of apoptosis (XIAP), relieving the inhibition of caspase-mediated programmed cell death pathways.<sup>66</sup> miR-122-induced apoptosis was similar to levels seen in the high glucose conditions, which is consistent with our previous *in vivo* findings of increased cell death in the endocardial cushion of E12.5 hearts from diabetic dams.<sup>43</sup> Targeting of the cardiogenic factors, *Gata4* and *Hand2*, as well as induction of apoptosis by miR-122 may contribute to the diabetes-induced outflow tract defects, such as TGA, truncus arteriosus and DORV in E18.5 fetuses.

Regulated cell proliferation is vital for cardiac morphogenesis and growth of the fetal heart. Proliferation deficiencies can result in thin, non-compact myocardium, shortening of the outflow tract and its incomplete septation, leading to the spectrum of CHDs.<sup>67,68</sup> In the present study, miR-122 targeted and inhibited the expression of Cyclin D1, thereby halting cell cycle progression, which may translate into a reduced number of pHH3-positive cells in these heart explants. AntimiR-122 in high glucose conditions restored both Cyclin D1 levels and cell proliferation to normal. In addition to inhibiting cell cycle progression, miR-122 targets the growth factor receptors, TGF $\beta$ R2, IFG1R and FGFR1 in the liver.<sup>69,70</sup> Ligands for these receptors, TGF- $\beta$ , FGF-10 and IGF-2, originate from the epicardium and promote proliferation and expansion of the adjacent myocardium.<sup>71-73</sup> Furthermore, in the present study, E12.5 heart explants grown on collagen exhibited stunted outgrowth and epicardial EMT with miR-122 transfection. Their migratory capacity and outgrowth mirrored the hearts in high glucose conditions, which is in agreement with our previous findings.<sup>42</sup> In fact, in a similar model of diabetes we have demonstrated an *in vivo* increase in E-cadherin expression, decreased Wt1-positive cells in the epicardium, as well as a downregulation of transcriptional drivers of epicardial EMT.<sup>42</sup> Here, we demonstrate that miR-122 targets and significantly reduces the transcript abundance of *Snail*, *Slug* and *EPO* by 2-fold. This is consistent with its role as a tumor suppressor, inhibiting EMT.<sup>74</sup> Recently, studies have explored the association of miR-122 with TGF- $\beta$ 1/Smad signaling or the Wnt/ $\beta$ -catenin signaling pathway in the development of liver fibrosis or cancer, particularly focusing on EMT and tumorigenesis.<sup>45,75</sup> They indicate that miR-122 reverses the ‘cadherin switch’ necessary for EMT, by increasing E-cadherin expression and decreasing N-cadherin levels via its

inhibition of Smad4.<sup>75</sup> Likewise, addition of miR-122 mimic to HCCs significantly diminished Wnt1 and  $\beta$ -catenin protein expression, decreasing tumor size.<sup>45</sup> Finally, miR-122 targets the transcription factor RUNX2, which functions independent of Snail1/2 in mediating EMT<sup>76,77</sup> and should be investigated in the developing heart in future studies.

The presented study is constrained by only examining a T1D model, and currently the prevalence of pregestational T2D is on the rise.<sup>78</sup> This is of particular interest as recent studies have revealed elevated levels of miR-122 in patients with obesity, insulin resistance and diabetic retinopathy, along with its already established roles as a biomarker for myocardial infarction and coronary artery disease.<sup>31,32,34,79-82</sup> The reason for this upregulation remains to be determined, however there is an inverse association between miR-122 and leptin, which is deregulated in diabetic patients.<sup>83,84</sup>

In conclusion, the present study is the first to reveal the role of miR-122 in embryonic heart development, and provide novel insights into the mechanisms underlying pregestational diabetes-induced CHDs. We show that embryonic hearts from diabetic dams have elevated levels of primary and mature miR-122, and that this nucleic acid could be stabilized in the cytosol by increased expression of GLD2. miR-122 targets the 3' UTR of many genes responsible for cardiogenesis, including *Gata4*, *Hand2*, *Wnt1* and *Snail1/2*, and specifically inhibits their expression *ex vivo*. This epigenetic modulation impairs key developmental processes of cell proliferation, apoptosis, and epicardial EMT, mirroring the negative effects of high glucose. In addition, we utilized a LNA form of the experimental drug antimiR-122 to effectively reduce the incidence of pregestational diabetes-induced CHDs and restore cardiac function. AntimiR-122

treatment had no adverse effects on litter size, fetal liver histology, or heart development, and can be considered safe for studies on fetal mice. Currently, undergoing phase II clinical trials for the treatment of chronic hepatitis C infection, our study suggests that antimiR-122 may have therapeutic potential in the prevention of CHDs in pregestational diabetes.

## 4.6 References

1. Benjamin EJ, Virani SS, Callaway CW, Chamberlain AM, Chang AR, Cheng S, Chiuve SE, Cushman M, Delling FN, Deo R, de Ferranti SD, Ferguson JF, Fornage M, Gillespie C, Isasi CR, Jimenez MC, Jordan LC, Judd SE, Lackland D, Lichtman JH, Lisabeth L, Liu S, Longenecker CT, Lutsey PL, Mackey JS, Matchar DB, Matsushita K, Mussolino ME, Nasir K, O'Flaherty M, Palaniappan LP, Pandey A, Pandey DK, Reeves MJ, Ritchey MD, Rodriguez CJ, Roth GA, Rosamond WD, Sampson UKA, Satou GM, Shah SH, Spartano NL, Tirschwell DL, Tsao CW, Voeks JH, Willey JZ, Wilkins JT, Wu JH, Alger HM, Wong SS, Muntner P, American Heart Association Council on E, Prevention Statistics C and Stroke Statistics S. Heart Disease and Stroke Statistics-2018 Update: A Report From the American Heart Association. *Circulation*. 2018;137:e67-e492.
2. Hoffman JI and Kaplan S. The incidence of congenital heart disease. *J Am Coll Cardiol*. 2002;39:1890-900.
3. van der Bom T, Zomer AC, Zwinderman AH, Meijboom FJ, Bouma BJ and Mulder BJ. The changing epidemiology of congenital heart disease. *Nat Rev Cardiol*. 2011;8:50-60.
4. Dolk H, Loane M and Garne E. The prevalence of congenital anomalies in Europe. *Adv Exp Med Biol*. 2010;686:349-64.
5. Oyen N, Diaz LJ, Leirgul E, Boyd HA, Priest J, Mathiesen ER, Quertermous T, Wohlfahrt J and Melbye M. Prepregnancy Diabetes and Offspring Risk of Congenital Heart Disease: A Nationwide Cohort Study. *Circulation*. 2016;133:2243-53.
6. Liu S, Joseph KS, Lisonkova S, Rouleau J, Van den Hof M, Sauve R, Kramer MS and Canadian Perinatal Surveillance S. Association between maternal chronic conditions and congenital heart defects: a population-based cohort study. *Circulation*. 2013;128:583-9.
7. Jenkins KJ, Correa A, Feinstein JA, Botto L, Britt AE, Daniels SR, Elixson M, Warnes CA, Webb CL and American Heart Association Council on Cardiovascular Disease in the Y. Noninherited risk factors and congenital cardiovascular defects: current knowledge: a scientific statement from the American Heart Association Council on Cardiovascular Disease in the Young: endorsed by the American Academy of Pediatrics. *Circulation*. 2007;115:2995-3014.
8. Loffredo CA, Wilson PD and Ferencz C. Maternal diabetes: an independent risk factor for major cardiovascular malformations with increased mortality of affected infants. *Teratology*. 2001;64:98-106.

9. Cho NH, Shaw JE, Karuranga S, Huang Y, da Rocha Fernandes JD, Ohlrogge AW and Malanda B. IDF Diabetes Atlas: Global estimates of diabetes prevalence for 2017 and projections for 2045. *Diabetes Res Clin Pract.* 2018;138:271-281.
10. Dabelea D, Mayer-Davis EJ, Saydah S, Imperatore G, Linder B, Divers J, Bell R, Badaru A, Talton JW, Crume T, Liese AD, Merchant AT, Lawrence JM, Reynolds K, Dolan L, Liu LL, Hamman RF and Study SfdiY. Prevalence of type 1 and type 2 diabetes among children and adolescents from 2001 to 2009. *Jama.* 2014;311:1778-86.
11. Mayer-Davis EJ, Lawrence JM, Dabelea D, Divers J, Isom S, Dolan L, Imperatore G, Linder B, Marcovina S, Pettitt DJ, Pihoker C, Saydah S, Wagenknecht L and Study SfdiY. Incidence Trends of Type 1 and Type 2 Diabetes among Youths, 2002-2012. *N Engl J Med.* 2017;376:1419-1429.
12. Bardenheier BH, Imperatore G, Gilboa SM, Geiss LS, Saydah SH, Devlin HM, Kim SY and Gregg EW. Trends in Gestational Diabetes Among Hospital Deliveries in 19 U.S. States, 2000-2010. *Am J Prev Med.* 2015;49:12-9.
13. Eriksen NB, Damm P, Mathiesen ER and Ringholm L. The prevalence of congenital malformations is still higher in pregnant women with pregestational diabetes despite near-normal HbA1c: a literature review. *J Matern Fetal Neonatal Med.* 2019;32:1225-1229.
14. Burchill LJ, Gao L, Kovacs AH, Opotowsky AR, Maxwell BG, Minnier J, Khan AM and Broberg CS. Hospitalization Trends and Health Resource Use for Adult Congenital Heart Disease-Related Heart Failure. *J Am Heart Assoc.* 2018;7:e008775.
15. Meilhac SM and Buckingham ME. The deployment of cell lineages that form the mammalian heart. *Nat Rev Cardiol.* 2018;15:705-724.
16. Kelly RG, Buckingham ME and Moorman AF. Heart fields and cardiac morphogenesis. *Cold Spring Harb Perspect Med.* 2014;4.
17. Soufan AT, van den Berg G, Ruijter JM, de Boer PA, van den Hoff MJ and Moorman AF. Regionalized sequence of myocardial cell growth and proliferation characterizes early chamber formation. *Circ Res.* 2006;99:545-52.
18. Kwon C, Arnold J, Hsiao EC, Taketo MM, Conklin BR and Srivastava D. Canonical Wnt signaling is a positive regulator of mammalian cardiac progenitors. *Proc Natl Acad Sci U S A.* 2007;104:10894-9.
19. Poelmann RE and Gittenberger-de Groot AC. Apoptosis as an instrument in cardiovascular development. *Birth Defects Res C Embryo Today.* 2005;75:305-13.
20. von Gise A and Pu WT. Endocardial and epicardial epithelial to mesenchymal transitions in heart development and disease. *Circ Res.* 2012;110:1628-45.



21. Mu H, Ohashi R, Lin P, Yao Q and Chen C. Cellular and molecular mechanisms of coronary vessel development. *Vasc Med*. 2005;10:37-44.
22. Winter J, Jung S, Keller S, Gregory RI and Diederichs S. Many roads to maturity: microRNA biogenesis pathways and their regulation. *Nat Cell Biol*. 2009;11:228-34.
23. Shantikumar S, Caporali A and Emanuelli C. Role of microRNAs in diabetes and its cardiovascular complications. *Cardiovasc Res*. 2012;93:583-93.
24. Liu N and Olson EN. MicroRNA regulatory networks in cardiovascular development. *Dev Cell*. 2010;18:510-25.
25. Ibarra A, Vega-Guedes B, Brito-Casillas Y and Wagner AM. Diabetes in Pregnancy and MicroRNAs: Promises and Limitations in Their Clinical Application. *Noncoding RNA*. 2018;4.
26. Dong D, Zhang Y, Reece EA, Wang L, Harman CR and Yang P. microRNA expression profiling and functional annotation analysis of their targets modulated by oxidative stress during embryonic heart development in diabetic mice. *Reprod Toxicol*. 2016;65:365-374.
27. Shi R, Zhao L, Cai W, Wei M, Zhou X, Yang G and Yuan L. Maternal exosomes in diabetes contribute to the cardiac development deficiency. *Biochem Biophys Res Commun*. 2017;483:602-608.
28. Bandiera S, Pfeffer S, Baumert TF and Zeisel MB. miR-122--a key factor and therapeutic target in liver disease. *J Hepatol*. 2015;62:448-57.
29. Hsu SH, Wang B, Kota J, Yu J, Costinean S, Kutay H, Yu L, Bai S, La Perle K, Chivukula RR, Mao H, Wei M, Clark KR, Mendell JR, Caligiuri MA, Jacob ST, Mendell JT and Ghoshal K. Essential metabolic, anti-inflammatory, and anti-tumorigenic functions of miR-122 in liver. *J Clin Invest*. 2012;122:2871-83.
30. Tsai WC, Hsu SD, Hsu CS, Lai TC, Chen SJ, Shen R, Huang Y, Chen HC, Lee CH, Tsai TF, Hsu MT, Wu JC, Huang HD, Shiao MS, Hsiao M and Tsou AP. MicroRNA-122 plays a critical role in liver homeostasis and hepatocarcinogenesis. *J Clin Invest*. 2012;122:2884-97.
31. de Candia P, Spinetti G, Specchia C, Sangalli E, La Sala L, Uccellatore A, Lupini S, Genovese S, Matarese G and Ceriello A. A unique plasma microRNA profile defines type 2 diabetes progression. *PLoS one*. 2017;12:e0188980.
32. Jones A, Danielson KM, Benton MC, Ziegler O, Shah R, Stubbs RS, Das S and Macartney-Coxson D. miRNA Signatures of Insulin Resistance in Obesity. *Obesity (Silver Spring)*. 2017;25:1734-1744.

33. Wang R, Hong J, Cao Y, Shi J, Gu W, Ning G, Zhang Y and Wang W. Elevated circulating microRNA-122 is associated with obesity and insulin resistance in young adults. *Eur J Endocrinol.* 2015;172:291-300.
34. Ortega FJ, Mercader JM, Catalan V, Moreno-Navarrete JM, Pueyo N, Sabater M, Gomez-Ambrosi J, Anglada R, Fernandez-Formoso JA, Ricart W, Fruhbeck G and Fernandez-Real JM. Targeting the circulating microRNA signature of obesity. *Clin Chem.* 2013;59:781-92.
35. Willeit P, Skrobilin P, Moschen AR, Yin X, Kaudewitz D, Zampetaki A, Barwari T, Whitehead M, Ramirez CM, Goedeke L, Rotllan N, Bonora E, Hughes AD, Santer P, Fernandez-Hernando C, Tilg H, Willeit J, Kiechl S and Mayr M. Circulating MicroRNA-122 Is Associated With the Risk of New-Onset Metabolic Syndrome and Type 2 Diabetes. *Diabetes.* 2017;66:347-357.
36. Delic D, Eisele C, Schmid R, Luippold G, Mayoux E and Grempler R. Characterization of Micro-RNA Changes during the Progression of Type 2 Diabetes in Zucker Diabetic Fatty Rats. *Int J Mol Sci.* 2016;17.
37. Engineer A, Saiyin T, Lu X, Kucey AS, Urquhart BL, Drysdale TA, Norozi K and Feng Q. Sapropterin Treatment Prevents Congenital Heart Defects Induced by Pregestational Diabetes Mellitus in Mice. *J Am Heart Assoc.* 2018;7:e009624.
38. Varkonyi-Gasic E, Wu R, Wood M, Walton EF and Hellens RP. Protocol: a highly sensitive RT-PCR method for detection and quantification of microRNAs. *Plant Methods.* 2007;3:12.
39. Liu Y, Lu X, Xiang FL, Poelmann RE, Gittenberger-de Groot AC, Robbins J and Feng Q. Nitric oxide synthase-3 deficiency results in hypoplastic coronary arteries and postnatal myocardial infarction. *Euro Heart J.* 2014;35:920-31.
40. Liu Y, Lu X, Xiang FL, Lu M and Feng Q. Nitric oxide synthase-3 promotes embryonic development of atrioventricular valves. *PLoS one.* 2013;8:e77611.
41. D'Ambrogio A, Gu W, Udagawa T, Mello CC and Richter JD. Specific miRNA stabilization by Gld2-catalyzed monoadenylation. *Cell Rep.* 2012;2:1537-45.
42. Moazzen H, Lu X, Liu M and Feng Q. Pregestational diabetes induces fetal coronary artery malformation via reactive oxygen species signaling. *Diabetes.* 2015;64:1431-43.
43. Moazzen H, Lu X, Ma NL, Velenosi TJ, Urquhart BL, Wisse LJ, Gittenberger-de Groot AC and Feng Q. N-Acetylcysteine prevents congenital heart defects induced by pregestational diabetes. *Cardiovasc Diabetol.* 2014;13:46.
44. Huang X, Huang F, Yang D, Dong F, Shi X, Wang H, Zhou X, Wang S and Dai S. Expression of microRNA-122 contributes to apoptosis in H9C2 myocytes. *J Cell Mol Med.* 2012;16:2637-46.

45. Cao F and Yin LX. miR-122 enhances sensitivity of hepatocellular carcinoma to oxaliplatin via inhibiting MDR1 by targeting Wnt/beta-catenin pathway. *Exp Mol Pathol.* 2019;106:34-43.
46. Wang W, Yang J, Yu F, Li W, Wang L, Zou H and Long X. MicroRNA-122-3p inhibits tumor cell proliferation and induces apoptosis by targeting Forkhead box O in A549 cells. *Oncol Lett.* 2018;15:2695-2699.
47. Fisher SA, Langille BL and Srivastava D. Apoptosis during cardiovascular development. *Circ Res.* 2000;87:856-64.
48. Gunthel M, Barnett P and Christoffels VM. Development, Proliferation, and Growth of the Mammalian Heart. *Mol Ther.* 2018;26:1599-1609.
49. Jin Y, Wang J, Han J, Luo D and Sun Z. MiR-122 inhibits epithelial-mesenchymal transition in hepatocellular carcinoma by targeting Snail1 and Snail2 and suppressing WNT/beta-cadherin signaling pathway. *Exp Cell Res.* 2017;360:210-217.
50. Liu N, Jiang F, He TL, Zhang JK, Zhao J, Wang C, Jiang GX, Cao LP, Kang PC, Zhong XY, Lin TY and Cui YF. The Roles of MicroRNA-122 Overexpression in Inhibiting Proliferation and Invasion and Stimulating Apoptosis of Human Cholangiocarcinoma Cells. *Sci Rep.* 2015;5:16566.
51. Hu J, Xu Y, Hao J, Wang S, Li C and Meng S. MiR-122 in hepatic function and liver diseases. *Protein Cell.* 2012;3:364-71.
52. Saiyin T, Engineer A, Greco ER, Kim MY, Lu X, Jones DL and Feng Q. Maternal voluntary exercise mitigates oxidative stress and incidence of congenital heart defects in pre-gestational diabetes. *J Cell Mol Med.* 2019;00:1-13.
53. Sivan E, Reece EA, Wu YK, Homko CJ, Polansky M and Borenstein M. Dietary vitamin E prophylaxis and diabetic embryopathy: morphologic and biochemical analysis. *Am J Obstet Gynecol.* 1996;175:793-9.
54. Siman CM and Eriksson UJ. Vitamin E decreases the occurrence of malformations in the offspring of diabetic rats. *Diabetes.* 1997;46:1054-61.
55. Siman CM and Eriksson UJ. Vitamin C supplementation of the maternal diet reduces the rate of malformation in the offspring of diabetic rats. *Diabetologia.* 1997;40:1416-24.
56. Porrello ER. microRNAs in cardiac development and regeneration. *Clin Sci (Lond).* 2013;125:151-66.
57. Zhao Y, Samal E and Srivastava D. Serum response factor regulates a muscle-specific microRNA that targets Hand2 during cardiogenesis. *Nature.* 2005;436:214-20.

58. Huang ZP, Chen JF, Regan JN, Maguire CT, Tang RH, Dong XR, Majesky MW and Wang DZ. Loss of microRNAs in neural crest leads to cardiovascular syndromes resembling human congenital heart defects. *Arterioscler Thromb Vasc Biol.* 2010;30:2575-86.
59. Singh MK, Lu MM, Massera D and Epstein JA. MicroRNA-processing enzyme Dicer is required in epicardium for coronary vasculature development. *J Biol Chem.* 2011;286:41036-45.
60. Thakral S and Ghoshal K. miR-122 is a unique molecule with great potential in diagnosis, prognosis of liver disease, and therapy both as miRNA mimic and antimir. *Curr Gene Ther.* 2015;15:142-50.
61. Deng XG, Qiu RL, Wu YH, Li ZX, Xie P, Zhang J, Zhou JJ, Zeng LX, Tang J, Maharjan A and Deng JM. Overexpression of miR-122 promotes the hepatic differentiation and maturation of mouse ESCs through a miR-122/FoxA1/HNF4a-positive feedback loop. *Liver Int.* 2014;34:281-95.
62. Gatfield D, Le Martelot G, Vejnar CE, Gerlach D, Schaad O, Fleury-Olela F, Ruskeepaa AL, Oresic M, Esau CC, Zdobnov EM and Schibler U. Integration of microRNA miR-122 in hepatic circadian gene expression. *Genes Dev.* 2009;23:1313-26.
63. Zhou L, Liu J, Xiang M, Olson P, Guzzetta A, Zhang K, Moskowitz IP and Xie L. Gata4 potentiates second heart field proliferation and Hedgehog signaling for cardiac septation. *Proc Natl Acad Sci U S A.* 2017;114:E1422-E1431.
64. Tsuchihashi T, Maeda J, Shin CH, Ivey KN, Black BL, Olson EN, Yamagishi H and Srivastava D. Hand2 function in second heart field progenitors is essential for cardiogenesis. *Dev Biol.* 2011;351:62-9.
65. Holler KL, Hendershot TJ, Troy SE, Vincentz JW, Firulli AB and Howard MJ. Targeted deletion of Hand2 in cardiac neural crest-derived cells influences cardiac gene expression and outflow tract development. *Dev Biol.* 2010;341:291-304.
66. Hua Y, Zhu Y, Zhang J, Zhu Z, Ning Z, Chen H, Liu L, Chen Z and Meng Z. miR-122 Targets X-Linked Inhibitor of Apoptosis Protein to Sensitize Oxaliplatin-Resistant Colorectal Cancer Cells to Oxaliplatin-Mediated Cytotoxicity. *Cell Physiol Biochem.* 2018;51:2148-2159.
67. Leung C, Liu Y, Lu X, Kim M, Drysdale TA and Feng Q. Rac1 Signaling Is Required for Anterior Second Heart Field Cellular Organization and Cardiac Outflow Tract Development. *J Am Heart Assoc.* 2015;5.
68. Feng Q, Song W, Lu X, Hamilton JA, Lei M, Peng T and Yee SP. Development of heart failure and congenital septal defects in mice lacking endothelial nitric oxide synthase. *Circulation.* 2002;106:873-9.

69. Sun Y, Wang H, Li Y, Liu S, Chen J and Ying H. miR-24 and miR-122 Negatively Regulate the Transforming Growth Factor-beta/Smad Signaling Pathway in Skeletal Muscle Fibrosis. *Mol Ther Nucleic Acids*. 2018;11:528-537.
70. Xu H, Xu SJ, Xie SJ, Zhang Y, Yang JH, Zhang WQ, Zheng MN, Zhou H and Qu LH. MicroRNA-122 supports robust innate immunity in hepatocytes by targeting the RTKs/STAT3 signaling pathway. *Elife*. 2019;8.
71. Azhar M, Schultz Jel J, Grupp I, Dorn GW, 2nd, Meneton P, Molin DG, Gittenberger-de Groot AC and Doetschman T. Transforming growth factor beta in cardiovascular development and function. *Cytokine Growth Factor Rev*. 2003;14:391-407.
72. Li P, Cavallero S, Gu Y, Chen TH, Hughes J, Hassan AB, Bruning JC, Pashmforoush M and Sucov HM. IGF signaling directs ventricular cardiomyocyte proliferation during embryonic heart development. *Development*. 2011;138:1795-805.
73. Hubert F, Payan SM and Rochais F. FGF10 Signaling in Heart Development, Homeostasis, Disease and Repair. *Front Genet*. 2018;9:599.
74. Bai S, Nasser MW, Wang B, Hsu SH, Datta J, Kutay H, Yadav A, Nuovo G, Kumar P and Ghoshal K. MicroRNA-122 inhibits tumorigenic properties of hepatocellular carcinoma cells and sensitizes these cells to sorafenib. *J Biol Chem*. 2009;284:32015-27.
75. Cheng B, Zhu Q, Lin W and Wang L. MicroRNA-122 inhibits epithelial-mesenchymal transition of hepatic stellate cells induced by the TGF-beta1/Smad signaling pathway. *Exp Ther Med*. 2019;17:284-290.
76. Ding CQ, Deng WS, Yin XF and Ding XD. MiR-122 inhibits cell proliferation and induces apoptosis by targeting runt-related transcription factors 2 in human glioma. *Eur Rev Med Pharmacol Sci*. 2018;22:4925-4933.
77. Tavares ALP, Brown JA, Ulrich EC, Dvorak K and Runyan RB. Runx2-I is an Early Regulator of Epithelial-Mesenchymal Cell Transition in the Chick Embryo. *Dev Dyn*. 2018;247:542-554.
78. Coton SJ, Nazareth I and Petersen I. A cohort study of trends in the prevalence of pregestational diabetes in pregnancy recorded in UK general practice between 1995 and 2012. *BMJ Open*. 2016;6:e009494.
79. Pastukh N, Meerson A, Kalish D, Jabaly H and Blum A. Serum miR-122 levels correlate with diabetic retinopathy. *Clin Exp Med*. 2019;19:255-260.
80. D'Alessandra Y, Devanna P, Limana F, Straino S, Di Carlo A, Brambilla PG, Rubino M, Carena MC, Spazzafumo L, De Simone M, Micheli B, Biglioli P, Achilli F, Martelli F, Maggiolini S, Marenzi G, Pompilio G and Capogrossi MC.

Circulating microRNAs are new and sensitive biomarkers of myocardial infarction. *Euro Heart J.* 2010;31:2765-73.

81. Wang YL and Yu W. Association of circulating microRNA-122 with presence and severity of atherosclerotic lesions. *PeerJ.* 2018;6:e5218.
82. Cortez-Dias N, Costa MC, Carrilho-Ferreira P, Silva D, Jorge C, Calisto C, Pessoa T, Robalo Martins S, de Sousa JC, da Silva PC, Fiuza M, Diogo AN, Pinto FJ and Enguita FJ. Circulating miR-122-5p/miR-133b Ratio Is a Specific Early Prognostic Biomarker in Acute Myocardial Infarction. *Circ J.* 2016;80:2183-91.
83. Zhai X, Cheng F, Ji L, Zhu X, Cao Q, Zhang Y, Jia X, Zhou Q, Guan W and Zhou Y. Leptin reduces microRNA-122 level in hepatic stellate cells in vitro and in vivo. *Mol Immunol.* 2017;92:68-75.
84. Azar ST, Zalloua PA, Zantout MS, Shahine CH and Salti I. Leptin levels in patients with type 1 diabetes receiving intensive insulin therapy compared with those in patients receiving conventional insulin therapy. *J Endocrinol Invest.* 2002;25:724-6.

## Chapter 5

### 5 Chapter 5

#### 5.1 Summary of Major Findings

The overall aim of this thesis was to explore the pathogenesis of pregestational diabetes-induced congenital heart defects (CHDs) and coronary artery malformations (CAMs), and investigate the efficacy and mechanisms behind two preventative strategies. Specifically, I studied the impact of elevated levels of eNOS uncoupling/oxidative stress and miR-122 during gestation on embryonic heart development in a model of streptozotocin-induced (STZ) pregestational diabetes in mice. Concurrently, we tested the efficacy of sapropterin and antimiR-122 pharmacotherapy on preventing a range of defects induced by pregestational diabetes. Altered gene expression, impaired protein activity and function, and deregulated cellular processes in embryos of diabetic dams resulted in morphological and functional congenital heart abnormalities at birth, which were reduced in incidence by both treatments. The experimental approaches used to carry out these experiments included histological analysis of heart structure, using a serial sectioning technique to accurately diagnose heart malformations. Next, we employed *in vivo* lineage tracing using transgenic mice to specifically map a group of cardiac progenitors. In addition, we performed *ex vivo* heart explant cultures to examine certain cellular processes under normal and high glucose conditions. Finally, we conducted immunostaining to identify certain cells, and molecular analysis of embryonic hearts via Western blotting or qPCR analysis.

Pregestational diabetes in the mother increases the risk of a CHD in the child by over 4-fold.<sup>1</sup> In **Chapter 2**, I investigated the effects of maternal sapropterin treatment on

CHDs induced by pregestational diabetes in mice. To carry out this aim, C57BL/6 adult female mice were made diabetic via STZ administration, a model of pregestational diabetes previously employed in our lab. Mice were categorized as diabetic if non-fasting blood glucose measurements were above 11 mM. Pregnant diabetic dams steadily increased in hyperglycemia throughout gestation. The offspring of these mice were born in smaller litters, had a lower body weight, impaired cardiac function, and a spectrum of morphological anomalies, including both cardiac and neural tube defects. Daily sapropterin treatment throughout gestation did not impact the hyperglycemic state of the pregnant dams; however, it prevented a decrease in fetal weight, and improved the functional and morphological defects in the hearts of the offspring. Importantly, oral sapropterin treatment to diabetic dams significantly decreased the incidence of CHDs from 59.4% to 26.5%, and all major malformations, such as AVSD and DORV, were absent in the treatment group. A higher proportion of male offspring had CHDs, and sapropterin treatment was effective in lowering the incidence of CHDs in both sexes. Fetal hearts from diabetic dams had thinner ventricular free walls, and thicker aortic, pulmonary and mitral valves, indicating defects in myocardialization and valve remodeling, respectively. Sapropterin treatment recovered the thickness of ventricular compact myocardium, and improved cardiac valve remodeling. In addition, treatment with insulin to diabetic dams restored normal blood glucose levels and resulted in no any CHDs, indicating that malformations in the offspring of diabetic dams were due to hyperglycemia. To determine the mechanism of hyperglycemia-induced CHDs, cardiogenesis was examined at different time-points during embryonic development. Lineage tracing of cardiac progenitors using the SHF-specific *Mef2c<sup>cre/+</sup>* transgenic



mouse and the global double fluorescent *Cre* reporter line *Rosa26<sup>mTmG</sup>* was conducted at E9.5 and E12.5. Analysis revealed a lower commitment of SHF progenitors to the OFT, endocardial cushions, and ventricular myocardium of the fetal heart. In fact, embryonic hearts from diabetic dams had a shortened OFT length at E10.5, along with less cell proliferation in both the OFT and ventricle, which was normalized with sapropterin treatment. Accordingly, gene expression analysis of E12.5 hearts demonstrated lower mRNA levels of key cardiac transcription factors, such as *Gata4*, *Tbx5*, *Nkx2.5*, *Gata5*, which were restored to normal with sapropterin treatment. Sapropterin treatment also restored the expression of dihydrofolate reductase (*Dhfr*), responsible for the conversion of BH<sub>2</sub> to BH<sub>4</sub>. These cellular and molecular alterations, induced by pregestational diabetes, could be attributed to elevated levels of ROS, observed in E12.5 hearts of diabetic dams via DHE-probe. Sapropterin treatment reduced ROS to the same levels as L-NAME and superoxide dismutase pre-treatment to embryonic hearts from diabetic dams, indicating eNOS-derived superoxide production. Furthermore, analysis of eNOS dimerization via western blotting showed a loss of the functional eNOS dimer in E12.5 hearts from diabetic dams, and re-coupling of the enzyme with sapropterin treatment. Overall, this study demonstrated the efficacy of the FDA-approved drug sapropterin (Kuvan®) at preventing pregestational diabetes-induced CHDs by restoring gene expression profiles, improving eNOS coupling, reducing ROS, and increasing cell proliferation.

The development of coronary vessels that perfuse the cardiac muscle occurs concurrently with heart development.<sup>1</sup> This process is reliant on coordinated epicardial EMT and eNOS-derived NO, and missteps can result in CAMs.<sup>2</sup> In fact, eNOS<sup>-/-</sup> mice

display hypoplastic coronary arteries and postnatal myocardial infarction.<sup>3</sup> To this end, in **Chapter 3**, we examined the effects of sapropterin on coronary artery development in embryonic hearts of mice with pregestational maternal diabetes. This study was conducted using the same model of pregestational diabetes and sapropterin administration as **Chapter 2**. Treatment with sapropterin to mice with pregestational diabetes resulted in a lower incidence of CAMs in their offspring from 50.0% to 20.6%. Histological analysis revealed coronary arteries with marked decreases in luminal diameters, abundance and volumes in fetal hearts from diabetic dams. In addition, capillary density within the myocardium was lower in these hearts. Sapropterin treatment prevented diabetes-induced fetal hypoplastic coronary arteries and restored capillary density. One source of coronary artery progenitors is the epicardium. Epithelial cells delaminate and migrate into the myocardium, where they differentiate into vascular smooth muscle cells, fibroblasts and endothelial cells, the components of coronary arteries.<sup>2</sup> As such, the epicardium of E12.5 hearts from diabetic dams was examined, and fewer actively proliferating cells were noted. In addition, these hearts had a lower number of Wt1<sup>+</sup> cells and higher expression of E-cadherin, indicating an impairment in epicardial EMT, which was returned to normal with sapropterin treatment. To further explore the behavior of epicardial-derived (EPDC) coronary artery progenitors, E12.5 embryonic hearts were explanted onto a collagen matrix and cultured *ex vivo*. Consequently, tetrahydrobiopterin, infused into the culture media, prevented the lower EPDC outgrowth and number under high glucose conditions. In a similar manner as **Chapter 2**, the mRNA levels of key molecular regulators of coronary artery development involved in EMT, differentiation, and growth, were examined. The expression of *Hif-1 $\alpha$* , *Snail1*, *Aldh1a2*,  *$\beta$ -catenin* and *bFGF*, was

lower with maternal diabetes and reestablished with sapropterin treatment. Mechanistically, these compromised molecular pathways and cellular processes can be attributed to increased oxidative stress in the ventricular myocardium of E12.5 hearts from diabetic dams. The increase in lipid peroxidation was attenuated with sapropterin treatment. Moreover, Akt and eNOS phosphorylation was lower in embryonic hearts from diabetic dams, and was returned to basal levels with sapropterin treatment. Taken together, this data demonstrated the therapeutic potential of the FDA-approved drug sapropterin at preventing pregestational diabetes-induced CAMs. This study also provides insight into factors contributing to altered coronary artery development, such as impaired Akt/eNOS activity and oxidative stress.

Thus far, in **Chapter 2** and **Chapter 3** of this thesis, oxidative stress and impaired eNOS-derived NO signaling was been investigated as a major driver of diabetic embryopathy. In addition to elevated oxidative stress, pregestational diabetes may alter maternal/fetal microRNA profiles, leading to the pathogenesis of CHDs.<sup>4,5</sup> Recent clinical data indicates that miR-122 is elevated in patients with impaired glucose tolerance, insulin resistance and obesity, and is a biomarker for cardiovascular disease.<sup>6-9</sup> In **Chapter 4**, I studied the role of miR-122 in the pathogenesis of pregestational diabetes-induced CHDs. To achieve this goal, we implemented *ex vivo* and *in vivo* experimental approaches to determine the effect of miR-122 on heart development, and anti-miR-122 pharmacotherapy on mitigating diabetes-induced CHDs in mice. Along with confirming higher levels of miR-122 in E12.5 hearts from diabetic dams, an upregulation of primary-miR-122 was also noted. As miR-122 functions to inhibit the expression of mRNA transcripts, the levels of key cardiogenic targets of miR-122 were examined by

qPCR. Genes critical for cell cycle progression, angiogenesis, and heart development, such as *Cyclin D1*, *Snail1*, *Gata4* and *Hand2*, were downregulated in normal E10.5 hearts transfected with miR-122. Antagonism using antimiR-122 to hearts cultured in high glucose media restored normal expression of these genes. Furthermore, transfection of miR-122 to heart explants inhibited cell proliferation, increased apoptosis and inhibited epicardial EMT, to the same level as explants exposed to high glucose levels. The high glucose-induced deregulation of these cellular processes was prevented by antimiR-122 transfection. Since these experiments suggest that elevated levels of miR-122 disturb key process of cardiac development, *in vivo* administration of antimiR-122 was tested for its effects on pregestational diabetes-induced CHDs. To this end, diabetes was induced in female C57BL/6 female mice using the same method as in **Chapter 2** and **3**; however, prior to breeding, diabetic mice were administered 10 mg/kg LNA antimiR-122 or scramble control, subcutaneously. Another dose was injected at E7.5, and heart morphology was examined at E18.5 following fetal echocardiography. The blood glucose levels of diabetic dams increased progressively throughout gestation, and neither LNA treatment had any effect on glycemic levels. An equal number of males and female offspring from scramble LNA-treated diabetic dams had CHDs, and antimiR-122 treatment was more effective in reducing the incidence of CHDs in male offspring. No significant changes in offspring litter size was noted between groups. Further, antimiR-122 treatment prevented cardiac dysfunction, measured through M-Mode analysis of LV ejection fraction and fractional shortening, in offspring of diabetic dams. A spectrum of CHDs was observed in offspring of scramble LNA-treated diabetic mice, which were consistent with the malformations observed in **Chapter 2**. In fact, the total ratio of

abnormal fetal hearts was stable, upwards of 50%, between this thesis and previous studies using the same model of pregestational diabetes.<sup>10</sup> Notably, the incidence of CHDs in the offspring of diabetic dams was reduced from 55.6% to 23.0% by antimiR-122 administration. Overall, this study is the first to reveal the role of miR-122 in the pathogenesis of pregestational diabetes-induced CHDs, and demonstrates the efficacy of *in vivo* antimiR-122 treatment at reducing the incidence of these cardiac malformations.

In summary, the results of this thesis highlight the potential protective effects of sapropterin and antimiR-122 treatment against pregestational diabetes-induced CHDs. We show that daily sapropterin therapy to diabetic dams inhibits oxidative stress and eNOS dysfunction in the embryonic heart, which regulates cardiogenic gene expression. This normalized impairment in cell proliferation and epicardial EMT, leading to normal heart and coronary artery development. Additionally, we showed that the incidence of CHDs in offspring of diabetic dams could be reduced via a miRNA-mediated mechanism. By relieving the repression of targets of miR-122, antimiR-122 treatment restored cellular processes of cell proliferation, apoptosis and epicardial EMT to normal levels, reducing the incidence of CHDs. A summary of findings from these studies is illustrated in **Figure 5.1**.

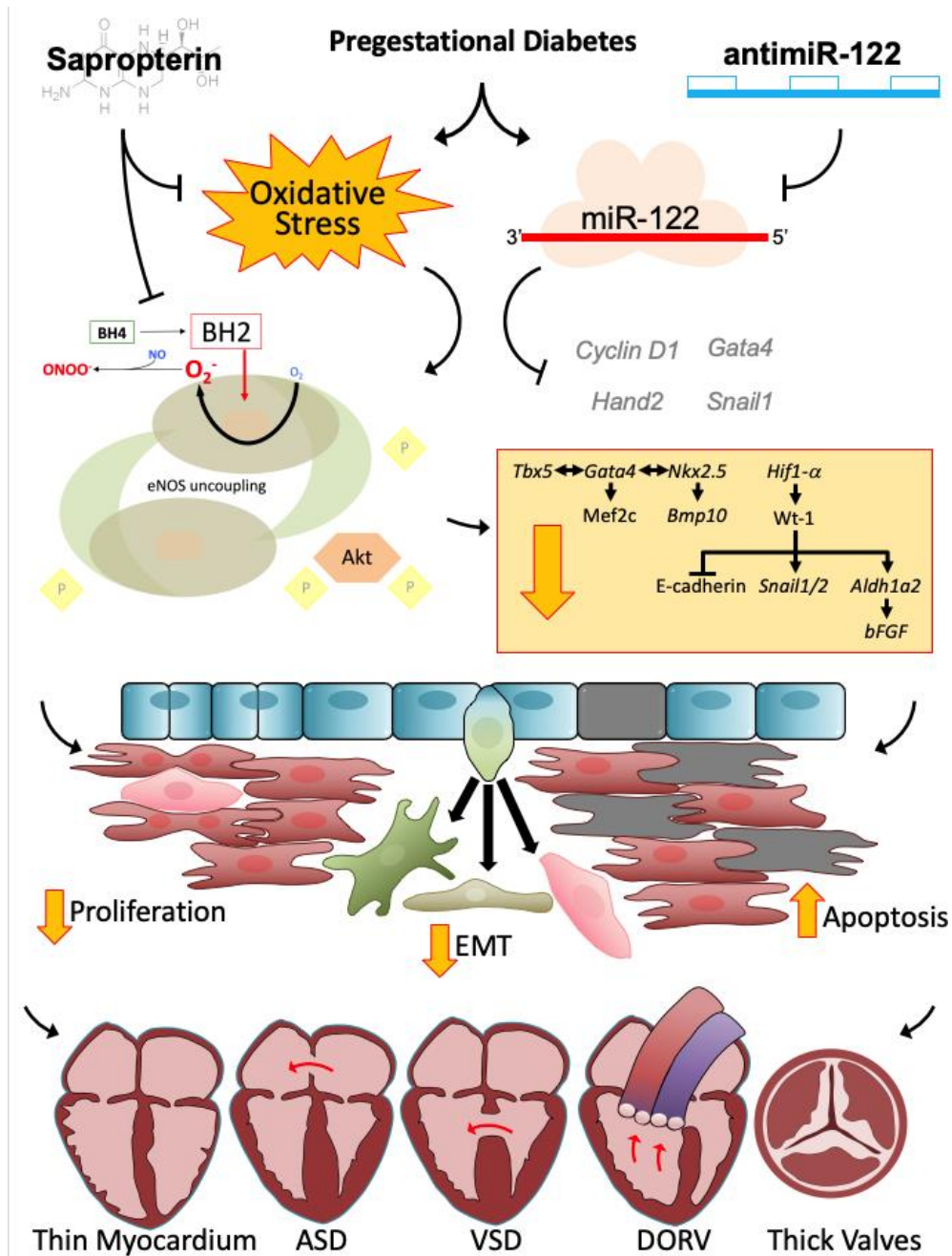


**Figure 5.1. The role of eNOS uncoupling/oxidative stress and miR-122 in the pathogenesis of pregestational diabetes-induced congenital heart defects.**

Pregestational diabetes leads to a concurrent increase in oxidative stress and miR-122 in the embryonic heart. This brings about eNOS uncoupling, leading to a reduction in many critical factors. Cell proliferation, apoptosis, and epicardial EMT are perturbed, and lead to CHDs. Treatment with sapropterin or antimiR-122 reduces the incidence of these malformations by regulating heart development, albeit through different mechanisms.

## 5.2 Study Limitations

### 5.2.1 Justification of a Mouse Model of Pregestational Diabetes

Diabetes is a global health issue with a rapidly increasing prevalence, and is estimated to affect 693 million people by 2040.<sup>11</sup> Currently, 40% of women with diabetes are of reproductive age.<sup>12</sup> T1D is characterized by autoimmune destruction of pancreatic  $\beta$ -cells, resulting in a lack of insulin production; whereas, T2D is the result of insulin resistance and usually has a later onset, but is much more prevalent.<sup>13</sup> Biomedical research utilizes various experimental approaches to study diabetes. In animal models, diabetes can be induced via many techniques, including diet, drugs, surgery, or genetic alterations. A common, established method for the generation of a T1D model in rodents is STZ administration.<sup>14, 15</sup> This chemical agent is a glucose analogue, which is taken up by pancreatic  $\beta$ -cells via the glucose transporter 2 (GLUT2). STZ within the cell causes DNA damage, oxidative stress, and ultimately results in cell death.<sup>16</sup> This depletion of pancreatic  $\beta$ -cells and thereby insulin supply recapitulates T1D in humans. A benefit of using this model of diabetes is the relatively quick induction period, taking approximately 7 days for the onset of hyperglycemia. In addition, this method is fairly cost-effective, and requires a simple high dose or multiple low doses of intraperitoneal injections. However, a drawback to this approach remains the potential off-target effects of STZ, such as carcinogenesis.<sup>17</sup> Nevertheless, as seen in **Chapters 2 and 3**, insulin administration to STZ-induced diabetic dams did not result in CHDs or CAMs, suggesting that STZ does not impose any teratogenic effects on the heart. Another limitation of this model is that clinically, most women with pregestational diabetes are insulin resistant, meaning they have T2D.<sup>12</sup> The pathogenesis of T2D has environmental

and lifestyle components, altering a patient's metabolism.<sup>13</sup> Although a T2D model may be more clinically relevant, effectively reproducing it without confounding variables, such as a high-fat diet or genetic modifications, remains difficult. In fact, previous experiments done in our lab indicate that mice on a prolonged period of high-fat diet rarely reach hyperglycemic levels needed to induce CHDs in their offspring. While T1D and T2D have systemic physiological differences, in this study, elevated levels of blood glucose was regarded as the primary factor behind diabetic embryopathy.<sup>18</sup> Importantly, in the clinic, both types of diabetes in women confer an equal risk of having a child with a CHD.<sup>19</sup> Therefore, by using a STZ-induced model of pregestational diabetes in this thesis, a consistently high rate of CHDs and CAMs were noted, which enabled testing the efficacy of two pharmacotherapies.

## 5.2.2 Genetically Altered Mice

Mice represent a practical and appropriate model organism to study physiological concepts, understand human diseases, and develop potential therapies. Embryonic heart development and the genetic and molecular mechanisms leading to congenital heart disease in humans, have been extensively studied using mouse models.<sup>20</sup> Cardiac anatomy and developmental pathways are very similar between humans and mice.<sup>21</sup> Sequencing of the mouse genome revealed approximately 99% homology of genes to the human genome.<sup>22</sup> In addition, manipulation of the mouse genome is relatively simple, even more so now with the advances in CRISPR technology, allowing for endless possibilities in studying development and disease. One of these genetic engineering technologies utilized in **Chapter 2** of this thesis was the Cre/loxP system, which enabled lineage tracing of SHF cardiac progenitors.<sup>23</sup> Specifically, we used the anterior SHF-



specific *Mef2c-Cre* transgenic mouse and the global double fluorescent *Cre* reporter line *Rosa26<sup>mTmG</sup>* to trace and characterize the development of SHF-derived cardiac structures, broadening our knowledge of heart development under pregestational diabetes.<sup>24</sup> Along with the many benefits of using this technology, some possible limitations of the Cre/loxP system exist. The insertion of the Cre recombinase gene or the lox P sites into the mouse genome could alter expression of surrounding genes.<sup>25</sup> In addition, endonuclease activity of Cre recombinase can have toxic effects.<sup>26</sup> Although driven by a tissue-specific promoter, the expression of Cre can occur in unwanted tissues. For instance, in lineage tracing experiments, all descendants of the original cell expressing Cre will be labeled with the reporter. Moreover, the *Mef2c-Cre* transgene is considered a “leaky” Cre, as mesodermal cells in other organs can also be labeled. In fact, in these mice, full body expression of Cre recombinase has been noted when this transgene is inherited via females. To mitigate this, the *Mef2c-Cre* transgene remained on a single allele and was inherited as a single copy in male mice.<sup>27</sup> In spite of the drawbacks, the ability to lineage trace the SHF using the Cre/loxP system in this thesis demonstrated a specific insult of diabetic pregnancy to SHF progenitors, directly contributing to the septal and OFT defects in fetal mice.

### 5.2.3 Use of *ex vivo* Organ Culture Systems

In **Chapters 3** and **4** of this thesis, embryonic hearts were explanted and grown *ex vivo* to delineate the effects of high glucose, tetrahydrobiopterin (BH4), miR-122 or antimiR-122 on many parameters intimately linked to heart development. Specifically, in **Chapter 3**, E12.5 heart ventricles from control dams were isolated in sterile conditions and explanted onto a collagen matrix to study epicardial EMT and migration of

epicardial-derived cells (EPDCs). This enabled us to determine the migratory capacity of coronary artery progenitors under conditions of high glucose and when exposed to BH<sub>4</sub>, providing support to our immunohistological data *in vivo*. Similarly, in **Chapter 4**, this EMT assay was performed; however, in addition to simulating a diabetic pregnancy *ex vivo* with high glucose, miR-122 and anti-miR-122 were transfected into these explants. In addition, E10.5 hearts from non-diabetic dams were explanted onto plastic and exposed to the above conditions for gene expression, cell proliferation and cell death analysis. Limitations exist with using these types of organ culture systems. For instance, in the embryo, blood vessels supply cardiac progenitors with continuous nourishment and remove cellular waste products. This is not matched in experimental conditions as growing heart explants on top of a collagen matrix or plastic well does not effectively replicate the *in vivo* environment of the cells, and could result in an altered response. In addition, the biomechanical forces within the live embryo, including the shear stress on cells by blood flow, cannot be simulated in this *ex vivo* setting. Finally, in **Chapter 4**, miR-122 or anti-miR-122 were delivered to embryonic heart explants using the JetPrime transfection reagent and buffer system. Although considered generally less toxic and more efficient method of delivery compared to electroporation, sonoporation or viral transduction, the incubation time and ratio of nucleic acid to transfection reagent must be carefully optimized. Despite these drawbacks, employing this organ culture system was critical to advance our understanding on the impact of high glucose, BH<sub>4</sub>, and miR-122 on embryonic cardiovascular development, and support our *in vivo* findings.

### 5.3 Suggestions for Future Studies

This thesis investigated the pathogenesis of congenital abnormalities of the heart induced by pregestational maternal diabetes. We tested two clinically relevant pharmacotherapies and elucidated developmental pathways leading to a spectrum of cardiac and coronary artery defects. However, further research is warranted regarding the effects of sapropterin and antimiR-122 on diabetic embryopathy.

All three chapters of this thesis investigate a model of T1D in mice. Indeed, both pregestational T1D and T2D diabetes in patients induce CHDs in newborns.<sup>19</sup> However, T2D is more prevalent in the population, encompassing 90-95% of cases, and can be brought about by environmental factors, such as obesity, which can also impact fetal heart development.<sup>13</sup> Future animal studies should try to model T2D and its metabolic complications, while testing therapeutics like sapropterin and antimiR-122 on fetal cardiovascular malformations. The FDA-approved drug sapropterin (Kuvan ®) has an acceptable safety rating and with very minor adverse effects, and represents a viable option for pregnancies affected with T2D.<sup>28</sup>

This thesis examined the impact of two distinct treatments on diabetes-induced CHDs. Sapropterin and antimiR-122 decreased the incidence of CHDs from 59.4% to 26.5%, and from 55.6% to 23.0%, respectively. As such, neither therapy had complete penetrance at preventing cardiac malformations. Although sapropterin prevented all major CHDs, such as AVSD, VSD, and DORV, minor defects like ASD, valve thickening and ventricle thinning were still present. Since sapropterin and antimiR-122 function via distinct mechanisms on mitigating perturbations in heart development, as

demonstrated in this thesis, a combination of both agents may further reduce the incidence of CHDs and should be examined in future studies. Correspondingly, previous studies in the same model of diabetes have demonstrated the beneficial effects of N-acetylcysteine (NAC) and maternal exercise on reducing the incidence of these defects by maintaining the oxidative balance within the embryonic heart.<sup>10, 29</sup> Future studies should test attenuating elevations in oxidative stress and miR-122 by sapropterin, NAC or maternal exercise, and antimiR-122 together, and investigate possible synergistic effects at preventing CHDs induced by pregestational diabetes.

In **Chapter 2**, I performed lineage tracing experiments to map SHF progenitors using the anterior SHF-specific *Mef2c-Cre* transgenic mouse, as many of the CHDs present at birth were in structures originating from the SHF. All SHF-derived cells and structures were GFP<sup>+</sup> and therefore easily identifiable, and our findings indicated a specific insult of diabetic pregnancy on these progenitors, which could account for the septal and OFT defects. However, the impact of sapropterin treatment on this group of cells in particular was not examined, and should be tested in future studies. Conversely, in **Chapter 3**, we observed pregestational diabetes-induced CAMs and demonstrated a deficiency in epicardial EMT as a causal factor, reversed by sapropterin treatment. Indeed, coronary artery progenitors delaminate from the epicardium via EMT and migrate into the myocardium where they differentiate into vascular smooth muscle cells and fibroblasts, forming vessels.<sup>2</sup> However, lineage tracing experiments confirm that the sinus venosus and endocardium also contribute to the formation of these arteries.<sup>30</sup> In fact, the majority of the coronary arteries that perfuse the septum are endocardial-derived.<sup>30</sup> Future studies should employ lineage tracing using the *Apj-CreER* and the

*Nfatc1-Cre* transgenic mice to map sinus venous and endocardial contributions to coronary arteries in the embryonic heart from diabetic dams, respectively.<sup>30</sup> This analysis should be conducted with both sapropterin and antimiR-122 treatment. In **Chapter 4**, antimiR-122 is effective at restoring epicardial derived cell (EPDC) outgrowth and number *ex vivo*, however the efficacy of antimiR-122 treatment at reducing the incidence of CAMs should also be defined *in vivo*.

Cardiac and coronary artery malformations were the focus of this thesis. However, in **Chapter 2**, one extra-cardiac defect, exencephaly, was reported. It has been well documented that along with CHDs, neural tube defects in the offspring can result from gestational hyperglycemia.<sup>31-33</sup> In fact, a study using a similar model of STZ-induced diabetes noted a 3-fold increase in offspring neural tube defects in comparison to our study.<sup>32</sup> The pathogenesis of these defects may differ from CHDs; however, sapropterin or antimiR-122 therapy should be tested on the formation of cranial structures during diabetic pregnancy. Similarly, in **Chapter 3**, the development of the coronary vasculature was analyzed; however, pregestational diabetes may have consequences on vessel development in other parts of the body. Mouse models of maternal diabetes have demonstrated hyperglycemia-induced vasculopathy in the yolk sac, with specific insult to vascular endothelial cells by oxidative stress.<sup>34</sup> Although the role of eNOS has not been explored in these studies, sapropterin therapy may have potential in mitigating these vascular abnormalities.

Additionally, in **Chapter 4**, I demonstrated that *in vivo* treatment with antimiR-122 reduced the incidence of CHDs in pregestational diabetes. This study utilized a pharmacological approach to correct a genetic irregularity. It would be of particular

interest to also determine if conditional knockout of miR-122 in the developing heart can reduce the incidence of CHDs induced by pregestational diabetes to the same extent. Using the Cre/loxP system, a floxed miR-122 could be excised by Cre recombinase in the diabetic embryonic heart driven by the cardiac-specific Nkx2.5 promoter. A complete knockout of miR-122 would not be ideal as it is necessary for liver homeostasis and could result in hepatocellular carcinoma.<sup>35</sup> Finally, as discussed before, a T2D model may have greater relevance, especially as an extension of **Chapter 4**. In patients with obesity, insulin resistance, and diabetic retinopathy, elevated circulating levels of miR-122 have been reported.<sup>6-9, 36</sup> Therefore, plasma levels of miR-122 should be analyzed in both a T2D and STZ-induced model of diabetes. In addition, plasma samples from diabetic patients should be analyzed to confirm reported findings. As miR-122 plays an important role in cholesterol and fatty acid metabolism in the liver, and is a potential prognostic marker for adult cardiovascular disease, elucidating its deregulation in diabetes is imperative.<sup>37-40</sup>

## 5.4 Conclusion

This thesis provides evidence for the critical roles of oxidative stress, eNOS and miR-122 in heart and coronary artery development in a mouse model of pregestational diabetes. Here, I demonstrate for the first time that pregestational diabetes impairs eNOS coupling and elevates levels of oxidative stress and miR-122, leading to functional and morphological cardiovascular anomalies in the offspring of diabetic dams. These malformations range in severity, and include ASDs, VSDs, OFT defects, ventricular myocardium defects, and hypoplastic coronary arteries. Additionally, I have shown that deficits in cardiogenic gene expression, enzyme activity, cell proliferation, and epicardial

EMT, induced by pregestational diabetes, contribute to the development of these defects. Importantly, this thesis exhibits the efficacy of two clinically relevant pharmacotherapies at regulating heart development disturbed by diabetic pregnancy. Treatment with sapropterin (BH<sub>4</sub>), a cofactor of eNOS, or antimiR-122 reestablishes normal cardiovascular development and reduces the incidence of pregestational diabetes-induced CHDs in mice. These results suggest that sapropterin and antimiR-122 may have therapeutic potential in preventing CHDs in children of women with pregestational diabetes.

## 5.5 References

1. Oyen N, Diaz LJ, Leirgul E, Boyd HA, Priest J, Mathiesen ER, Quertermous T, Wohlfahrt J and Melbye M. Prepregnancy Diabetes and Offspring Risk of Congenital Heart Disease: A Nationwide Cohort Study. *Circulation*. 2016;133:2243-53.
2. Tian X, Pu WT and Zhou B. Cellular origin and developmental program of coronary angiogenesis. *Circ Res*. 2015;116:515-30.
3. von Gise A and Pu WT. Endocardial and epicardial epithelial to mesenchymal transitions in heart development and disease. *Circ Res*. 2012;110:1628-45.
4. Liu Y, Lu X, Xiang FL, Poelmann RE, Gittenberger-de Groot AC, Robbins J and Feng Q. Nitric oxide synthase-3 deficiency results in hypoplastic coronary arteries and postnatal myocardial infarction. *Eur Heart J*. 2014;35:920-31.
5. Lock MC, Botting KJ, Tellam RL, Brooks D and Morrison JL. Adverse Intrauterine Environment and Cardiac miRNA Expression. *Int J Mol Sci*. 2017;18.
6. Ibarra A, Vega-Guedes B, Brito-Casillas Y and Wagner AM. Diabetes in Pregnancy and MicroRNAs: Promises and Limitations in Their Clinical Application. *Noncoding RNA*. 2018;4.
7. de Candia P, Spinetti G, Specchia C, Sangalli E, La Sala L, Uccellatore A, Lupini S, Genovese S, Matarese G and Ceriello A. A unique plasma microRNA profile defines type 2 diabetes progression. *PLoS one*. 2017;12:e0188980.
8. Jones A, Danielson KM, Benton MC, Ziegler O, Shah R, Stubbs RS, Das S and Macartney-Coxson D. miRNA Signatures of Insulin Resistance in Obesity. *Obesity (Silver Spring)*. 2017;25:1734-1744.
9. Ortega FJ, Mercader JM, Catalan V, Moreno-Navarrete JM, Pueyo N, Sabater M, Gomez-Ambrosi J, Anglada R, Fernandez-Formoso JA, Ricart W, Fruhbeck G and Fernandez-Real JM. Targeting the circulating microRNA signature of obesity. *Clin Chem*. 2013;59:781-92.
10. Pastukh N, Meerson A, Kalish D, Jabaly H and Blum A. Serum miR-122 levels correlate with diabetic retinopathy. *Clin Exp Med*. 2019;19:255-260.
11. Moazzen H, Lu X, Ma NL, Velenosi TJ, Urquhart BL, Wisse LJ, Gittenberger-de Groot AC and Feng Q. N-Acetylcysteine prevents congenital heart defects induced by pregestational diabetes. *Cardiovasc Diabetol*. 2014;13:46.
12. Cho NH, Shaw JE, Karuranga S, Huang Y, da Rocha Fernandes JD, Ohlrogge AW and Malanda B. IDF Diabetes Atlas: Global estimates of diabetes prevalence for 2017 and projections for 2045. *Diabetes Res Clin Pract*. 2018;138:271-281.



13. Rezai S, LoBue S and Henderson CE. Diabetes prevention: Reproductive age women affected by insulin resistance. *Womens Health (Lond)*. 2016;12:427-32.
14. Olokoba AB, Obateru OA and Olokoba LB. Type 2 diabetes mellitus: a review of current trends. *Oman Med J*. 2012;27:269-73.
15. Mansford KR and Opie L. Comparison of metabolic abnormalities in diabetes mellitus induced by streptozotocin or by alloxan. *Lancet*. 1968;1:670-1.
16. Graham ML, Janecek JL, Kittredge JA, Hering BJ and Schuurman HJ. The streptozotocin-induced diabetic nude mouse model: differences between animals from different sources. *Comp Med*. 2011;61:356-60.
17. Szkudelski T. The mechanism of alloxan and streptozotocin action in B cells of the rat pancreas. *Physiol Res*. 2001;50:537-46.
18. Cojocel C, Novotny L, Vachalkova A and Knauf B. Comparison of the carcinogenic potential of streptozotocin by polarography and alkaline elution. *Neoplasma*. 2003;50:110-6.
19. Eriksson UJ and Wentzel P. The status of diabetic embryopathy. *Ups J Med Sci*. 2016;121:96-112.
20. Liu S, Joseph KS, Lisonkova S, Rouleau J, Van den Hof M, Sauve R, Kramer MS and Canadian Perinatal Surveillance S. Association between maternal chronic conditions and congenital heart defects: a population-based cohort study. *Circulation*. 2013;128:583-9.
21. Krishnan A, Samtani R, Dhanantwari P, Lee E, Yamada S, Shiota K, Donofrio MT, Leatherbury L and Lo CW. A detailed comparison of mouse and human cardiac development. *Pediatr Res*. 2014;76:500-7.
22. Wessels A and Sedmera D. Developmental anatomy of the heart: a tale of mice and man. *Physiol Genomics*. 2003;15:165-76.
23. Mouse Genome Sequencing Centre, Waterston RH, Lindblad-Toh K, Birney E, Rogers J, Abril JF, Agarwal P, Agarwala R, Ainscough R, *et al*. Initial sequencing and comparative analysis of the mouse genome. *Nature*. 2002;420:520-62.
24. Doetschman T and Azhar M. Cardiac-specific inducible and conditional gene targeting in mice. *Circ Res*. 2012;110:1498-512.
25. Barnes RM, Harris IS, Jaehnig EJ, Sauls K, Sinha T, Rojas A, Schachterle W, McCulley DJ, Norris RA and Black BL. MEF2C regulates outflow tract alignment and transcriptional control of Tdgf1. *Development*. 2016;143:774-9.

26. Schmidt EE, Taylor DS, Prigge JR, Barnett S and Capecchi MR. Illegitimate Cre-dependent chromosome rearrangements in transgenic mouse spermatids. *Proc Natl Acad Sci U S A*. 2000;97:13702-7.
27. Naiche LA and Papaioannou VE. Cre activity causes widespread apoptosis and lethal anemia during embryonic development. *Genesis*. 2007;45:768-75.
28. Leung C, Lu X, Liu M and Feng Q. Rac1 signaling is critical to cardiomyocyte polarity and embryonic heart development. *J Am Heart Assoc*. 2014;3:e001271.
29. Qu J, Yang T, Wang E, Li M, Chen C, Ma L, Zhou Y and Cui Y. Efficacy and safety of sapropterin dihydrochloride in patients with phenylketonuria: A meta-analysis of randomized controlled trials. *Br J Clin Pharmacol*. 2019;85:893-899.
30. Moazzen H, Lu X, Liu M and Feng Q. Pregestational diabetes induces fetal coronary artery malformation via reactive oxygen species signaling. *Diabetes*. 2015;64:1431-43.
31. Chen HI, Sharma B, Akerberg BN, Numi HJ, Kivela R, Saharinen P, Aghajanian H, McKay AS, Bogard PE, Chang AH, Jacobs AH, Epstein JA, Stankunas K, Alitalo K and Red-Horse K. The sinus venosus contributes to coronary vasculature through VEGFC-stimulated angiogenesis. *Development*. 2014;141:4500-12.
32. Salbaum JM and Kappen C. Neural tube defect genes and maternal diabetes during pregnancy. *Birth Defects Res A Clin Mol Teratol*. 2010;88:601-11.
33. Phelan SA, Ito M and Loeken MR. Neural tube defects in embryos of diabetic mice: role of the Pax-3 gene and apoptosis. *Diabetes*. 1997;46:1189-97.
34. Pani L, Horal M and Loeken MR. Polymorphic susceptibility to the molecular causes of neural tube defects during diabetic embryopathy. *Diabetes*. 2002;51:2871-4.
35. Dong D, Reece EA, Lin X, Wu Y, AriasVilella N and Yang P. New development of the yolk sac theory in diabetic embryopathy: molecular mechanism and link to structural birth defects. *Am J Obstet Gynecol*. 2016;214:192-202.
36. Hsu SH, Wang B, Kutay H, Bid H, Shreve J, Zhang X, Costinean S, Bratasz A, Houghton P and Ghoshal K. Hepatic loss of miR-122 predisposes mice to hepatobiliary cyst and hepatocellular carcinoma upon diethylnitrosamine exposure. *Am J Pathol*. 2013;183:1719-1730.
37. Prats-Puig A, Ortega FJ, Mercader JM, Moreno-Navarrete JM, Moreno M, Bonet N, Ricart W, Lopez-Bermejo A and Fernandez-Real JM. Changes in circulating microRNAs are associated with childhood obesity. *J Clin Endocrinol Metab*. 2013;98:E1655-60.

38. D'Alessandra Y, Devanna P, Limana F, Straino S, Di Carlo A, Brambilla PG, Rubino M, Carena MC, Spazzafumo L, De Simone M, Micheli B, Biglioli P, Achilli F, Martelli F, Maggiolini S, Marenzi G, Pompilio G and Capogrossi MC. Circulating microRNAs are new and sensitive biomarkers of myocardial infarction. *Eur Heart J*. 2010;31:2765-73.
39. Wang YL and Yu W. Association of circulating microRNA-122 with presence and severity of atherosclerotic lesions. *PeerJ*. 2018;6:e5218.
40. Cortez-Dias N, Costa MC, Carrilho-Ferreira P, Silva D, Jorge C, Calisto C, Pessoa T, Robalo Martins S, de Sousa JC, da Silva PC, Fiuza M, Diogo AN, Pinto FJ and Enguita FJ. Circulating miR-122-5p/miR-133b Ratio Is a Specific Early Prognostic Biomarker in Acute Myocardial Infarction. *Circ J*. 2016;80:2183-91.
41. Tsai WC, Hsu SD, Hsu CS, Lai TC, Chen SJ, Shen R, Huang Y, Chen HC, Lee CH, Tsai TF, Hsu MT, Wu JC, Huang HD, Shiao MS, Hsiao M and Tsou AP. MicroRNA-122 plays a critical role in liver homeostasis and hepatocarcinogenesis. *J Clin Invest*. 2012;122:2884-97.

# Appendix

**Qingping Feng**

---

**From:** eSirius3GWebServer <esirius3g@uwo.ca>  
**Sent:** Thursday, November 1, 2018 9:02 AM  
**To:** Qingping Feng; Animal Care Committee  
**Subject:** eSirius3G Notification -- 2016-099 Annual Renewal Approved



2016-099:8:

**AUP Number:** 2016-099  
**AUP Title:** Modulation of Myocardial Function in Myocardial Infarction, Sepsis and Diabetes  
**Yearly Renewal Date:** 11/01/2019

**The YEARLY RENEWAL to Animal Use Protocol (AUP) 2016-099 has been approved by the Animal Care Committee (ACC), and will be approved through to the above review date.**

Please at this time review your AUP with your research team to ensure full understanding by everyone listed within this AUP.

As per your declaration within this approved AUP, you are obligated to ensure that:

- 1) Animals used in this research project will be cared for in alignment with:
  - a) Western's Senate MAPPs 7.12, 7.10, and 7.15  
[http://www.uwo.ca/univsec/policies\\_procedures/research.html](http://www.uwo.ca/univsec/policies_procedures/research.html)
  - b) University Council on Animal Care Policies and related Animal Care Committee procedures

[http://uwo.ca/research/services/animalethics/animal\\_care\\_and\\_use\\_policies.html](http://uwo.ca/research/services/animalethics/animal_care_and_use_policies.html)

- 2) As per UCAC's Animal Use Protocols Policy,
  - a) this AUP accurately represents intended animal use;
  - b) external approvals associated with this AUP, including permits and scientific/departmental peer approvals, are complete and accurate;
  - c) any divergence from this AUP will not be undertaken until the related Protocol Modification is approved by the ACC; and
  - d) AUP form submissions - Annual Protocol Renewals and Full AUP Renewals - will be submitted

and attended to within timeframes outlined by the ACC.

[http://uwo.ca/research/services/animalethics/animal\\_use\\_protocols.html](http://uwo.ca/research/services/animalethics/animal_use_protocols.html)

- 3) As per MAPP 7.10 all individuals listed within this AUP as having any hands-on animal contact will

- a) be made familiar with and have direct access to this AUP;
- b) complete all required CCAC mandatory training ([\\_training@uwo.ca](mailto:_training@uwo.ca)); and
- c) be overseen by me to ensure appropriate care and use of animals.

- 4) As per MAPP 7.15,

- a) Practice will align with approved AUP elements;
- b) Unrestricted access to all animal areas will be given to ACVS Veterinarians

and ACC Leaders;

- c) UCAC policies and related ACC procedures will be followed, including but not

limited to:

- i) Research Animal Procurement
- ii) Animal Care and Use Records

iii) Sick Animal Response  
iv) Continuing Care Visits  
5) As per institutional OH&S policies, all individuals listed within this AUP who will be using or potentially exposed to hazardous materials will have completed in advance the appropriate institutional OH&S training, facility-level training, and reviewed related (M)SDS Sheets, <http://www.uwo.ca/hr/learning/required/index.htm>

Submitted by: Copeman, Laura  
on behalf of the Animal Care Committee  
University Council on Animal Care



Western Ontario  
Council on Animal Care

The University of  
Animal Care Committee / University

London, Ontario Canada

N6A 5C1  
519-661-2028

519-661-2111 x 88792 Fax

[auspc@uwo.ca](mailto:auspc@uwo.ca)  
<http://www.uwo.ca/research/services/animalethics/index.html>

\*\*\* THIS IS AN EMAIL NOTIFICATION ONLY. PLEASE DO NOT REPLY \*\*\*

# Curriculum Vitae

## Anish Engineer

---

### Post-secondary Education and Degrees

---

- PhD in Physiology and Pharmacology and Developmental Biology (PhD. 2019)**  
 The University of Western Ontario, (London, Ontario)  
 Schulich School of Medicine and Dentistry  
 Supervisor: Dr. Qingping Feng, MD/PhD.  
 Thesis Title: *Pregestational Diabetes Induced Congenital Heart Defects and Coronary Artery Malformations: Mechanisms and Preventative Therapies*
- Bachelors of Medical Sciences (BMSc. 2014)**  
**Honors Specialization in Medical Sciences, Minor in Pharmacology**  
 The University of Western Ontario, (London, Ontario)  
 Schulich School of Medicine and Dentistry

---

### Publications

---

- 2019 **Sapropterin reduces coronary artery malformation in offspring of pregestational diabetes mice.** Submitted to *Nitric Oxide* NOX\_2019\_137  
 A Engineer, YJ Lim, X Lu, K Norozi, Q Feng
- 2019 **Maternal voluntary exercise mitigates oxidative stress and incidence of congenital heart defects in pre-gestational diabetes.** Published in *Journal of Cellular and Molecular Medicine* DOI: 10.1111/jcmm.14439  
 T Saiyin, A Engineer, ER Greco, MY Kim, X Lu, DL Jones, Q Feng
- 2019 **The role of submaximal exercise-induced skeletal muscle remodeling in HFREF patients.** Published in *Journal of Physiology* 2019 Feb;597(3):669-671  
 A Engineer, S Albers, A Kucey
- 2018 **Sapropterin treatment prevents congenital heart defects induced by pregestational diabetes in mice.** Published in *Journal of the American Heart Association* 2018 Nov 6;7(21):e009624  
 A Engineer, T Saiyin, X Lu, A Kucey, B Urquhart, T Drysdale, K Norozi, Q Feng
- 2018 **MiRAR-miRNA activity reporter for living cells.**  
 Published in *Genes (Basel)* 2018;9(6)  
 M Turk, C Chung, E Manni, S Zukowski, A Engineer, Y Badakhshi, Y Bi, I Heinemann

---

### Honours and Awards

---

- 2019 **Canadian Society of Pharmacology & Therapeutics (CSPT) Publication Award**  
 Awarded by CSPT for outstanding first author publication in 2018 \$ 500.00 (CAD)
- 2019 **Lucille & Norton Wolf London Health Research Day Trainee Publication Award**  
 Awarded by the Bernard & Norton Wolf Family Foundation for outstanding first author publication \$ 1000.00 (CAD)

- 2019 **Collaborative Specialization in Developmental Biology Travel Bursary**  
Awarded for travel to the Canadian National Perinatal Research Meeting \$ 500.00
- 2018 **Canadian Institutes of Health Research (CIHR) Travel Award**  
Awarded by CIHR & Institute of Circulatory and Respiratory Health \$ 966.00 (CAD)
- 2018 **Canadian Society of Pharmacology and Therapeutics (CSPT) Travel Bursary**  
Awarded by CSPT and Department of Physiology & Pharmacology \$ 350.00 (CAD)
- 2017 **Children's Health Research Institute (CHRI) Travel Award**  
Awarded by the CHRI Trainee Travel Fund \$ 750.00 (CAD)
- 2017 **Canadian Student Health Research Forum (CSHRF) Gold Prize for Best Poster Presentation**  
Awarded by the Canadian Institutes of Health Research (CIHR), competition held at The University of Manitoba, Winnipeg, Manitoba. \$500.00 (CAD)
- 2017 **Malcolm Arnold Presentation Award in Cardiovascular Sciences**  
Awarded by the Department of Physiology and Pharmacology \$ 200.00 (CAD)
- 2017 **Canadian Nitric Oxide Society Best Oral Presentation (2<sup>nd</sup> Place)**  
Competition held at The University of Windsor \$150.00 (CAD)
- 2017 **Physiology and Pharmacology Graduate Student Council Leadership Award**  
Awarded by the Department of Physiology and Pharmacology \$ 400.00 (CAD)
- 2016 **Queen Elizabeth II Graduate Scholarship in Science and Technology**  
Awarded by the Ministry of Training, Colleges and Universities \$ 15, 000.00 (CAD)
- 2016 **Pediatric Research Day First Prize Best Oral Presentation**  
Children's Health Research Institute \$100.00 (CAD)
- 2015 **6<sup>th</sup> Annual Diabetes Research Day First Prize Best Poster Presentation**  
Lawson Health Research Institute \$300.00 (CAD)
- 2015 **Department of Physiology and Pharmacology Annual Research Day First Place in the Developmental Biology Category**  
Schulich School of Medicine and Dentistry \$250.00 (CAD)
- 2014–  
*present* **Western Graduate Research Scholarship**  
The University of Western Ontario \$ 4, 500.00 (CAD)
- 2015 **Sanofi Biogenius Challenge – 1<sup>st</sup> Place Poster and 2<sup>nd</sup> Place Oral Presentation**  
Recipients: Mella Kim and Anish Engineer
- 2010–  
2014 **Dean's Honor List – Every year of undergraduate education**  
The University of Western Ontario
- 2010 **The Western Scholarship of Excellence**  
The University of Western Ontario \$2, 000.00 (CAD)

---

 Academic Conferences and Presentations
 

---

- 2019 **Canadian National Perinatal Research Meeting – Plenary Lecture**  
 “The Role of microRNA-122 in Pregestational Diabetes-Induced Congenital Heart Defects” (Mont-Tremblant, Quebec)
- 2019 **London Health Research Day – Selected Poster Presentation**  
 “The Role of microRNA-122 in Pregestational Diabetes-Induced Congenital Heart Defects” (London, Ontario)
- 2018 **Canadian Society of Pharmacology and Therapeutics – Selected Oral Presentation**  
 “Tetrahydrobiopterin Prevents Coronary Artery Malformations Induced by Pregestational Diabetes” (Toronto, Ontario)
- 2018 **Experimental Biology 2018 – Poster Presentation**, American Physiological Association  
 “Tetrahydrobiopterin Prevents Coronary Artery Malformations Induced by Pregestational Diabetes” (San Diego, California)
- 2018 **London Health Research Day – Selected Poster Presentation**  
 “The Role of microRNA-122 in Pregestational Diabetes-Induced Congenital Heart Defects” (London, Ontario)
- 2018 **Department of Physiology and Pharmacology Monday Seminar**  
 “Pregestational Diabetes-Induced Congenital Heart Defects and Coronary Artery Malformations; Mechanisms and Preventative Therapies” (London, Ontario)
- 2018 **Physiology and Pharmacology Research Day – Poster Presentation**  
 “The role of microRNA-122 in Pregestational Diabetes-Induced Congenital Heart Defects” (London, Ontario)
- 2017 **Canadian Student Health Research Forum 2017 by CIHR – Selected Presentation**  
 “Tetrahydrobiopterin Prevents Coronary Artery Malformations Induced by Pregestational Diabetes” (Winnipeg, Manitoba)
- 2017 **Canadian Nitric Oxide Society – Selected Oral Presentation**  
 “Tetrahydrobiopterin Prevents Coronary Artery Malformations Induced by Pregestational Diabetes” (Windsor, Ontario)
- 2017 **Weinstein Cardiovascular Development Meeting 2017 – Poster Presentation**  
 “Tetrahydrobiopterin Prevents Congenital Heart Defects and Coronary Artery Malformations Induced by Pregestational Diabetes” (Columbus, Ohio)
- 2017 **Developmental Biology Research Day – Poster Presentation**  
 “Tetrahydrobiopterin Prevents Congenital Heart Defects and Coronary Artery Malformations Induced by Pregestational Diabetes” (London, Ontario)
- 2017 **Pediatric Research Day – Poster Presentation**  
 “Tetrahydrobiopterin Prevents Congenital Heart Defects and Coronary Artery Malformations Induced by Pregestational Diabetes” (London, Ontario)
- 2016 **Experimental Biology 2016 – Poster Presentation**, American Physiological Association  
 “Tetrahydrobiopterin Prevents Congenital Heart Defects Induced by Pregestational Diabetes” (San Diego, California)



- 2016 **Physiology and Pharmacology Research Day** – Poster Presentation  
“Tetrahydrobiopterin Prevents Congenital Heart Defects and Coronary Artery Malformations Induced by Pregestational Diabetes” (London, Ontario)
- 2016 **Developmental Biology Research Day – Selected Platform Presentation**  
“Tetrahydrobiopterin Prevents Congenital Heart Defects and Coronary Artery Malformations Induced by Pregestational Diabetes” (London, Ontario)
- 2016 **London Health Research Day – Selected Platform Presentation**  
“Tetrahydrobiopterin Prevents Congenital Heart Defects and Coronary Artery Malformations Induced by Pregestational Diabetes” (London, Ontario)
- 2016 **Pediatric Research Day – Selected Platform Presentation**  
“Tetrahydrobiopterin Prevents Congenital Heart Defects and Coronary Artery Malformations Induced by Pregestational Diabetes” (London, Ontario)
- 2015 **6<sup>th</sup> Annual Diabetes Research Day** – Poster Presentation  
“Tetrahydrobiopterin reduces Congenital Heart Defects Induced by Pregestational Diabetes” (London, Ontario)
- 2015 **Physiology and Pharmacology Research Day** – Poster Presentation  
“Tetrahydrobiopterin reduces Congenital Heart Defects Induced by Pregestational Diabetes” (London, Ontario)
- 2015 **Developmental Biology Research Day** – Poster Presentation  
“The Effects of Tetrahydrobiopterin on Congenital Heart Defects Induced by Pregestational Maternal Diabetes” (London, Ontario)
- 2015 **London Health Research Day** – Poster Presentation  
“The Effects of Tetrahydrobiopterin on Congenital Heart Defects Induced by Pregestational Maternal Diabetes” (London, Ontario)
- 2015 **GradCast Radio CHRW 94.9 FM** – Broadcasted Interview (London, Ontario)  
“Episode #4: The Dark Side of Being a Sweetheart with Anish Engineer”
- 2015 **Retiring with Strong Minds** – Oral Presentation (London, Ontario)  
“Maternal Diabetes and Congenital Heart Disease” - Simplifying science for senior citizens

---

#### Work Experience

---

- 2016–  
2018 **Graduate Teaching Assistant and Course Co-Coordinator** – Molecular Techniques 9550  
The University of Western Ontario
- Laboratory skills training for incoming graduate students
- 2014–  
2016 **Graduate Teaching Assistant** – Physiology Laboratory 3130Z  
The University of Western Ontario
- Accessibility in Teaching and Service Certification (09/10/2014)
  - Safe Campus Community Certification (09/10/2014)

---

 Community & Committee Involvement
 

---

2016 – **Chair, Physiology and Pharmacology Graduate Student Council**  
 present *Elected Position*

**Collaborative Specialization in Developmental Biology Steering Committee**

2017 – Children’s Health Research Institute and UWO  
 present

- Graduate student representative responsible for planning and discussing academic matters pertaining to this inter-departmental collaboration

**Western Senate – Graduate Student Senator**

2014 – University Secretariat – The University of Western Ontario  
 2016

- Responsible for forming, amending and upholding academic policy
- Acting as a representative for graduate students on the highest governing body of the university. *Elected Position*

**University Disciplinary Appeals Committee**

2014 – University Secretariat – The University of Western Ontario  
 2016

- Serving on a panel with two faculty senators to grant or deny appeals to sanctions imposed by the VP Student Affairs to students committing academic or scholastic offences; *Elected Position*